

Soft matter food physics—the physics of food and cooking

This content has been downloaded from IOPscience. Please scroll down to see the full text.

2015 Rep. Prog. Phys. 78 124602

(<http://iopscience.iop.org/0034-4885/78/12/124602>)

View the [table of contents for this issue](#), or go to the [journal homepage](#) for more

Download details:

IP Address: 130.237.165.40

This content was downloaded on 13/11/2015 at 12:37

Please note that [terms and conditions apply](#).

Report on Progress

Soft matter food physics—the physics of food and cooking

Thomas A Vilgis

Max-Planck-Institute for Polymer Research, Ackermannweg 10, 55129 Mainz, Germany

E-mail: vilgis@mpip-mainz.mpg.de

Received 23 December 2014, revised 11 May 2015

Accepted for publication 9 June 2015

Published 5 November 2015



Abstract

This review discusses the (soft matter) physics of food. Although food is generally not considered as a typical model system for fundamental (soft matter) physics, a number of basic principles can be found in the interplay between the basic components of foods, water, oil/fat, proteins and carbohydrates. The review starts with the introduction and behavior of food-relevant molecules and discusses food-relevant properties and applications from their fundamental (multiscale) behavior. Typical food aspects from ‘hard matter systems’, such as chocolates or crystalline fats, to ‘soft matter’ in emulsions, dough, pasta and meat are covered and can be explained on a molecular basis. An important conclusion is the point that the macroscopic properties and the perception are defined by the molecular interplay on all length and time scales.

Keywords: soft matter, food structure, proteins, emulsions

(Some figures may appear in colour only in the online journal)

1. Introduction

Food and physics: at first sight, such a combination seems strange. Food is considered often as a daily need, and is frequently consumed without thought in order to satisfy hunger. The objects that are put into the mouth, chewed and masticated before being swallowed seem remote from physical systems, which require investigations by physical methods. Even a closer look at bread rolls, sausages, cheese, milk or breakfast cereals does not suggest their close relationship to soft matter physics. Nevertheless, food can be bitten with the teeth, crushed between tongue and palate, and lubricated with saliva to form a bolus, which finally can be swallowed. The oral processing of food requires relatively small forces and thus suggests that food is soft matter.

A closer look shows that foods are complicated multicomponent molecular systems with competing interactions, which appear too diverse to be treated by the conventional physical methods known from condensed matter physics. Foods are mainly associated with nutrition, pleasure, importance and of course ‘flavor’, which consists of the basic taste qualities

sweet, sour, salty, bitter and umami, but also with the olfactory sense via a large number of aroma compounds, with oral and nasal trigeminal stimulation, such as coolness, heat, astringency, prickling, irritation and pain, and finally with the texture, which defines a large part of the mouth-feel (Lawless and Heymann 2010). The taste of food may be judged as ‘good’, ‘excellent’ or, in the best case, ‘sensational’. If food is processed in the mouth (Chen and Engelen 2012) the thermo-senso-mechanical materials properties are significant for the ‘mouth-feel’, the taste and release of aroma, its flavor and the pleasure it gives. The expression ‘it tastes good’ contains only part of the truth, because the flavor of foods is based on a multitude of actions on different physical levels. Volatile aroma compounds are released; taste-relevant ions and compounds are liberated during oral processing and finally the original food structure breaks down during chewing and mastication. Only if these physically very different processes are in full accord with the sensory expectations does the food taste ‘really good’. The processing in the mouth thus follows thus a number of hierarchically organized steps and corresponds to the ‘testing’ of soft matter under shear, temperature changes

and the breakdown of the structures, which can either be natural for raw foods, or designed by chefs. These naive considerations already suggest the multiscale nature of foods.

Nevertheless, all foods are bio-materials whose biological, physical and chemical properties define their methods of preparation, processing and cooking, and even the way they will be served. The engineering and preparation of food is considered a highly technological process, based on a mixture of empirical laws and long-standing experience. The successful preparation of a bread dough, for example, has a very narrow range of parameters concerning the ratio of water to flour, the concentration of salt and the amount of yeast. Even kneading times, proofing times and baking temperatures need to be considered. Small deviations from the documented values often lead to baking accidents, and the bread fails. Small details can have a large impact, as is well known from home baking, but also in the baking industry, where great effort is put into the production of bread with controlled properties, when the initial conditions of the natural product, flour, fluctuate strongly. Indeed, these statements seem to be addressed in food technology, but all flour consists at least of proteins and starch, which are themselves molecules with defined arrangements and properties. Their temperature-dependent inter- and intramolecular interactions with the added water define most of the macroscopic processes. The parameters used by food engineers can thus be attributed to the physical and chemical behavior on molecular scales, and end up in structure–property relationships, as known from materials sciences. However, any structure–property relationship in foods need to be associated with ‘texture’ as well as the taste and release of aroma. Simple examples of ‘textural properties’ are based on physical quantities: mechanical moduli of gels, melting points in chocolates, melting point distributions and nano- and microstructure in ice creams, the viscosity of sauces, crack propagation in crisps and the tenderness of meat. Most of these properties are also established in soft matter physics and soft matter materials.

Each piece of natural and processed food consists of numerous molecules, which interact at given temperatures and define, in addition to taste and aroma impressions, the materials properties of the foods. The size of the molecules in foods ranges from small aroma compounds and ions up to typical protein and polymer sizes. The physics of foods therefore links many different length scales and physical methods. Some large-scale properties seem to be appropriate for approaches well known from statistical physics, whereas small-scale properties, especially when water and/or aroma compounds are involved, need closer consideration of molecular details, far beyond statistical physics. Thus foods, from the pure physics point of view, are ‘dirty’ systems, which appear too complicated, too applied, and too advanced in engineering, processing and applied science. Natural and processed foods are multicomponent molecular systems with too many competing interactions on a wide range of time and length scales and thus far away from the well-defined model systems that are usually investigated by clear physical methods.

On the other hand, food science is very often associated with chemistry, technology and engineering, and naturally

with biology, but only little with physics. Clearly, a large part of food science is far apart from one basic principle, which has been used in statistical physics for a long period of time: universality, e.g. in second-order phase transitions (Brézin and Zinn-Justin 1990, Stanley 1971) or classical polymer theory (Doi and Edwards 1986, de Gennes 1979, des Cloizeaux and Jannink 1990), when universal exponents are sufficient to describe the general (equilibrium) properties without the influence of lattice properties or chemical composition. Indeed, this universality hypothesis enabled the development of new methods for soft matter systems, especially polymers, and their breakthrough in theoretical physics in various aspects.

The behavior of foods with changing (external) physical parameters, in most cases temperature, does not generally show universal properties; the final properties depend on the process. Molecular control is essential, because foods are in general non-universal systems (Fellows 2009), as noted in many (everyday) experiences: cooking of natural foods depends strongly on the chosen piece, on its origin, or even on the season. For example, the cooking behavior of a piece of beef and its final flavor depend to a large extent on its origin, even when it is taken from the same species and race. Many properties of the ‘sample’ cannot be controlled: how the meat was aged, how it was slaughtered, where the animals were raised, how their feed was composed. This ‘prehistory’ defines the final muscle structure, water content or fat composition of the meat during cooking and eating—and, of course, under physical investigations. Obviously, food systems appear to be far from the well-defined, ‘clean’ model systems that are usually investigated in physics. Nevertheless, to a large extent all foods consist of polymers, often of different molecular architectures, such as starch and cellulose, polar small molecules and polymers (carbohydrates), polyelectrolytes (hydrocolloids), proteins (eggs, muscles, meat), fat, oil and water (Walstra 2007). Indeed their relative ratios define texture, taste and aroma, but also most of the physical parameters that define sensory quantities like mouth-feel.

Most of these remarks apply to all foods, no matter whether naturally grown, raw, cooked, processed or reconstructed. So, why is there a need for ‘food physics’ beyond food chemistry and food engineering? Indeed, physics can bring some ‘order’ into food systems, especially to the large variety of fats, oils, proteins, food polymers and carbohydrates which, together with the actual and local water content, determine the nano-structure of the foods. Thus physics can use simple model systems, which allow fundamental aspects of processes, and physics can define simple, also sometimes universal principles in the behavior of food. Physics thus enables us to understand food from a fundamental molecular point of view and provides a basis for new ideas, fundamental aspects and the predictability of a structure–texture–property–flavor relationship, based on molecular grounds.

One of the key issues is the immiscibility and the strong thermodynamic competition of oil/fat and water. This provides indeed one of the minimal driving forces for food structure. Protein folding and the secondary, tertiary and quartic structure of proteins is one example of structure formation, based on the different water solubilities of the protogenic amino acids (Dill 1999) and the ‘quenched disorder’ of the primary structure

defined by the sequence of the amino acids (Bryngelson and Wolynes 1987, Plotkin and Onuchic 2002, Onuchic and Wolynes 2004). Such simple models inspired by statistical mechanics are not sufficient to understand proteins in foods, where the interplay between function and process properties is important. Especially in protein-rich foods, such as eggs, fish or meat, the precise protein structure matters and defines the pathway of processing and even simple home cooking, when proteins are denatured and change their molecular shape and dynamic properties at well-defined temperatures. After denaturation of some proteins, new, network-like structures are formed (Tornberg 2005). However, the food material consists of numerous different proteins, which are associated with their original biological function. Connective tissues show different local ‘mechanical’ properties than muscle proteins. Therefore, these proteins respond differently to temperature changes. Consequently, some muscle proteins denature at lower temperature, i.e. they ‘cook’ earlier. Moreover, during such denaturation processes their water holding capacity changes and, depending on the water loss during cooking, mouth-feel properties such as tenderness undergo a ‘culinary–non-culinary’ transition, when the mechanical properties of a mistreated piece of meat change from soft to rubbery and leathery. Evidently, the water (meat juices) acts as a ‘plasticizer’, which helps mastication and chewability. However, with modern techniques, such as ‘*sous-vide*’ cooking (Baldwin 2012, Tzschirner and Vilgis 2013), when food is vacuum-sealed and cooked in a water bath at precisely controlled temperatures, proteins can be denatured (meaning cooked) selectively. Thus, protein physics meets meat science. The results are textures controlled and predicted by physics that define taste and aroma perception, mechanical properties and the texture in the mouth, where food is processed by chewing, mastication, bolus formation and swallowing.

Bond	Energy ($k_B T$)	Energy (J)	Remarks
van der Waals	1	4.1×10^{-21}	molecule–molecule
Ionic	2.5	1×10^{-20}	ion–ion
Hydrogen	10	4.1×10^{-20}	water–water
Covalent	200	8.2×10^{-19}	chemical bond

Only soft matter can be processed in the mouth. Simple examples are soft solid foods, such as gels and protein networks, semi-solid foods, such as emulsion, and other complex fluids. The modulus and viscosity need to be of magnitudes that can be handled by the teeth, tongue and palate. In physical terms, energies needed to bite and eat food need to be of the order of magnitude of $E \lesssim 50 k_B T$ per molecule, in contrast to hard matter, where typical energies per molecule are a factor of 10–100 larger (see e.g. Chaikin and Lubensky (2000), Walstra (2007)). The relevant binding potentials thus correspond to van der Waals and electrostatic forces, hydration between ions and polar molecules, such as water, and strong hydrophobic interactions by the interplay of hydrophilic and hydrophobic molecules (or parts of molecules). Moreover, molecular sizes, molecular geometry and shape entropic effects play a major role, as well as cooperative effects as seen in jamming transitions and shear thinning of viscoelastic fluids.

Many foods appear therefore as a typical example of ‘soft condensed matter’: protein gels, hydrocolloid gels, swollen and unswollen networks, natural and reconstructed emulsions. Even the few examples of hard matter, e.g. fat crystals in chocolate, are prepared such that they melt at normal mouth temperatures of 37 °C. Brittle glass-like materials, e.g. potato crisps, break easily between tongue and palate under relatively small forces.

The overall flavor of food, however, comes from a complicated interplay between many other ‘small’ molecules, such as numerous aroma compounds, responsible for the scent, and ions responsible for the taste. Many of these have additional trigeminal stimulation, which completes the perception. Their perception and the interplay with structural and textural properties complete the overall impression, i.e. the flavor. Salts, however, also play a major roles. Apart from their contribution to taste perception, monovalent ions, such as delivered from sodium chloride screen interactions, are well known from the physics of polyelectrolytes, whereas bivalent ions in many cases form strong ionic bonds with charged hydrocolloids, as is well known from pectin in plant cells or alginate in algae cells.

To understand the physical behavior, structure and texture of food, it appears useful to bring at least some naive order to the large variety of molecules and competing interactions. The simplest idea is to identify water and fats as immiscible but basic solvents, which dissolve aroma compounds and ions, solubilize proteins and carbohydrates selectively, and organize more or less defined structures. Food is a material that is ‘tested’ in the mouth: texture as a result of the breakdown of the food structure; taste as the release of ions, protons (acids) and polar molecules, trigeminal sensations by the release of polyphenols, alkaloids and certain aroma compounds, and retronasal perception by the release of volatile compounds. These are many coupled processes that happen simultaneously. Perception has thus many quantitative physical and chemical aspects. To understand some of these mechanisms by physical methods is one of the goals of this review and is summarized in figure 1.

Given the different functions and sizes of the molecules, food physics and food science can be considered as ‘multi-scale’ (Aguilera and Lillford 2008). This almost trivial statement unfolds its detailed importance only during perception, when the interplay between structural properties and the senses of taste and aroma determines the final judgment of the food in the mouth. Thus the entire range of length and time scales, from angstroms to macroscopic, are of (almost) equal importance, as indicated in figure 2.

At small scales, small non-volatile molecules and ions determine the taste detected on the tongue, and low-molecular-weight and volatile aroma compounds are responsible for the scent. The basic food structure is already given at nanoscales by the size of lipids, proteins, hydrocolloids and their self-organization. Emulsion droplets cover nano- to micrometer scales and define viscosity and the behavior under shear, which are detected by tactile sensors in the mouth. Macroscopic properties like shape surface properties, shapes and forms provide the first impression and contact in

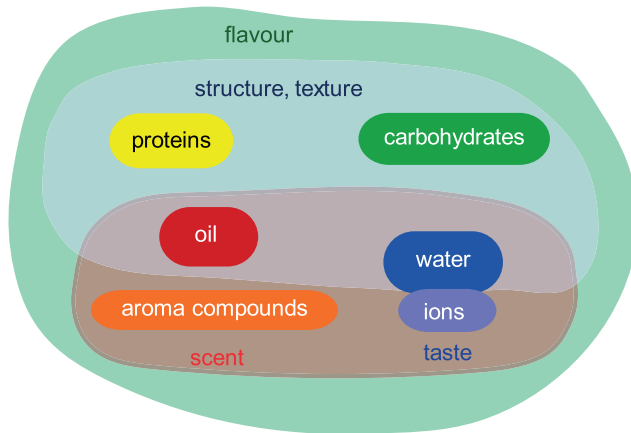


Figure 1. The basic classes of molecules in foods. Proteins, carbohydrates, fat and water, along with ions, define most of the structure and texture properties. Fat acts as a good solvent for aroma compounds, whereas water dissolves the basic molecules, and ions are responsible for the taste.

the mouth. Thus, all length scales of food define physical and sensory properties, which need to be discussed below.

The review is organized as follows: after brief historical remarks, the basic food molecules—water, fat/oils, proteins and carbohydrates—are discussed, where the main emphasis is on their physical behavior and function. Simple (but tasty) foods such as chocolate, oils and fats offer a deep insight into their structure formation by (partial) crystallization and their corresponding melting behavior in the mouth. The behavior of proteins and their relations to polymer structures and network formation are discussed, mainly using the example of gluten. Starch, as a typical carbohydrate, offers the interplay between linear and highly branched macromolecules. The following section reports on the interplay between proteins and starches, which are the main components in doughs for breads and pasta. Their difference is mainly given by their different water content. If pasta dough is dried, the material undergoes a rubber-to-glass transition, common for other polymeric materials. Protein-rich foods, such as eggs and meat are discussed, before the last sections treat model systems, such as the physics of gels and emulsions.

2. When food systems and cooking entered physics

The science of food was (and still is) dominated by the disciplines of food chemistry, food engineering and food technology. Physics as a food-relevant science entered only recently, when the principal theories and experimental techniques in soft matter sciences were developed. Indeed, the developments in polymer physics appeared as a key issue for food physics. Hydrogels, which consist of food-relevant biopolymers, have been studied in detail by Ross-Murphy (1987, 1995). Such studies on model systems have been driven very much from polymer physics, see e.g. Doi and Edwards (1986), the physics of gels as published in Burchard and Ross-Murphy (1990), or the early studies of the physics of polyelectrolytes and polysaccharides (Rees 1977). Another early milestone is

the review by Donald (1994), where methods from polymer physics have been discussed intensively.

The kitchen was introduced to physical science by Kurti (1980) and was advanced by Kurti and This-Benckhard (1994). ‘Molecular gastronomy’ was born and cooking, physics and chemistry have been brought together. The term molecular gastronomy (This 2005, van der Linden *et al* 2008, Vega and Ubbink 2008, de Solier 2010, Barham 2013, Liberman 2014) was very much debated for along time, as to whether it is a scientific discipline or not.

Nevertheless, it certainly needs to be considered as cross-disciplinary research (Barham *et al* 2010), when, for example, systematic investigations show that different ways of preparation influence the results of ‘simple’ sauces, such as the classical hollandaise (Rognså *et al* 2014). However, molecular gastronomy cannot be considered as a scientific discipline like physics, chemistry or biology. Molecular gastronomy is a multidisciplinary branch of science ranging from fundamental physics, connected to biology and chemistry, to food technology, sensory sciences, physiology, fragrance theory, perception and cultural sciences (Vilgis 2012b, 2013b).

The use of combining science and cooking became clearly evident to chefs and scientists with the avant-garde kitchen revolution, initiated mainly by the chefs Ferran Adria (Adrià *et al* 2002, Adria *et al* 2006, Adrià *et al* 2010) and Heston Blumenthal (Blumenthal 2008, 2009). A new level of cooking with scientific background emerged. These novel techniques have been summarized by Myhrvold and Smith (2011), which has become a standard reference for advanced chefs, and the new techniques of the photography shown there are very instructive and most useful for chefs and scientists. However, the topics of this six-volume book stop in most cases at the macroscopic level and do not explain molecular details.

Molecular cooking and molecular gastronomy play only subordinate roles in this review, although they are spreading fast and have become popular recently. However, at various places it is shown via small ‘recipes’ how the basic physical understanding of the molecular interplay can help cooking and food preparation.

3. Water, and its physical relevance in food systems

All foods consists at least of water, fat/oil proteins and carbohydrates in different ratios. In this basic section several examples are introduced and discussed in their basic physical context, which shows the interplay between natural function, food relevance, processing, mouth-feel and cooking of the food system. However, some ‘physically basic’ foods are composed of only one or two molecular classes, e.g. egg white, which consists of proteins and water, chocolate, dominated by the behavior of fats, or puddings, where the properties can be traced back to carbohydrates, especially starches.

3.1. Basics

Water is in most cases the main component of foods. Natural edible foods, no matter what their origin (vegetables or

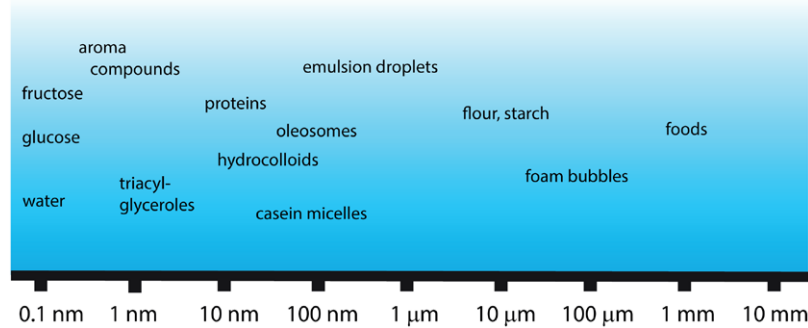


Figure 2. The relevant length scales in food systems span from nanometers to centimeters. All scales play different but important roles in food preparation, processing, perception and sensory properties. The flavor can be defined as an overall perception including taste, scent and texture.

animal), contain between 70% and 90% water, see e.g. Belitz *et al* (2009) and it is thus one of the major components that determines ‘parts of the texture’, as can be seen from tasting the same food with varying water content after different stages of drying. The strong dipole moment of 1.85 D (Gregory *et al* 1997) of the (free) water molecules is responsible for many local, small-scale properties. Water forms temporary clusters and the local dipole moment might change in different environments (Gregory *et al* 1997). The dipole moment is also responsible for the formation of hydrate shells of water molecules with high cooperativity (Tielrooij *et al* 2010) and charge-dependent orientation around ions and thus salt in foods (Kunz *et al* 2004). Even when hydrophobic or amphiphilic low-molecular-weight (aroma) compounds are immersed in water, e.g. in hydrolates, it has been assumed that water molecules ‘encapsulate’ small molecules in a cage formed by hydrogen bonds. This effect is called hydrophobic hydration (Lazaridis and Paulaitis 1992). In recent experiments on solutions of tetramethylurea in water (Tielrooij *et al* 2010) this idea is supported by dielectric relaxation spectroscopy.

These observations have many consequences for food systems, which contain many different ions, polar and charged molecules. Except for salts, whose hydrate shells increase the water binding, water interacts with sugars, e.g. sucrose (Engelsen and Pérez 1996), carbohydrate polymer, such as amylose or molten amylopectin in starch (Fringant *et al* 1995), and proteins via hydrophilic amino acids (Ebbinghaus *et al* 2007). Strong water binding is recognized in the slowing down of the dynamics of the water molecules (Saenger 1987). It has been shown that water partly determines the folding and function of proteins (Levy and Onuchic 2004).

Moreover, the polarity of water allows polar molecules and ions to dissolve. This almost trivial remark has a deeper meaning for foods, food processing and cooking. All taste-relevant molecular groups, which trigger the taste buds for the basic taste qualities salty, sour, bitter, sweet and umami, are water-soluble, a point that will be discussed in more detail below.

3.2. Water activity

The large dipole moment and the ionic and polar nature of many food polymers are especially important for the texture and the biophysics and biochemistry of foods. Water

molecules bind closely to polar monomers (or subunits) of food polymers and form strong and large hydrate shells. Water molecules in the hydrate shells are less ‘active’, i.e. less mobile, and show slower dynamics. For food systems it is useful to define a phenomenological value for the water activity a_w with $a_w = 1$ for entirely free water and $a_w = 0$ for completely bound water. More precisely, the water activity can be measured via the ratio of the vapour pressure of bound water and free water under the same external pressure p and temperature T (Lewicki 2004):

$$a_w = \left[\frac{p}{p_0} \right]_{p,T}. \quad (1)$$

The water activity and the actual water content are in general not simply proportional, because they depend on the precise local properties and interactions. The water activity is determined by sorption isotherm measurements and shows a typical sigmoid bending for most natural foods. The exact shape of the isotherms depends on the composition and the state of the food matter, e.g. viscous liquids, amorphous or crystalline matter. Most foods exhibit three different regimes, as indicated by I, II and III in figure 3 (Troller and Christian 2012, Duckworth [chapter 1]139). When water is added to absolutely dry food, at very low water activities (and therefore low water content as indicated in regime I) it is concluded that water molecules are closely located in the vicinity of the hydrophilic portions, which can be either small molecules with a polar nature, e.g. sugars, or ions, such as salts, but also food macromolecules, such as starch or polyelectrolytes, and proteins. The water molecules diffuse into foods and occupy successively hydrophilic environments. In this regime that water is strongly bound. The dynamics of the water is slow and appears, for example, unfreezable (Duckworth 1974). In regime II ‘multilayer binding’ appears to be predominant. The water is only loosely bound but cannot be considered to be free either. Water molecules exchange their positions rapidly. However, the water cannot be considered as ‘free’ because it is in regime III. In regime II food still appears ‘dry’. At high water activities, where the value of a_w approaches 1, most of the water is ‘free’ and thus non-bound. In regime III foods are wet, examples being fruits, raw meat and fresh dairy products.

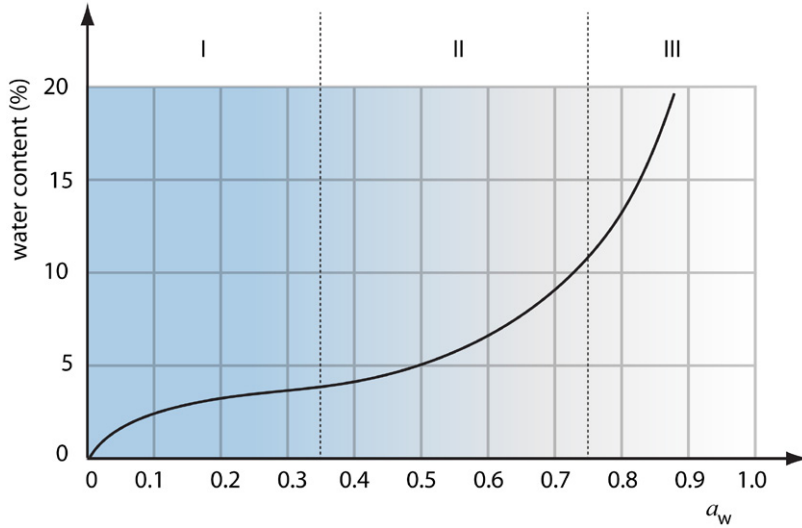


Figure 3. Typical sorption isotherm for food. Regimes I, II and III correspond to different types of water binding.

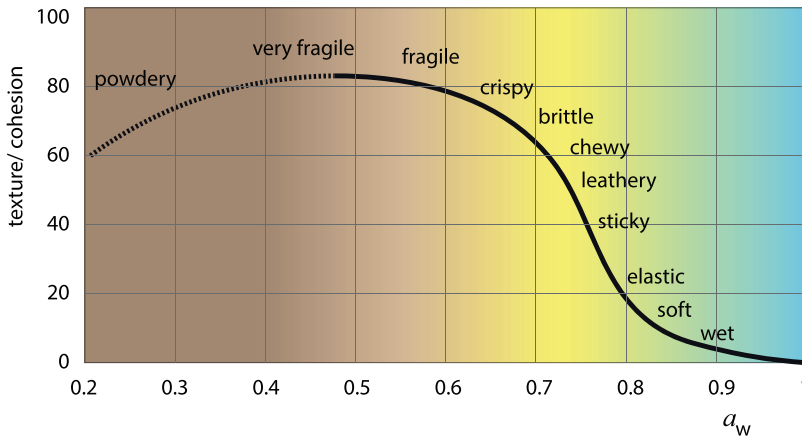


Figure 4. Water activity and typical textural properties and descriptions for foods. The curve is not meant to be unique for all foods; the precise curvature depends on the molecular structure and composition of the food itself.

This heuristic description already suggests a strong relation between the water activity a_w and the texture of foods. At values close to $a_w \rightarrow 0$ the foods appear very dry, even powdery; at the other extreme, the food is practically liquid. The water activity is thus an important parameter for the food texture. Another effect is that at a certain value of the water activity a_w the ‘crispiness’ decreases, as shown for example in figure 4 where it appears around $a_w^c \approx 0.5$. The structure breaks down and the food disintegrates under weak mechanical forces.

It has been suggested to describe the relationship between water activity and the elastic response modulus G empirically by fitting it to equations that recall the Fermi function known from electron theory (Wollny and Peleg 1994), e.g.

$$G = \frac{G_g}{1 + \exp\{(a_w - a_w^c)/b\}}. \quad (2)$$

Although these are plausible fitting functions, they have not been derived from physical theories. The parameters a_w^c and b are food-dependent materials constants and G_g is the modulus of the food in its dry or glassy state. The glassy state of the foods (Slade *et al* 1991) is an important aspect for all foods as discussed later in more detail. However, the relation

to the glassy nature becomes visible in figure 4. At low water activity values, foods are more brittle and crunchy, i.e. less elastic, which are typical properties known for glassy materials (see for example Tomozawa (1996)). Thus it appears natural to apply these concepts to food systems also (Meste *et al* 2002, Ahmed and Rahman 2014). The glass temperature T_g can be (intuitively) defined as the freezing temperature; therefore the molecular motion of the molecules ceases dramatically, and the material changes its mechanical properties from elastic (rubbery) to brittle. Because many solid foods are rich in water it is clear that water and its mobility have strong impacts on the glass transition temperature. The free water in foods with high water activity acts as a lubricant. The foods are soft, tender and elastic. The evaporation of the free water leaves ‘bound’ water in the food, the texture then becomes more leathery, and at even higher drying states, food becomes glassy and brittle by undergoing its glass transition (Neri *et al* 2014). The glass transition temperature in single-component systems (with and without plasticizers) is not a universal property but depends strongly on the structure on atomistic length scales and the local interactions between the molecules (Daniels and Cabrera 2014). Its prediction from first principles

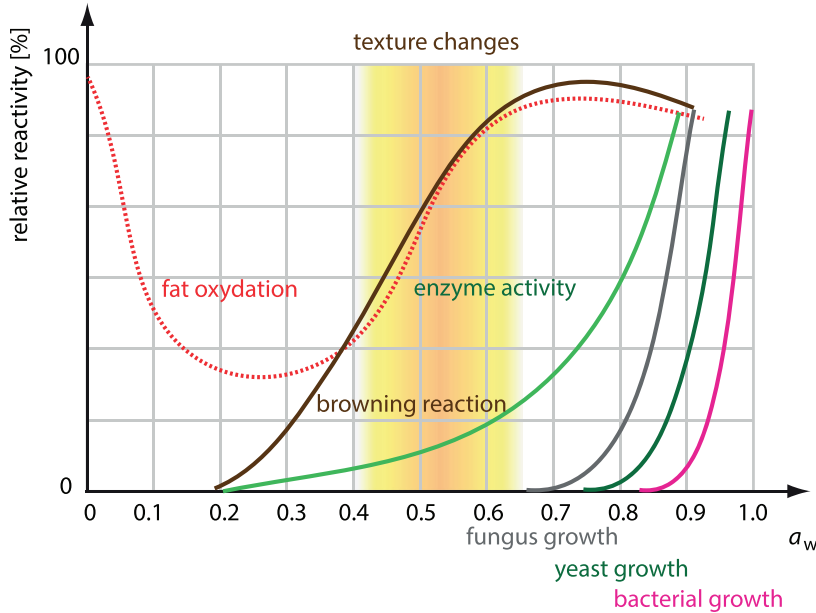


Figure 5. Water activity and the processes in foods. At lower values of a_w the growth rates for microorganisms decrease significantly. The (non-enzymatic) browning reactions during roasting, frying and barbequing increase significantly by the evaporation of free water. Significant textural changes take place in the shaded range around $a_w \approx 0.5$.

is not simple (Langer 2014). Naturally, all natural foods are complex multicomponent systems, and each class of molecules present possesses a distinct glass transition temperature, possibly significantly separated from the others. Thus foods have, in general, broader ‘glass transition ranges’, in contrast to single-component materials. Generally, the glass transition temperature T_g increases with decreasing water activity a_w (Slade *et al* 1991). The glass transition temperature can be measured by the use of standard differential scanning microscopy and other caloric methods (Höhne *et al* 2003).

Apart from its physical, structural and textural relevance the water activity is an important quantity for food safety, see e.g. Troller and Christian (2012). Microorganisms need free water for their metabolism. The growth of fungi, yeast and bacteria, which are responsible for food spoilage, is much lower at lower water activity values $a_w < 0.7$, where the food texture is more crispy and brittle (Barbosa-Cánovas *et al* 2008).

As indicated in figure 5 the water activity determines many processes in foods. Lower values for a_w stop the growth of microorganisms and foods can be stored for longer provided that no additional moisture is taken up from the humidity of the air. These facts are important for practical purposes in food processing and even cooking at home. Roasted and fried foods are more ‘tasty’ because frying produces new aroma and flavor compounds, but only at temperatures above 130 °C. However, as long as free water evaporates from fresh foods, the temperature cannot increase significantly above 100 °C. Browning begins only if the water activity is reduced during the first stages of the frying process, and then a significant concentration of aroma compounds is produced by chemical reactions, e.g. the Maillard reaction (Baynes *et al* 2005). Indeed the browning rate increases when the difference $a_w - a_w^c$ decreases, or in other words, the temperature difference between the actual temperature and the glass temperature

$T_g(a_w)$ decreases, as has been shown in detail by Karmas *et al* (1992), depending again on the precise molecular composition of the foods under consideration.

3.3. A hypothetical state diagram—implications for processing and cooking

The water activity determines many properties in foods when the temperature is changed also. Free water molecules at high water activity values are able to crystallize whereas water at low a_w values does not form proper crystals. These differences are important during freezing of foods, e.g. during storage. The water fraction (and its activity), or equivalently the fractions of the solids in foods, translates into phase diagrams as shown schematically in figure 6.

For figure 6 it is assumed that simple foods can be characterized by their solid parts only, which are not further characterized at this stage. These solid parts in simple (model) foods can be sugars, starch or one-component protein solutions (Slade *et al* 1991). Nevertheless, such simple phase diagrams offer already a fundamental understanding of the role of water in foods as a basic component. At low solid fractions (high water fractions) most of the water is free and forms ice crystals when the temperature is low enough. The results are larger water crystals, whose size becomes comparable to or larger than the relevant molecular distances; elementary structural elements, for example plant cells in vegetables, fruits or salad leaves, will rupture at slow cooling rates. When such foods are thawed again, the texture and mechanical properties are eventually destroyed: frozen (in ordinary freezers) and thawed strawberries have lost all their attraction. Foods with high water activity need fast quenches to low temperatures to form brittle glasses. Herbs, like parsley, chervil or chives can be made glassy/crispy by cooling them quickly below 130 °C,

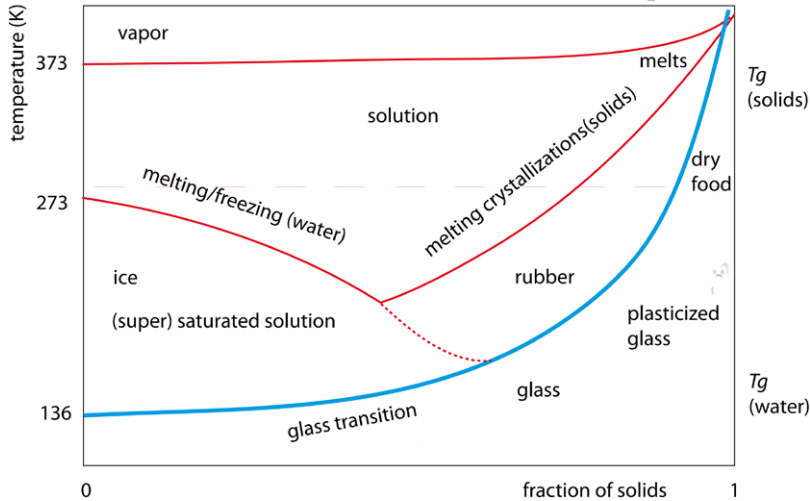


Figure 6. Simplified phase diagram of simple (model) foods.

for example by plunging them in liquid nitrogen. Because such leaves are thin they freeze immediately, form a glass and can be a delicious component when eaten in the glassy state.

At higher temperatures water acts as a solvent. In pure water the limiting temperature is (at high quenching rates) its glass transition, which has been found experimentally to be 136 °C (Angell and Tucker 1980), whereas some simulations conclude higher values (Giovambattista *et al* 2004). Glass transitions of water solutions have been studied by Katkov and Levine (2004) and compared to different phenomenological or empirical models.

At intermediate solids fractions and above the glass transition line food takes on a rubber-like state with a leathery texture. It can be chewed and masticated several times before it breaks apart. In such regimes the water activity values are around four to five. Depending on the exact composition of the food, water molecules can only crystallize in parts and form small crystals. A slightly increasing water fraction lowers the glass transition accordingly by increasing the molecular mobility (and thus entropy). This effect is well known in daily life: freshly prepared potato crisps (thinly sliced potatoes, fried in oil) are in a glassy state at room temperature and have a very crunchy texture. After some time they may take up humidity from the air. The glass transition temperature increases by the uptake of water and the texture changes from glassy to rubbery. The crisps are then soggy and their fracture behavior is very different.

The phase diagram (figure 6) also allows a physical definition of the term ‘dried food’. It can be defined as the small area between room temperature and the line for the glass transition at high solid fractions. For applications in food technology such fundamental principles are important, for example when fresh vegetables, such as carrots, are dried below their glass transition temperature (Xu *et al* 2014). The exact influence of the pre-drying on the vegetables has an important influence on the glass transition temperature and the corresponding texture.

Glassy foods, cooked and dried to a very well-defined water activity, have many practical and gastronomic applications. A well-known example is popcorn, where these thermophysical parameters define not just the textural parameters but also the

final volume of the popped corn (Shimoni *et al* 2002). Corn is cooked until it reaches its amorphous state (see section 6) and dried afterwards to a moisture content between 12% and 15%. These corn grits are in a glassy state. When the grits become quickly heated far above the glass transition temperature the solid parts get a high mobility, and the water evaporates quickly and expands the volume of the corn grits (see Virot and Ponomarenko (2015) for a recent discussion of the macroscopic physics). The method has been adopted in modern gastronomy for many different foods, such as puffed rice, puffed cereals (wheat, oats etc); even cooked and dried pork skin can be puffed by frying it in oil or heating in a microwave oven to get light and crispy textures of different tastes.

4. Fat/oil: triacylglycerols

4.1. Fats—fatty acids

Fats and oil play an important role in foods and nutrition. All natural foods contain a certain amount of oils and fats, at least in the seeds, where fats are used to store energy for germination (see for example Raven *et al* (2005)). Examples of fat-dominated foods are sausages (Frisullo *et al* 2009), cheese (Dufour *et al* 2000), cream and butter (Precht 1988), margarine (de Bruijne and Bot 1999), frying oils (Choe and Min 2007), cacao butter (Marangoni and McGauley 2003) and, last but not least, chocolate (Beckett 2000). The latter especially can be used as a culinary model example to study the phase behavior of fats, where the melting of fat crystals leads to the food’s sensory properties. Moreover, since fat dissolves most aroma compounds, it plays a major role in the flavor release in foods (see for example Carrapiso (2007)).

In general, natural oils and fats consist of a distribution of non-polar molecules, known as triacylglycerols (TAG), which are sometimes also called triglycerides. These molecules contain fatty acids, which are carbon chains containing an even number of carbon atoms from 2 to 24. Food-relevant fatty acids with an odd number of carbon atoms exist too, and appear naturally in milk fats of ruminants in small concentrations.

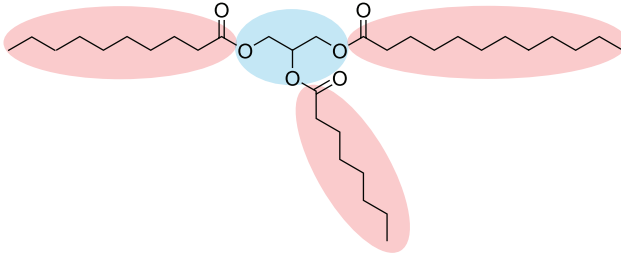


Figure 7. Example of a triacylglycerol (TAG). The glycerin part in the center of the molecule carries three (here saturated) fatty acids with different chain lengths.

Natural and food TAGs contain three fatty acids (FAs), esterified to glycerol, which can be of different chain length within the same TAG (see figure 7). The chain length of a FA is measured by the number n of carbon atoms and generally characterized by C_n . The carbon–carbon bonds can be saturated (all *trans* C–C bonds are single bonds) or unsaturated (*cis*-double bond), which makes a big difference in the structure formation and thus the physical behavior of oils. From the chemical structures shown in figure 8 the influence of the degree of saturation already becomes obvious. Single carbon–carbon bonds can rotate according to the energies in chemical bonds, see e.g. Flory (1989), where different models and transfer matrix methods have been developed to describe the effect of the statistical physics of C–C bonds on the conformation of oligomers and polymers. Figure 8 shows the conformations of a common fatty acid containing 18 C-atoms at different degrees of saturation s , $C_{18:s}$, $C_{18:0}$ (stearic acid), $C_{18:1}$ (oleic acid), $C_{18:2}$ (linoleic acid) and $C_{18:3}$ (alpha-linolenic acid). The change of the conformation by the presence of *cis*-double bonds in the fatty acids changes their crystallization behavior. Saturated FAs may form crystal structures with fewer defects than unsaturated FAs (Garti and Sato 1988). In pure monodisperse melts of FAs the chain length n and the saturation s control the melting temperature of the crystals (Vaclavik *et al* 2008, Belitz *et al* 2009, Knothe and Dunn 2009). Typical melting temperatures of FAs are shown in figures 9 and 10. The melting temperature increases with the chain length n and decreases with increasing degree of saturation s due to more crystal imperfections.

The fits in figures 9 and 10 have been achieved by use of the equations derived for chain homologs as predicted by Flory and Vrij (1963) (see also Broadhurst (1966) for a clearer discussion), which has been extended to unsaturated FAs by using a simple entropy argument for the mobility of the bound FAs (Vilgis 2010):

$$T_M(n, s) \approx T_M^{(\infty)} \frac{a + n}{(b + n)} \frac{1}{(1 + cs \log s)}. \quad (3)$$

The parameters a and b can be associated with the enthalpies and entropies of the end groups (Broadhurst 1966). The parameter c depends on the nature of the unsaturated FA, i.e. on the location the first double bond from the end opposite to the carboxyl bond ($C=O$) (number 3 for n_3 FAs, number 6 for so-called n_3 FAs, or omega3 or omega6 FAs in nutritional terminology). The temperature $T_M^{(\infty)}$ corresponds to the melting temperature for a homolog with infinite chain length, which

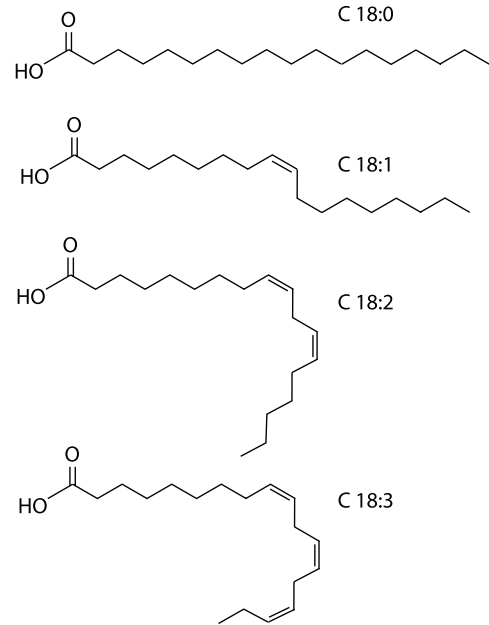


Figure 8. Fatty acids can be saturated or unsaturated. As an example the FA C18 is shown with different degrees of saturation, $s = 0, 1, 2, 3$. (Note that the two-dimensional graphical representation of the FA does not show the complete number of possible conformations in the different saturation degrees s .)

is a hypothetical temperature because chain-folding will produce differently shaped crystals. Nevertheless, $T_M^{(\infty)}$ has been estimated on thermodynamic grounds which can be related to experimentally detected values, e.g. by extrapolation (Jain *et al* 2004). For unsaturated FAs, $s = 0$, equation (3) reduces to the classical Flory–de Vrij equation (Flory and Vrij 1963), which is well known and often used in polymer physics (Jain *et al* 2004).

As a side remark it is mentioned that for very short chain lengths the difference in odd and even numbers of n chemical details matters and a systematically higher melting point is measured for even compared to odd values of n ; this has its origin in the different steric situation at the surfaces of the crystallites (Knothe and Dunn 2009) (which changes the parameters a and b in equation (3) slightly).

Mixtures of different FAs show phase diagrams similar to those known for paraffin mixtures (Maximo *et al* 2014). Binary mixtures of saturated FAs follow similar rules as for other materials with waxy melting regions and a clearly defined eutectic composition. In a series of papers Costa *et al* (2009a, 2009b, 2009c) studied the phase diagrams of mixtures of different FAs with a systematic length variation and determined their phase diagrams. It is also shown in detail how the difference in the chain lengths determines precisely the phases and the coexistence regions. Recently, mixtures of FAs have also been considered as phase change materials for energy storage (Yuan *et al* 2014).

4.2. Simple triacylglycerols: monoacid TAGs as physical model systems

The crystallization and melting of free FAs, however, can provide only indications of the phase behavior of fats and oils

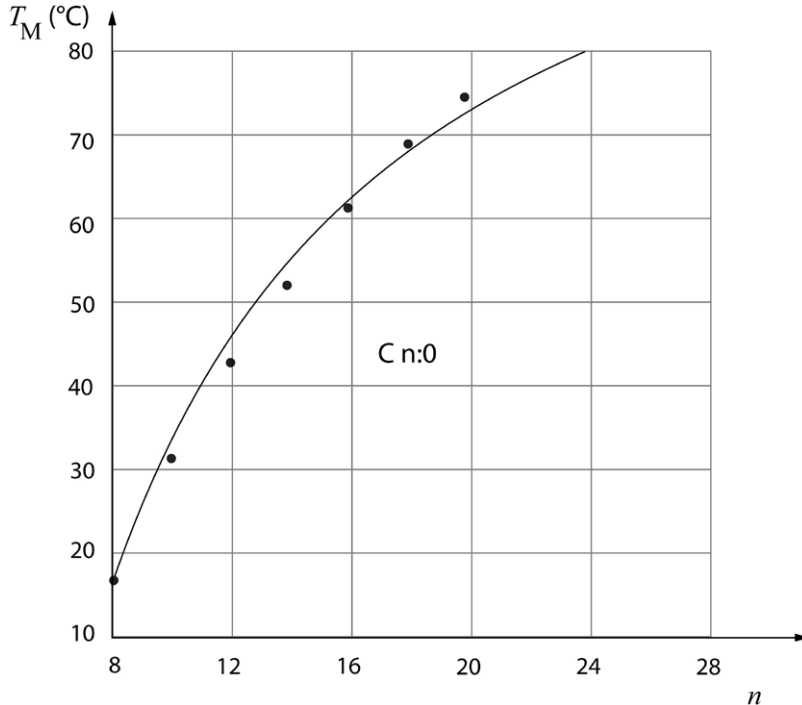


Figure 9. Melting temperatures of saturated ($s = 0$) fatty acids as a function of the chain length n .

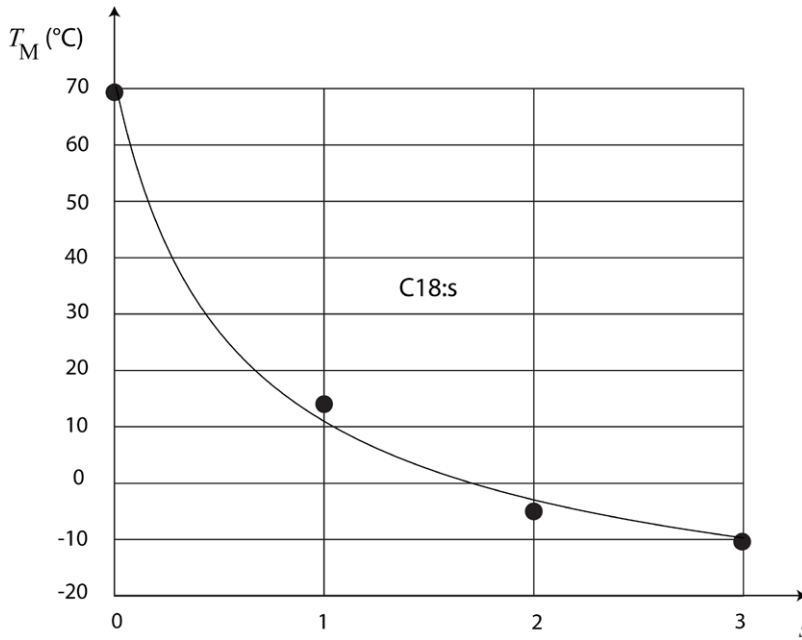


Figure 10. Melting temperature of the fatty acids $n = 18$ at different values of s .

that consist of triacylglyceroles (TAG), i.e. three FAs bound to a glycerin molecule. Natural food fats and oils consist of a more or less broad mixture of different TAGs having different FAs. Thus, no melting point exists; instead the melting regime is characterized by waxy and pasty consistencies that consist of many mixed crystals (Belitz *et al* 2009). A well-known, everyday example is butter, which is solid below 15 °C, liquid above 40 °C, but spreadable, waxy, pasty and semi-liquid at intermediate temperatures. The broad regime and special rheological properties (Wright *et al* 2001) between solid and liquid are a consequence of the broad distribution of TAGs

in the natural milk fat (Jensen *et al* 1991). As will be shown below, butter has a liquid fraction of low-molecular-weight TAGs, even at temperatures below 10 °C, which is encapsulated in the solid phase (Precht 1988).

Simple model fats, which consist of only one TGA, such as trilaurin (3-C 12:0, or LLL) or tristearin (3-C 18:0, or SSS), have the additional advantage for their crystallization properties of being saturated. Therefore, relatively simple crystal structures will emerge. Trilaurin (very prominent in coconut oil) has been studied thoroughly by scattering methods by Lee *et al* (2010) and Cebula *et al* (1992). The structural transition of

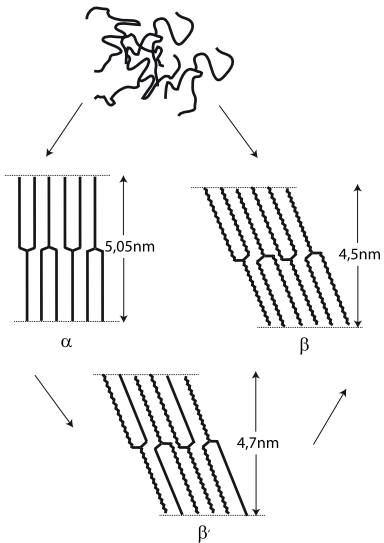


Figure 11. The basic structures (α , β , β') of tristearin SSS at different rates of cooling. At fast cooling (quench) the crystal structure (left) is different from that at slow cooling and tempering (Mayama 2009). Redrawn after (Mayama 2009) with permission from RSC.

tristearin has been discussed, for example, by Mayama (2009). The general behavior of the basic phases is shown in figure 11. Similar phases are obtained in other TAGs of similar types, i.e. LLL or other TAGs of the type C k:0, C k:0, C k:0 (Sato 2001). At high temperatures, the TAGs are in a disordered melt phase. At fast quench (left path in figure 11) a so-called α -phase is formed with a certain thickness. The TAGs are arranged in a hexagonal lattice with a ‘fork structure’ with a melting point of 54 °C. At slow cooling rates a stable β -structure with a melting point of 74 °C appears, which corresponds to the thermal equilibrium. Here the FAs are tilted compared to the crystal plane and form a triclinic lattice. However, the TAGs also show an unstable β' -structure, where they form a hexagonal lattice and a steeper tilt, which is expressed in a slightly larger long period (4.7 Å compared to 4.5 Å) of the crystals. This form has a melting temperature of 63.5 °C and is thus significantly lower than that of the stable β -structure.

For trilaurin (LLL) a similar picture is found (Lee *et al* 2010). The α -form has a tilt of 90° and a melting point of 15.0 °C, the β' -form a tilt angle of 66° and a melting point of 35.0 °C, and finally the stable β -structure a tilt angle of 66° and a melting temperature of 46.5 °C. These results have been confirmed also by neutron scattering. Since the α - and β' -structures are not stable they recrystallize to the stable β -form. In such solid–solid transitions the structures recrystallize slowly over a long period and form ‘blooms’ (Mayama 2009), a more general effect not restricted to SSS or similar TAGs, which is important for chocolate, when the (partial) recrystallization is visible at the surface (Beckett 2000).

The unsaturated model fat triolein (3-C 18:1, or OOO) has been studied recently by Akita *et al* (2006) using infrared techniques combined with scattering and by Cebula *et al* (1992) using diffraction methods. It was shown (Akita *et al* 2006) that despite the *cis*-double bond the structural characteristics of the

β - and β' -phases are similar to tristearin. The α -phase, however, does not show a very pronounced appearance. The steric hindrance by the *cis*-double bond seems to prevent the formation of such structures. The melting temperatures (Kodali *et al* 1987) are –32.0 °C for the α -phase, –13.0 °C for the β' -phase and 5.5 °C for the β -phase.

4.3. Triacylglycerols with different fatty acids

The TAGs discussed in section 4.2 are nice model systems that provide basic and fundamental answers for physicists. In natural foods the TAGs contain different FAs with different values for n and s , which will affect the crystal structures, the number of phases, defects and melting temperatures. The ‘non-universality’ of natural TAGs is obvious when the crystal structure and the melting temperature depend on the local arrangement of the FAs at the glycerol, e.g. a TAG lmn has different properties from those with different possible permutations in the arrangement of the FAs, as shown in the work by Knoester *et al* (1972) and Timms (1984). The results for the melting temperatures of the permutations in a ‘model fat’, which contains different compositions and permutations of stearinic (C 18:0) and palmitic acid (C 16:0), are shown in figure 12. The crystallization, kinetic effects and kinetic phase behavior under different cooling rates have been studied in detail by Bouzidi and Narine (2012).

An important TAG consists of two stearic acids (S, C 18:0) and one oleic acid (O, C 18:1), in the configuration SOS, where the O is located between the two S (Sato 2001). SOS allows for more polymorphs, which are very important for food technological and culinary applications. For detailed studies of the different β -polymorphs, see the papers by van Mechelen *et al* (2006a, 2006b). The behavior of the SOS TAG is of special culinary interest, since the melting temperature of the β' -form is slightly lower than the temperature in the mouth, which will be of special importance for physically driven sensory sensations and mouth-feel, as indicated by the melting points of its polymorphs in figure 13.

4.4. Mixtures of triacylglycerols

Detailed studies of TAG blends are of special interest for food technology (Sato 2001, Aguilera and Lillford 2008, Rajah 2014, Sato and Ueno 2014). Mixtures of tristearin and triolein have been studied by Ahmadi *et al* (2009). Recent studies show how well-defined mixtures of triacylglycerols and diacylglycerols can be used to control crystal structures, polymorphism and melting temperatures (Silva *et al* 2014). Such ideas open new applications for margarine, fat or chocolate constructions. The spatial structural arrangement of the solid crystals and their resulting properties have been discussed in Narine and Marangoni (1999b). In recent molecular-dynamics (MD) simulations (Greiner *et al* 2012) the densities and self-diffusion coefficients of a range of liquid monoacid triacylglycerols have been studied as a function of temperature and pressure. The response of the TAGs is qualitatively similar to temperature and pressure changes. Application of pressure was found to significantly

	SSS	72,0 °C
	PSP	68,2 °C
	SPS	67,7 °C
	SSP	66,2 °C
	PPP	66,0 °C
	PPS	63,5 °C

Figure 12. Melting points of model fats containing two fatty acids differing in length, e.g. FAs C 18:0 (S) and C 16:0 (P). The difference in length has been exaggerated in the cartoon. Data taken from Knoester *et al* (1972).

increase densities and reduce diffusion of the TAG molecules, suggesting that pressure may play as much a role in processing and crystallizing TAGs as supercooling does. A solution of glycerol tripalmitate and glycerol trihexanoate was also studied, showing that the application of pressure should lead to a significant decrease in the saturation point of the solution, which is an important consideration for processing TAGs. Different solid/liquid interfaces of glycerol tripalmitate have also been investigated. The obtained results suggest that the melting of TAGs may be cooperative in nature, rather than involving dissolution of individual TAG molecules (Greiner *et al* 2012).

4.5. Chocolate

A special and well-accepted ‘fat construction’ is dark (or bitter) chocolate (Beckett 2000). Its bases are the special polymorphs of cacao butter, which contribute to the slow melting in the mouth, the release of taste, which stems from finely ground cacao powder, and finally a small amount of sugar, which attenuates some of the bitter taste of the cacao powder. The exceptional melting behavior of cacao butter in the mouth has its origin in the composition of its TAGs. Its main component, about 80%, is a TAG consisting of palmitic acid C 16:0 (P), stearic acid C 18:0 (S) and oleic acid C 18:1 (O) in the form POS (Beckett 2000, Talbot 2014). Regional differences come from the different compositions of SOS, POP, POS, as well as SOO and POO, which are liquid at room temperature (as known for example from olive oil). Other TAGs are PPP, SPP, PSS, SSS and SOO. The composition shows an important principle of natural fats. Around a dominant component, a broader distribution of other TAGs influences small details which can be sensed during eating, e.g. the mouth-feel

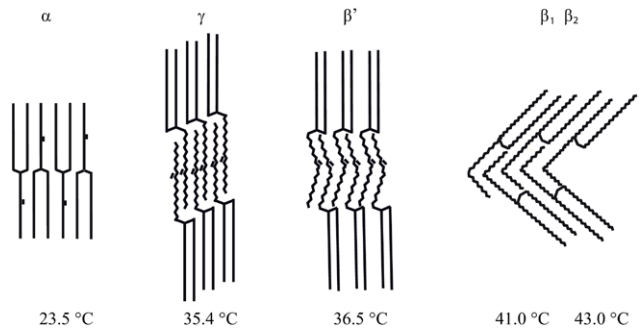


Figure 13. The polymorphs of SOS. A three-layer γ -form appears. The β -structures show two modifications, which are not drawn explicitly. The melting points increase from left to right.

of the regional differences in chocolates (Chaiseri and Dimick 1989). Such differences have quite an impact on the crystallization behavior, the crystallization kinetics and the melting kinetics (Dimick 1999), which are used by confectioners and patisseries to control sensory properties and taste release. The crystal structure of such fat compositions has been studied, for example, by Kaneko *et al* (1998) and Talbot (2014), whereas the structure of pure POS amongst others has been analyzed by van Mechelen *et al* (2006a, 2006b), and mixtures and blends of POS by Wille and Lutton (1966). Figure 14 shows the melting temperature of the six different crystal forms associated with the structure and the corresponding melting temperatures. The most preferred form corresponds to a β -structure with a melting point of 33.8 °C. Such forms melt in the mouth in an appropriate time; taste and aroma compounds are released sufficiently slowly to provide a pleasant mouth-feel. Moreover, it has been reported recently that several aroma compounds undergo chemical reactions during mastication and contact with saliva in the mouth, which enhance the sensory quality (Granvogl *et al* 2012).

However, kinetic effects play an important role in the selection of the crystal form Marangoni and McGauley (2003). Figure 15 shows how the crystal form changes with time at a given temperature. The phase diagram was obtained by x-ray diffraction methods. The crystallization temperature and the time define the resulting crystal form, the melting temperature and thus the mouth-feel. To obtain appropriate parameters for excellent chocolates, the pathway from liquid to solid phases needs to be controlled in detail. To ensure crystal forms providing an excellent mouth-feel special temperature programs have been developed, which involve cooling rates and tempering times, as indicated in figure 16 (see e.g. Beckett (2000), Fryer and Pinschower (2000), Sato and Ueno (2014), Schenk and Peschar (2004)). The first step consists of a relatively rapid cooling, which enables nucleation, which is well known from all crystallization phenomena (see e.g. Chaikin and Lubensky (2000), Mandelkern (1964))). Cooling by about 25 °C, according to figure 15, allows nuclei of the α -, β - and β' -types to form. Brief reheating allows the unstable α -nuclei to melt whereas subsequent tempering periods enable slow growth of the desired crystal form. When slow cooling to the usual storage temperature follows, the β -crystals with well-defined melting temperatures remain.

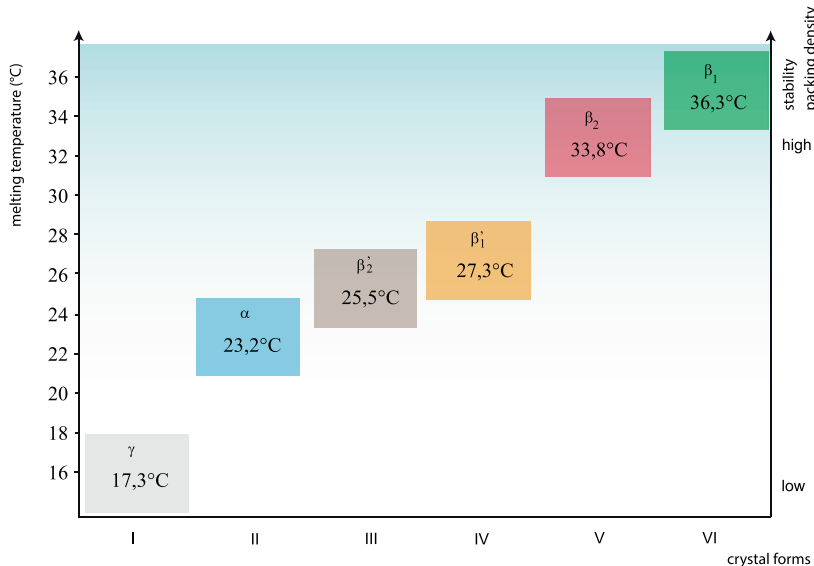


Figure 14. Crystal forms in cacao butter. The most acceptable form is an unstable β -structure with a melting temperature of 33.8 °C.

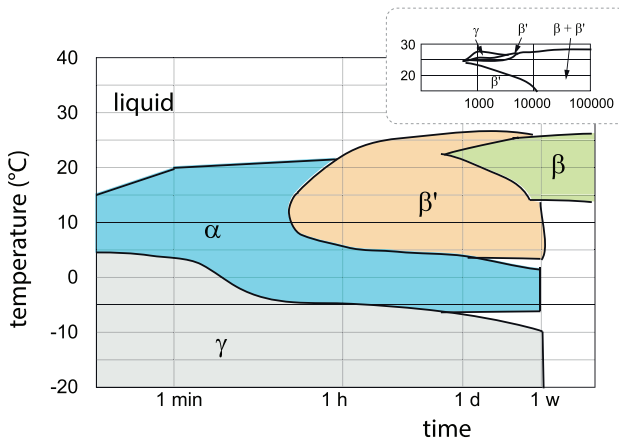


Figure 15. When cacao butter is cooled ‘statically’ at certain temperatures different crystal forms are adapted and change with time. (Redrawn with the results from Marangoni and McGauley (2003) (inset) and Schenk and Peschar (2004) with permission from ACS.)

However, chocolate undergoes so-called ‘blooming’ transitions with increasing storage times, which indicates slow dynamic recrystallization, and healing of crystal defects can be observed. The surface of chocolates shows white areas (Beckett 2000). In such solid–solid transitions ‘flakes’ of different crystal structure form. Mayama (2009) used a simple argument concerning the energy of additional tilting from α -to the β -phase for tristearin (SSS) to estimate the size of such flakes which form the bloom. The free energy of deformation of a (rectangular) flake (with length l and deformation ϵ due to the relative change of height $\Delta h/h$ caused by tiling) can be expressed as $F_d \approx \frac{1}{2}E\epsilon^2 l^2 h$, where E is the elastic modulus of the crystal. To form a crack at the surface, the deformation free energy must be of the same order as the surface free energy $F_s \approx 2\gamma l^2$, where γ is the surface energy. Comparing both free energies yields

which can be used to analyze sizes to $l \approx 10 \mu\text{m}$ and $h \approx 0.3 \mu\text{m}$ when the values for the moduli, Poisson’s ratio and surface tensions are used.

A widely used practice is to add ‘seed crystals’ of the desired types of crystal form as nuclei to prevent cacao butter forming ‘wrong’, undesired crystal structures. Moreover other added seed crystals, e.g. BOB crystals, where the letter B stands for behenic acid, a longer fatty acid of the C 22:0 type, also prevent blooming (Hachiya *et al* 1989a, 1989b). Crystallization of cacao butter/chocolate under shear has been studied by Campos and Marangoni (2014). Different shear rates influence the formation of nuclei (together with seed crystals) and decrease the cooling rate dependences of the melting process.

Note that cacao butter describes only the ‘fat part’ of chocolate. As mentioned earlier (dark) chocolate contains sugar and cacao powder. In milk chocolate some of the cacao powder (cacao mass) is replaced by milk powder. Emulsifiers are added to improve the viscous properties of the molten chocolate during conching (Beckett 2000). These additional components complicate the physics of real chocolate considerably. In many cases phospholipids (‘lecithin’) are used as emulsifiers.

4.6. Fat crystal networks

When natural fat (e.g. milk fat or cacao butter) crystallizes, the structures are more complicated than the model blends discussed so far (Wright *et al* 2001). The distribution of TAGs is broad, and the highly unsaturated and short-chain TAGs remain in the liquid state. Consequently, the unsaturated or singly unsaturated and long-chain TAGs crystallize in spherical forms. The liquid fat (oil) is dispersed freely between the spherical crystals. The crystal form is nodular, and a scale-dependent distribution of the fat particles has been suggested (Wright *et al* 2001, Aguilera and Lillford 2008), especially

when shear is applied during cooling. The solid spheres form a random network, as shown in figure 17. At scales of ‘blobs’ of mean size ξ the structure is assumed to be fractal, where the number n_b of particles inside the blob scales with a certain exponent, i.e. the fractal dimension:

$$(\xi/b)^{d_f} = cn_b \quad \text{or} \quad \xi^{d_f-d} \propto \phi \quad (5)$$

where ϕ is the volume fraction of particles inside the d -dimensional sphere ($d = 3$) and c a non-universal proportionality constant. At larger scales the blobs pack closely according to the degree of crystallinity. The size ξ decreases with increasing degree of crystallinity. The hierarchical structure implies scale-dependent elastic and rheological properties which provide information on the model parameters. The elastic properties are determined entirely by the solid fat fraction as has been argued by Ball (1989) and Brown and Ball (1985). The fractal dimension alone is not sufficient to characterize (random) fractals. The spectral dimension, d_s , describes the connectivity ($d_s = 1$ for one-dimensionally connected chains/polymers), and the ‘walk dimension’, d_w , determines the distance traveled at a given time t by a random walker placed on the object, $R^{d_w} \propto t$. Fractal, spectral and walk dimensions are connected by the simple relation $d_s = 2d_f/d_w$ (Alexander and Orbach 1982). The walk dimension d_w can be written as $d_w = d_f + x$, where x is the fractal dimension of the backbone (de Gennes 1979, Cates 1985).

The model allows for two different stress/deformation regimes (Shih *et al* 1990). At low deformations and shear amplitudes, the entire networks stays intact. The modulus is determined by the entire structure of the solid part. At large deformation/shear amplitudes the links between the blobs of size ξ break and the fat network breaks into several pieces. The elastic response decreases. At still higher shear amplitudes the bonds inside the blobs break. Eventually the system becomes liquid. A crucial parameter for the elasticity is the volume fraction ϕ of the solid part (Shih *et al* 1990), which discriminates between the breaking of bonds under shear inside and outside ξ . The scaling theory for rigid (but weakly linked) fractals shows two distinct regimes for the moduli:

$$G \propto \phi^{-\frac{d_f+x}{3-d_f}} \quad \gamma_{nl} \propto \phi^{\frac{1+x}{3-d_f}} \quad (6)$$

and

$$G \propto \phi^{-\frac{1}{3-d_f}} \quad \gamma_{nl} \propto \phi^{\frac{1}{3-d_f}} \quad (7)$$

where γ_{nl} describes the shear amplitude at which the nonlinear deformation regime starts and strong structural changes, e.g. the breakage of the links, take place and the total elasticity gets weaker. Several slight modifications of equations (6) and (7) have been proposed to fit the data better: for example, an interpolation between the two regimes by Wu and Morbidelli (2001) which allows the regime between linear and nonlinear deformation to be better described.

These ideas have been further developed and applied to cacao butter and other food fats by Marangoni (2002), Marangoni and Rogers (2003), Marangoni and Rousseau (1996), Narine and Marangoni (1999a), where it was shown

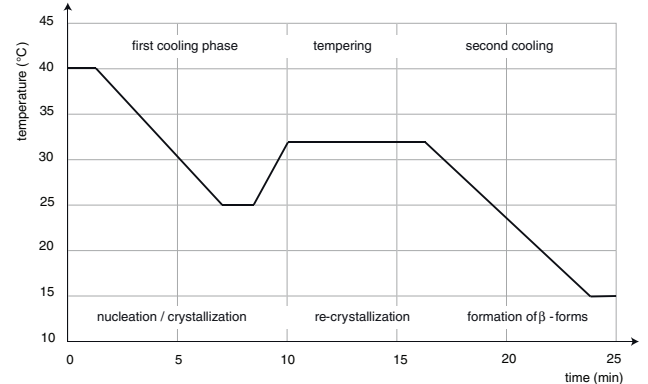


Figure 16. Typical cooling and tempering phases of cacao butter/chocolates. Three different phases are needed until the crystal form has acceptable mouth-feel. The precise temperatures and times vary with the type and regional origin of the cacao butter.

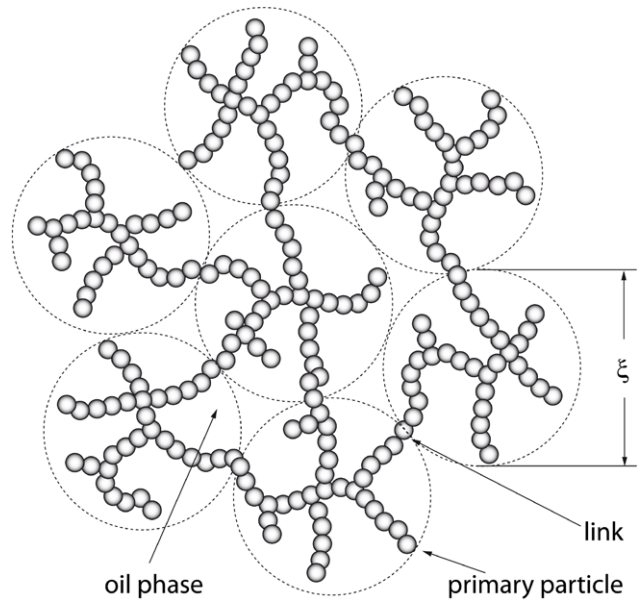


Figure 17. Hierarchical spatial arrangement of fat. At distances less than a typical lengths scale ξ a ‘fractal’ distribution of the primary particles with diameter b is assumed. The liquid fat phase is distributed in the ‘meshes’ of the fat network.

that rheological data can be well understood with such ideas. When prefactors are taken into account, the storage modulus as a function of the shear γ for the fat network obeys (Tang and Marangoni 2006)

$$G \simeq \frac{mA}{6c\pi b\xi d^3} \phi^{-\frac{1}{3-d_f}}, \quad (8)$$

where A is Hamaker’s constant, m is the coordination number of the blobs of size ξ , c defined in equation (5), b is the mean diameter of the primary particles and d is the average mean distance between the blobs, of the order of b , when the blobs are closely linked. The yield stress Σ^* , at which the fractal structure breaks down, can also be determined (Tang and Marangoni 2006) as

$$\Sigma^* \simeq \frac{6\sigma}{b} \phi^{-\frac{1}{3-d_f}}, \quad (9)$$

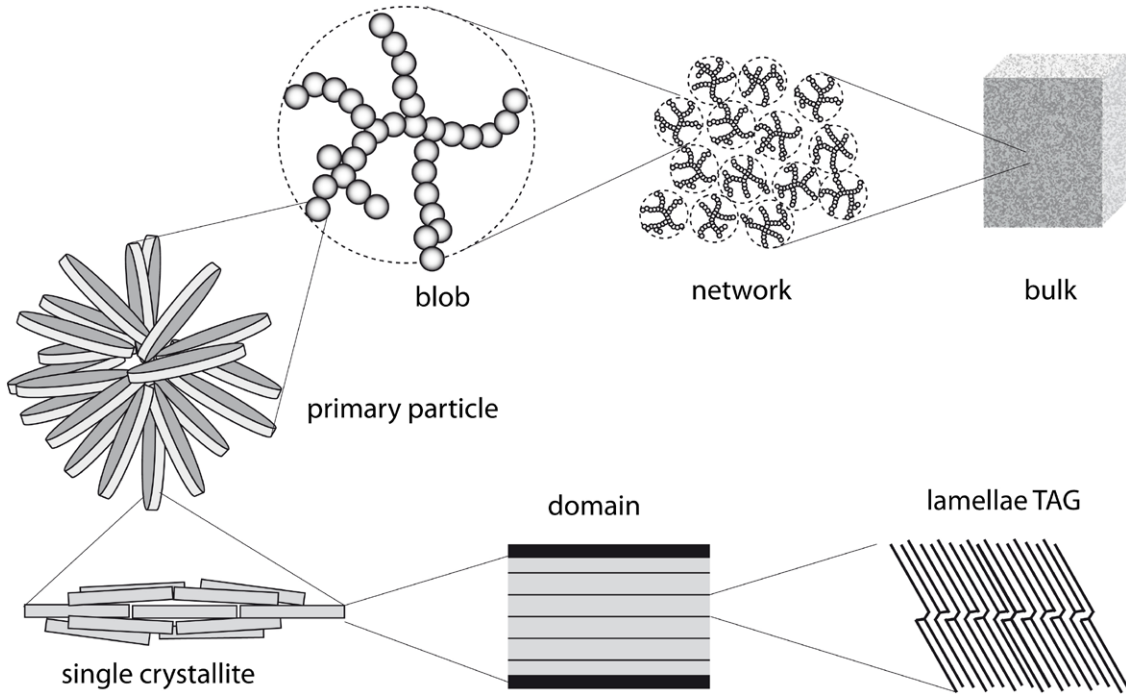


Figure 18. Solid fat at various length scales (redrawn after Tang and Marangoni (2006) with permission).

where σ is the interface tension between the liquid and solid phases.

Awad *et al* (2004) showed how the fractal dimension may change with the increasing solid fat content of several model fats, in addition to the blob size ξ , which shows that the fractal structure of the fats does not always have a universal nature and depends on the material used. In addition, the measured value for fractal dimension depends strongly on the method (Tang and Marangoni 2006). So far, fractal dimensions between $1.7 \leq d_f \leq 2.8$ have been reported (Aguilera and Lillford 2008). The value depends on the crystallization kinetics, on the nature of the fatty acids in terms of their length and their saturation degree, and on the width of the distribution of TAGs, which yields a polydisperse diameter distribution of the primary particles.

Finally a structural hierarchy of food fats emerges from the considerations (Tang and Marangoni 2006) and is depicted in figure 18. Such physical hierarchies are important in other fields of materials physics as well. Similar ideas have been independently proposed and used for particle-reinforced elastomers (Witten *et al* 1993, Huber *et al* 1996, Vilgis *et al* 2009), where the primary particles form clusters of a certain (process-dependent) fractal dimension which are immersed in an elastic rubber matrix (Vilgis *et al* 2009). Related mechanisms are responsible for the softening of the material at larger amplitudes when the network of the filler particles breaks down. The decrease of the modulus can also be assigned to the breakdown of the partially fractal structure of the network spanned by the filler particles.

4.7. Culinary experiments with fat and oil

The physics of such fat blends can be applied daily in the kitchen. One of the simplest physical ideas is a mixture of

olive oil and cacao butter. The TAG composition of olive oil varies regionally, but nevertheless the most important TAG composition can be determined (Boskou *et al* 1996, Ollivier *et al* 2006). The main TAG components in olive oil are OOO (3 C 18:1), POO (C 16:0, 2 C 18:1) and LOO (C 18:2, 2 C 18:1) and are responsible for the structure formation. At room temperature olive oil is liquid, cacao butter solid. Blending both in their molten state and cooling under shear (stirring) produces a fat network as discussed in the previous section. By the composition of the blend, the texture and melting can be adjusted to the culinary use. For a spreadable, almost buttery blend, two thirds of olive oil and one third of cacao butter give a spreadable fat blend. Since cacao butter has almost no aroma, the aroma of the blend is dominated by the olive oil.

Another application is ‘cooling chocolate confection’, a blend of dark chocolate (cacao butter) and coconut oil, which contains mainly saturated short-chain FAs and a broad distribution of CCLa (2 C 10:0, C 12:0), CLaLa, LaLaLa, LaLaM (2 C 12:0, C 14:0) and LaMM (Marina *et al* 2009); the abbreviations La, C and M stand for lauric acid, capric acid and myristic acid respectively. The melting temperature of coconut oil is about 22 °C (Tan and Che Man 2002) for small cooling rates. Therefore, a coconut oil-dominated blend with chocolate decreases the melting point to below 24 °C. If the blend is cooled rapidly, mostly very unstable α - and γ -forms result, which melt very quickly at 37 °C, the temperature in the mouth. The energy for the melting enthalpy is taken from the tongue and cannot be delivered as quickly from the blood circulation. The local temperature of the tongue falls quickly below 24 °C, which is recognized as a cooling sensation by the trigeminal temperature receptors. These are only two examples of the application of the basic component fat in foods and pleasure. Of course, liquid fat blends (fat emulsions) are also

of interest, for example tasty peanut oil with a note of dark chocolate, which is served so that its crystallization temperature is slightly above the temperature of the plate it is served on. During eating the liquid fat blend will partially solidify and change its texture; this may also be in combination with other foods at lower temperature placed on the plate. Such gastronomic physical kitchen stories just never end.

5. Proteins

5.1. Forms and function

Proteins are macromolecules with special functions, which give foods their structure (see for example the book by Finkelstein and Ptitsyn (2002) for an introduction). Proteins are chain-like molecules, but unlike polymers (de Gennes 1979), which show a large number of statistically equivalent conformations, proteins possess only a limited number of shapes, often just one, which defines its biological and biophysical function. In the simplest case, long-chain polymers consist of one type of sub-unit, the monomer. The degree of polymerization defines the chain length N , which is, apart from a constant, proportional to the degree of polymerization or the number of monomers forming the chain. The size of a polymer chain R_g , i.e. the radius of gyration of the chain, has always been a valuable measure (de Gennes 1979, Doi and Edwards 1986). Single chains obey simple scaling laws of the form $R_g = bN^\nu$ for the chain size with certain limits, where b is a typical size of a statistical repeat unit (Flory 1989). The size of the chains is ruled by the thermodynamic environment and in some cases by the ‘chemistry’ of the monomers. The exponent ν has basic limits for linear, flexible excluded volume chains: $\nu \approx 3/5$ for chains in good solvents, $\nu = 1/2$ for chains in a Θ -solvent, where repulsive excluded volume forces balance each other, and $\nu = 1/3$ for totally collapsed chains in a poor solvent. Another extreme is given by $\nu = 1$ for totally rigid chains (de Gennes 1979, Vilgis 2000). When monomers in polyelectrolytes (Van der Maarel 2008) are charged, the charges repel each other and the chains adopt more stretched conformations (de Gennes 1979, Holm *et al* 2004, Dobrynin and Rubinstein 2005), see figure 19 for the different scaling regimes. Copolymers with more than one type of monomer can have a (multi) block structure, which shows a richer number of conformations in selective solvents (see e.g. Hamley (2005), Wang *et al* (2005)). Random and amphiphilic copolymers (Matsuoka *et al* 2012) can be specially designed for structuring, but have also been used as simple models for the behavior of proteins, conformation and protein folding (Thirumalai 1995, Shakhnovich 1997, Garel and Orland 1988, Khokhlov and Khalatur 1998, Dill 1999, Onuchic and Wolynes 2004, Clementi 2008). Some of the theories use for simplicity quenched random excluded volume potentials (Garel and Orland 1988, Sfatos *et al* 1993) with replica theories, which are difficult to apply to proteins. Their primary structure is well defined and practically unique for each protein, and defines their structure and function, see figure 21 for an illustration.

Proteins are ‘copolymers’ where the ‘monomers’, i.e. the amino acids, define the primary structure. The 20 protogenic amino acids have different chemical structures and properties.

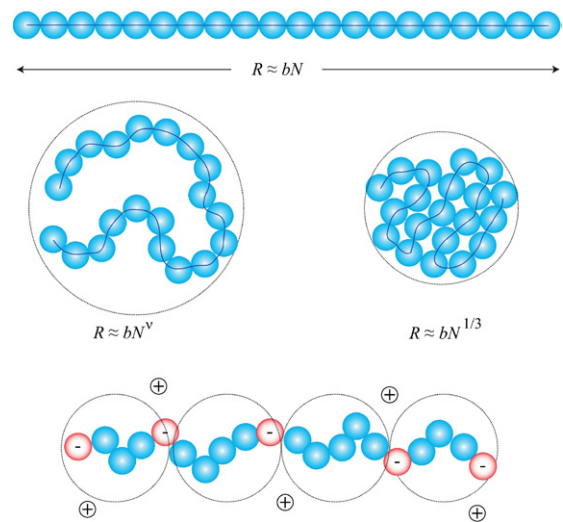


Figure 19. Elementary conformations in polymers. The subunits (‘monomers’) are indicated as spheres. A fully extended, stretched chain conformation is entropically not favored, and exists only for chemically rigid rod polymers. In a good solvent the chain is extended; in a poor solvent the chain collapses. In polyelectrolytes a new length scale (electrostatic blob) is introduced, which depends on the number of charges. The overall conformation is stretched. Counterions ensure electroneutrality.

The amino acids differ in their solubility due to different pK values of their zwitterionic nature. Thus, amino acids change their solubility when the pH value of the solutions or the environment changes, and the overall behavior of the proteins changes also (Yang and Honig 1993). To ensure their stability and function in the natural environment, the appropriate primary structure enables different possibilities of structural elements: helices, which stiffen parts of the protein, and β -sheets, which allow aggregation. The local sequences of the primary structure define exact conformations of the proteins. Each stable conformation corresponds to a low energy bound. If the energy increases, the native structures become unstable and denature at sufficiently high temperatures; the protein conformation corresponds to a random copolymer, which happens in cooking. It has to be noted that the process of denaturing involves several successive processes according to the local stability of the structural elements. Partial denaturation has become a very recent principle in scientifically based low-temperature cooking (Tzschorner and Vilgis 2013), as will be discussed later in section 10.

5.2. Some basic protein physics features

The remark in section 5.1 suggests that proteins do not have any ‘physical universal’ properties. This is not quite true as has been shown by Hong and Lei (2009), who have worked out several universal features that are relevant to food, when the denatured, polymeric state of the proteins matters. The simplest idea is to distinguish only between the number of hydrophilic (T, S, W, Y, P, H, E, N, Q, D, K, R) and hydrophobic (I, V, L, F, C, M, A, G) amino acids in the protein chain, in the one-letter code in figure 20. The fraction of hydrophobic amino acids defines the hydrophobicity h of the protein

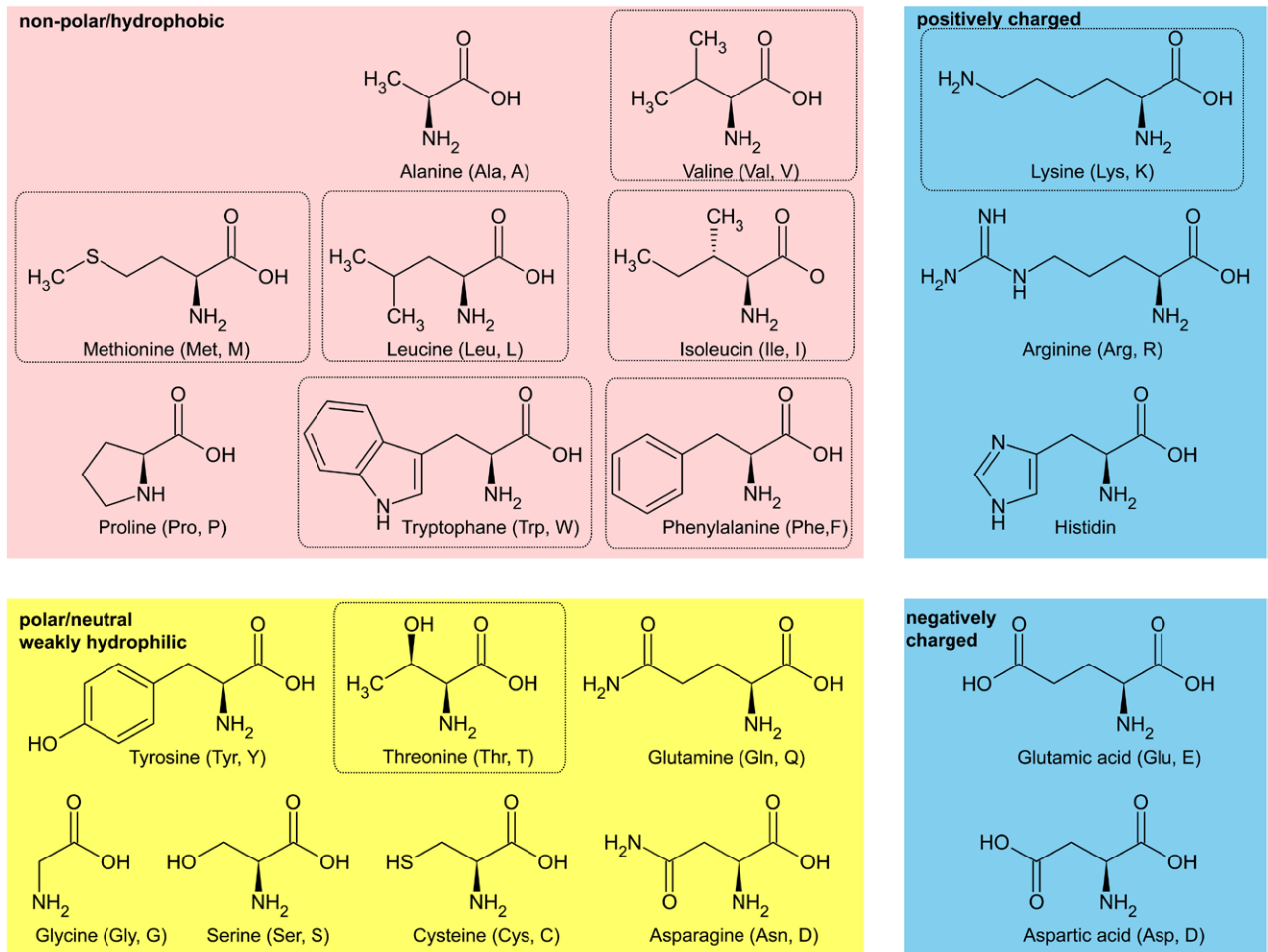


Figure 20. The 20 basic amino acids in proteins. Their solubility in water determines more or less the structure of the protein. The abbreviations correspond to the three- and two-letter codes used often in biophysics and biochemistry.

(Kyte and Doolittle 1982). It has been shown by analyzing numerous proteins that the value of h interpolates between the extremes defined by the radius of gyration of a polymer chain, i.e. $1/3 \leq h \leq 3/5$ (Hong and Lei 2009), which is not surprising because $h = 0$ corresponds to a chain in a good solvent (water) or to an (eventually slightly overcharged) polyampholyte, following the good solvent regime. In contrast $h = 1$ defines a polymer chain in a poor solvent that should be completely collapsed. However, most of the natural proteins need to be more or less water-soluble, so that their hydrophobicity lies between $0.4 \leq h \leq 0.6$ and they have more or less the same scaling exponent $\nu \approx 2/5$, compare these discussions with figure 22. The secondary structural elements, helices and β -sheets, impose stiffness within the chains and prevent the proteins from a total dense packing as in totally collapsed chains. The scaling behavior can be motivated by a very heuristic argument. During folding proteins do not form knots (Taylor and Lin 2003), so that the molecules form loosely connected self-similar structures, which can be described by a d_s -dimensional connected object ('polymeric fractal' in the frame of Cates (1985) and Vilgis (1987)) with a bare fractal dimension defined of $d_f^0 = 2d_s/(2 - d_s)$, which leads to an elastic energy of the order of $k_B T R^2/N^{d_f^0}$. The minimum requirement is the excluded volume repulsion energy, which is of the order of

$k_B T b^3 N^2/R_g^3$. The balance yields an excluded volume exponent $\nu = (d_s + 2)/5d_s$, which is $\nu = 2/5$ for two-dimensionally non-knotted chains with $d_s \approx 2$ and recovers the classical Flory exponent for one-dimensionally connected polymer chains.

5.3. Wheat proteins: polymers, food rubbers, seitan

Why are such oversimplified considerations important for foods? Foods form 'polymer networks' when proteins are denatured and processed. A typical example is the large-scale elasticity of gluten networks, the proteins from wheat (Charalambides *et al* 2006). They play an important role in the processing of dough (Belton 1999, Shewry *et al* 2002) by forming networks (Mann *et al* 2013, Schiedt *et al* 2013). The physical behavior strongly resembles the mechanical behavior of cross-linked rubbers (Treloar 1975, Vilgis *et al* 2009, Mark *et al* 2013). The wheat protein gluten itself consists of mainly two different proteins, gliadin and glutelin (Wieser 2007, Belitz *et al* 2009). The structure of gliadin has recently been studied by Ang *et al* (2010), but only the glutelin is responsible for the large-scale elasticity and the large deformation regime obtained in gluten networks (Shewry and Tatham 1997), by cross-linking the long molecules via disulphide bridges via the sulfur-containing amino acid cysteine. The glutelin

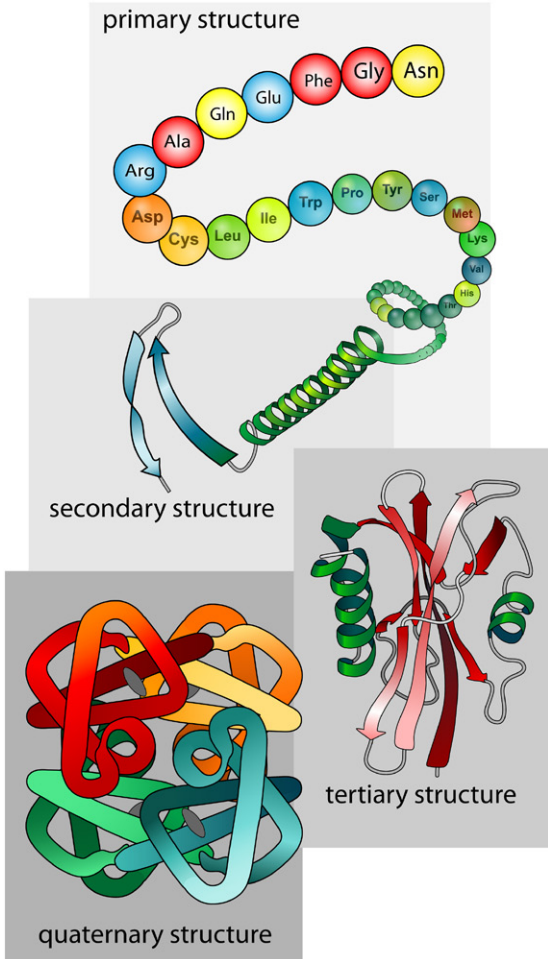


Figure 21. Basic structure of proteins.

fraction is divided into fractions of low and high molecular weight, which differ in molecular weight by a factor of two (Wieser 2007). The positions of the cysteine are important for the network formation and the addition water to the gluten. The cysteine is placed in gliadin along the chain. Consequently gliadins are mostly ‘self-cross-linked’ molecules, whereas in low-molecular-weight glutenin, cysteine is placed towards the chain ends, as well as in the center of the primary structure. Hence, low-molecular-weight glutenin (about 250–300 amino acid residues per chain) takes part in the network formation. The cysteine amino acids for the high-molecular-weight (about 700–800 amino residues) fraction of the glutenin are placed at the termini of the chains (Wieser 2007). Thus a part of the glutenin networks can be viewed as ‘end-linked’ networks, which governs the large-scale elasticity.

The scaling considerations provide a rough estimate of the maximum extension of the gluten network. The chains can (ideally) be stretched totally; their maximum stretching ratio λ_{\max} behaves roughly as

$$\lambda_{\max} \approx \frac{Nb}{R_g} \approx N^{3/5}, \quad (10)$$

when the scaling exponent $\nu = 2/5$ is taken into account, which is a larger value than for Gaussian chains ($N^{1/2}$) due to the hydrophobicity h . Using five to six residues as a crude

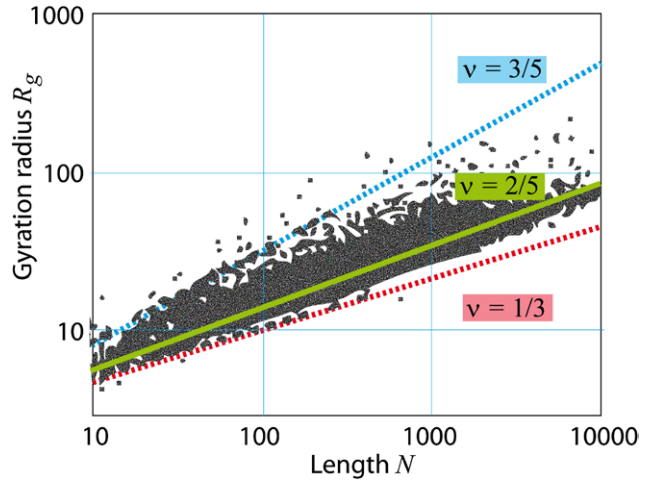


Figure 22. Radius of gyration of 37 162 proteins as a function of the number of amino acids (chain length N). Redrawn from Hong and Lei (2009) with permission. The limiting lines $\nu = 3/5$, $\nu = 1/3$ and the fit $\nu = 2/5$ are indicated.

estimate for a statistically independent unit Flory (1989), λ_{\max} can be between 10 and 20, which corresponds to typical strains in gluten networks (Kokelaar *et al* 1996, Singh and MacRitchie 2001). However, such estimates appear very simple when water as solvent and polar and hydrophilic amino acids are taken into account. The formation of complexes between charged amino acids or hydrophobic residues provides additional effects (Belton 1999, Tatham and Shewry 2000, Tolstoguzov 2003), which are summarized in figure 23. The gliadin is a self-cross-linked molecule and does not take part in the network formation. It acts more or less as a ‘soft filler lubricant’ in the network. The different glutenin fractions cross-link with disulphide bonds. Water plays a central role in the network formation. Apart from enabling the cross-linking via sulfur bridges it enables electrostatic complex formation and hydrophobic interactions, when hydrophobic amino acids form clusters or, eventually, β -sheets (Belton 2005), which may act as transient cross-links. On a larger scale and in a different hydration state the number of loops and trains between different glutenin chains changes accordingly. Only an optimal hydrated gluten network develops its full elastic and high-performance deformation properties (MacRitchie 2014).

The ionic amino acids and their electrostatic interactions show that added salt is not only a question of taste, but also a physical quantity. Salt ions, such as sodium chloride, screen the Coulomb interactions to lowest order (Chaikin and Lubensky 2000). This prevents strong complex formation and lowers the repulsion of the chains. More entanglement-like contributions to the elasticity (Doi and Edwards 1986) might show up. However, its precise contribution on a molecular level is not quite clear yet (Tuhumury *et al* 2014).

A nice culinary application of gluten networks is seitan, well known in Asian cultures, prepared from water, gluten and salt. By kneading gluten and pre-salted (or spiced) water (or vegetable broth) a network as described above is formed. The kneading process aligns the gluten molecules, which provides a meat-type mouth-feel. This texture makes gluten a

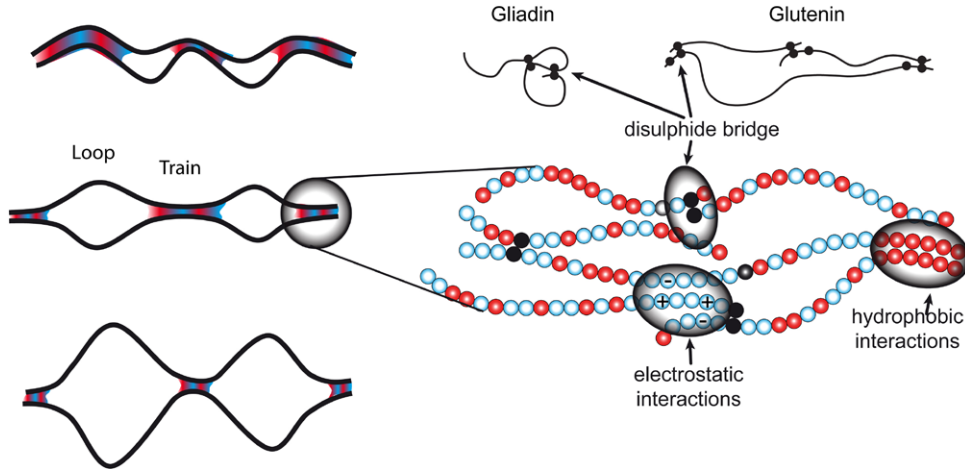


Figure 23. Schematic representation of the structural elements of gluten networks.

well accepted meat substitute. The permanent cross-linked network allows boiling and pan-frying.

5.4. Proteins and acid

It is not only heat and temperature that matter, but also acid. Changes in the pH value may denature proteins (Yang and Honig 1993). Lowering the pH value increases the concentration of protons (more precisely, hydronium in water), which increases the concentration of ‘positive charges’. Thus the interactions in the protein change, and hydrogen bonds and charge complexes from positive and negative charged amino acids get weaker. The protein gets denatured (Bashford and Karplus 1990, van Vlijmen *et al* 1998).

Each isolated amino acid i has a certain pK_{a}^i value (defined e.g. under physiological conditions, $\text{pH} = 7.4$), which changes in the protein by its interaction with water and other amino acids in the folded state to (Tanford and Roxby 1972, Bashford and Karplus 1990, 1991, Yang *et al* 1993)

$$pK_{\text{a}} = pK_{\text{a}}^0 - \frac{1}{2.3}\Theta_i\beta\Delta U_i \quad (11)$$

where $\Delta U_i = \sum_{i \leq j} U_{ij}$ is the change of the electrostatic energy of amino group i in the protein, β is the inverse temperature $1/k_B T$, and $\Theta = 1$ for acidic and $\Theta = -1$ for basic groups. For the electrostatic potential U_{ij} different approximations can be used (Tanford and Roxby 1972). The numerical factor in equation (11) is based on the iteration scheme of Tanford and Roxby (1972) for the protonation f_i of ionizable groups at a given pH value:

$$\log(f_i(1 - f_i)) = 2.3(\text{pKa} - \text{pH}). \quad (12)$$

The free energy of the folded state can then be defined as $\beta F_F = -\log Z_F$, where Z_F is the partition function of the folded state, given as

$$Z_F = \sum_n \exp\{-\beta F_F(n)\}, \quad (13)$$

and $\beta F_F(n)$ for a given pH value can be written as

$$\beta F_F(n) = \sum_i \left(x_n(i) \Theta_i 2.3(\text{pH} - pK_{\text{a}}^i) + \sum_{1 \leq j \leq i} x_n(i)x_n(j) U_{ij} \right). \quad (14)$$

The vector \mathbf{x}_n with its components $x_n(i)$ defines the reference state free energy of non-ionized groups. The resulting free energy needs to be compared to the free energy of the unfolded state βF_U , which can be computed from its partition function $\beta F_U = -\log Z_U$, where the corresponding expression for $\beta F_U(n)$ for the unfolded state is given by the pK_{a} value for the isolated state, when each amino acid is far away from the others, i.e. the interactions $U_{ij} = 0$,

$$\beta F_U(n) = \sum_i x_n(i) \Theta_i 2.3(\text{pH} - pK_{\text{a}}^0). \quad (15)$$

The free energy of the unfolded state can thus be expressed as

$$\beta F_U = - \sum_i \log\{1 + \exp(-2.3\Theta_i(\text{pH} - pK_{\text{a}}^0))\}. \quad (16)$$

These ideas can be used to understand the titration curves of protein solutions, when at a certain pH value the proteins denature and change their shape (Tanford and Roxby 1972, Bashford and Karplus 1990, 1991).

5.5. Cooking with acids

In food technology and cooking the change of the pH value is a basic principle of ‘cooking’ at room temperature, when no food-relevant protein denatures under normal circumstances. Some proteins denature by the treatment of acids, such as vinegar or lemon juice ($2 < \text{pH} < 4$). When raw salmon is sprinkled with culinary acids, its color changes from red to white, which originates from the coagulation of certain proteins. Egg white treated with acid shows similar effects. The transparent viscous liquid changes to white and opaque, similarly when cooked under heat. This is relevant also for food safety. Bacteria and microorganisms cannot grow at low pH values, which apply to foods of similar relevance as those with low water activity values, as described in section 3.2. Dishes with low pH dishes

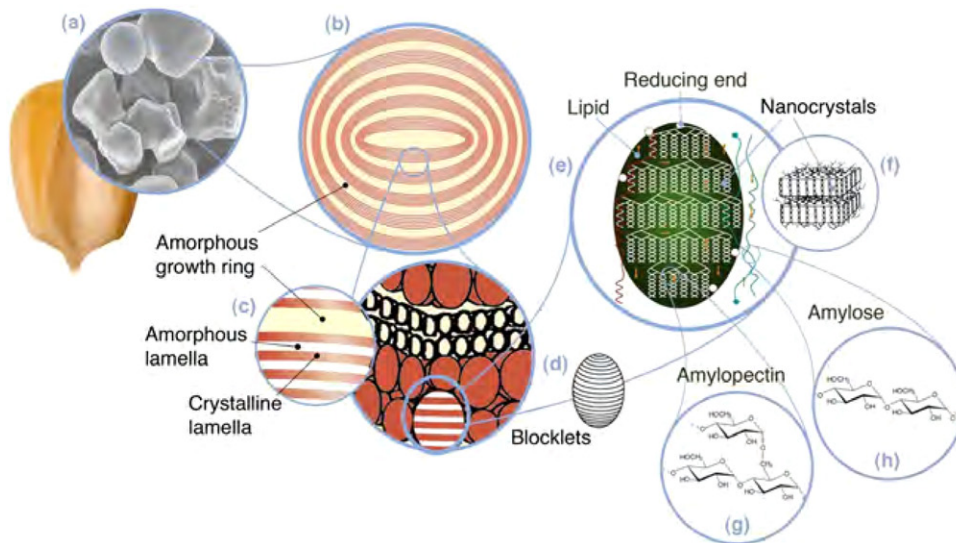


Figure 24. The structural hierarchy in natural starch grains. Reprinted from Dufresne (2014) with permission.

have been created worldwide and in most cultures. Fish dishes such as ‘ceviche’ from South America have recently become very popular. Fresh fish is thinly sliced and covered with onions, herbs and garlic, and marinated for some time in lime juice. Some proteins of the fish muscle denature. The appearance and the color can be associated with ‘cooked’ fish, and the texture resembles a state between cooked and raw.

Some recipes for Italian carpaccio, the famous thinly sliced lean beef, suggest a short marination time in vinegar to giving a tender and melting-type texture and taste.

6. Carbohydrates

6.1. General remarks

Starch, i.e. linear and branched macromolecules of glucose, is another fundamental nutrient and is present in corn maize, potatoes, rice, wheat, manioc roots and other plants and grains. It provides energy and can be relatively easily digested. A rich source of carbohydrates are plants, grains and seeds, where starch is used as energy storage for germination of the grain/seed (Chapin *et al* 1990). The storage needs to be effective, which means that the number of glucose molecules in a small volume of starch granules must be high, providing a high energy density. This defines the form and conformation of the starch molecule. Obviously, starch needs to be highly polymerized: small molecules consisting one to 10 glucose units would cause high osmotic effects, and the starch granules burst and would not be stable. Dense packing can be achieved in crystals, and starch in granules shows a high degree of crystallinity (Zobel 1988, Buléon *et al* 1998). Nature created two types: linear amylose chains and highly branched amylopectin polymers. The physical and biological reason is simple: linear chains can be better cleaved by enzymes (α -amylases) than branched ones (β -amylase, cleaving the branching points first), energy is thus quickly available and reliable during germination. A typical molecular assembly in starch granules is shown in figure 24. The amylose and amylopectin ratio varies in

different plants and grains, from 15% to 25% of amylose and 75% to 85% of amylopectin. An amylose molecule contains 1000–10 000 glucose residues. In amylopectin the molecule branches after each 20–30 glucose residues; a typical amylopectin molecule contains 10 000–100 000 glucose residues. Although the molecular weight of the amylose and amylopectin and their ratio differ in the species the organization of the starch grains is similar. Even today new kinds of starch are being considered for food applications (N’dia Kouamé *et al* 2011). Figure 24 shows the hierarchy in starch particles (here, for example, corn maize). The grains (a) show a typical arrangement of crystalline (b) and amorphous regions (c). The crystalline regions contain blocklets (d) in which most of the starch can be found as nanocrystals. The branched amylopectin and linear (helixed) amylose arrange themselves into tightly packed crystalline and partially into more loosely packed amorphous regions. Lipids in the form of free fatty acids, and eventually TAGs, are placed in the blocklets as well. Amylopectin and amylose consist of glucose monomers.

The structural hierarchy in starch grains determines the physical behavior as well as the resulting processing of starch in cooking and food technology. The difference in structure between amylose and amylopectin makes starch a fundamental system for food physics. The highly branched amylopectin behaves completely differently to the linear amylose molecule when molten and in an aqueous environment.

6.2. Melting and water binding of starch

Cold starch granulates do not take up water and form a highly thixotropic suspension. Heat is needed to melt the crystals and enable the helix–coil transition of the amylose molecules. Only in the presence of heat and water do starch grains melt and dissolve.

Starch grains show high degrees of crystallinity at low temperatures, as visualized in polarized light between crossed polarization filters. At 65 °C the crystals begin to melt and crystallinity decreases, while at the same time the starch grain begins to swell. Water is taken up. The melting and swelling

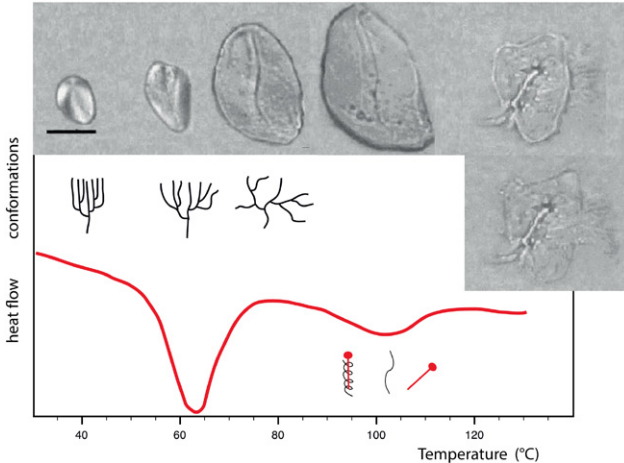


Figure 25. Typical differential scanning calorimetry experiment on starch. The corresponding structural changes during melting of a highly branched amylopectin molecule are indicated. Microscopic pictures of wet potato starch grains heated in oil (taken at 30 °C, 65 °C, 75 °C, 80 °C, 120 °C and 180 °C from left to right) are taken from Aguilera *et al* (2001) with permission. The scale bar corresponds to 20 μm . The heating rate for the microscopic pictures was 40 $^{\circ}\text{C min}^{-1}$ and is too high for a precise state–temperature correlation for equilibrium.

progress with further increase in temperature. At temperatures around 120 °C starch–lipid complexes (Biliaderis and Galloway 1989, Godet *et al* 1995) separate, and the remaining amylose is able to melt. The thermal behavior is summarized in figure 25. The melting of individual starch components under different moisture contents is shown in figure 26. Lipid–amylose complexes consist of fatty acids, which provoke helix formation of amylose. The helix winds itself around the tail of the fatty acid.

The swelling of the grains has reached its maximum extent at about 80 °C. Nevertheless, at very high temperatures ‘ghosts’ (Carrillo-Navas *et al* 2014, Zhang *et al* 2014) of the grain remain visible, which have an impact on the physical, thermal and rheological properties of starch pastes. However, the nature of such ghost particles is still debated and their appearance is mostly attributed to non-polysaccharidic components, such as lipids and proteins (Debet and Gidley 2007, Zhang *et al* 2014). van de Velde *et al* (2002) used confocal scanning laser microscopy (CSLM) to visualize the remaining ghosts, which are supposed to contribute to the thickening and gelatinization process.

Aguilera *et al* (2001) showed that dry starch does not show any swelling behavior; the starch grains remain of the same size. Slight changes in the crystal structure are due to the natural moisture content of the starch granules. Therefore, the melting temperature and melting process depend strongly on the moisture content and the availability of water during heating; this is true the lipid amylose complexes as well (Jovanovich *et al* 1992). Shogren (1992) discussed the melting of starch as a function of the moisture content and analyzed the melting of the different starch constituents in detail. Starch melts selective and in steps, depending on the different types of molecules, their conformation and complexion. Starch melting and the corresponding gelatinization have also been studied in detail by small-angle x-ray diffraction (Cameron and Donald

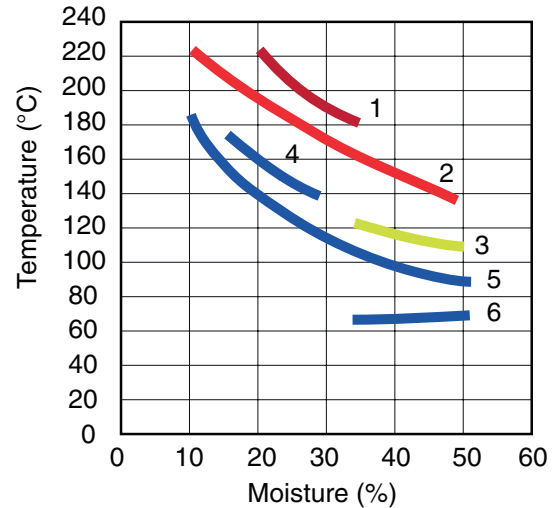


Figure 26. The melting temperatures of the different components of corn maize starch as a function of the moisture content. 1, degradation of the granules; 2, amylose; 3, amylose–lipid complexes; curves 4, 5, 6 correspond to amylopectin melting in different crystal forms.

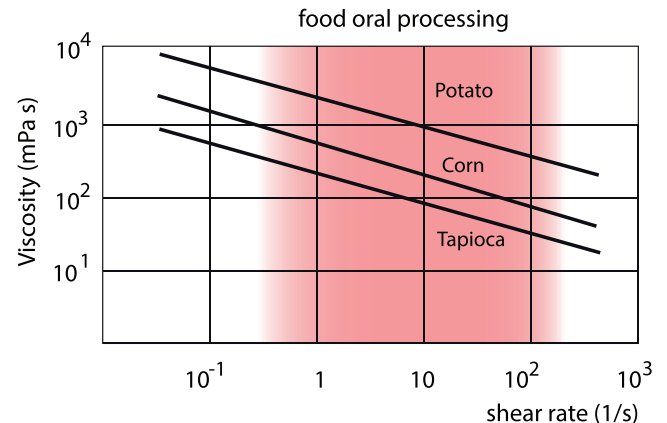


Figure 27. Shear thinning of potato (2.3%), corn (4.9%) and tapioca starch (2.9%) solutions. The relevant shear rates for oral processing are indicated by the shaded range (data from Evans and Haisman (1980)).

1992, Jenkins and Donald 1998). In particular, Vermeylen *et al* (2006) concluded that the melting of amylopectin is accompanied by the formation of the amylose network, which forms at larger-scale fractal structures. The latter is known from gel-forming systems in general in the vicinity of the gel point, see for example Aharony and Stauffer (2003).

6.3. The use of starch in culinary applications

The large amount of swelling and especially the strong water binding by the amylopectin molecules have been found applications in cooking. Starches (mainly potato or corn starches) are still used for binding sauces and soups. Indeed, different starches from different species show different shear thinning properties (see figure 27), which are even relevant for the oral processing. A small amount of starch is sufficient to increase the viscosity of the liquids significantly, which gives a better mouth-feel. The key issue is the high amount of amylopectin

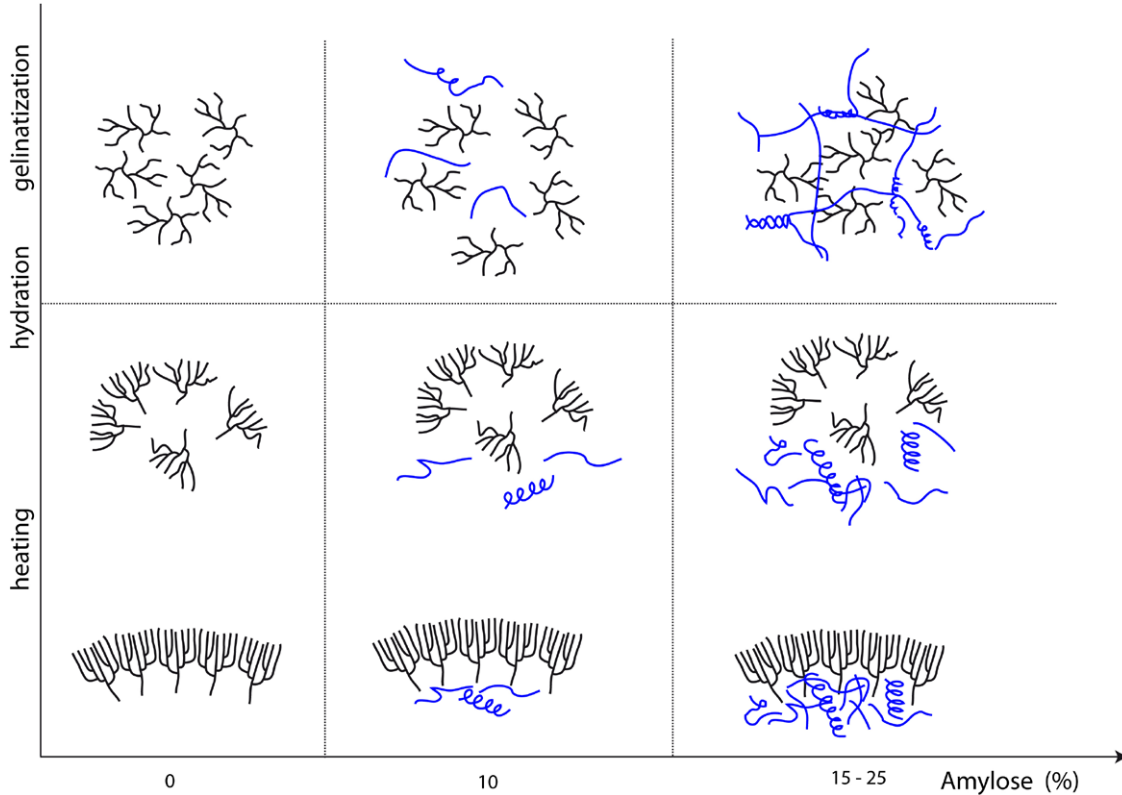


Figure 28. Starches with different amylose content behave differently. Amylopectin shows strong thickening (left). Starches with sufficient amylose content (right) form solid gels by network formation of linear amylose chains during cooling (schematic representation only, not to scale). Remaining ‘ghosts’ are not drawn.

and its branched structure. In terms of polymer physics, amylopectin is a hyperbranched molecule and has almost an ideal tree structure when it is molten. There are no closed loops between the different branches of the molecule and the high molecular weight allows for simple scaling considerations (de Gennes 1979) and can be described as a polymeric fractal. Hyperbranched trees correspond to a spectral dimension of $d_s = 4/3$ (Alexander and Orbach 1982, Cates 1985, Vilgis 1987, Daoud and Leibler 1988, Feder 1988). The size of an amylopectin molecule in the molten state is then determined by its excluded volume in solution and can be found by simple scaling arguments (Daoud and Joanny 1981) as $R^{d_f} \simeq bM$, where $d_f = 2$ in three dimensions. The size of the amylopectin in a crystal can be estimated as $R \simeq b(g - 1) \log M$, where g is its generation number, which is of the order of 10–20. The swelling ratio by volume expansion from the crystalline state to the molten fully hydrated state is thus of the order of

$$Q = V_{\text{swollen}}/V_{\text{crystal}} \simeq \frac{M^{3/2}}{((g - 1) \log M)^3} \propto M^{3/2}/\log^3 M. \quad (17)$$

Although this theoretical factor overestimates the swelling ratio for a single amylopectin molecule, it shows the potential for water binding and viscosity enhancement. Viscosity enhancement is often described by Einstein’s equation (see for example Brady (1983) for a nice revisit of Einstein’s classical work (Einstein 1906)):

$$\eta = \eta_0 \left(1 + \frac{5}{2} \phi + \dots \right) \quad (18)$$

where η_0 is the viscosity of the fluid and ϕ the volume fraction of the particles, which can be considered as the first term of a series for ϕ . During heating the volume expands by melting and swelling, so ϕ increases. A special point is the overlap concentration, when the swollen amylopectin molecules start to get close to each other. At that overlap concentration the amylopectin interacts strongly. However, in contrast to linear chain molecules the amylopectin molecules cannot interpenetrate each other, because their spectral dimension (connectivity) with $d_s = 4/3$ is larger than the critical spectral dimension $d_c = 6/5$ for interpenetration (Vilgis 1987). The molecules repel each other with a roughly logarithmic repulsive potential (Witten and Pincus 1986), when it is assumed that the outer shell of the amylopectin can be approximated as a large, many-armed star-like polymer molecule. At maximum swelling the viscosity is very high; the dynamics of the amylopectin due to strong steric hindrance is exponentially slow and the mouth-feel is pasty.

Nevertheless, starch solutions are shear-thinning (Rao 2014), which is very important for the mouth-feel and the behavior of the solution in the mouth during oral processing and swallowing (Chen and Engelen 2012), compare also figure 27. Therby, the conformation and shape of the molecules are responsible for the mouth-feel and thus partly for whether the food is liked or disliked.

Since all starches also contain linear amylose, the mixture and the phase behavior of linear and branched molecules need to be considered. From a purely physical point of view such mixtures are exceptional systems. Amylopectin and amylose consist

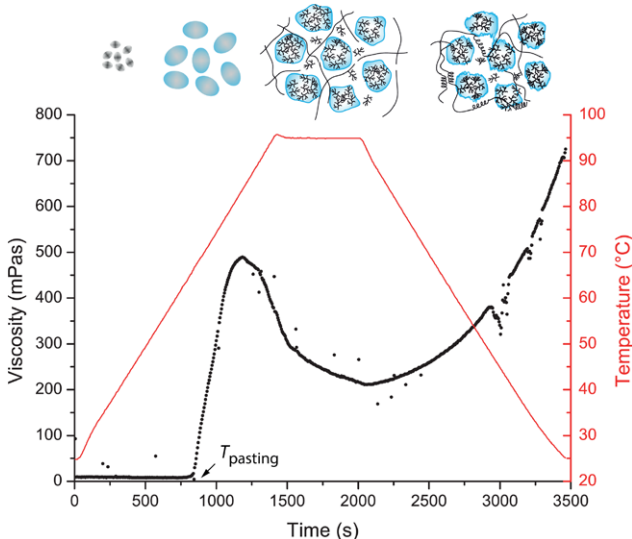


Figure 29. Viscosity of tapioca starch as a function of time and temperature, from Natalie Russ, PhD Work, Max-Planck-Institute for Polymer Research, in preparation.

of the same monomer (glucose), thus their local interaction is practically identical. Only the structure, molecular weight and spectral dimension matter (Vilgis 1992), where the effective fractal dimensions in the presence of other polymeric objects have been calculated by taking into account their size, condensation and mutual screening of excluded volume interactions.

Starches with high amylopectin content do not form strong gels, as seen in figure 28. As mentioned before, the branched molecules do not penetrate each other. Amylose-rich starches show an effective increase in solutions; such starches are the best choice for pure thickening (without crosslinking). Amylose-rich species can be used to form food gels based on starch. The amylose content has a significant influence on the rheological properties of starch, as has been shown explicitly for rice starch by Lii *et al* (1996).

6.4. Rheology of starch solutions: gelatinization

The swelling and thickening of starch suspensions can be studied by rheometric experiments while simultaneously changing the temperature, which shows the corresponding processes on macroscopic scales. The suspension is heated in a rheometer (Vain geometry) by a temperature ramp as indicated by the red curve in figure 29. At the pasting temperature T_{pasting} the viscosity reaches a maximum; when the temperature is kept constant, the viscosity drops again. After cooling, the viscosity decreases, before it rises again and reaches its final value at the viscosity of the starch paste. The change in viscosity occurs along with the structural changes as indicated at the top of the figure. At low temperatures the starch grains are found in their native state. At the pasting temperature they swell and take up water. Similarly the amylose gets released and the amylopectin begin to melt. Some of the branched molecules dissolve, some remain and swell more. In grains that grow larger, the viscosity increases until most of the amylose molecules leave. The grains swell further, become softer and

the deformation (constant shear) separates the network and the particles. The viscosity decreases. The grains form weakly elastic ‘ghost’ particles. Upon cooling, the amylopectin partially recrystallizes and the amylose partially forms helices again. They aggregate and form harder cross-links. The starch hardens and forms a paste with high viscosity.

This also shows a ‘mistake’ in the application of starch in the kitchen: too much starch and the sauce is spoiled. The sauce forms a gel upon cooling on the plate during eating. The dynamics of the amylose chain is fast enough for a further gelation and forms larger growing gel-like clusters. The viscosity of the sauce becomes too high, since the large amylopectin particles still bind a large amount of water, and the pleasure is gone.

Structural changes in starches can also be followed by mechanical spectroscopy. Amplitude sweeps also provide structural information. Low shear amplitudes have no effects on the large-scale structure of the starch paste. At a critical shear rate the structure breaks down and the ‘ghost particles’ are reorganized. Since they are highly swollen they interact with each other and enhance the modulus again. Only at larger strains does the amylose network rupture and the elastic modulus decrease considerably, see figure 30.

6.5. Culinary application: linseed starch glass

Starch that has been previously cooked, cooled down and subsequently dried does not recrystallize to its completely native state. It forms rubbery or glassy states according to the remaining water activity (Capron *et al* 2007). The amorphous states will be more prominently present after drying. Therefore, a very pronounced glassy state with a brittle texture will remain. Such glassy states are very important for technological applications (Steiger *et al* 2014), but are also well known in daily life: when, for example, bread becomes stale parts of the starch will retrograde (recrystallize) as water evaporates, but most of the amylopectin remains in the amorphous state and forms glassy states.

Such physical aspects can be easily transformed in culinary applications, which even enter restaurants of high gastronomy (Nilsson 2014). Linseed is embedded in a glassy matrix, which provides a deconstructed ‘gluten-free bread’ with nice crunchy, crispy texture. Take about 200 g of linseed and mix it with 40 g potato starch and 5 g salt. Bring 700 ml water to the boil and pour it over the starch–linseed mixture. Let it rest for about 20 min, to rehydrate the starch and linseed. The large amount of water and the high temperature will melt the amylopectin; amylose will be released during that time and form a paste. When the paste is spread out in a thin film (defined by the thickness of the linseed) and dried in the oven at 150 °C for about 10–15 min, the water content reduces below 12–15%. During the relatively quick drying the starch film between the linseed undergoes a transition from a rubbery to a glassy state. The remaining water acts as a plasticizer, guaranteeing the crispiness and the cohesion of the starch glass. The taste and texture of these crisps remind one of crispy bread.

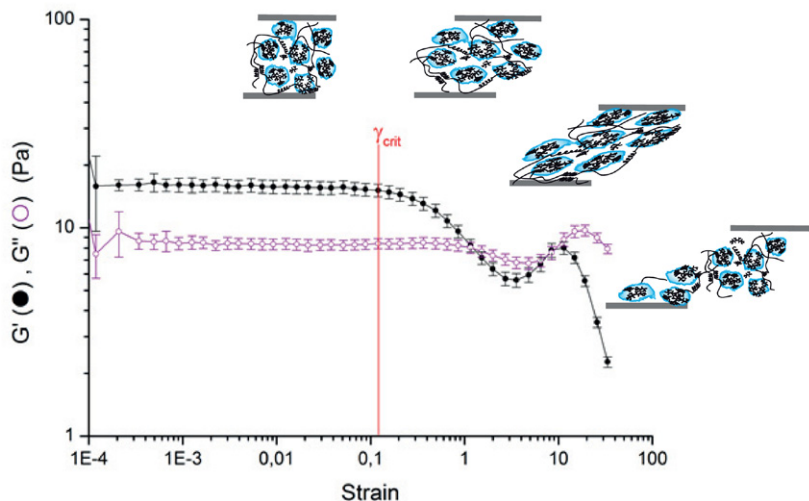


Figure 30. Amplitude sweeps of gelatinized tapioca starch, from Natalie Russ, PhD Work, Max-Planck-Institute for Polymer Research, in preparation.

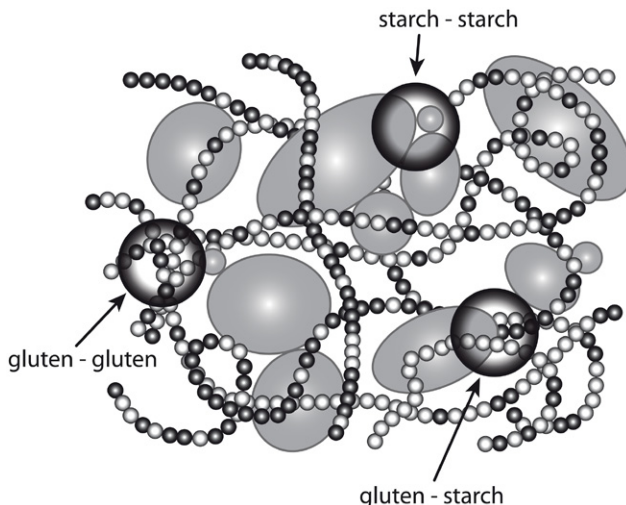


Figure 31. A simple model of the interactions in dough. The different interactions are indicated. Air bubbles are omitted—their size is much larger.

7. Gluten and starch: dough and pasta

7.1. Flour and its dough

The natural presence of gluten and starch in wheat and other cereal flours combines with structurally related physics in the well-known system, dough (Delcour and Hoseney 2010). Gluten in dough consists mainly of long linear amphiphilic polymers of different lengths, which form permanent cross-links. Hard, solid starch grains contain densely packed linear amylose chains and hyperbranched amylopectin polymers. The protein component changes its ‘native’ structure during kneading and water contact, whereas the crystalline structure of starch melts only at higher temperature. The formation of dough can thus be physically attributed to protein network elasticity, whereas the micrometer sized solid starch grains act as ‘filler particles’, as shown in figure 31 (Menjivar 1990, Kim *et al* 2008). The different contributions of solid starch particles and the highly elastic and permanently cross-linked gluten

network suggests similar physical approaches to nanoparticle-reinforced elastomers (Tatham and Shewry 2008, Vilgis *et al* 2009). The structural changes of the starch molecules, their swelling and water binding only become relevant during heating processes. Despite the similarities in network formation and network structure when compared to reinforced elastomers, a number of important differences need to be considered. The most obvious difference is the ratio between the elastic matrix and the filler particle distribution. The filler particles in reinforced elastomers are distributed in a cluster-like manner. In wheat dough the starch particles are packed more densely and do not form a significant structure such as the carbon black or silica particles in elastomers. In addition, the relative concentration of network-forming polymers with respect to the filler particles is far below that in reinforced rubbers. The (wheat) starch particles show almost a bimodal size distribution and their concentration is far above the percolation threshold.

Another difference to rubbers is the formation and development of the dough structure and its physical properties. The flour is first hydrated with water, and kneading forms the elastic matrix by changing the structure of the gluten. This process can be viewed by electron microscopy. During the formation of gluten the cross-links and complexes are as shown in figure 23. The starch particles are not hydrated; consequently their form and size remain unchanged. They get only rearranged by the mechanical work during kneading. Figure 33 shows how the elastic matrix is formed in the space between the starch grains. The proteins, previously arranged in storage grains, become extended and place themselves as gluten between the starch particles. The gluten matrix is not homogeneously distributed between the starch grains, as has been quantified in greater detail by confocal light microscopy (Jekle and Becker 2011).

A minimal model for the physics of dough and its mechanical behavior is governed by four different types of interactions, which define the modulus of the dough. The situation in doughs is thus more complicated than in simple reinforced networks. The gluten–gluten interaction contains permanent

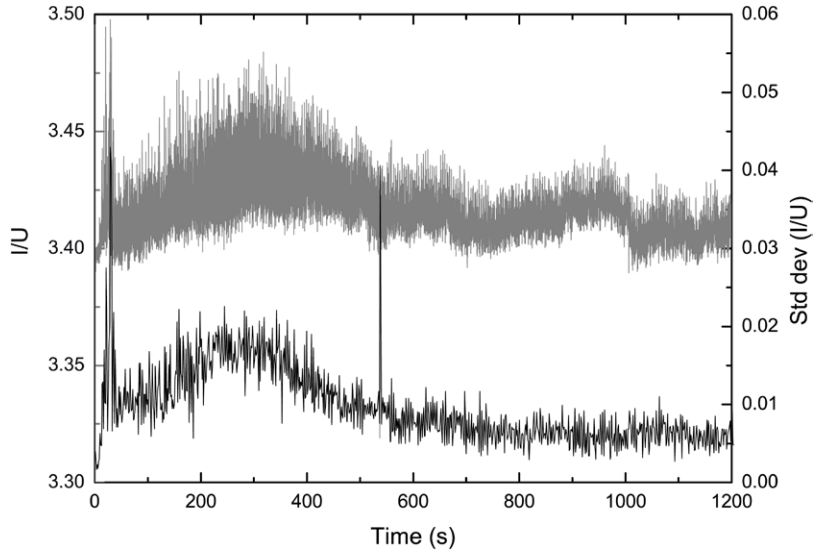


Figure 32. Typical mixing curve for a wheat dough containing 40% water. The increase of power reaches a maximum. At this kneading time the elasticity has its optimum value. The lower curve corresponds to the standard deviation (right vertical axis), see also Schiedt *et al* (2013).

sulfur cross-links, but also electrostatic and hydrophobic interactions (see figure 23). The starch–starch interactions can be assigned to the contact between the particles and their space-filling, and is additional to the detailed interactions between the surfaces of the grains, which depend on the exact composition, and eventual starch modification during milling and flour processing. The gluten–starch interaction is due to the contact of the proteins and the surface of the starch grains and depends on the amino acids that are in the vicinity of the starch grains. Because the amino acids are hydrophilic, neutral and hydrophobic, the starch–protein interaction cannot be described by a simple (universal) adsorption problem, even if the polar solvent water and hydrogen bonding are completely neglected:

$$G(t) = G_G(t) + G_S(t) + G_{SG}(t) + G_A(t). \quad (19)$$

The different terms in equation (19) come from the starch–starch (S), gluten–starch (SG) and gluten–gluten (G) interactions. The contribution $G_A(t)$ corresponds to air inclusions during kneading, which would make the dough softer (Huber and Vilgis 2002), since the compression modulus of air bubbles is much lower than the modulus of the gluten–starch matrix (Bloksma 1990). The arrangement of the different components in the dough can be investigated with new visualization techniques (Kokawa *et al* 2012, 2013).

The mixing time has a great influence on the dough’s properties (Gomez *et al* 2011). When water is added the dough becomes more elastic with increasing kneading time. However, after some further time the elasticity decreases again with further kneading. The viscoelastic properties can be measured during well defined kneading in so-called mixographs (Gras *et al* 2000). In a simpler method that provides similar qualitative results, small laboratory mixers are used for measurement. A typical mixing curve is shown in figure 32. It is apparent that the properties and the local interactions of the dough change during kneading. Sulfur bridges, electrostatic and hydrophobic

complexes are formed during gluten formation. At the same time the spatial distribution of the starch particles is rearranged. The gluten formation and the changes during kneading time can be followed by scanning electron microscopy, as shown in figure 33. At longer mixing times the gluten again becomes disrupted and the elasticity decreases. The decrease in elasticity can be explained by a partial disruption of the gluten network. According to the lower binding energies the hydrophobic complexes are dissolved first, yielding a lower modulus but a larger extension. In addition, the electrostatic complexes are disrupted and cause further rearrangement of the water molecules. The overall dough strength gets weaker. Formed β -sheets may be disrupted; the loops and the trains (see figure 23) become larger. Finally some of the sulfur bridges might be broken as well. The precise processes during dough mixing are not clearly understood and many different suggestions have been made. Hanft and Koehler (2006) studied the development of dough with the aid of different enzymes and their effect on free sulfur and cross-linking, Joye *et al* (2009) addressed similar issues in the context of the gluten structure. Aussennac *et al* (2001) studied the solubility of gluten proteins during mixing with SDS-PAGE by extraction of different mixing stages, where it was shown that the concentration of extractable (soluble) protein decreases exponentially during mixing before the peak time, corresponding to the formation of the gluten network. Kuktaite *et al* (2005) found that the amount of unextractable protein remains unchanged until the peak in mixing time and suggested the rupture of the disulphide bonds during overmixing, i.e. mixing to times beyond the peak. Danno and Hoseney (1982), however, found no significant decrease of the disulphide cross-links during overmixing, which supports the idea that mainly electrostatic complexes and hydrophobic clusters become dissolved and rearranged. Skerritt *et al* (1999) studied in detail the possibility of depolymerization of the glutenin network during mixing by determining the size and molecular weight, which decreases after the mixing peak. Weegels *et al*

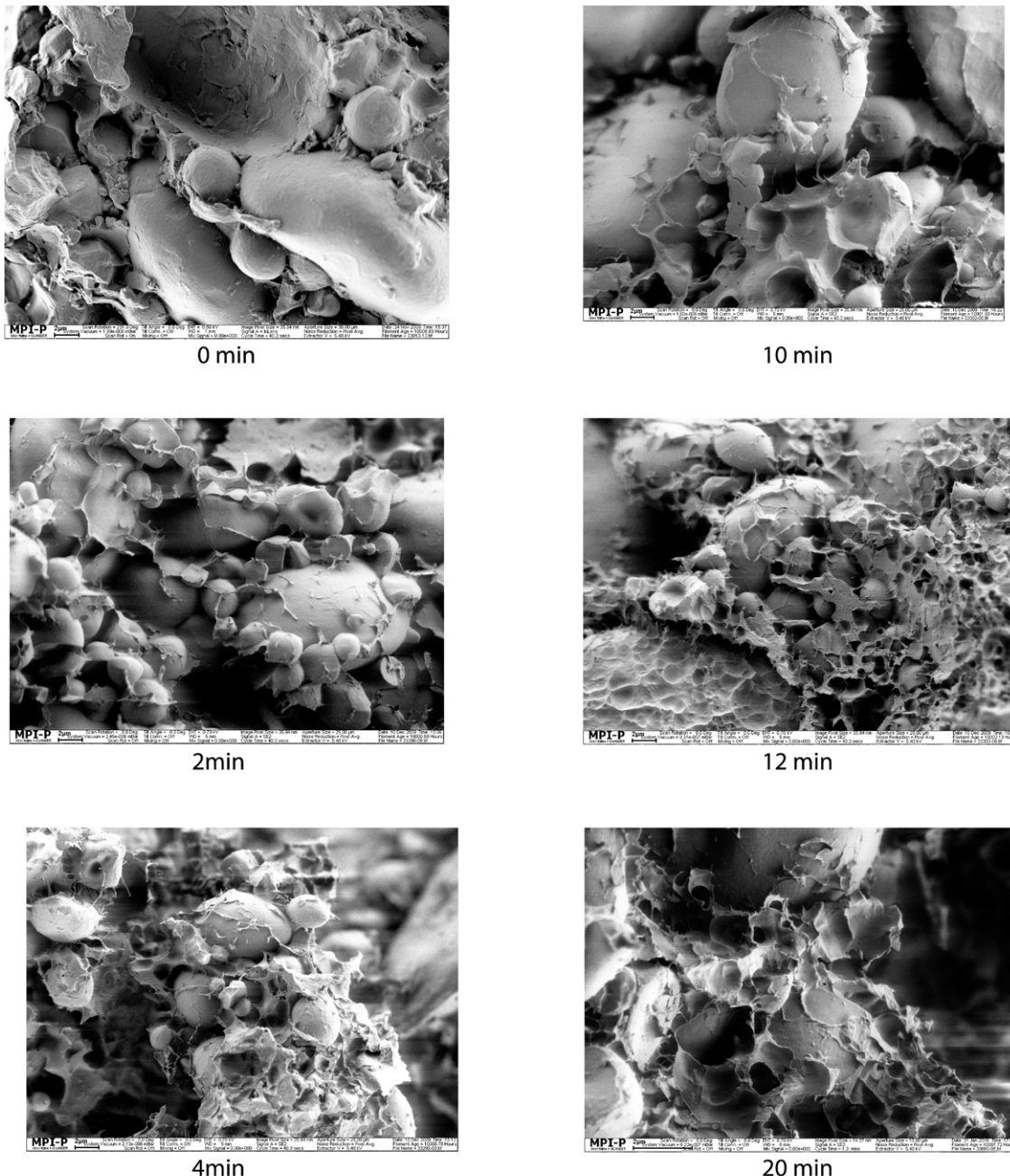


Figure 33. The evolution of the dough with kneading time for a given amount of water. The magnification is the same in all pictures; the scale bar corresponds to $2 \mu\text{m}$. (B Zielbauer, T Vilgis, MPI for Polymer Research.)

(1997) studied the functional behavior of the different gluten components during mixing and dough resting at longer times. The present state of the art of dough formation is summarized in figure 34. The intensive research on this special issue has a practical reason: highly elastic doughs with pronounced strength are essential for rising and baking, see for example Wieser (2007).

Another problem needs to be mentioned: wheat and other flours of cereals are natural products, and thus their composition and quality (e.g. measured in terms of the distributions of their high- and low-molecular-weight glutenin) fluctuate significantly. Therefore food technological approaches develop systematic methods to compensate such natural variations

to improve the quality of gluten. The use of cross-linking enzymes (e.g. transglutaminase) and the addition of the sulfuric amino acid cysteine are only two examples, see e.g. Zhou *et al* (2014). These methods have high impact on the molecular processes during dough formation, but are beyond the scope of this work.

7.2. Rheology of model doughs

Model doughs are excellent systems in which to learn more about the different fundamental interactions between gluten and starch. Defined starches and gluten can be mixed in defined proportions and studied as a function of the amount

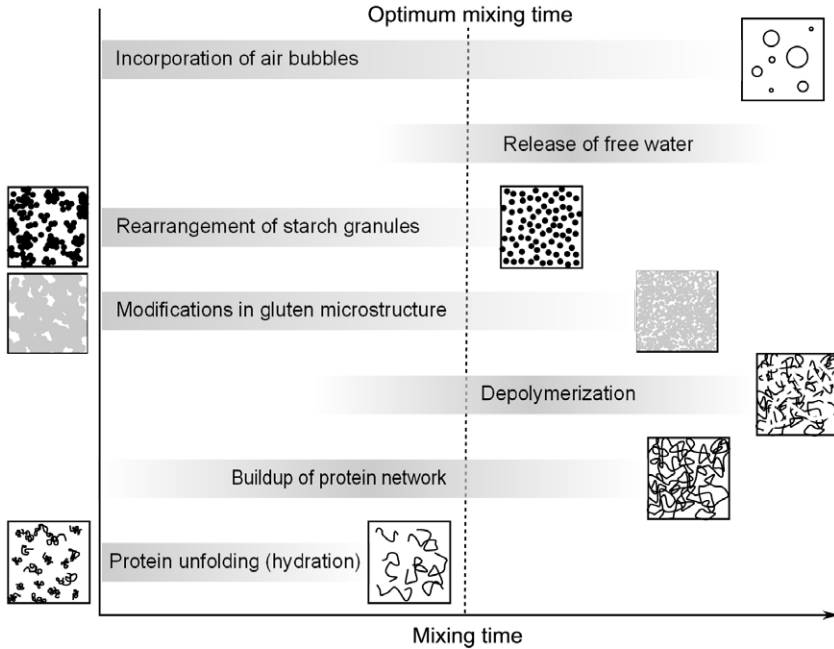


Figure 34. The current state of the art of dough formation (from Schiedt *et al* (2013) with permission). The optimal mixing time (peak) is indicated (dashed line).

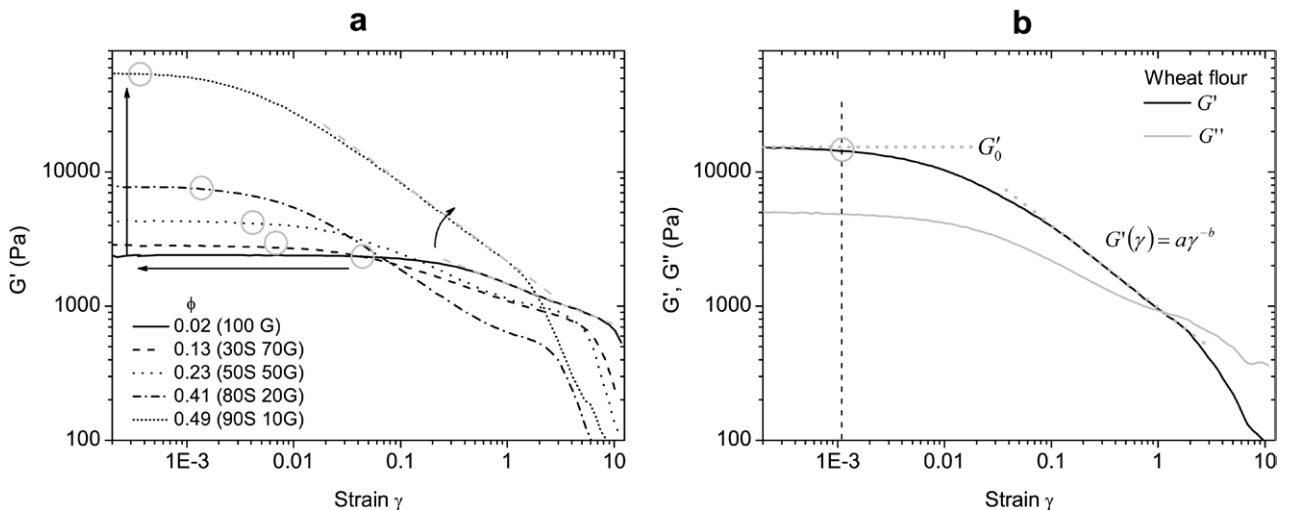


Figure 35. The amplitude sweeps for the different model doughs (a) in comparison with dough from flour (b). The composition of the starch (S) and gluten (G) content, as well as the calculated volume fraction ϕ , are indicated. The circles indicate the onset of the nonlinear regime, which has been defined as $G^o = 0.95G_0$. (From Schiedt *et al* (2013) with permission.)

of added water. Shear, amplitude and frequency sweeps show how the different interactions will influence the modulus (Schiedt *et al* 2013). Model doughs of systematic starch–gluten and water ratio have been produced and measured with amplitude sweeps. Typical curves are shown in figure 35. The moduli show different but characteristic behavior. The lowest curve in figure 35 shows the behavior of pure gluten. The linear regime is most pronounced. At large amplitudes the elastic modulus drops, and the network changes structure according to the opening of electrostatic complexes, hydrophobic lumps and eventual ruptures of sulfur bonds. With increasing starch content, the linear regime shortens significantly due to the rearrangement of starch particles. The significant increase of the linear modulus G' with increasing starch content at higher

starch concentrations ($\geq 50\%$) can be assigned to the direct interactions between the starch particles which form a ‘connected particle network’. This phenomenon is well known from nanoparticle-reinforced elastic materials (Vilgis *et al* 2009) and defines the so-called Payne effect. The nonlinear part and the stronger decrease of the storage modulus at higher starch content can be attributed to the rearrangement and the breakdown of the particle network, as well as the change in the gluten–starch interactions. In filled elastomer networks the form of the modulus amplitude can be described by a Kraus-type law:

$$G'(\gamma) = G'_\infty + (G'_0 - G'_\infty) \frac{1}{1 + (\gamma/\gamma_c)^a} \quad (20)$$

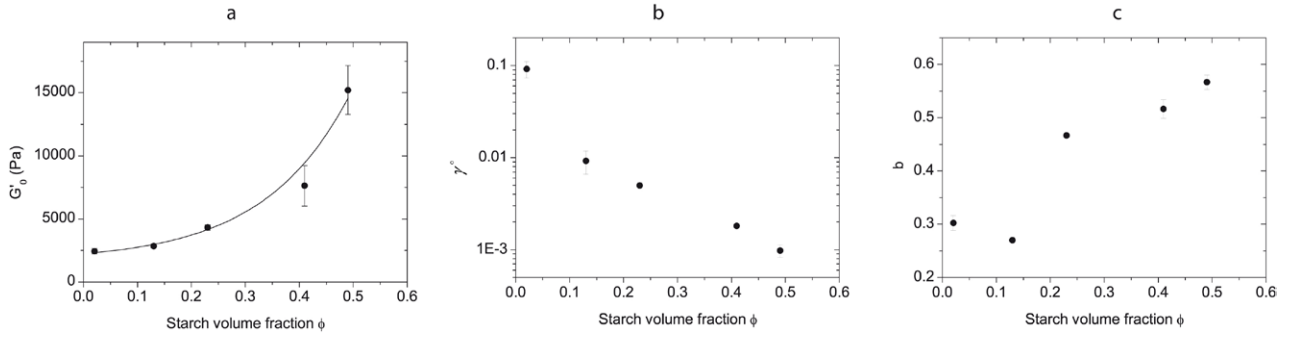


Figure 36. Results for the model dough. The initial modulus (a), width of the linear regime (b) and the exponent b (c) for the characteristic decay of the modulus in the nonlinear viscoelastic regime.

where the exponent a can be assigned to the (fractal) properties of the particle-cluster network, G'_0 and G'_{∞} are the storage moduli for zero and infinite amplitudes, and γ_c is a reference shear rate that can be determined and assigned to the structure of the filler clusters (Huber *et al* 1996, Vilgis *et al* 2009). The particle structure in starch–gluten networks does not show a fractal nature, and a clear value for G'_{∞} cannot be measured. Thus a better representation,

$$G' \propto \gamma^b, \quad (21)$$

has been chosen to analyze the experimental data. The onset of the nonlinear regime (indicated by the circles in figure 35) and b can be used to describe the strength of the starch–starch and the starch–gluten interactions. The comparison of the model doughs with dough from wheat flour shows the similarities of the general behavior. A complete agreement of the moduli cannot be expected.

The results are shown in figure 36. The initial modulus increases with the starch volume fraction. The width of the linear viscoelastic regime drops with a power law ($\gamma^\circ \propto \phi^{-r}$) as the starch volume fraction increases.

Most interesting is the observation of a two-stage process in the parameter b during the development of the model dough as a function of the mixing time, which has been observed for all compositions (Schiedt *et al* 2013). This is similar to network formation in classical rubbers.

For entropic rubber networks with a well-defined and fixed number of cross-links, the modulus can be described as $G \propto k_B T n = k_B T / \xi^3$ where $k_B T$ is the thermal energy, n the number of cross-links and ξ the mesh size of the network. The functionality of the cross-links together with the number of chains fixes the mesh size to a precise value. However, this is not the case in gluten networks, as shown in figure 37 and the discussion below. Different types of cross-links such as disulphide bonds, hydrogen bonds, hydrophobic associations, entanglements as well as their opening and re-formation do not yield a simple relationship between the number of cross-links and the corresponding mesh size. Thus, these can be treated as independent (and time-dependent) structural parameters. Several mechanisms can lead to the observed decrease in G_0 . Assuming a cross-linked polymer network as a very simplified model for the gluten matrix, the developing network suggests an increase in G_0 with increasing mixing time, due to an increasing number n of cross-links. However, if n and the mesh

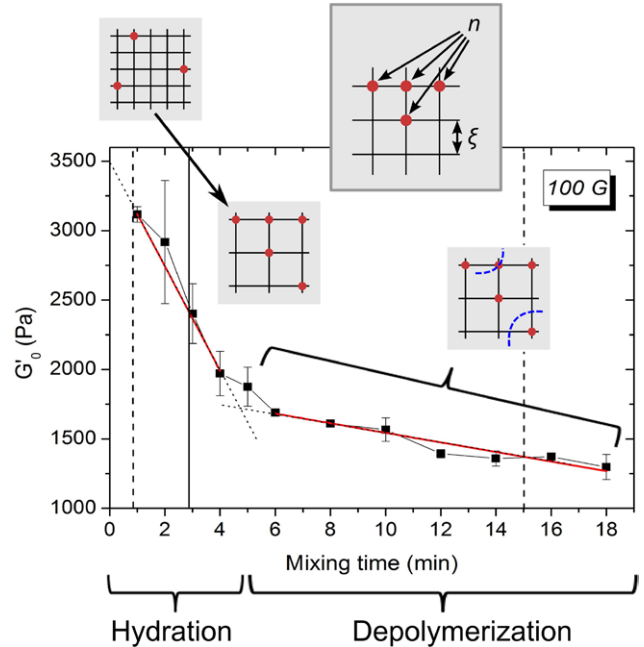


Figure 37. Two-stage processes during the development of dough.

size are independent parameters, the storage modulus of such a network is not only proportional to the number of cross-links, but also inversely proportional to the mesh size of the network and can therefore be written as $G_0 \propto n/\xi$. Thus, a strong increase in mesh size leads to a decrease in G_0 , even if n is increased. This is the case when gluten proteins unfold, as occurs during the first step of mixing, due to increasing hydration. This is in accordance with the loop and train model (Belton 1999), where at low hydration mainly hydrogen bonds and hydrophobic associations between adjacent molecules are formed, leading to a new distribution in trains and loops (see figure 23).

7.3. Culinary application: loosely cross-linked bread

A tasty application of the physics of dough is a bread made from unknaded, underdeveloped and strongly hydrated wheat dough. For this type of very tasty homemade bread, mix without kneading 220 g flour 1 teaspoon salt, 1/4 teaspoon dry yeast with 120 ml warm water (37 °C) and 50 ml beer (Pils/lager). Let it rest for 18–20 h for slow proofing then put it in a covered cast iron pot in a preheated oven at 250 °C

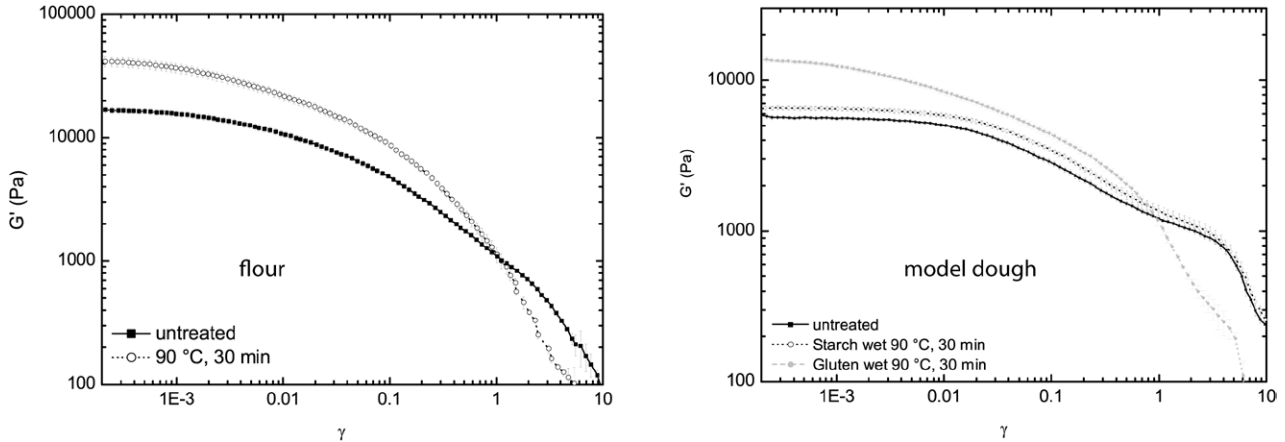


Figure 38. Amplitude sweeps of different flour and model doughs. Left: elastic modulus G'_0 of untreated and heat-treated ($90\text{ }^\circ\text{C}$, 30 min) flour with a moisture content of 16–17%. Right: model dough prepared from untreated (MC(starch) 12.6%, MC(gluten) 7.4%) and heat-treated ($90\text{ }^\circ\text{C}$, 30 min) starch (MC 15.5%) and gluten (MC 10%).

for 20–25 min and finish it with the lid removed at $220\text{ }^\circ\text{C}$ for an additional 15 min.

The very slow proofing of the dough by the small amount of yeast leads to a slow formation of bubbles by the production of carbon dioxide, which deforms the weak gluten network at very small deformation rates. The glutenin chains are prevented from forming a tight network, and it is thus very loose. The pleasure of eating such bread has its origin in physics, especially when the bread is tasted fresh and still slightly warm. The bread crumb is able to developed larger pores so the bread will be soft and show an almost melting texture. The glutenin network is only weakly linked and the structure resembles the aligned structure of seitan. Its elasticity will be higher, since only a light cross-linking of the gluten has been formed and the water content is slightly higher than in classical breads. The disadvantage is that it goes stale quickly. The higher water activity in the bread enables the starch to recrystallize more quickly due to higher molecular mobility.

7.4. Heat treatment of starch and gluten—physical modifications

As seen in section 6.2 starch changes its structure when heated. The starch may melt, depending on the water content. When starch is (partially) molten it takes up water faster and binds water at lower temperatures. Such purely physical ‘starch modifications’ by heat treatment allow a systematic control of dough formation and the resulting rheological behavior of dough. Additionally, the heat treatment can be carried out under controlled humidity (Mann *et al* 2013). The use of model doughs has the advantage that both components, starch and gluten, can be modified separately. The results will also provide insight into the different interactions. Heat treatment of starch modifies the surface and eventually, depending on the water content, the size of the grains; heating the gluten changes the conformation of the proteins. The formation of dough is modified by purely physical effects.

Typical results are shown in figure 38: the heat treatment of flour dough shows significant effects on the elastic modulus

G'_0 , which becomes higher than in the untreated case. On the other hand, there is a strong decrease at higher shear rates: the exponent b becomes steeper under heat treatment. The experiments on model doughs show that the main effect is due to the elastic properties of the gluten network. A separate heat treatment of starch shows only small effects on the elastic properties, whereas the separate heat treatment of gluten shows similar properties to those seen in the dough made from wheat flower. Mann *et al* (2013) proposed a physical model, suggesting that some of the glutenin chains are cross-linked during heat treatment and act as ‘soft filler’ in the space between the starch grains. The self-cross-linking is supported by the natural moisture content of the gluten and the temperature of $90\text{ }^\circ\text{C}$, which is higher than the glass transition temperature of the gluten. The chain mobility is thus higher, enabling the self-cross-linking. The slight modification during the heat treatment of the starch granules does not have significant effects.

7.5. Pasta: glassy, rubbery and *al dente* states

The most well-known starch–gluten system is pasta. In pasta most of the effects described become important. For industrially fabricated pasta, flour and water are mixed, the dough is formed until it is processable and the pasta is made into its desired shape. Then the pasta is dried in controlled temperature and moisture steps, which means that it undergoes a rubber-to-glass transition as shown in figure 39. Depending on the drying temperatures (up to $85\text{ }^\circ\text{C}$ according to the process (Bruce Litchfield and Okos 1992, Waananen and Okos 1996, Güler *et al* 2002)), starch melts and hydrates accordingly. The drying process affects the surface of the pasta, and apart from the physical processes on molecular scales, the porosity and thus the cooking quality of pasta depend strongly on the control of the drying, which required modeling (Cunningham *et al* 2007) and refined testing (Cuq *et al* 2003, Ogawa 2014).

Dried pasta has a typical moisture content of 5–10% and needs to be rehydrated during cooking. In addition, the remaining crystalline starch needs to be molten according to the actual moisture content during cooking. This brings an interesting

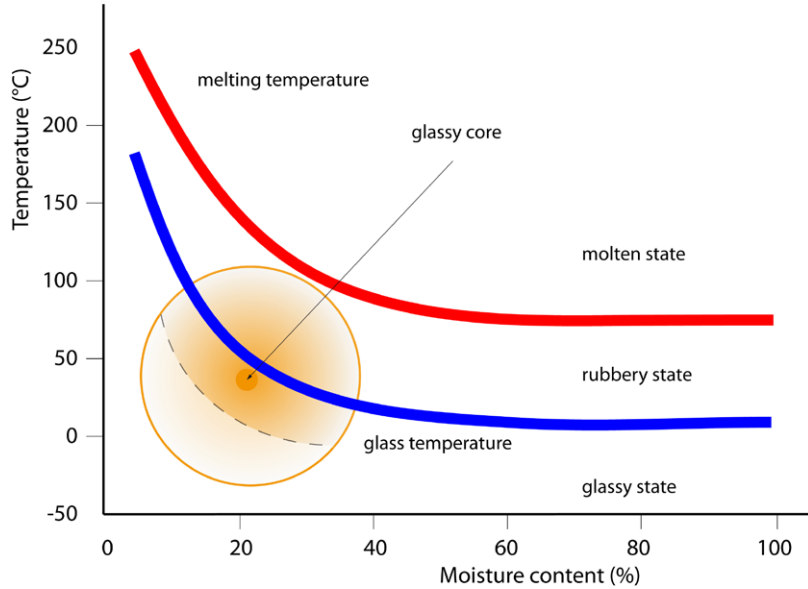


Figure 39. Schematic description of the physical definition of *al dente*. Dried pasta is in a glassy state. Cooking rehydrates the pasta by diffusion. In the ideal case the pasta contains a glassy core. For simplicity, no distinction is made between the different melting and glass transitions of starch and gluten: only one symbolic glass and melting line for both is drawn.

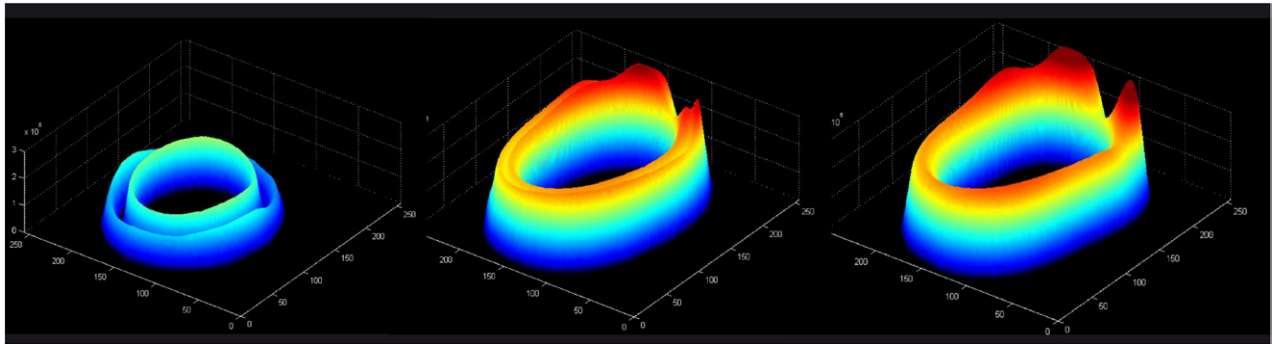


Figure 40. Qualitative visualization of the water uptake in Italian penne. The hollow pasta takes up water from both sides. The water content (vertical axes) changes during cooking time (horizontal axis). The picture in the center shows a small glassy region in the middle of the noodle. (P Zänker, MPI for Polymer Research.)

aspect to the culinary term ‘*al dente*’, the Italian way of cooking pasta, where a ‘harder’ center of the pasta remains (see shaded circle in figure 39). The additional texture obviously provides greater pleasure than very soft pasta. Cuq *et al* (2003) suggested to quantify the strength S of the pasta (spaghetti) by

$$S = S_{\text{rubber}} + \frac{S_{\text{glass}} - S_{\text{rubber}}}{1 + (t/t_0)^p} \quad (22)$$

for the rehydration of the pasta, which interpolates between the glassy state at $t = 0$ and the completely soft and rubbery state at large times. The strength (force) S can be measured (in N) by texture analysis. Since equation (22) is purely phenomenological the exponent p remains a fitting parameter. Nevertheless at finite time t the rehydration is not complete. Because the rehydration is associated with the diffusion of water into the center of the pasta, the center remains glassy at a finite cooking time. In *al dente* pasta the center remains glassy, whereas the outer parts are already in the rubbery state. A practical example is shown in figure 40. The diffusion and uptake of water during cooking inside an Italian penne

(hollow noodle) is followed by NMR imaging. The water can diffuse into the glassy pasta from both sides. After a short cooking time both edges undergo a glass-to-rubber transition (left picture). At the right cooking time, a small glassy cylinder remains in the center (middle picture). Overcooking (right picture) yields a completely moist and soggy pasta.

8. Protein-rich food

In contrast to wheat protein, which has many polymer-like properties, many foods show very individual and typical protein effects, which correspond to their denaturation and imply structural changes. In foods this is connected to consistency and textural changes. Most prominent examples are animal-based foods such as eggs, fish and meat (Belitz *et al* 2009). In the future, protein foods based on extracted plant or insect proteins will gain more importance. A well-known example is tofu, which consists of structured proteins from the soy bean and is well established in Asian culture (Cai and Chang 1999).

Table 1. The main proteins in egg white and their basic properties.

Protein	Average percentage (%)	T_c (°C)	Basic property
Ovalbumin	54	72	denatures under shear, foam stabilizer
Conalbumin	12	62	ovotransferrin, binds iron
Ovomucoid	11	77	glycoprotein, heat stable
Ovomucin	3.5	—	heat stable
Lysozyme	3.4	78	antibacterial
S-Ovalbumin	—	81	forms during storage

8.1. Egg—a ‘simple’ example

Cooking an egg seems to be simple, but it is not. Everybody knows the problems: sometimes too hard, sometimes undercooked, sometimes a perfect yolk but slimy white, part of the egg white still remaining uncooked, the difference between fresh and two-week-old eggs, and other problems of such kinds. In an impressive paper Vega and Mercadé-Prieto (2011) have shown the rich and complicated phase behavior of eggs, especially the egg yolk. Phase, consistency, texture and mouth-feel change in a very narrow temperature range far below that of the ‘classical boiling’ of an egg.

Indeed, many authors discuss cooking an egg in detail from a phenomenological point of view as a well used example of heat conduction and to find the perfect egg (Unsworth and Duarte 1979, Williams 1998, Roura *et al* 2000). Such macroscopic views are only partly helpful. The diffusion of heat, energy and thus temperature follows classical diffusion laws for homogeneous bodies:

$$\left(\frac{\partial}{\partial t} - D \nabla^2 \right) T(x, t) = 0 \quad (23)$$

where D is the thermal diffusivity, $D = k/(\rho c_p)$, k is the thermal conductivity, ρ the density and c_p the specific heat capacity of the body. The exact solutions of equation (23) can be formulated but depend on the specific geometry of the body. The equation can be solved by Fourier methods for different geometries. Several geometrical approximations, such as spheres or ellipsoids for eggs, are helpful and provide some agreement with experiments, when using known values for c_p , ρ and k . From the dimensionless variable of equation (23), $x = tk/(TR^2\rho c_p)$, it can be concluded that the typical cooking time for an egg of typical diameter R is determined by

$$t \propto (\rho c_p/k) TR^2 \quad (24)$$

i.e. that the time increases with the square of the diameter of the egg.

Phenomenological considerations help only marginally in understanding eggs on a molecular basis. The changes in texture and consistency need to be addressed for the proteins. Even the complex fluid egg white consists of many different proteins, which respond differently to temperature changes (Mine *et al* 1990). Cooking eggs at different temperatures thus provides very different textures that can be visualized by simple photography (Vilgis 2010, Myhrvold and Smith 2011, Baldwin 2012) and show the fundamental problem. Eggs

consist of egg white and egg yolk, and the two behave differently under physical processes and have different values for ρ , k and c_p . Egg whites and yolks undergo structural transitions via protein denaturation, which eventually change the values of the physical constants. During protein denaturation thermal energy is absorbed. Crystalline fat in the yolk finally melts. All these effects together might contribute and add to the general macroscopic picture. A more detailed view is necessary to understand the cooking on molecular levels.

Egg white contains about 88% water and several different proteins, which are listed in table 1. The proteins are globular proteins, and their size can be described well with the basic model depicted in section 5.2. Their surface is strongly hydrophilic and binds water strongly. Thus egg white shows well-known viscoelastic properties. The main protein, ovalbumin, contains 365 amino residues. It is the only protein in egg white that contains cysteine, and is thus, like wheat proteins, able to form temperature-stable cross-links under thermal activation (see e.g. Mine (1995)). Like gluten, ovalbumin forms stable edible gels, which are permanently cross-linked. Ovotransferrin consists of 686 amino acids and binds iron. It has bacteria-inhibiting properties. Ovomucoid, a glycoprotein, contains sugar residues in addition to amino acids. The structure of ovomucoid remains stable under heating at low pH values. It is also well known for its trypsin inhibitory activity. Ovomucin is also a glycoprotein and highly water-soluble, and is mainly responsible for the viscoelastic and ‘slimy’ properties of raw egg white. It provides surface activity and contributes to the foam stability when egg white is beaten. Ovomucin does not show a thermal denaturation at mprmal food processing temperatures.

S-ovalbumin is a special form of ovalbumin. It is created by the formation of sulfur cross-links if the pH value changes during storage (Donovan and Mapes 1976, Herald and Smith 1992). As a result, the denaturation temperature increases by about 9 °C, which explains the higher cooking temperatures for the albumin of ‘older’ egg whites. The concentration of S-ovalbumin can even be used as an indicator of the freshness of eggs (Huang *et al* 2012). Lysozyme is an enzyme and shows antibacterial properties. For many food applications extracted lysozyme is used for food safety reasons. Only the most important physical properties of the proteins are listed in the table. A complete proteomic analysis of hen egg white can be found, for example, in Guérin-Dubiard *et al* (2006).

A typical differential scanning calorimetry (DSC) analysis (figure 41) shows the denaturation of the principal proteins in egg white (Ferreira *et al* 1997), with distinct denaturation steps. The proteins denature at distinct temperatures, which allows selective ‘cooking’ at protein-specific denaturing temperatures, perfect for advanced cooking applications.

However, time matters as well as temperature. By holding an egg white at a certain temperature for longer times the denaturation process continues. In figure 42 egg white was cooked at 71 °C for one or two hours (temperature precision 0.05 °C). The differences in structure and texture are clearly visible. According to table 1 and the DSC analysis (figure 41), only conalbumin and lysozyme denature at 71°C. However, the temperature is just one degree below

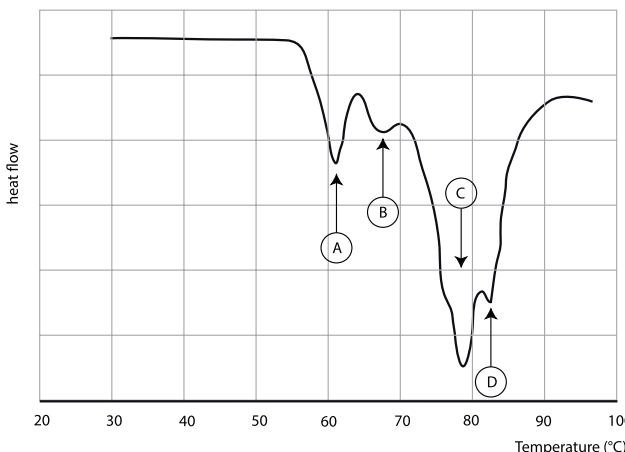


Figure 41. Typical DSC curve from fresh egg white. The peaks correspond as follows: A, conalbumin; B, ovalbumin; C, lysozyme; D, S-ovalbumin.

the denaturing temperature of ovalbumin. With a relatively high Boltzmann factor ovalbumin denatures within a time span $\tau \propto \exp(\Delta U - k_B T_b)/k_B T$, where T_b is the temperature of the water bath and ΔU the energy of denaturing ovalbumin. Because the difference in the exponent is very small, the probability of denaturation becomes close to one. Once ovalbumin is denatured, it will not return to the native state. Thus with accumulating time, more and more ovalbumin will denature and the egg white protein gel becomes tighter and binds more water. Water evaporation is excluded because the egg white has been sealed during cooking. When ovalbumin denatures at temperatures over 72 °C, elastic solid gels are formed by permanent sulfur bridges. However, it has been shown that ovalbumin also forms aggregates of β -sheets (Mine *et al* 1990). At higher temperatures the S-ovalbumin denatures as well; this state of the egg white is known well from ‘hard-boiled eggs’.

When egg white is cooked at 65 °C the selective denaturation of the conalbumin is more likely. Egg white forms an almost transparent, very soft gel and is part of the physical secret of the ‘Onsen egg’ (Yamashita *et al* 1998), well known in Japan, where eggs are cooked in hot springs with temperatures between 63 °C and 66 °C.

8.2. Function and culinary value of egg white proteins: foams and gels

The functionality of most egg white proteins has been discussed by Mine (1995) in more detail. Another most useful and more general discussion of protein functionality in food can be found in Foegeding and Davis (2011), where egg white foams are discussed in a more general context. The latter have direct applications to foods, where foams play a very important role in many food processes and kitchen applications.

Egg white forms stable foams, which can be easily dried at temperatures up to 100 °C. Dried egg white foams are used on their own (known as meringues or baisers) but also used to bring an airy structure to cakes and mousses. To get stable foams some of the proteins need to have surface-active properties, which are due to the different water-soluble natures of

the amino acid residues (Hailing and Walstra 1981, Davis and Foegeding 2007). Imposing mechanical energy by beating egg white denatures ovalbumin. At the same time, air bubbles are trapped in the egg white. The denatured proteins are thus exposed to the air–water interface, where hydrophobic and hydrophilic parts of the protein distribute themselves similarly to multiblock copolymers at selective interfaces (Leclerc and Daoud 1997, Eastwood and Dadmun 2002, Malik *et al* 2013). When egg white foams are dried at moderate temperatures between 60 °C and 80 °C, the foam is stabilized by the cross-linking of ovalbumin and the simultaneous removal of water. Sweet meringues additionally contain a large amount of sugar, which increases the viscosity and partially crystallizes during drying in the water cells, which separates the air bubbles. The strong dipolar interaction of the sugars (e.g. sucrose) via their hydroxyl groups with the polar and charged amino acids of the proteins prevents the formation of perfect crystals. The semicrystalline and partially amorphous state along with the low water activity yield very crunchy meringues, with a very pleasant mouth-feel.

Special culinary effects can be achieved with (spray) dried hen’s egg white (albumin). The egg white powder retains most of the functional properties of the natural hen’s egg white (Lechevalier *et al* 2007). For example, if concentrated broths or juices (fruit or vegetables) are used for rehydration, unusual meringues with very strange tastes can be produced. The alternative use of less sweet sugars or sugar alcohols, such as isomalt, erythritol or xylitol, provides additional crunchiness and specially attractive mouth-feel. Additional spicing, e.g. salt or glutamic acid, enhances the overall taste. If using vinegar and other strongly acid liquids, the shift of the isoelectrical point has effects on the texture, which need to be kept in mind.

The presence of surface-active proteins in egg white also allows the preparation of culinary emulsions (see section 13). When oil is added to lightly beaten egg white and mixed at high speed, (salted, soured and spiced) tasty and creamy emulsions (mayonnaise) are formed, which indeed have a very high stability (classical recipes use egg yolk).

Such a mayonnaise containing a lot of oil can also be gelled by heating it up to temperatures between 71 °C, when most of the proteins are denatured and form gels, and 80 °C, when S-ovalbumin denatures and gels. At these temperatures, the water is still bound in the gels, which, along with the oil (as depicted in figure 43), provides a positive mouth-feel and an exceptional taste (Vilgis 2007, Vilgis and Caviezel 2012).

8.3. Culinary highlights: Onsen eggs

In Japan ‘Onsen eggs’ are a well-known specialty (Aye 2014). Raw eggs are cooked in hot springs, where the water has a temperature between 63 °C and 68 °C. When eggs are placed in the hot water, they cook in a very special way, since some of the proteins become denatured due to the temperature. Even those proteins with higher denaturation temperatures eventually denature kinetically with time (this point will be discussed in a later section in greater detail). The resulting taste and texture are exceptional and can also be obtained in temperature-controlled water baths, when eggs are placed



Figure 42. Hen egg white cooked at 71 °C for one hour (left) and two hours (right), heated and sealed in a water bath. (N Russ, T A Vilgis, Max-Planck-Institute for Polymer Research.)

for different times and temperatures to control structure and texture precisely (Vilgis 2010, Myhrvold and Smith 2011, Baldwin 2012).

Vega and Mercadé-Prieto (2011) carried out a most valuable and thorough study on a library of texture of eggs as a function of temperature and time. In this detailed rheological study, eggs were heated to temperatures of $(60 + x)$ °C, and gave, due to gelling, very creamy egg white and egg yolk. This finding is of great culinary interest and important not only to the mouth-feel but also for egg-containing preparations in confectionery.

The proteins in egg yolk are immunoglobulins (IgG), which denature in different steps concerning the different domains in the protein. Relevant temperatures for textural changes are 60 °C and 71 °C. At higher temperatures their coagulation is completed; the egg yolk becomes hard, dry and mealy. One of the most important results of Vega and Mercadé-Prieto (2011) is shown in figure 44, which shows the increase in the apparent viscosity of egg yolk at different heating temperatures as a function of cooking time. The (horizontal) gelation line is indicated. An important message is that time matters and changes the cooking state of the eggs at a given temperature, which has been also explained earlier by a thermostatic model (Vilgis 2010) and confirmed by precise experiments. As mentioned before, the molecular processes in food materials are far away from thermal equilibrium, as is shown even in simple processes, such as ‘boiling’ eggs.

In cooking an egg, both the egg white and the egg yolk have to be considered. Figure 45 shows the relevant denaturation temperatures of the egg white and yolk of hen’s eggs. Immunoglobulins denature at about 60 °C, conalbumin at about 62 °C and most of the yolk parts around 65 °C. It is most important for any food formulation that thermal denaturation occurs when the corresponding denaturing temperature is reached. Kinetic denaturation is determined by the Boltzmann factor and the difference between the denaturing temperature and the actual cooking temperature. The closer these temperatures are ($T_b \leq T_d$), the more likely the protein is to denature; and the more denatured and structure-forming proteins

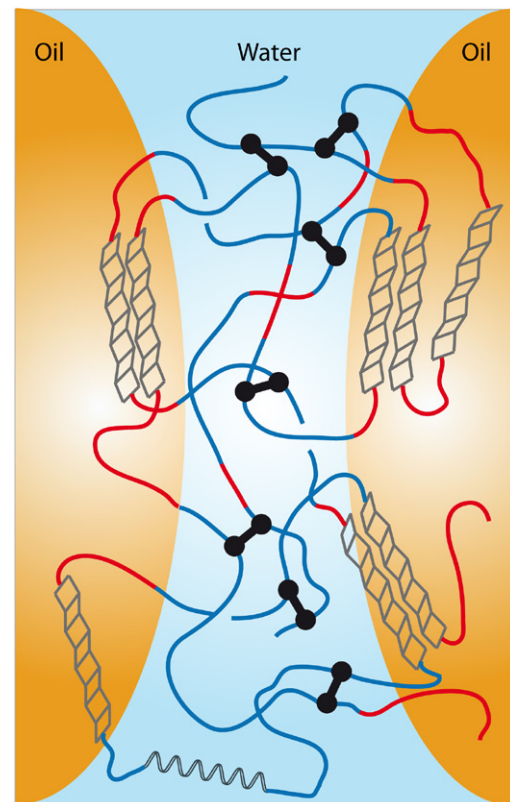


Figure 43. Highly schematic presentation of a solid albumin gel containing oil. Ovalbumin and S-ovalbumin form a network by sulfur crosslinks (black links) and more hydrophobic β -sheet aggregates. The hydrophobic unstructured parts of the proteins are drawn in red/grey.

accumulate with time. “There is no such thing as a 65 °C egg”, as stated clearly by Vega and Mercadé-Prieto (2011).

For many applications that use whole eggs (mixed together) the gelling properties are reported in Raikos *et al* (2007), where the precise pH value, ionic strength (salt) and dipolar interactions (sugars) matter and determine the gel point and gel strength, moduli and mouth-feel. However, similar considerations as given in figure 45 need to be taken into account

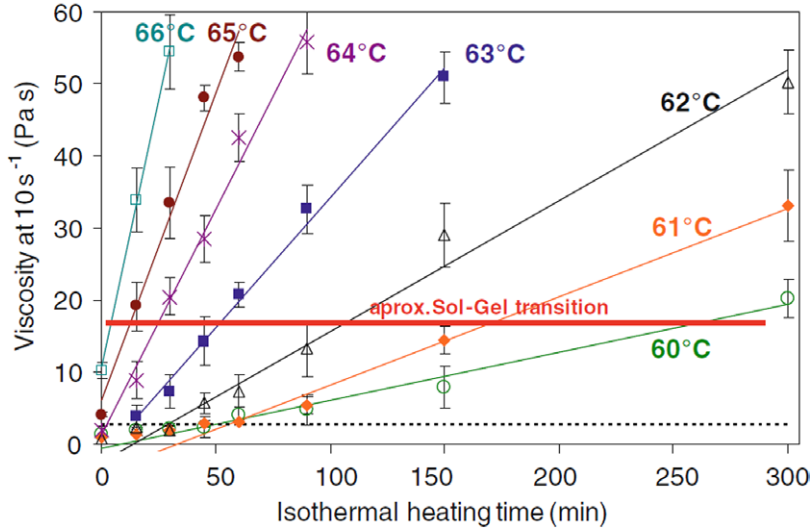


Figure 44. The increase in the apparent viscosity of egg yolk at different heating temperatures as a function of cooking time. The (horizontal) gelation line is indicated. Reprinted from Vega and Mercadé-Prieto (2011) with permission.

for a more precise prediction of gelling and binding with food formulations using whole hen's eggs.

However, it is interesting to note that not only raised temperature yields nice creamy textures, but also freezing. ‘Raw cooked’ egg yolks yield textures very similar to Onsen eggs. Freezing the eggs for about 24 h lets egg yolks ‘gel’ to a very creamy structure by maintaining their spherical shape. The texture resembles that of egg yolks cooked between 64 °C and 67 °C but the taste is completely raw. The Spanish avant-garde chef Aduriz (2012) from the restaurant Mugaritz used this idea to great perfection.

9. Protein-rich food, mainly fibrillar proteins in meat

9.1. Muscle meat as fibrous biomaterial

The considerations made for eggs apply for more complicated systems as well. Meat is another example, and contains even more proteins of different structure (Forrest *et al* 1975, Hedrick 1994, Hui *et al* 2001, Bechtel 2012). In addition, the temperature range of denaturation is wider and the cooking varieties are greater, where the water-holding capacity also matters. The literature concerning meat is widely developed and cannot be reviewed here in all its detail. Therefore, only the most important issues on the changes on molecular scales can be addressed. As a natural product from a living body, meat exhibits strong fluctuations in its composition, which is hard to control for experiments in a physics laboratory. Each animal is different, each race produces its own sample, and even the type of feeding influences the composition (Warriss 2010, Bechtel 2012).

The simplest example is pure muscle meat, where the proteins are best defined in the samples. The thermal behavior of such muscle proteins can be measured precisely by DSC and other techniques. However, at certain temperatures it is not simple to distinguish the different contribution to the different proteins. As is well known from the biophysics of muscles (Squire 1997), the muscle follows a structural hierarchy,

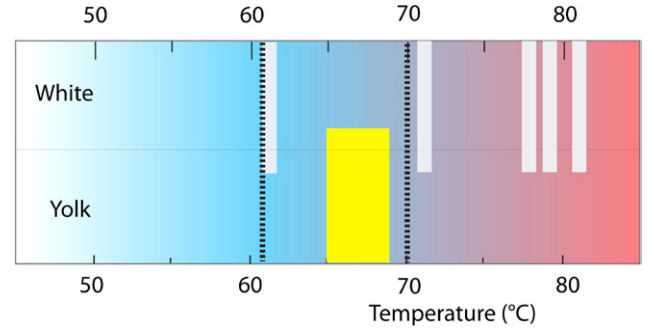


Figure 45. The most interesting temperature range for cooking eggs from a culinary point of view, indicated by dashed lines, involves the thermal denaturation of conalbumin and proteins from egg yolk.

which is schematically shown in figure 46. The basic muscle cell is represented by myofibrils, which are surrounded by a membrane composed of phospholipids and several membrane proteins. The ‘disks’ that separate the different bands (Luther 2009) also consist of proteins, especially the so-called z-disk, and they have been described in detail by Sheikh *et al* (2007) and Luther (2009). Figure 47 shows the biophysical binding of the proteins in the z-disks and the biological formation of ‘cross-links’ in the highly anisotropic ‘gel’ muscle meat. In addition, figure 47 shows some of the molecular principles that need to be taken into account during cooking and processing of meat. Titin and dystrophin connect z-disk proteins with the cell membrane (top in figure 47).

The complex structure and the large number of proteins inside a muscles show the complexity of meat as food. Nevertheless, most relevant in the context of food physics is the thermal behavior of the myosin–actin complex, the collagen and eventually the sacroplasmatic proteins. Figure 48 shows internal hierarchies in the proteins. The myosin–actin motor enables muscle contractions by shifting its head (Ebashi and Endo 1968, Rayment *et al* 1993) in the presence of multivalent ions (calcium and ATP). The F-actin fibrils consist of a chain of globular actin (red circles) and this itself is dressed with other functional proteins, such as different

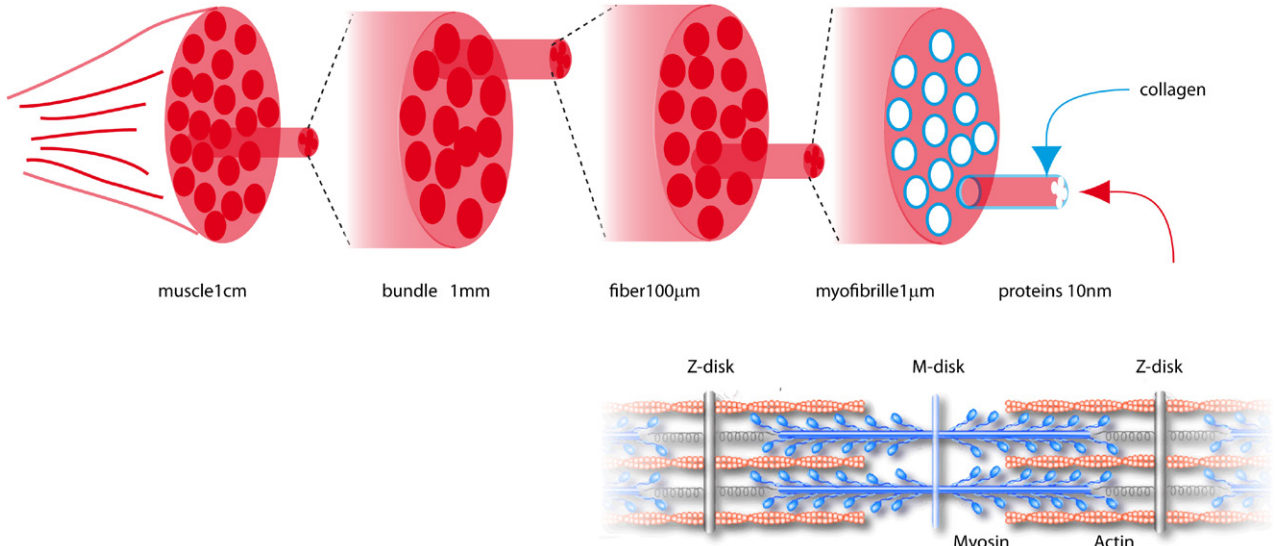


Figure 46. The architecture of muscles. Macroscopic muscles are divided into muscle fibers, and these in turn into myofibrils, which contain the most relevant muscle proteins actin and myosin, responsible for muscle contraction. The fibrils are surrounded by a thin layer of collagen.

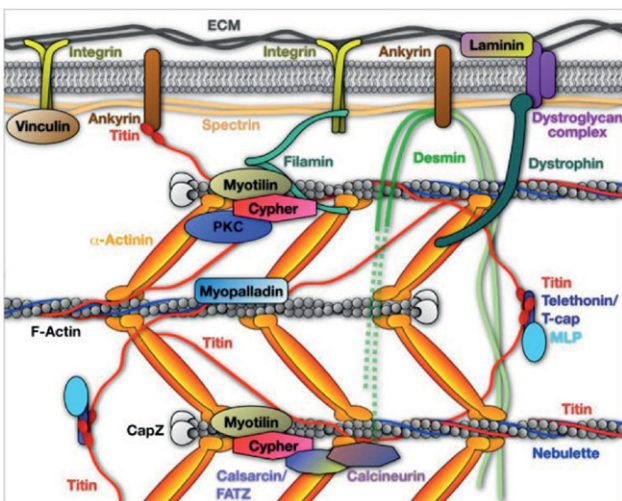


Figure 47. The model of the binding in the z-disc. Highly elastic proteins such as titin fix muscle proteins, the F-actin in crosslinks. (Reprinted from Sheikh *et al* (2007).)

troponins. Myosin consists of a head part and double α -helical parts. Detailed investigations of the structure of such giant muscle proteins have been recently reported (Meyer and Wright 2013). Active muscles, however, are not meat. They define the basic structures but not quite the properties of meat, and it is indeed important how muscles are transformed into meat (Pearson 2012, Smulders *et al* 2014). After slaughtering, many different parameters, such as temperature changes, the pH value, post-mortem enzymatic activity etc, determine the quality of meat (Kim *et al* 2014) and thus the physical and chemical properties of cooking and processing, which determine in the end the mechanical, textural and structural properties of the meat, in other words the mouth-feel and pleasure. The biochemistry of the post-mortem processes has been discussed, for example, by Huff-Lonergan *et al* (2010) and modeled by Vetharaniam *et al* (2010). It was shown how

temperature, the presence of proteases and oxidation change the structural properties, along with their effects on the main muscular protein composition, myosin and actin, titin, nebulin, troponin-T, desmin and filamin, which are mainly responsible for the mechanical properties.

The conversion of muscle into meat post-mortem needs to avoid the two ‘phase transitions’, as pointed out recently by Hamoen *et al* (2013): first, the transition of the lipid bilayer of the cell membrane—it loses its liquid state, and second, the denaturation/deactivation of calpain enzymes (see figure 47), which controls the release of calcium from the muscle (Goll *et al* 2003). Thus post-mortem temperature and pH value need to be controlled strictly (Hamoen *et al* 2013) to avoid cold or heat shortening, which means the shortening of the overall sarcomere length at temperatures between 0 °C and 15 °C and between 35 °C and 40 °C, where the first proteins start their denaturation processes in the meat state, which provokes hard and chewy textures. When glucose (from glycogen) becomes transformed to lactic acid, the pH value drops, starting from pH values around 7. The breakdown of glycogen produces energy, which contracts the muscles, and also produces lactic acid, which lowers the pH value. Without blood circulation lactic acid stays in the muscle tissue and contributes to the taste. However, when the pH value is too low, the meat loses its water-binding ability and becomes pale and watery. On the other hand, if the pH value remains too high, the meat will be tough and dry.

Low pH values also increase the release of calcium, which causes further muscle contraction. As glycogen supplies are depleted, ATP regeneration stops, and the actin and myosin remain locked in a permanent contraction (rigor mortis). Cooling the carcass of the freshly slaughtered animal too soon after death results in very tough meat. Aging allows enzymes in the muscle cells to break down the overlapping proteins, which makes the meat tender.

At about pH ≈ 6, the rigor mortis sets in, and when the temperature is too low, cold shortening takes place. At temperatures

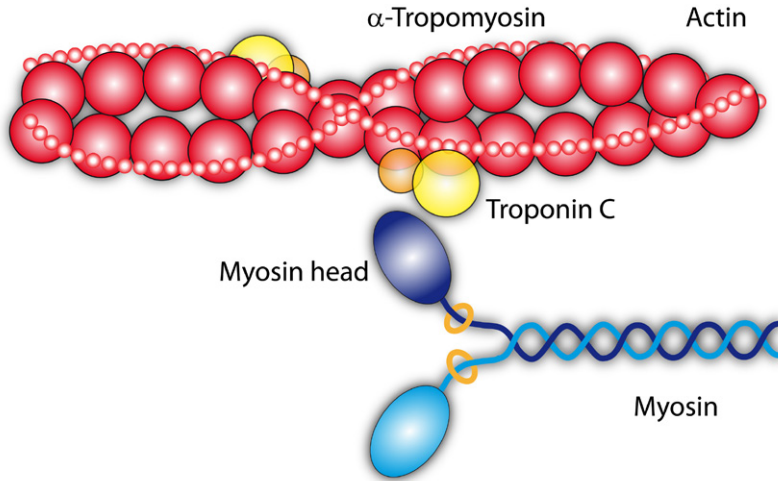


Figure 48. The basic proteins in muscle meat: actin and myosin.

higher than 20 °C cold shortening is very unlikely (Kim *et al* 2014). Meat quality is determined by these initial conditions. These different conditions give rise to a ‘state diagram’ for meat quality (see figure 49 and Hamoen *et al* (2013)), which summarizes the post-mortem changes when muscle changes to meat. When the temperature is too low after slaughtering, and the pH value remains high, the meat contracts, and after cooking it remains hard with unpleasant textures (blue area). The origin of ‘meat failures’ thus has deep physical grounds in the interaction of proteins, driven by bivalent interactions, isoelectric points and ‘wrong’ temperature changes. Wyrwisz *et al* (2012) carried out a thorough analysis of meat tenderness as a function of composition and pH values.

Muscles and muscle meat contain a large number of proteins, which have different functions, structures and denaturation temperatures, and show once more the complexity of natural food systems. Indeed cooking and processing of meat seem to be too remote from a proper system for physical models. Nevertheless, muscle-type meat of fish, pork, beef, poultry or game is cooked and processed at relatively low temperatures between 35 °C and 70 °C, where mainly myosin, collagen, actin and several serum proteins show significant changes that define essential structural changes with implications for texture and mouth-feel. Of course the precise range depends on the species and their living temperatures (lowest for fish, highest for birds). A recent study on pork meat (Vujadinović *et al* 2013) underlines as well the denaturation of specific proteins within the significant range between 50 °C and 71 °C. The denaturation of most of the troponins (see figure 48) takes place between 34 °C and 44 °C and depends strongly on the calcium ion concentration present (Jacobson *et al* 1981). Troponins lose their function but do not have much impact on the textural changes of fish and meat.

The denaturation of myosin has a strong impact on texture-relevant structural changes. Detailed investigations of myosin extracted from fish or chicken show the gelation during heat changes. The denaturation of myosin is revealed in these pictures using (field emission) electron microscopy (Yamamoto 1990, Hayakawa *et al* 2012), where it can be seen that isolated myosin molecules aggregate first with their heads as the temperatures increases, and this is followed by the

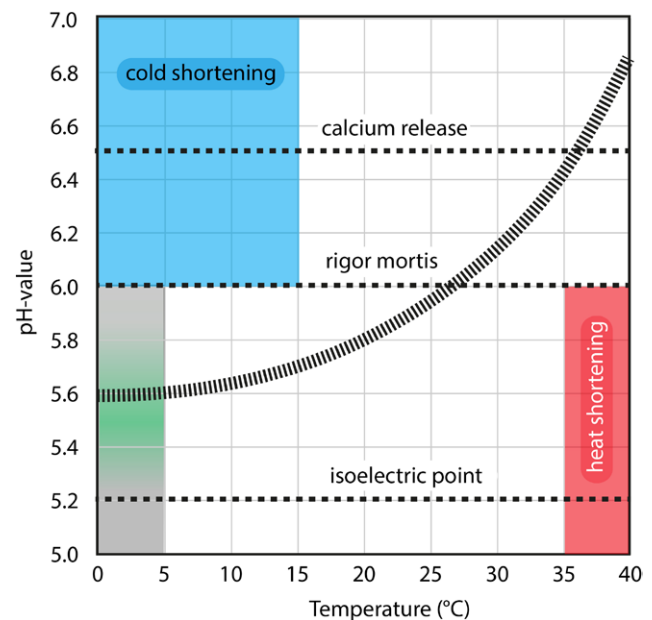


Figure 49. The pH–temperature state diagram with the regions of likely cold shortening (blue) and heat shortening (red). The drop of the pH value (dashed curve) ends up at values around 5.4, i.e. below the rigor line, but above the typical isoelectric point of muscle proteins (myosin). (Redrawn from Hamoen *et al* (2013) with permission.)

formation of intermolecular aggregates into star-like objects; with further increase of the temperature aggregates form on larger scales with partial unfolding of the rod-like helix parts. These particles again form themselves into a particle network with high water binding. A simplified cartoon is shown in figure 50, which has been drawn according to these observations. The precise temperatures where the different steps happen depends strongly on the species and the type of muscle from which the myosin is extracted. Other influences are the salt concentration, the concentration of bivalent ions (Ca^{2+}) or the presence of positively charged amino acids, such as L-histidine (Hayakawa *et al* 2012). Such properties observed in solutions are of significance for weakly gelled fish products like surimi and sashimi (Lanier *et al* 2013) or ground meat products (Tornberg 2005), where the gelation properties

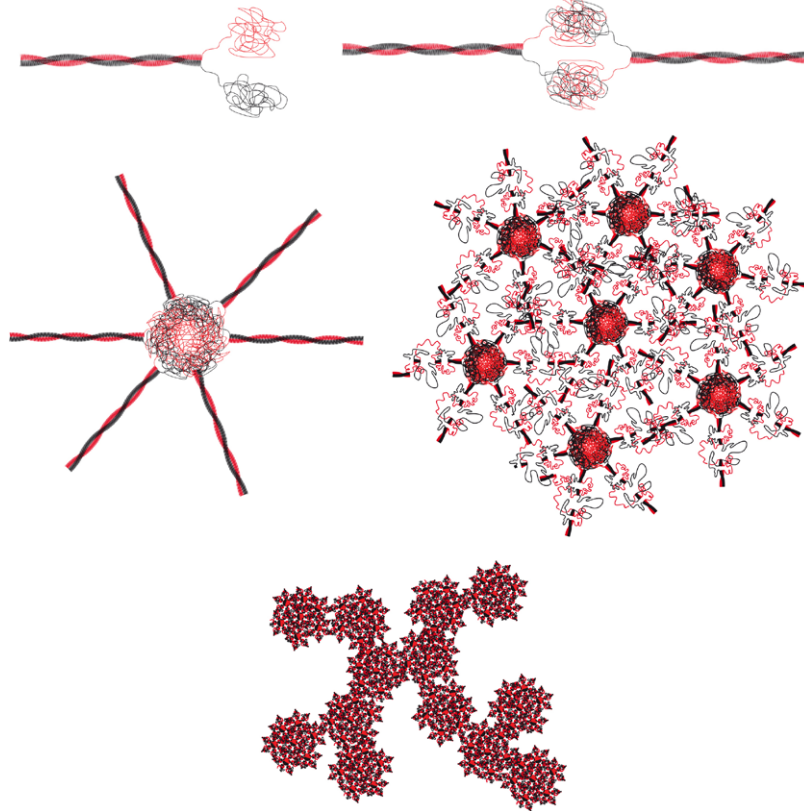


Figure 50. Successive aggregation of isolated myosin under heating.

determine a large part of the mouth-feel and the water binding. On the other hand, the presence of other muscle proteins has a strong influence on the resulting gel structure (Lanier *et al* 2013). In addition the ‘light chains’ of myosin have not been taken into account yet. These are proteins that are associated with the myosin heads and are indicated in blue in figure 48; they denature first, making little contribution to the texture. However, their conformational changes enable the heavy chains to form the rod-like conformation and the heads to denature.

Actin denatures only at higher temperatures. A summary of the different denaturation stages and corresponding temperatures and enthalpies has been provided by Bertazzon *et al* (1990). A more recent study confirms the basic ideas in more detail (Levitsky *et al* 2008), where *in vivo* denaturation can also be investigated by the use of actin in cells. Actin itself consists of globular actin (G-actin), which is arranged in helical filaments (F-actin). The denaturation temperatures and the corresponding specific heats are indicated in figure 51. It can be seen that free G-actin denatures at lower temperatures than F-actin, as indicated by the dotted line. F-actin can be stabilized by different agents. Levitsky *et al* (2008), for example, used toxic phalloidin (and aluminium fluoride AlF₃, not indicated in figure 51), which binds to F-actin and shifts its denaturation temperature to larger values. Although the results shown in figure 51 do not represent the situation in post-mortem muscles, they indicate the basic processes. Nature protects actin by so-called small heat shock proteins (Lomiwes *et al* 2014), which have similar effects. A very instructive review of heat shocks and their effect on the molecular structure of

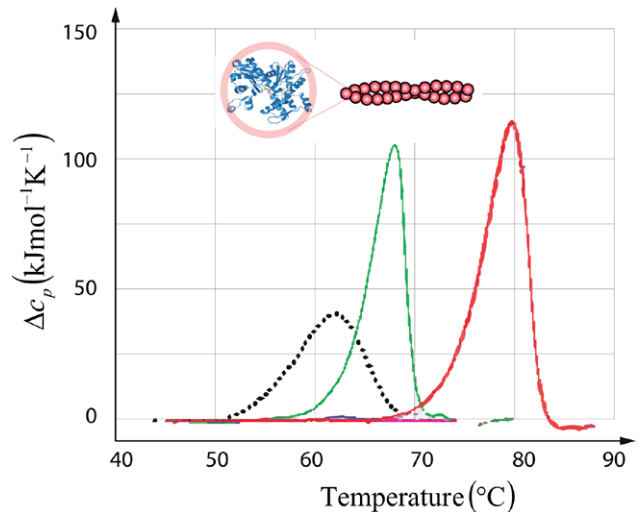


Figure 51. The denaturation of cellular actin. F-actin denatures between 65 °C and 72 °C (green line). Globular actin (dotted line) denatures at lower temperatures between 50 °C and 68 °C. However, the presence of other factors (here phalloidin) stabilizes F-actin significantly (red line). Data from Levitsky *et al* (2008) with permission.

proteins and the resulting macroscopic phenomena, e.g. ‘tenderness’, is provided by (Lomiwes *et al* 2014).

Although the collagen does not belong to the most dominant fraction in muscle meat (see figure 52), it contributes to the thermodynamics and to textural properties (Purslow 2014). Collagen is a fiber of a triple α -helix with high tensile strength and is found in the connective tissue of the muscle

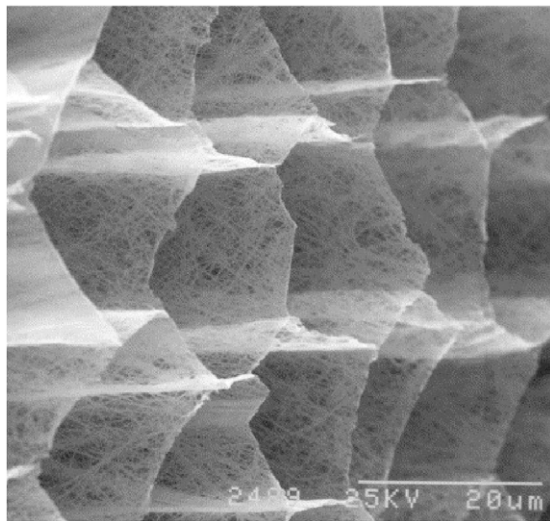


Figure 52. Collagen in muscle meat, when muscles proteins are removed. From Purslow (2005) with permission.

fibers. Collagen also changes by post-mortem aging, which is known from cooking meat and kitchen experience. Dry aged beef is stored at temperatures slightly above 0 °C for at least two weeks (longer is better). During this time the collagen in the connective tissue gets weaker, and the muscle fibers are easy to separate. The meat becomes very tender, when for example fried in a pan without too much heat in the center. Monsón *et al* (2004) have studied the influence of different breeds and time of aging on the mechanical properties (mainly pressure) in detail. For most breeds the contribution of the collagen to aging was leveling off after 20 days.

Collagen denatures at about 58 °C to 65 °C, which can be directly observed and followed by second harmonic generation microscopy (Brüggemann *et al* 2010). The triple helices unwind in three highly water-soluble polymers, and collagen turns into gelatine. The unwinding of collagen to gelatine plays a major role in cooking braised meat, which has a much higher collagen content than muscle meat. In collagen-rich meats and foods the precise situation depends strongly on the nature and type of the collagen. Collagen fibers exists in several types containing more or less lateral cross-linking, when fibers show a high degree of internal cross-linking. Such collagen structures are very tight and need long cooking times, as for example in braising meat. These issues, however, are not discussed further in this review.

Other proteins do not play dominant roles in cooking or in temperature ranges relevant to food processing. The denaturation of titin has been reported at 76–78 °C by Pospiech *et al* (2002), which is higher than the denaturation temperatures of myosin, collagen and actin.

10. Meat and protein denaturation: temperature and time

10.1. General remarks

The cooking of meat has been investigated for a long time and still many points are not yet clear. The influence of breeds,

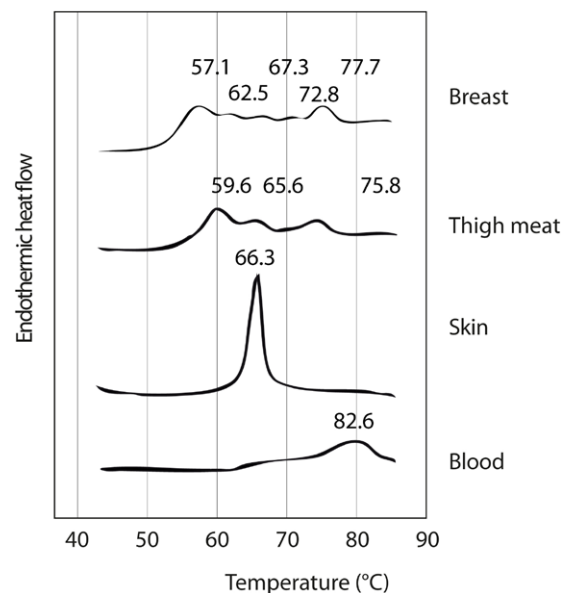


Figure 53. The denaturation of different pieces of chicken meat. Redrawn from Kijowski and Mast (1988) with permission.

races, even diets of the animals makes it hard to get well defined ‘samples’. As already mentioned, the precise denaturation temperatures of structure- and texture-relevant proteins depend on the species. Structural changes of aged beef are discussed in early studies by Martens *et al* (1982) and Leander *et al* (1980), and the consequences for meat and cooking quality can be found in a more recent study by Dikeman *et al* (2013). In the following, more fundamental properties of meat cooking are discussed.

The cooking properties as well as the resulting textures depend on many factors, such as breeds and feeding. Thermal denaturation in chicken meat has been investigated (Kijowski and Mast 1988). This early study shows an almost universal principle in meat cooking: different pieces of animal meat possess very different cooking properties, as is well known from home cooking (see figure 53). Chicken breast (typical muscle meat) shows the richest peak structure when measured by differential scanning microscopy. It shows about five peaks, which correspond to the denaturation of different proteins. The meat of the thighs appears to have a less rich protein variety, but shows a small peak at around 66 °C, which has a similar position of denaturation as the proteins in the skin. This indicates a higher concentration of collagen, which is also very present in the skin. Chicken blood, however, shows a very broad peak, starting at about 62 °C, and ends with the highest denaturation temperature at about 82 °C. It was reported that chicken blood serum contains several proteins known from chicken eggs (Marshall and Deutsch 1951), whose denaturation peaks show up in the DSC of the blood as well (Murphy *et al* 1998).

Various proteins from different parts of the chicken have been extracted and investigated by differential scanning calorimetry (DSC). Figure 54 shows the most important proteins and their denaturation temperatures relevant for practical uses. Myosin is the first to start denaturing at temperatures around 57 °C, which is indicated in the isolated (washed)

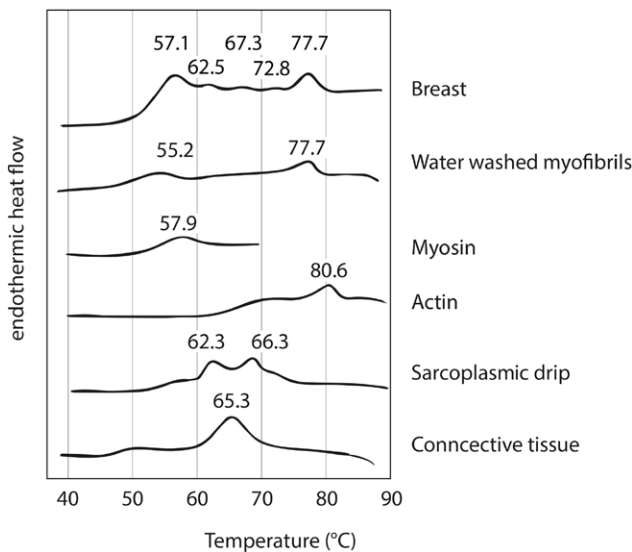


Figure 54. The denaturation of different proteins and parts of the chicken meat and their denaturation temperatures are indicated. The vertical axis does not correspond to values: the lines are drawn so that the peaks can be directly compared. Redrawn from Kijowski and Mast (1988) with permission.

myofibrils, showing a slightly lower denaturation temperature, presumably induced by the manipulation. Myosin is definitely present in the chicken breast as the dominant muscle protein, as well as actin, which denatures at temperatures around 80 °C. Again in the water-washed myofibrils the actin peak appears at a slightly lower temperature (77.7 °C). An important observation has been made in the sarcoplasmic drip ('meat juice'), where two dominant peaks appear at 62.3 °C and 68.3 °C, which can be seen as well in the chicken breast (with a slight shift). These two peaks can be assigned to (globular) membrane proteins, which become dissolved post-mortem in the serum. The connective tissue (collagen) denatures around 65 °C. Thus in the temperature range around 65 °C collagen and sarcolasmatic proteins denature, and they might not always be clearly separated in DSC experiments. These observations appear in the meat of other species as well, with similar shifted temperatures. Empirically it can be said that the denaturation temperature of myosin occurs at around $T \approx T_{\text{living}} + 25$ K, where T_{living} is the average living temperature of the animal. Thus it is lowest for fish and highest for birds. Indeed when myosin denatures in any meat the texture become nicely gelly by maintaining a high water-holding capacity. In other words, the meat is tender and juicy.

Similar observations have been made for beef (see e.g. Martens *et al* (1982)), which are summarized in figure 55. The denaturation temperatures are shifted to lower values compared to chicken, according to the living temperatures of cattle. Nevertheless the proteins denature in the same sequence as those of chicken. Haem proteins are proteins that are also found in the sacroplasmatic drip of muscular meat. They color pigments (the haem group) in the meat and provide the dark red color. They are present in chicken blood as well (see figure 53) but less prominent in chicken breast meat

and the sarcoplasmic drip (see figure 54). So far, only 'ideal meat' (pure muscle meat) has been considered. For a review of the heat treatment of meat including most factors, such as fat, ionic strength, pressure and other details, see for example the publication of Sun and Holley (2011).

11. Sous-vide cooking

Apart from its relevance in gastronomy, *sous-vide* cooking of meat provides a solid basis for studying meat in a clearly defined way. The sample meat is packed and sealed under vacuum in polymer bags, and cooked in water baths with precise temperature control. It is already obvious from the previous sections that the important parameters are temperature and time. When meat is cooked under controlled conditions, the temperature and time dependence of the cooking state and texture can be investigated. Zielbauer *et al* (2015) measured the water loss and protein denaturation and analysed the textural properties for pork meat. In these experiments the meat in each sample was frozen to ensure equal initial conditions for the beginning of the measurements (see figure 56). Thus the curves without cooking (meat at room temperature, here 24 °C), with and without sealing are compared as well. Obviously the higher water loss for sealed meat can be attributed to the vacuum. These results show different aspects of the denaturation of meat proteins. The top-left diagram in figure 56 shows denaturation of meat at a fixed heating time, 10 min, as a function of the temperature. For room temperature (24 °C) all three denaturation peaks, known from other meats, are visible. The first corresponds to myosin; the second is the common denaturation of the connective tissue and the sarcoplasmic serum proteins; the peak corresponding to the highest temperature denotes the denaturation of the actin. The peaks disappear with increasing temperature. Thus at 45 °C the enthalpy (area under the peak) of the myosin peak decreases, due to partial denaturation already at this low temperature, whereas the other proteins are still unaffected. At 51 °C the myosin peak has vanished. At 60 °C most of the sarcoplasmic proteins and the collagen are denatured and at 74 °C no further denaturation is visible. Obviously pork fillet is completely 'cooked' at this temperature. The three other diagrams show the time dependence when meat had been held a certain temperature for different times. The diagram marked 45 °C shows a clear time dependence of the myosin peak, which indicates further progress of the denaturation process. Apparently this can be interpreted as a kinetic effect, possibly mixed with some remaining (or temperature-enhanced) enzymatic activity. Enzymatic activity at such moderate temperatures is still likely and can be indicated by the change of the collagen peak as well. It has been reported that collagenase remains active in bovine muscles for cooking temperatures below 60 °C (Laakkonen *et al* 1970, Christensen *et al* 2011) and may thus contribute to the tenderness of meat. Enzymatic activity in porcine meat has also been investigated by Liu *et al* (2014). At higher temperatures, especially at 60 °C, the enzymatic contribution is less likely; the denaturation changes are purely of kinetic origin.

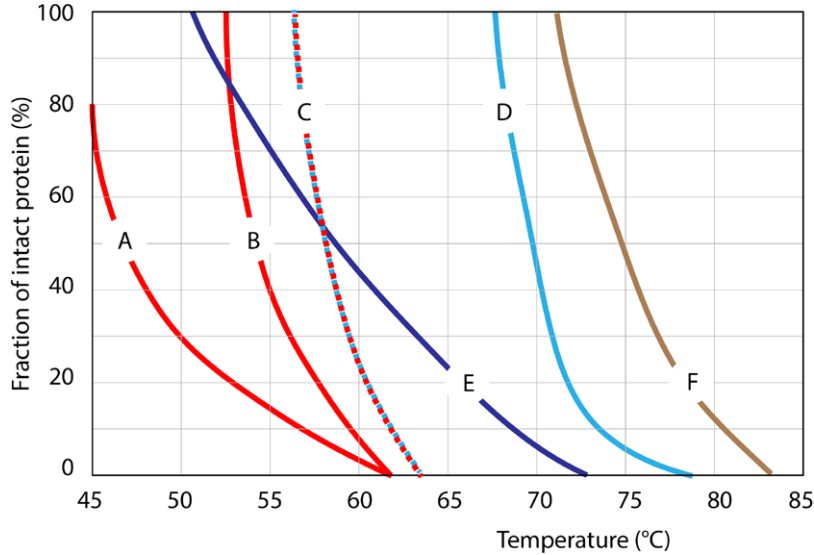


Figure 55. Denaturation of the main proteins contributing to the texture of beef muscle meat. A: myosin light chains, B: myosin heavy chains, C: collagen, D: actin, E: sarcoplasmic proteins, F: haem proteins. The meat samples have been held for 7 min at the corresponding temperatures.

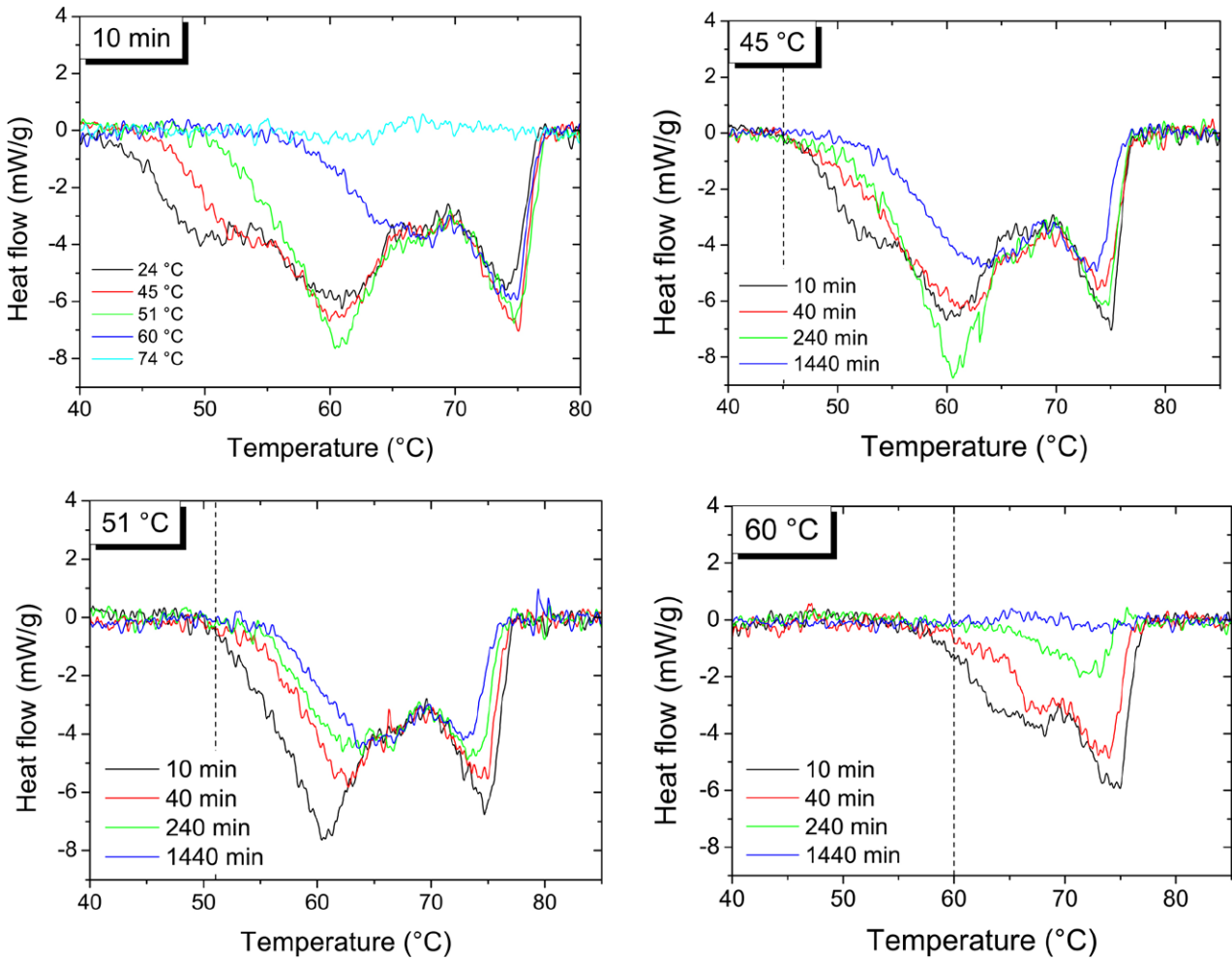


Figure 56. Denaturation of pork meat (fillet) as a function of time and temperatures.

In this case the reason for the time dependence can be understood by statistical arguments: the denaturation of proteins corresponds to crossing an energetic barrier, whose

height is roughly determined by the energy of the protein structure. For cooking temperatures in the water baths that are only slightly lower than the denaturing temperatures $T_b \leq T_d$

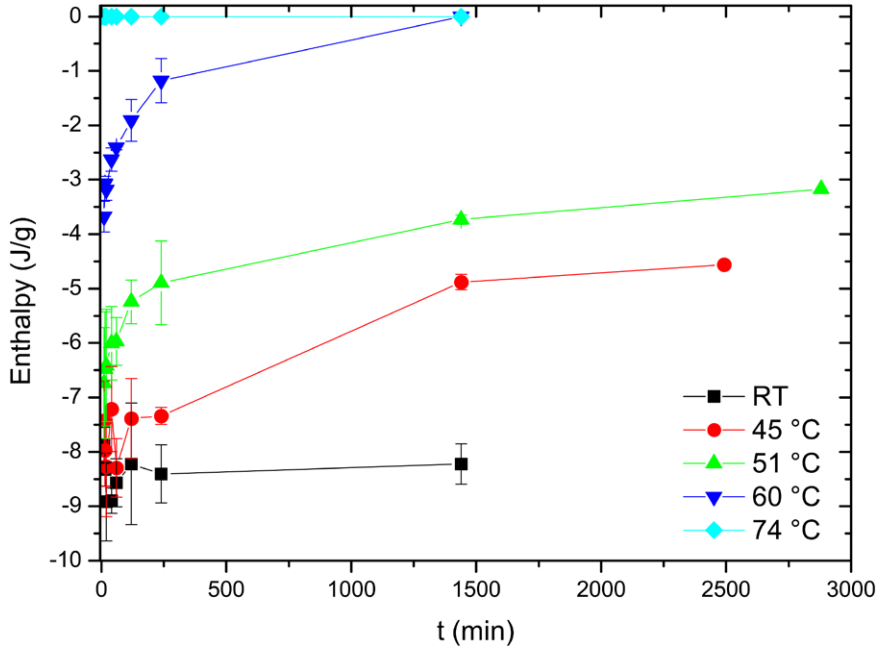


Figure 57. Remaining total specific enthalpy depending on cooking time for different cooking temperatures.

the effective barrier is reduced. The barrier crossing probability for a single process becomes of the order

$$p \propto \exp\left(-\frac{E_d - k_B T_b}{k_B T_b}\right). \quad (25)$$

In low-temperature cooking proteins can be denatured by bath temperatures below the actual denaturation temperatures.

For completeness the remaining enthalpy of the denaturation is shown in figure 57.

An interesting point comes with the very small peak at about 68 °C which persists for all temperatures. The appearance of the peak has been reported in the literature in several older experiments (Mietsch *et al* 1994, Cheah and Ledward 1996, Wright *et al* 1977, Ngapo *et al* 1999), but has been forgotten in the meantime. So far its relation to the protein structure is not clear. It is most likely that it corresponds to proteins dissolved in the sarcoplasmic drip (Di Luca *et al* 2011), because most of the literature is based on frozen and thawed meat, where the amount of drip increases due to freezing. The temperature for their denaturation seems to be higher than that of collagen. To underline this points the meat drip has been investigated by differential scanning calorimetry as well and compared to the meat (Zielbauer *et al* 2015). The results are shown in figure 58. It can be seen that the denaturation of proteins in the meat drip follows most of the peaks in the meat. The meat drip contains myosin (I), which has been dissolved during freezing, but no actin (V). More important is the shift of the minimum of the peak in region II to higher temperatures. The drip does not contain collagen, which cannot be transferred to solution without heating. Furthermore, collagen starts to denature before 60 °C and thus does not contribute to peak II. Peak II thus contains mostly sarcoplasmatic proteins. On the other hand, the peak in region III appears quite pronounced in the drip and appears at the same temperature as in meat. However, the assignment of the peaks in DSC

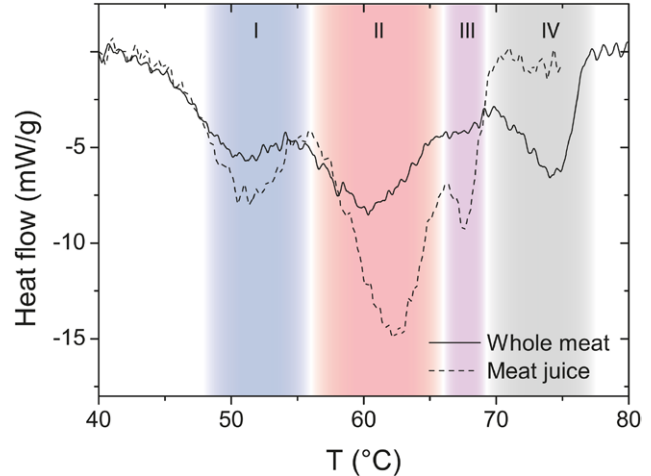


Figure 58. Comparison of the DSC of meat (solid line) and meat juice (dashed line). The peak regions I (myosin), II (connective tissue, sarcoplasmic proteins), III (unknown) and IV (actin) are indicated. The unheated drip was obtained from meat after freezing and thawing.

curves to specific proteins has been doubted recently. New developments in second harmonic generation (Brüggermann *et al* 2010) allow us to follow the denaturation of special protein groups during heat treatment more directly.

The measured water loss is shown in figure 59. The amount of water loss (or cooking loss) increases with time and temperature. When the temperature was fixed the water loss continued. It can be measured as the weight of drip in the bags. The water loss increases with time at a given temperature, which can be explained by equation (25). The inverse of the probability defines the typical time scale. When the total water binding energy is assumed to be proportional to the water concentration around a protein, the water loss becomes (for a single statistical process) logarithmic in time. However, the

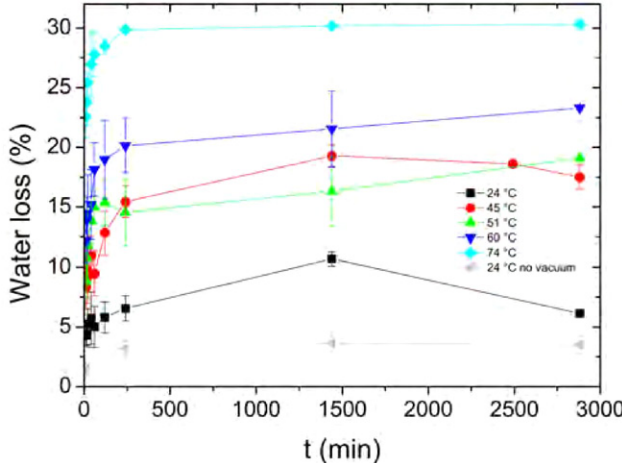


Figure 59. Denaturation of the main proteins provokes significant water loss at the temperatures marked ($24\text{ }^{\circ}\text{C}$, $45\text{ }^{\circ}\text{C}$, $51\text{ }^{\circ}\text{C}$, $60\text{ }^{\circ}\text{C}$ and $74\text{ }^{\circ}\text{C}$) and times (horizontal axis).

processes are more complicated in meat and cannot be modeled by a single barrier-crossing process. The water loss for $45\text{ }^{\circ}\text{C}$ remains higher than that at $51\text{ }^{\circ}\text{C}$ for a long period of time. Myosin heads denature and the water starts to bind. However, at $45\text{ }^{\circ}\text{C}$ gel formation is too little pronounced to keep the water in the meat. Water binding is not guaranteed by the denaturation of myosin heads alone. The denaturation of collagen (forming gelatine) and sarcoplasmatic proteins provides higher potentials for gelling and water binding. The latter can be easily seen when the sarcoplasmatic drip is heated and forms firm gels, which can be used as tasty elements in dishes to support the meaty flavor and special character of advanced avant-garde-type dishes in up-market restaurants.

11.1. Meat texture

The texture of meat has been investigated for a long time (Bailey 1972, Martens *et al* 1982, Purslow 1985, Bourne 2002). Classical texture studies are usually carried out in texture analyzers, see e.g. Hopkins *et al* (2011). The idea of such measurements is twofold: the technical apparatus can simulate the biting of meat between the incisor teeth and mastication with the molars (back teeth). Most well known for meat is the Warner–Bratzler method, where meat is cut with a triangular tool, while the force is measured as a function of the travel of the knife through the meat, see e.g. Møller (1981). Such data can be brought into context with sensory aspects (Caine *et al* 2003). A more general paper on the texture of foods including meat has been published by Lillford (2001), and shows some fundamental aspects, such as the stress–strain deformation curves for single muscle fibres from cooked meat, which closely resemble the behavior of rubber-like materials (Treloar 1975, Vilgis *et al* 2009).

In figure 60 the shear force as a function of the deformation (travel) and the cooking temperature of the pork meat is discussed and summarized. It can be seen that no simple correspondence to the temperature exists, as already observed for the water binding in figure 59. The reason is the combination of water holding capacity and protein denaturation. The

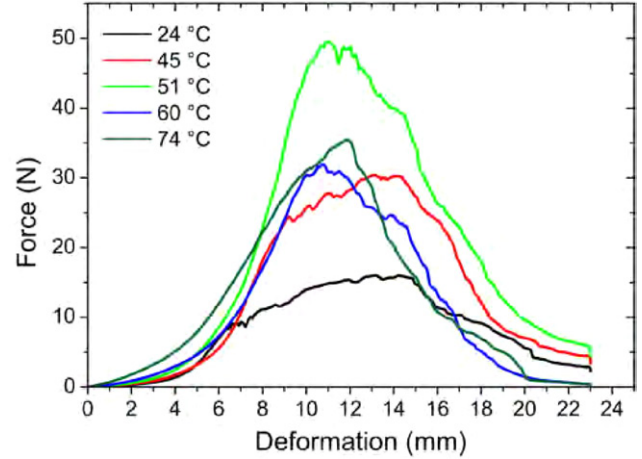


Figure 60. Denaturation of the main proteins provokes significant water loss at the marked temperatures ($24\text{ }^{\circ}\text{C}$, $45\text{ }^{\circ}\text{C}$, $51\text{ }^{\circ}\text{C}$, $60\text{ }^{\circ}\text{C}$ and $74\text{ }^{\circ}\text{C}$) and times (horizontal axis).

maximum force alone does not correspond to the mouth-feel, but also the width of the measured force, which correlates with the work needed to rupture the muscle fibers, which becomes lower for higher cooking temperatures. For practical applications it is important to mention the differences between roasting and cooking (Vujadinović *et al* 2013), which are ignored here.

11.2. Phenomenological approaches

Meat contains about 75% water and structural polymers. It appears attractive to consider meat as a ‘hydrogel’, and employ some well established theories from polymer and soft matter physics, such as the Flory–Rehner model (Flory and Rehner 1943, Khokhlov *et al* 1993, Osada and Khokhlov 2001). In soft matter food science these ideas are applied and developed in great detail by Van der Sman (2012) by studying the thermodynamics of meat proteins. The theoretical development indeed follows the classical Flory–Rehner hypothesis. One of the first applications of these ideas to muscle proteins goes back to investigations by Van Kleef *et al* (1978), who also studied egg white proteins and their elastic properties based on classical rubber elasticity (Treloar 1975), and Gosline (1978), who studied the swelling approach for elastin using the ideas of Flory and Rehner.

The models are based on the assumption of the additivity of the free energy of the different contributions, such as elastic deformations, mixing and electrostatic pressure and forces:

$$F = F_{\text{elastic}} + F_{\text{mix}} + F_{\text{electrostatic}} \quad (26)$$

where the classical expressions for gels have been used for the different contributions. Thus, the elastic part of the free energy is approximated by the Gaussian elasticity (Treloar 1975, de Gennes 1979) of the gel; the mixing free energy corresponds to the classical Flory–Huggins model (de Gennes 1979); for the electrostatic contribution ionic and (screened) Coulombic contributions are taken into account (Khokhlov *et al* 1993).

In the context of meat gels volume changes are most interesting. Thus equation (26) can be differentiated with respect to the volume to arrive at the swelling pressure

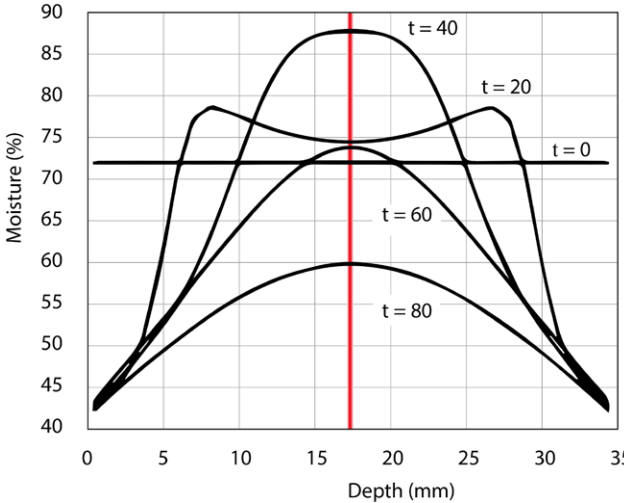


Figure 61. Theoretical moisture profiles at different stages of cooking a piece of meat of 35 mm thickness. At $t = 0$ the moisture is assumed to be equally distributed at about 72% (horizontal line). The profiles at different times t are shown accordingly. The vertical line indicates the core of the meat. (Redrawn after Van der Sman (2007) with permission.)

$$\pi_{\text{swelling}} = -\pi_{\text{elastic}} + \pi_{\text{mix}} + \pi_{\text{electrostatic}}, \quad (27)$$

with

$$\pi_{\text{elastic}} = k_B T \frac{\rho_c}{M_c} \left(\frac{1}{2} \phi - \phi^{1/3} \phi_0^{2/3} \right) \quad (28)$$

where ρ_c is the number density of the elastic material, M_c the mean molecular weight of a mesh between two subsequent cross-links, ϕ is the volume fraction of the swollen material and ϕ_0 corresponds to the unswollen state of the network. The equation is a direct consequence of the Gaussian network elasticity. The mixing pressure has its origin in Flory–Huggins pair interactions and reads

$$\pi_{\text{mix}} = \frac{k_B T}{V_w} (\ln(1 - \phi) + \phi + \chi \phi^2). \quad (29)$$

Here χ is the Flory–Huggins parameter, describing the interactions between the network material (meat) and the solvent (water). V_w is the specific (molar) volume of the solvent (water).

The final swelling pressure π_{swelling} is identical to zero in equilibrium states, because it needs to be balanced by the other contributions. Despite the simplicity of the approach, it appears to be very successful in the context of foods such as meat (Van der Sman 2012). When the thermodynamics is coupled to transport and diffusion equations, it becomes possible to compute the moisture transport and the moisture diffusion in meat as a function of cooking time (Van der Sman 2007, Van der Sman and Meinders 2013). A nice example is shown in figure 61, where the theoretically calculated profiles for the moisture distribution in a symmetric piece of meat are shown for different cooking times. The results from Van der Sman (2007) show the development of the moisture during cooking. At short cooking times water not only evaporates from the surface but diffuses inside into the still colder regions

until it reaches a maximum in the core (here at 40 min) before the meat dries out by outwards diffusion. The moisture drops below the value observed before cooking. The unexpected behavior at the earlier stages of the cooking process has its origin in the strong coupling between the temperature and mass transfer in the transport equations used in Van der Sman (2007), which is traced back to the local energy balance. It is interesting to note that the swelling pressure shows a similar behavior to the moisture content in figure 61.

The Flory–Rehner method can be extended to starch (Farhat and Blanshard 1997, Van der Sman and Meinders 2011, Van der Sman 2012) and generally to calculate the water activity, when the free energy becomes extended by a term involving the glass transition temperature via the free volume theory, known from polymer physics. Close to the glass transition the sorption of water can no longer be expressed by the binary contact between meat and water. The water activity then becomes modified as

$$\ln a_w = \ln(1 - \phi) + \phi + \chi \phi^2 - \mathcal{F}(\phi) \quad (30)$$

where

$$\mathcal{F}(\phi) = -M_w \frac{\Delta C_p}{k_B T} y_w \frac{dT_g}{dy_w} \frac{T - T_g}{T_g} \quad \forall T < T_g, \quad 0 \text{ otherwise.} \quad (31)$$

Despite successful data fitting, such phenomenological approaches, however, suffer in general from several drawbacks. First, it is not clear under which circumstances the assumption of the additivity of the different parts of the free energy, generally based on mechanics using strain invariance (Valanis and Landel 1967), is valid; cross-terms seem to play a role (Ball and Edwards 1980) in a more general context. Second, meat gels are at least locally strongly anisotropic in the muscle cells, which requires anisotropic elastic free energies (Warner *et al* 1988). Third, it is not obvious how meat containing a large number of proteins with different conformations and a large number local interactions via their amino acids can be treated with a low number of sensible phenomenological parameters. Moreover, the heat treatment of meat (and food in general) are often driven by non-equilibrium processes which are molecularly controlled. Finally, the finite extensibility suppresses the elastic free energy at higher local swelling ratios (Miao *et al* 2010), especially in spatially restricted gel conformations such as meat.

12. Viscoelastic model foods: viscoelastic fluids and gels

12.1. Thickening and gelling as fundamental processes

The physics of viscosity enhancement (thickening) and gelation in food systems is another fundamental problem, since it relates molecular structure and food texture on the basis of model systems, which allow more systematic studies. Simple water-based gels can be considered as physical model systems for foods. Their number of components, mainly water, gelling agents, possibly sugars or salts and aroma compounds, is limited. There exists a large variety of hydrocolloids from

plant cells, such as agarose, alginate, carrageenans, pectin or microbiologically fermented (starch) products, such as gelan gum and xanthan gum, or cellulose derivatives (Phillips and Williams 2009, Wuestenberg 2014). Their differences in molecular structure and molecular weight provide a basis for structuring liquids and gels in a physically very well defined way. A few examples are reviewed in the sections below, where the main emphasis is put on the multiscale behavior of the interactions of hydrocolloids with their environment.

Hydrocolloids are water-soluble polymers (Lee *et al* 2012, Morell *et al* 2014, Varela *et al* 2014), which change their rheological and textural behavior of water-based fluids according to their molecular properties. In food systems hydrocolloids are used for enhancing the textural properties. For example, creams with specially controlled flow properties stay longer in the mouth and release their taste more slowly, so that they match flow times for certain molecular processes in the mouth and are thus relevant to the sensory experience. Such applications are well known in the food industry. In most cases hydrocolloids are used to stabilize the mouth-feel of a certain product against the natural and possible variation of physical parameters, such as acidity, salt or sugar content and basically the temperature at which the product is eaten, e.g. directly out of the fridge or after some warming at room temperature. The taste receptors for sour, sweet, bitter, salty, umami and eventual fatty tastes are exposed for longer to the influence of the molecules that trigger them, so the perception becomes enhanced. A secondary effect is more important. During the time the food stays in the mouth, the temperature of the liquid changes. As this happens, more of the volatile compounds responsible for the retronal effects (Funami 2011) may escape from the liquid and evaporate. Hence the sensory effects are also enhanced. These naive thoughts suggest a number of physical requirements for a simple theory for the structure–property–taste relationship: (a) the description of the rheological flow properties, via the viscosity and the physical behavior of the fluid, (b) a more detailed description of possible mechanisms of taste release. However, since their use in ‘molecular cooking’ their special features have become available for new applications in restaurant kitchens, and the products are even used in home cooking (Vilgis 2010).

The elementary approach of viscosity enhancement by adding colloids even goes back to Einstein’s famous simple equation (Einstein 1906), which is expressed by the first term of a series,

$$\eta = \eta_0 \left(1 + \frac{5}{2} \phi + 14.1 \phi^2 + \dots \right) \approx \eta_0 1/(1 - \phi/\phi_{\max})^2 \quad (32)$$

where η_0 is the viscosity of the solvent and ϕ is the volume fraction of the added spherical colloids in solution. A large number of modifications of the Einstein equation for colloidal systems at larger volume fractions ϕ has been made, where the series has been casted in approximations showing singularities at the maximum volume fraction ϕ_{\max} . For a discussion of the different models and their experimental relevance see the recent work by Shewan and Stokes (2015). The shape of the colloids determines only numerical factors, and for strong dilution hydrocolloid polymers with a polymerization degree

N and a hydrodynamic radius $R \propto N^\nu$ occupy a volume fraction $\phi = n/R^3$, where n is the number density of chains, as long as the chains do not overlap (Doi and Edwards 1986). When the hydrocolloid chains of chain length N are sufficiently flexible, for example polar, non-ionic hydrocolloids, such as cellulose derivatives like methyl- or carboxy-methylcellulose, well-known results from polymer physics, such as Rouse scaling, i.e.

$$\eta \propto k_B T N \quad (33)$$

hold as well, below the overlap concentration. At higher concentrations, interactions yield a stronger rise of the viscosity, which leads to a chain length dependence $\eta \propto N^3$. Other phenomenological approaches and empirical equations have been proposed to describe the increase of viscosity with concentration, molecular weight or structure of the dissolved polymers, which can be found for example in Ferry (1980). Amongst these the Mark–Houwink relation should be mentioned, which finds many applications in food hydrocolloids, see e.g. Qiu *et al* (2015) and Szopinski *et al* (2015) for some recent references.

Charged chains are described theoretically as polyelectrolyte chains (Förster and Schmidt 1995, Barrat and Joanny 1997). The polyelectrolyte chains appear sufficiently stretched, depending on their charge. Simple scaling suggests (Barrat and Joanny 1997)

$$R \simeq b \left(\frac{l_B f^2}{b} \right)^{1/3} N \quad (34)$$

where b is the size of the repeat unit, l_B is the Bjerrum length and f is the charge fraction, which is the number of charged monomers in the chain. Thus the chain extension is proportional to the chain length itself, but on scales below the ‘blob size’ $\xi = b \left(\frac{b}{l_B f^2} \right)^{1/3}$ the conformation is coiled. For charged hydrocolloids this ‘chain of blobs’ implies electrostatic stretching by the charges placed along the chains and an additional stiffening of the backbone. The chains of charged (ionic) hydrocolloids are even ‘stiffer’ when immersed in food preparations, and this has an additional impact on the viscosity and the mouth-feel.

12.2. Salts, thickening and chain conformation

As is known from the theory of polyelectrolytes, salts and the increase of the ionic strength have a severe impact on the chain conformation and thus the thickening. In the presence of salt, interactions between charges become screened and the Coulomb repulsion changes to a Debye–Hückel screened potential between two charges:

$$U_C(\mathbf{r}) \propto \frac{1}{r} \quad \longrightarrow \quad U_{DH}(\mathbf{r}) \propto \frac{\exp(-\kappa r)}{r} \quad (35)$$

where $\kappa^2 = 4\pi l_B I$, I being the total ionic strength, and r denotes the distance between two charges. The electrostatic screening length $\xi = 1/\kappa$. The screening effect can be understood easily

in physical terms. The dissociated salt ions of opposite charge will be attracted by the charges along the polymer contour and will screen their effect. For very high salt concentrations, which means very small values of the screening length, the Debye–Hückel potential becomes very short-ranged. The effect of the charges then disappears more or less completely and the chains behave like self-avoiding chains in a good solvent.

The screening effect indeed has some relevance for culinary applications of any thickening (or gelling) agent. Since the presence of salt in any liquid such as a sauce or broth will screen the interaction, it will change the shape of the polymer and thus its effect on viscosity. The size of the chains in a more highly salted solution shrinks (Barrat and Joanny 1993, Micka and Kremer 1996). It was shown that the persistence length l_p of a chain in a salted solution is of the order of the electrostatic blob size, i.e. $l_p \approx 1/k$, and this scales with $l_p \propto 1/I^{1/2}$. The persistence length decreases with increasing ionic strength. All interactions are screened at very high salt concentrations and the interaction potential from equation (35) becomes short-ranged. The chain conformation shrinks from the extended state to that of a self-avoiding chain, $R_S \approx (Nb/l_p)^{3/5} l_p \propto bN^{3/5} I^{-1/5}$, which interpolates between the unsalted and highly salted regimes. Consequently the viscosity reduces, with the effect that salted liquids need a higher concentration of the thickening agent to compensate the conformational effects. This large-scale effect indicates already that thickening is strongly dependent on salt concentrations. For example, it is straightforward to estimate that the concentration c_S of hydrocolloids required in salty conditions scales inversely with the ratio of the chain size to the third power,

$$c_S = c_0 (R_0/R_S)^3 \propto I^{3/5} N^{6/5} \quad (36)$$

which increases with the ionic strength at fixed molecular weight. Since the chain size in the salty solution R_S is always lower than the size in the unsalted solution R_0 the concentration increases. This simple result suggests, for example, a ‘kitchen rule’ for the thickening of salted sauces.

12.3. Local interactions and salt types: Hofmeister series in foods

So far local aspects have been ignored. To better understand the physics of hydrocolloids on all relevant length scales, local interactions such as hydrogen bridges and local dipolar interactions need to be taken into account. Such local effects may change the Coulomb law between sodium and chloride ions at short distances (Hess *et al* 2006a, 2006b); sodium and chloride ions may form water-mediated complexes, despite their strong electrostatic repulsion. The physical origin of these effects is the strong orientation of dipolar water molecules in the first hydrate shell around the salt ion. The nature of interaction between two oppositely charged ions is highly distance-dependent. At larger distances they interact with the classical Coulomb potential (strictly valid only for point-like charges/ions). When they become close and their separation



Figure 62. Comparison of two identical tomato preparations, without xanthan (left) and with 0.3% xanthan (right).

is shorter than the radii of the hydrate shells, the oriented water dipoles interact as well. The interaction potential develops local minima, which correspond to metastable sodium–water–chloride complexes (Hess *et al* 2006a). In addition, these effects play a significant role in ionic hydrocolloids. Especially in food systems, the strong local water binding of ionic hydrocolloids is important for the mouth-feel, and the hydrate shells play an important role. The maximum number of charges in hydrocolloids is proportional to the chain length, and the concentration of ‘bound’ water is high.

Typical food-grade salts are sodium chloride (NaCl), potassium chloride (KCl), calcium chloride (CaCl₂) and others. The corresponding ions have different radii, thus form different hydrate shells (Ohtaki and Radnai 1993, Hummer *et al* 1996) and have a very distinct impact on the chains’ conformation and even the salty taste. The effects of salts in the Hofmeister series and solvent isotopes on the gelation mechanisms for hydroxy-propyl-methylcellulose gels have been investigated by Liu *et al* (2008). It was shown there how the use of different salts (not always food-grade systems) influences the gelling behavior and the structure formation in gels. The effect of konjac glucomannan in aqueous solutions have been established as well (Yin *et al* 2008). Frictional aspects have been investigated by Garrec and Norton (2012). Some Hofmeister effects in a more general context are discussed in Parsons *et al* (2011).

12.4. Xanthan: stiff polyelectrolyte with unusual properties

The interplay of both local and large-scale effects in the food context can be illustrated with the physical example of xanthan, a polysaccharide that is used as a standard food thickener. The molecules consist of a relatively stiff backbone of repeat units, each carrying an ionic side chain (Phillips and Williams 2009). The chains form very stiff, rod-like helices in solution. These are sufficiently charged (Kawakami and Norisuye 1991) to guarantee a high water binding by forming hydration shells around the macromolecules. In figure 62 the increased water holding capacity is visualized. One part of a ‘homemade’ tomato preparation (ketchup) has been left natural (on the left of the figure) and xanthan has been added to the other part (on the right of the figure). The sample without xanthan leaks water after a few minutes, whereas the other sample retains the water completely and has a much better mouth-feel.

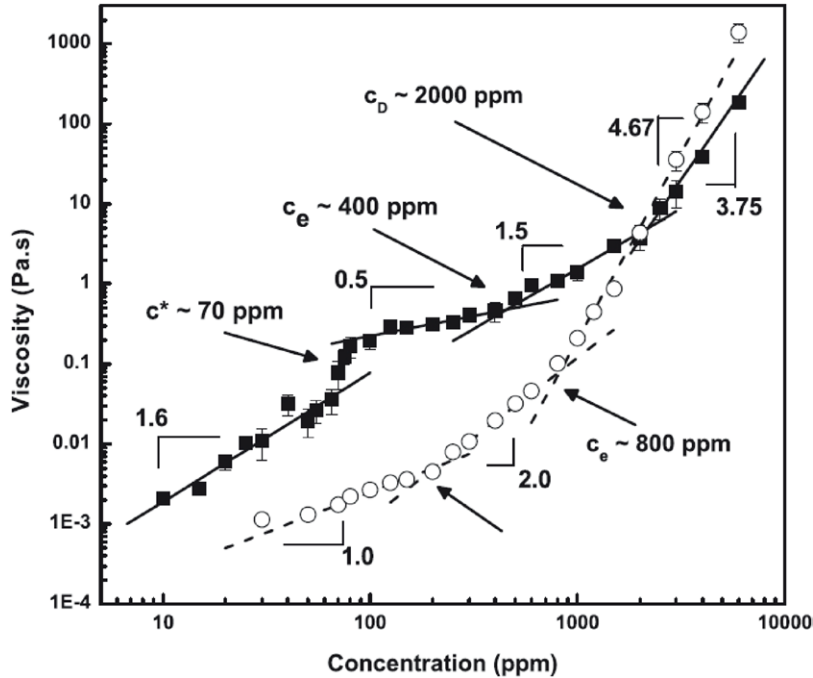


Figure 63. Concentration dependence of xanthan solution without (full squares) and with salt (NaCl, empty circles). Different concentrations are indicated. From Wyatt *et al* (2011) with permission.

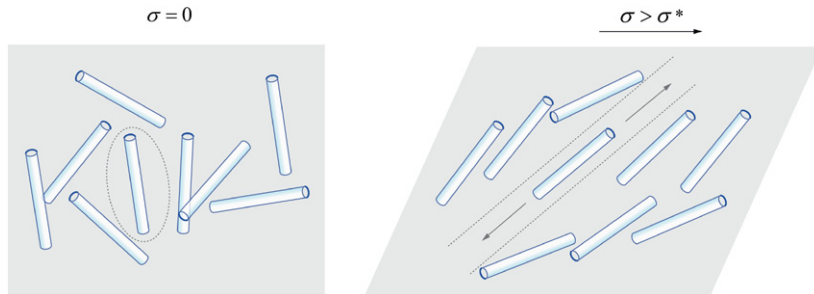


Figure 64. Jamming of rod-like molecules at low concentrations of xanthan solution. Under shear above the yield stress, the rods become oriented and slide alongside each other.

Xanthan solutions show a thixotropic flow behavior with a yield stress, at already very low concentrations, that is due to the stiffness and its charge. It is assumed that the rod-like polymers have a length L , thickness b and effective charge of the order $fe(L/b)$, and dissolve in water at very low concentrations. At concentrations of the order

$$c^* \simeq \frac{1}{bL^2(1 + (l_B f^2/b)^3(L/b))} \quad (37)$$

the hindrance between the repelling rods becomes larger; the rods ‘freeze’ in random orientations (Nordqvist and Vilgis 2011). The first term in the denominator corresponds to the Onsager transition in rigid polymers (De Gennes and Prost 1993), whereas the second term comes from the electrostatic repulsions. It is worth noticing that the dominant term for c^* shows an L^3 dependence, which indicates very low critical concentrations for jamming for large chain length. Low concentrations already have a strong effect on the viscoelastic behavior.

When the rods are uncharged they most likely form liquid crystalline phases at concentrations closely related to the

(Onsager) excluded volume bL^2 , as discussed in a very elegant way by Doi and Edwards (1986). Charged rods repel each other strongly, which shifts the critical concentration to much lower values, as expressed in equation (37). At the concentrations relevant for thickening, liquid crystalline phases are unlikely and the rods ‘quench’ in a random orientation. Such ideas go back to earlier toy models on the glass or jamming transitions (Edwards and Vilgis 1986), which follow general principles in (soft matter) physics (Liu and Nagel 2001, Olsson and Teitel 2007, Biroli 2011, Ikeda *et al* 2012).

The concentration dependence of the viscosity of xanthan solutions has been measured and discussed in detail by Wyatt and Liberatore (2009). Already at low concentrations the viscosity of salt-free solutions increases strongly as indicated by c^* , which suggests ‘jamming’ without strong packing effects.

At larger concentrations this becomes more and more difficult and it is not easy for the rods to remain separated from each other. Moreover the rods will not arrange themselves in ordered (liquid crystalline) phases, at moderate concentrations, since the energies of electrostatic repulsion of parallel charged rods are larger than when their orientations form

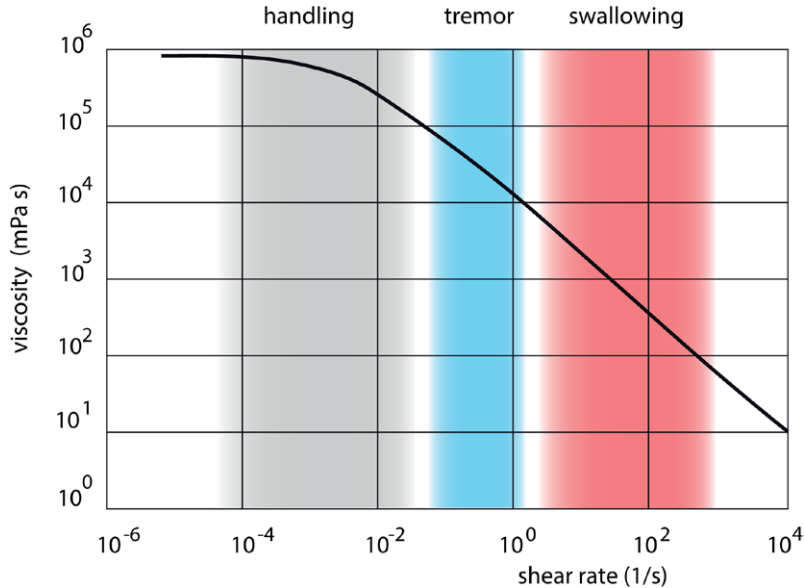


Figure 65. Typical nonlinear shear rate dependence of xanthan solutions. The viscosity drops over several decades when the shear rate is increased. Typical shear rate regimes for handling, tremor and swallowing during eating are indicated.

an angle between them. The concentration dependence of xanthan solutions is shown in figure 63.

Consequently, this idea suggests that with increasing concentration the stiff xanthan molecules will ‘freeze’ at a certain critical concentration. This immobilization of the rods causes the transition to the soft solid-like behavior of the ketchup-like liquid at zero shear. The immobilization is thus based on multiple compromises at finding the lowest energetic state of the molecules as an ensemble: on one hand, the molecules should maintain a large distance from each other; on the other hand the increasing density prevents them from doing so. It has been shown that counter-ion-induced attraction at higher concentrations and low energy (Grønbech-Jensen *et al* 1997, Ha and Liu 1997, Manning 2011) allows for ordered phases in rod-like polyelectrolytes.

Xanthan solutions with added salt show an increase of the viscosity at larger salt concentrations (Wyatt *et al* 2011); at low concentrations screening dominates. In solutions containing salt electrostatic screening lowers the repulsion and enables entanglements in the stiff chain solutions (Doi and Edwards 1986). The jamming becomes released under shear, see figure 64. Low-concentration xanthan solutions show a pronounced shear thinning if the shear stress is larger than the yield stress, which can be estimated as Nordqvist and Vilgis (2011)

$$\sigma^* \propto \frac{k_B T}{b^3} \frac{l_B f^2}{b} \left(\frac{L}{b} \right)^2. \quad (38)$$

This pronounced shear thinning with a yield stress defines very much the physical part of the sensory attraction of xanthan-thickened liquids that show this ‘ketchup effect’: at low shear rates the ketchup appears ‘solid’, at higher shear rates it becomes liquid. The shear rates during oral food processing (Chen and Engelen 2012) and the shear stresses (at large amplitude) in between tongue and palate yield significant viscosity changes in the mouth (see figure 65). The shear

rate-dependent behavior of xanthan solutions as shown in figure 65 makes their application in geriatric nutrition very attractive (Vilgis *et al* 2015). Such purely physical aspects are important in very practical applications: elderly people suffering from tremor (or Parkinson’s disease) can lift soups, drinks or juices by themselves from the plate to the mouth. At typical tremor frequencies the viscosity remains high: the liquid does not drop from the spoon. When processed orally at larger shear rates during swallowing the viscosity drops significantly. The liquid can be swallowed easily, even by patients suffering from dysphagia.

Very often xanthan is combined with other flexible hydrocolloids such as guar, locust bean gum or chitosan to enhance the sensory properties (see for example Vilgis *et al* (2015) for more details). In the case of chitosan the conformation has been studied by atomic force microscopy (Maurstad and Stokke 2004). Order-disorder transitions have been suggested (Viebke 2005). Combined, synergistic thickening by the use of xanthan and starch (potato) shows the culinary potential using different molecular structures—linear-stiff, linear-flexible and hyperbranched—to gain in sensory quality (Krystyan *et al* 2012).

12.5. Agarose gels as simple model food systems

One of the most well-known gelling agent is gelatine, which exists in the connective tissues in meat and stromal proteins. As already mentioned earlier, the collagen, consisting of triple helices, denatures to gelatine, a strongly water-soluble amphiphilic polymer, which forms soft and elastic gels (Johns and Courts 1977) when corresponding preparations are cooled (Ross-Murphy 1987). The gel formation under partial helix formation takes quite some time (Ross-Murphy 1992). Gelatin gels have been widely studied (Ledward *et al* 2000, Weiss and Terech 2006) and are not discussed in detail here. In the following, agarose gels are discussed in more detail, which will

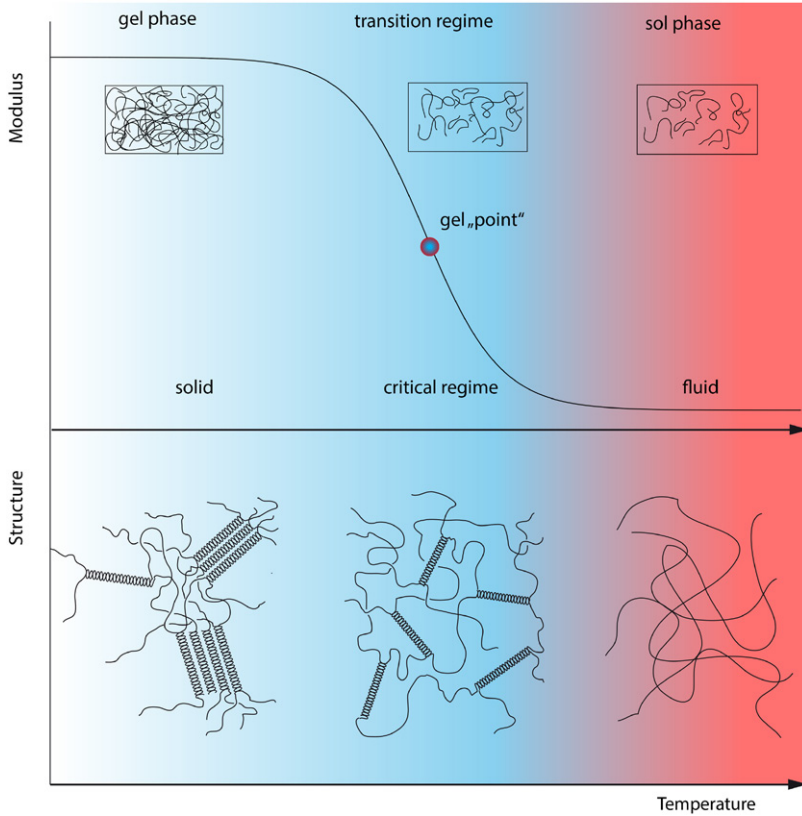


Figure 66. Typical view of the sol–gel transition of a helix-forming network. At high temperatures (right) chains are dissolved.

enable us to study interactions with water, and with other long food polymers (hydrocolloids) and small water-binding carbohydrates (sugars).

12.6. Pure agarose gels

Pure agarose gels are considered first, because they show many fundamental processes in the formation of soft solids in hydrogels. The common process taking place in most gelling agents is shown in figure 66. At high temperature the gelling agent forms a solution and the viscosity is enhanced. On lowering the temperature the viscosity increases, and at the gel point (Vilgis *et al* 2009, Seiffert and Sprakel 2012) gels are formed. The gelation corresponds to a liquid-to-solid transition and when it happens in equilibrium the process can be modeled by a percolation process (de Gennes 1979, Aharony and Stauffer 2003), which is described as a second-order phase transition with critical exponents close to the gelation point. The chains form larger clusters, where the largest grows to an ‘infinite’ cluster. The percolating system shows solid character with (small) moduli. The gelling system significantly shows a high modulus above the critical point, with a value that is determined by the physical properties of the percolating elements, e.g. chain stiffness, bending properties and the mean distance between the connecting points (Vilgis *et al* 2009). Gels in foods are in most cases far above the gel point and behave as soft elastic solids with sufficient brittleness. One of the most well used gelling agents from plants is agarose (Saha and Bhattacharya 2010, Imeson 2011), the gel-forming molecule in agar, which stems from the cell walls

of algae (Armisen 1997). Following Russ *et al* (2013), some important aspects of the recent developments in agarose gelling are reviewed below.

In the liquid phase near the boiling point of water, the agarose molecules form a random coil conformation and are distributed homogeneously in the solution (Labropoulos *et al* 2002). While gelling under cooling, this entropically preferred state has to be overcome and the single polysaccharide chains are forced to associate with other chains via hydrogen bonds. Below the gelling temperature the loss of entropy is thus compensated by a gain of energy. Arnott *et al* (1974) demonstrated by x-ray diffraction (XRD) and optical rotation measurements that agarose gels are formed by double helical structures of single polymer chains. The binding by hydrogen bonds leads to a double helical combination of two single agarose chains (Rees and Welsh 1977). Further cooling causes aggregation of these double helices. Therefore, a two-step gelation mechanism for agarose has been proposed (Normand *et al* 2000, Nordqvist and Vilgis 2011). First, the formation of a gel by joining the randomly distributed coils into a double helical association by hydrogen bonds, followed by the aggregation of the double helices into a tight three-dimensional network. In between the junction zones of this network, meshes are established that enable the enclosure of water molecules by forming hydrogen bonds with the hydroxyl groups of the agarobiose units facing outward (Arnott *et al* 1974).

The gelation process (Russ *et al* 2013) and the increase of the real part of the complex modulus with decreasing temperature are shown in figure 67. The hysteresis of the modulus between the cooling and heating curves indicates the non-equilibrium

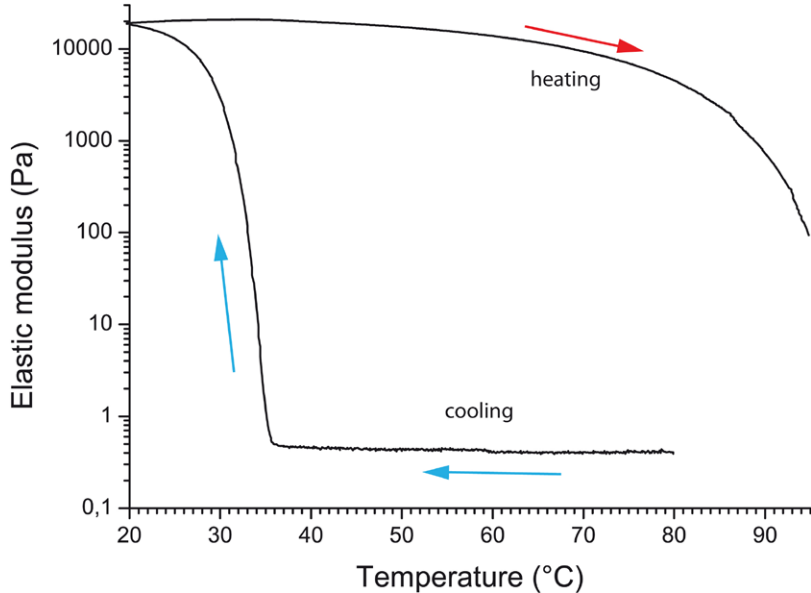


Figure 67. Measurement of the modulus in a rheometer at a cooling rate of 1 °C/min. The sample is again reheated in the rheometer at the same heating rate.

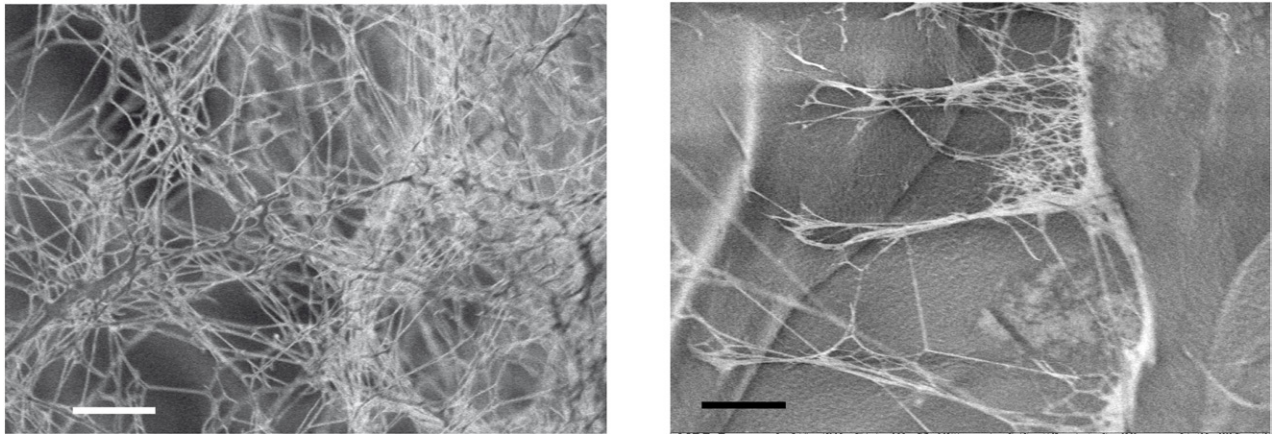


Figure 68. Scanning electron microscopy of the formation of agarose gels at two different temperatures Right: 45 °C, with incomplete network formation; left: 20 °C (room temperature) where the network has been completely developed. The scalebar is 2 μm.

nature of the gelation process (Mohammed *et al* 1998, Kara *et al* 2011). Indeed food systems are often far from being equilibrium physics and require, in general, non-equilibrium thermodynamic methods (Slade and Levine 1991). Nevertheless equilibrium studies offer first insights into the relevant physics. Figure 66 suggests a ‘two-stage’ process for the gel formation. It is interesting to verify these suggestions by scanning electron microscopy (SEM) (Nordqvist and Vilgis 2011). The results are shown in figure 68. The gel has been formed by cooling. Part of the gel is frozen in close to the gel-forming regime at 45 °C. The other part of the gel has set on further cooling to room temperature. The structure after freeze-drying is significantly different. At lower temperatures the gel has been formed completely, whereas at temperatures in the early stages of the gel-forming regime, only clusters of partial networks are visible, which supports the ideas depicted in figure 66.

The final strength is obviously given by the concentration of the gelling agent as shown in figure 69. According to the classical gel theory the shear modulus of a soft (polymer) gels scales as $G \simeq k_B T / \xi^3$ (de Gennes 1979), where ξ is the

mean mesh size of the network. Indeed this can also be verified with the agarose gels at different concentrations (Russ *et al* 2013). Therefore, it was necessary to stain the agarose molecules with a fluorescent dye (5-(4, 6-dichlorotriazinyl) aminofluorescein) to allow confocal laser scanning microscopy (CLSM), which enables one to visualize the mesh size and measure it in the agarose gels by image evaluation. Figure 70 shows the decreasing mesh size in pure agarose networks with increasing concentration. The figures can be evaluated more precisely. The mesh size can be measured in the two-dimensional picture and correlated with the modulus obtained in figure 69. Figure 71 shows the relation between the modulus obtained by rheology and the values of the two-dimensional mean mesh sizes as a function of the concentration. However, the mesh sizes from the CLSM are evaluated from two-dimensional pictures, which shows only two-dimensional projections of the three-dimensional network meshes. The plotted values obtained from CLSM are therefore too small by a factor of between $\sqrt{3}/2$ and $\sqrt{3}$, which would bring them closer to the rheological data, showing the

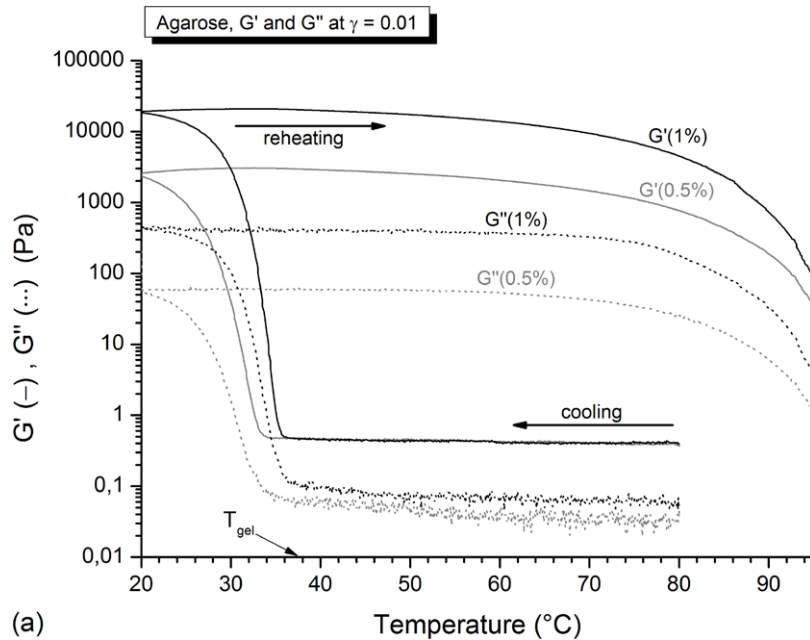


Figure 69. Temperature sweep and concentration dependence of gel formation for the concentrations 0.5% and 1%, which are above the gel concentration 0.2%. (From Russ *et al* (2013) with permission.)

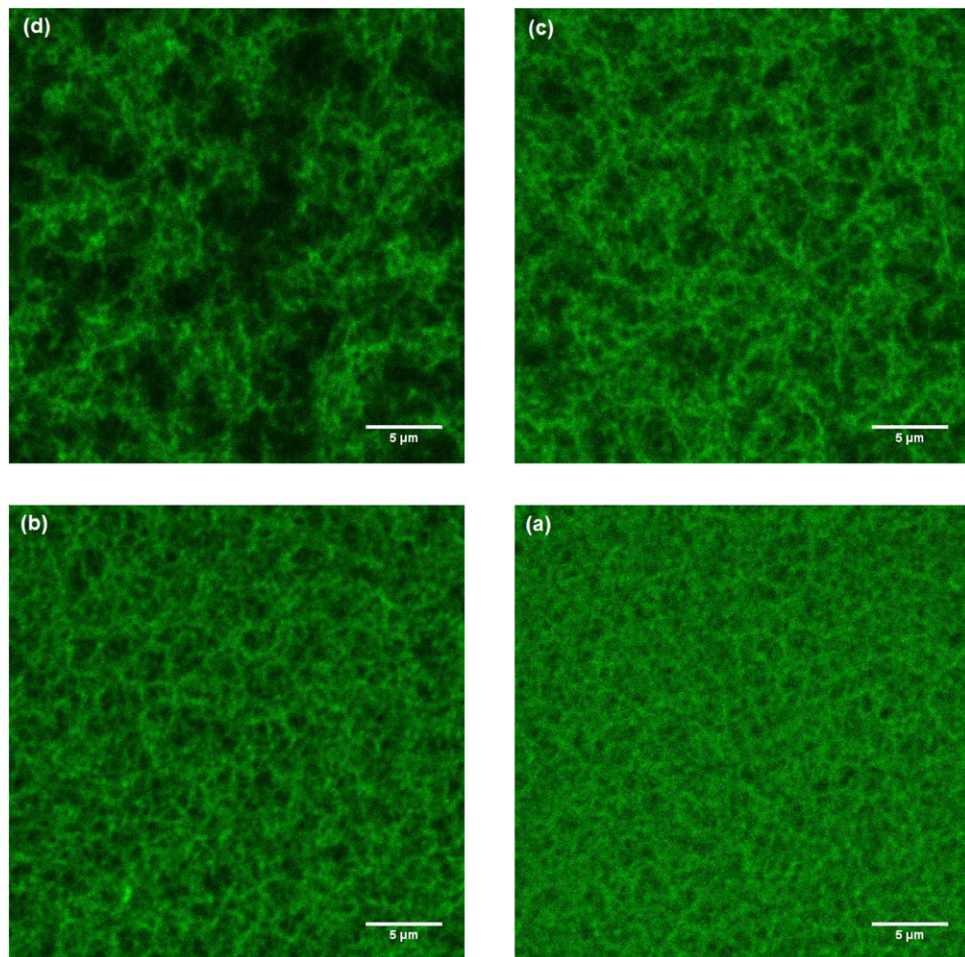


Figure 70. Mesh size as seen by CLSM at (a) 0.25%, (b) 0.5%, (c) 0.75% and (d) 1%. (From Russ *et al* (2013) with permission.)

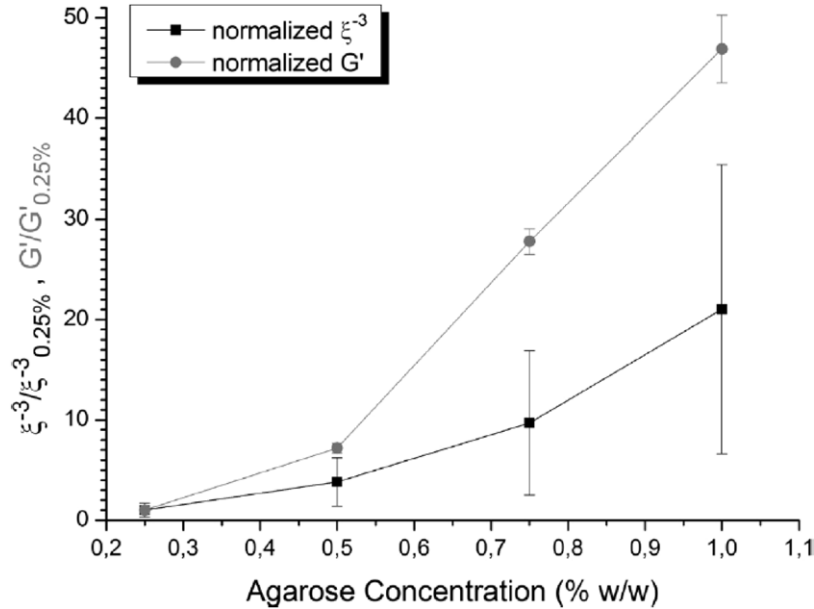


Figure 71. Correlation between the normalized mesh size ξ^{-3} and the modulus. (From Russ *et al* (2013) with permission.)

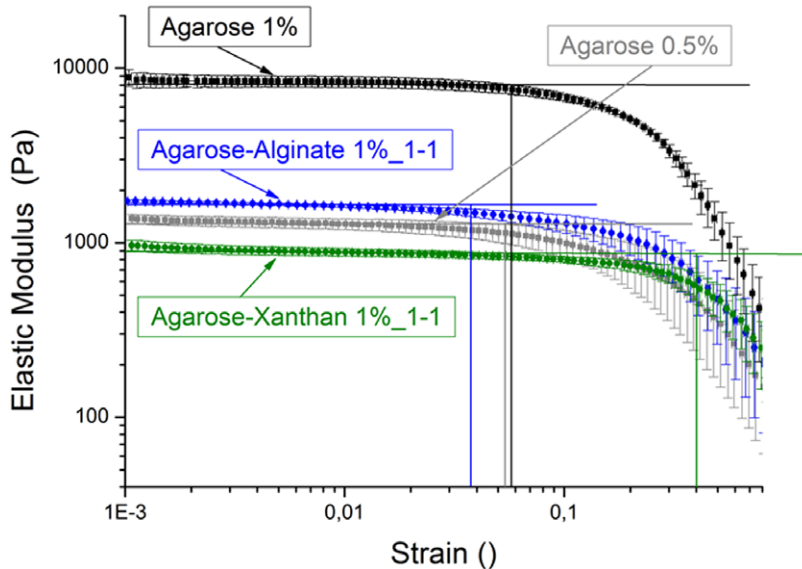


Figure 72. Modulus of agarose with xanthan and alginate.

trend better. Total agreement cannot be expected, since the actual structure of the agarose networks is more complicated than gels with simple point-like cross-links and fully flexible chains, for which the simple scaling relation is derived. The concentration dependence has been studied in terms of polymer scaling, for example by Normand *et al* (2000). However, kinetics plays an important role and the structure formation depends on thermal and mechanical histories of the preparation (Aymard *et al* 2001).

12.7 Agarose gels mixed with non-gelling agents

For many (culinary and industrial) applications it appears useful to add non-gelling thickening agents before the gels are settled, which enables a more precise texture control (Phillips

and Williams 2009, Saha and Bhattacharya 2010). There are many possibilities in the landscape of gelling and thickening agents to produce food-relevant mixtures, but so far no systematic investigations to allow some insight into the influence of the physical parameters. Systematic investigations with control of the parameters are lacking. Recently Russ *et al* (2013) studied the influence of the chain flexibility of added hydrocolloids on agarose gel formation. As examples two polyelectrolytes, xanthan and alginate (Imeson 2011) have been chosen. Alginate is a relative flexible polymer where parts of the block (guluronic acids) are charged. The macromolecules are water-soluble and are in most cases used with bivalent ions (calcium and magnesium) to form ionic networks of considerable strength (Draget *et al* 1994, Donati *et al* 2005, Phillips and Williams 2009) with many applications

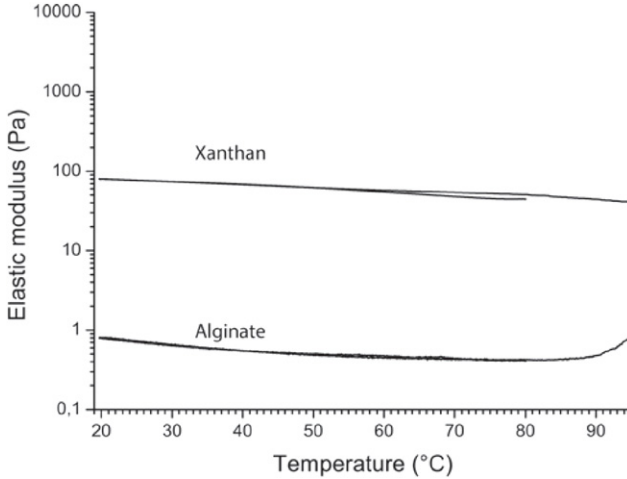


Figure 73. Temperature sweeps for alginate and xanthan solutions (each 1%) do not show a relevant temperature dependence, unlike the network formation.

in controlled drug release (Gombotz and Wee 2012, Lee and Mooney 2012) and physical and culinary aspects (Vilgis 2007, 2009, Vilgis 2010). Without the combination with bivalent ions alginate can be used as a thickening agent because its flexibility provides very different viscoelastic properties from xanthan (Russ *et al* 2013, Rao 2014).

In combination with the gelling agent agarose, alginate and xanthan provides different rheological properties and thus a very different mouth-feel, which can be traced back to the arrangements of the molecules with different flexibility. Figure 72 shows the influence of the chain flexibility of the hydrocolloids in agarose gels. The modulus of the agarose–alginate gels is slightly higher than that of the pure gel (0.5% agarose), whereas the xanthan lowers the modulus. For the interpretation it is important to note that neither xanthan nor alginate shows a significant temperature dependence of the low deformation modulus during a temperature sweep in the rheometer (see figure 73). This shows that xanthan and alginates do not show a pronounced temperature dependence. For xanthan this means that the formation of the jammed state in the linear deformation regime is not sensitive to temperature changes in the food-relevant temperature range.

In addition, the xanthan jamming state is formed before the gelling of the agarose network. Consequently the agarose gelation needs to take place in the presence of the jammed xanthan network. The presence of the stiff xanthan chains during network formation implies a strong limitation of diffusion and mobility for the agarose chains. While heating the mixture, the agarose has to be dissolved in the array of the xanthan chains. The dynamic time scale of the jammed xanthan structure is much longer than that of the motion of the flexible agarose chains. In addition, it is not much affected by heating, because the viscosity of xanthan solutions does not show a significant temperature dependence, which indicates that the time scale of motion of the xanthan molecules is very long. The jammed structure of the xanthan rods hinders the free diffusion of the agarose chains, and the formation of helices needs to be considered

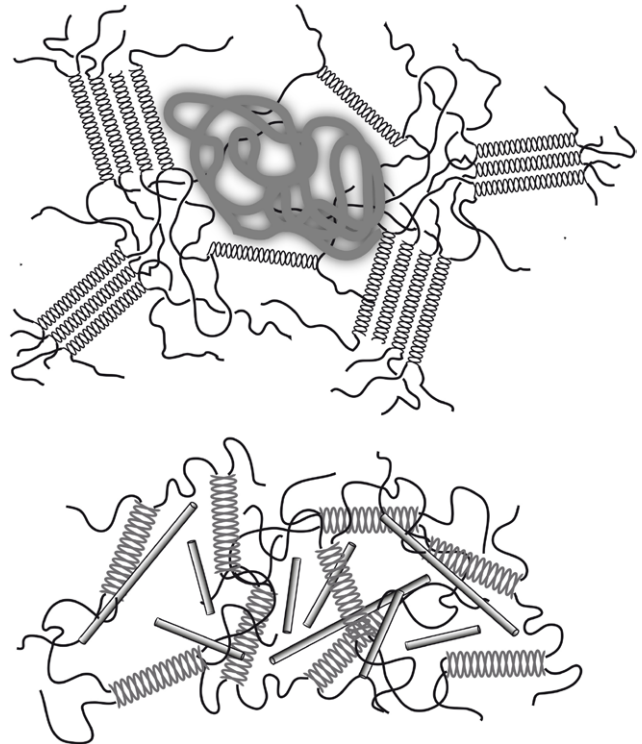


Figure 74. Different arrangements of gel-forming agarose chains in the presence of the xanthan ‘glass’ and the alginate solution.

in a restricted (phase) space that is formed by the random array of stiff xanthan molecules. Thus, it is assumed that during the gelation fewer agarose coils can transform into helices and, hence, fewer helices can agglomerate, and the resulting gel structure consists of fewer and weaker junction zones. To estimate the modulus the rod length is larger than the mesh size, $L > \xi$, which implies a lower modulus (Russ *et al* 2013):

$$G \approx \frac{k_B T}{\xi^3} \left(1 - \frac{3\xi}{L}\right) \quad (39)$$

compared to the gel without xanthan.

The mixture with alginate shows slightly higher values of the elastic modulus than 0.5% agarose gels. Alginate in solution has a structure of flexible, mobile and entangled coils of polymer chains which hardly affect the diffusion of the agarose helix. During gelation the aggregation of agarose double helices and the build-up of the three-dimensional network are hardly hindered (Edwards and Vilgis 1988). The entangled flexible polymer chains of the alginate are easily incorporated into the agarose meshes and act similarly to soft filler particles in the network. Thus, the formation of the agarose network is less restricted than the formation with added xanthan. Such swollen networks have already been observed for other mixtures of a gelling agent with non-gelling hydrocolloids (Cates and Edwards 1984). Effectively, the flexible alginate molecules provide larger entropy, which yields a larger modulus. In addition the embedded flexible alginate chains act as reinforcing ‘filler’ particles of self-avoiding walk shape in the network. From these plausible ideas emerges a picture

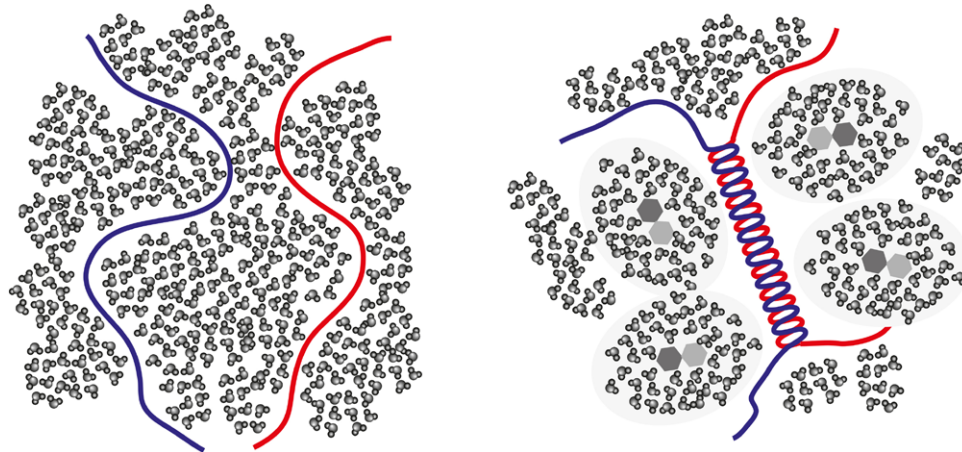


Figure 75. The addition of sugars or sugar alcohols restructures the water around the hydrocolloids and triggers the first step of gel formation (Shimizu and Matubayasi 2014).

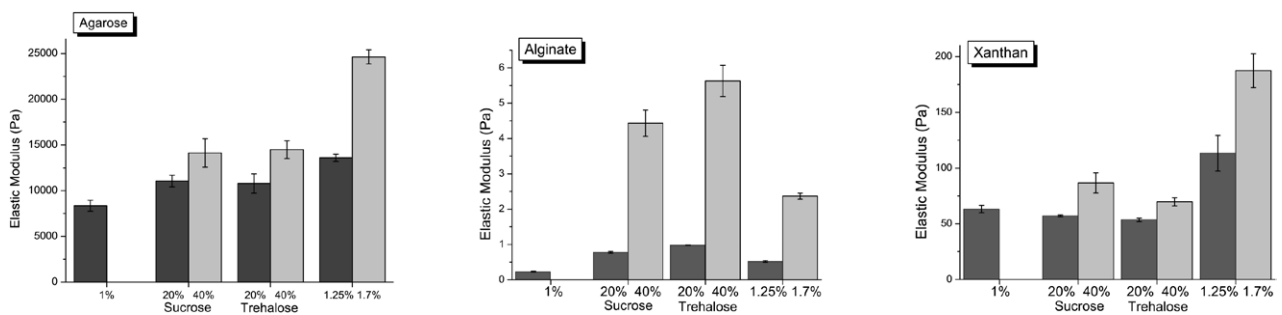


Figure 76. The addition of sugars or sugar alcohols has a strong impact on the dynamic shear behavior of the different hydrocolloids. From Russ *et al* (2014) with permission.

for the molecular arrangement in different scenarios and this is shown in figure 74. The alginate chains with their flexibility are able to arrange themselves more easily to act as soft filler. Rigid xanthan molecules act as disordered obstacles and restrict the phase space, which lowers the small deformation modulus.

12.8. Influence of sugars and other low-molecular-weight cosolvents

Low-molecular-weight sugars, often added to sweeten gels, have an important influence on the gelling properties of foods (Maurer *et al* 2012, Russ *et al* 2014). Kasapis *et al* (2003) and Kawai *et al* (1992) described the stabilizing effect of sugar molecules in hydrocolloid systems. They assumed that the hydrogen bonds between the polymer chains are strengthened by adding sugar molecules, and more stable and stronger junctions in the hydrogel networks develop. Nishinari and Watase (1992) also observed an increase of the elastic modulus of agarose gels by the addition of sucrose.

Sugars dissolve in water and restructure the water molecules locally in hydration shells, rather than using the models as discussed by Nishinari *et al* (1992). Thus water is not an inert background of good solvent, which manifests itself by the change of the gelling properties when different sugars are added. Following the previous section, it is useful to compare the pure agarose and the agarose/xanthan and agarose/

alginate gels with sugar. Obviously there is a ‘fight for water’ between the hydrocolloids and the low-molecular-weight sugars, which depends strongly on the nature and the structure of the sugars. In Maurer *et al* (2012) mono- and disaccharides have been studied whereas in Russ *et al* (2014) two sugars have been investigated because the nature of the sugars plays a non-negligible role, especially the positions of the hydroxyl groups (OH) that are responsible for the water binding. Thus local properties have a strong impact on large-scale properties of the gels. In the following the main results and physical ideas are reported, without going into further details.

In agarose + sucrose/trehalose systems there is an increase in the elastic modulus of the 1% w/w agarose gel by adding 20% or 40% sugar, see figure 76, as already observed by Deszczyński *et al* (2003a, 2003b). The main features are due to the reduced amount of water and the thus increased effective concentration of agarose, but further ideas are important and necessary. The presence of sugars and other polyols may trigger the first step of the helix formation, as has been pointed out by Shimizu and Matubayasi (2014). Low-molecular-weight carbohydrates bind water in their hydrate shells. Less free water is able to surround the hydrocolloids, which may face a stronger interaction, and helix formation may become enhanced (see figure 75). On the other hand, it is important to compare the gels with equal polymer-to-water ratios with and without sugar molecules as co-solutes, which has been done in agarose gels with rescaled concentrations (Russ *et al* 2014).

Table 2. Gelling temperatures, T_{gel} .

	1.7%	+ 40% sucrose	+ 40% trehalose
Agarose	37.3 ± 0.3	38.5 ± 0.1	40.6 ± 0.1
Agarose + alginate	33.7 ± 1.0	34.2 ± 0.1	37.1 ± 0.1
Agarose + xanthan	34.4 ± 0.6	36.0 ± 1.1	38.8 ± 1.2

This comparison to agarose gels of a concentration corresponding to the effective concentration of agarose in the sugar-containing gel (1.25% and 1.7% for the two corresponding sugar concentrations) shows a decrease in elasticity with the addition of sucrose as well as trehalose as shown in figure 76. In fact, the addition of sugars triggers the helix formation but they also prevent the aggregation of the helices at lower temperatures. As a result, the sugar-containing gel remains softer and less stable. Pure xanthan with added sucrose or trehalose shows a similar behavior of the modulus, as can be seen from figure 76, whereas alginate shows the opposite behavior. It has the lowest viscosity/modulus for the rescaled sugar-free concentrations. Obviously, this cannot be explained solely by the water binding of the sugars themselves, but is also a result of the nature of the hydrocolloid, keeping in mind that agarose is polar (non-ionic) and gel-forming, whereas xanthan is charged and stiff, and alginate charged and flexible. Russ *et al* (2014) have argued that local entropic and energetic contributions need to be taken into account. The sugars ‘bind’ via hydrogen bonding preferably on flexible molecules such as alginate with a higher probability than on stiff rods such as xanthan for entropic reasons. Thus the sugars link alginic acid molecules to a very soft transient network. Sugars slightly weaken the interactions in xanthan solutions between the rods. These findings are consistent with experiments on gels including sugars and hydrocolloids. Kasapis *et al* (2003) demonstrated also a decrease in elasticity with sugar concentrations above 40% w/w, indicating a disaggregation of the polysaccharide. This is explained by the increasing shortage of water molecules, which additionally form stable hydrogen bonds with sugar molecules, and thus gradually deprive the polysaccharides of a hydration layer, which is required for the thermodynamic stability of intermolecular helices and the subsequent building of a network. The presence of sugars shifts the gelling temperatures due to the hydration shells as indicated in table 2. The effect of the different sugars on the moduli are summarized in figure 77.

The effect of trehalose is more pronounced than for sucrose for all experiments, which is another indication of the impact of the precise local structures of the low-molecular-weight sugars. The position and the orientation of the hydroxyl groups in the sugars play the important role. This can be explained because trehalose has a better ability to bind water molecules in its hydration shell than sucrose. The positions and orientation of the OH groups can be described by equatorial (e) and axial (a) groups (Angyal 1969). Thus, Branca *et al* (2001) identified a stronger interaction between trehalose and water by viscosity measurements. Dissolved trehalose molecules have a distinctive tendency to form hydrogen bonds due to their higher number of e-OH groups. According to Kawai

et al (1992) $n(e\text{-OH})$ per saccharide is 6.3 for sucrose and 8.0 for trehalose. In hydrocolloid solutions containing sugar molecules, water molecules favor the hydrogen bonding with sugar molecules from an entropic point of view, especially with trehalose. Figure 78 shows schematically the different interactions of sucrose and trehalose with the surrounding water molecules. Regarding the molecular structure of the two disaccharides, trehalose possesses more equatorially oriented OH groups than sucrose. The number of water molecules in the co-sphere is in proportion to the number of OH groups in the sugar molecules, and the e-OH groups are able to interact with water in a manner that forms a long-lived hydration structure, since they match the unperturbed water structure better (Uedaira *et al* 1989). The special linkage of the two glucose rings in the trehalose molecule provides solely equatorially arranged OH groups, which facilitates the accommodation of solute molecules within the H-bond network due to the small perturbation induced on surrounding water molecules, and leads to a higher hydration number for trehalose (Branca *et al* 2001, Fioretto *et al* 2013), which results in larger hydrate shells. Nishinari and Watase (1992) and Watase *et al* (1992) investigated the effects of different polyols and sugars on the sol-gel transition of κ -carrageenan or agarose gels. They also suggested different influences related to the number of equatorially attached OH groups in the sugar molecules.

12.9. Resulting culinary aspects: texture and mouth-feel

The non-equilibrium process of gel formation and the pronounced hysteresis have made agarose gels one of the stars in culinary applications. The gels are served warm or hot, which enhances the taste and the mouth-feel (Vilgis 2010). When set agarose gels are reheated, the network becomes looser and less elastic (see figure 68). Also the release of taste-relevant ions and the volatility of the aroma compounds released from the gels at higher temperatures provide an agreeable and pleasurable perception. In the example shown in figure 79 apple juice has been slightly reduced to enhance the taste and gelled after adding some sugar and yuzu juice with agar. One side has been coated with breadcrumbs and cinnamon and this side has been fried in butter. It can be served as a ‘physically driven’ dessert component (Vilgis 2009).

The mouth-feel can easily be influenced by changing the concentration. In gastronomy most of the gel preparations have concentrations around 1%. However, from the physical point of view gels can be prepared between 0.2% and 1%, which leads to a very different taste release and aroma perception. Gels close to 0.2% are close to the critical gel concentration and form very irregular and soft ‘bite pieces’ as shown in figure 80. This example visualizes the interplay between texture and decreasing water retention in gels with increasing concentration. The water-holding capacity in agarose gels with and without different sugars has been studied in detail in Russ *et al* (2014).

Different gelling agents, such as gellan gum (Morris *et al* 2012), κ - and ι -carrageenan (Campo *et al* 2009) provide different fracture properties, which again yield different mouth-feels, and these can be very well designed. The bite pieces have a different structure and different water retention at their

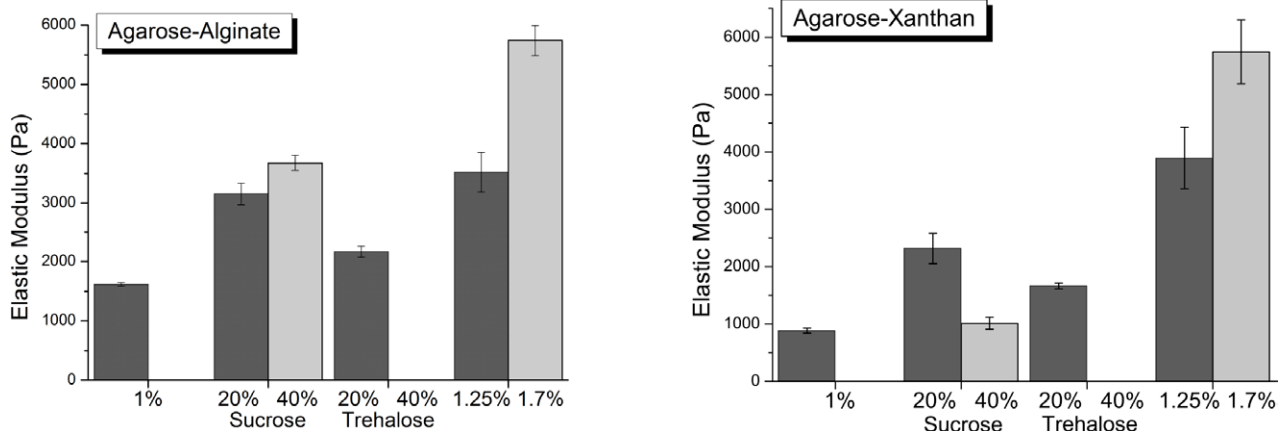


Figure 77. Moduli of the mixed gels with different sucrose and trehalose. From Russ *et al* (2014) with permission.

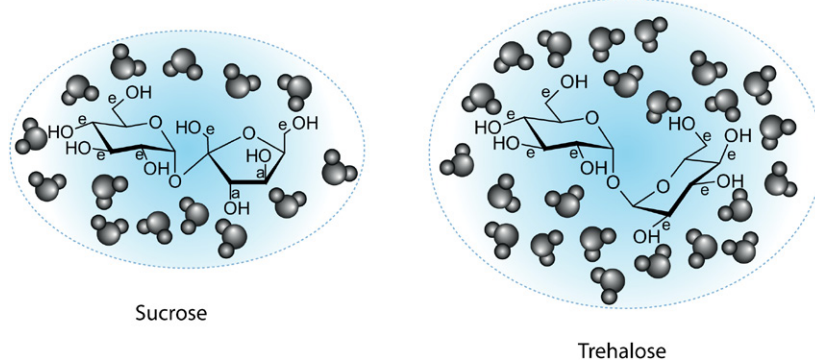


Figure 78. Axial (a) and equatorial (e) OH groups yield a different structuring of the water molecules in their surroundings. The hydration shell of trehalose is therefore larger.



Figure 79. Agarose gels (here spiced apple) can be fried in a buttered pan without melting.

surfaces, see figure 81. The gellan pieces appear dry from a brittle fracture, whereas ι -carrageenan melts under pressure. The κ -carrageenan behaves less elastically than agarose gels. Mills *et al* (2011) studied, for example, the salt release from different, well defined prepared gels from gelling agents as a function of time and temperature. These different properties make the application of gels in modern gastronomy very attractive. Chefs have several tools to control the impact on mouth-feel and sensory perception.

Other gastronomic applications with a scientific background are ‘fluid gels’ (Norton *et al* 2006). When a solid gel is destroyed in a blender to a puree, it has a well-defined ‘creamy-ness’ and a pleasurable smooth mouth-feel. The resulting

small particles slide upon each other, because the water on their surfaces acts as a lubricant between the individual gel particles. When the gels are broken, the surfaces of the particles are charged. The surface binds water via strong hydrogen bonding and lowers the friction between the gel particles, see figure 82(left). Alternatively, gels can be prepared under shear (de Carvalho and Djabourov 1997) at a given shear rate. The shear rate limits the size of the particles and provides a well defined mouth-feel. The average size of the particles can be estimated at low Pélet numbers by the Einstein diffusion of a particle of given size R within the time scale defined by the shear rate $\dot{\gamma}$ to be (West *et al* 1994, de Carvalho and Djabourov 1997).

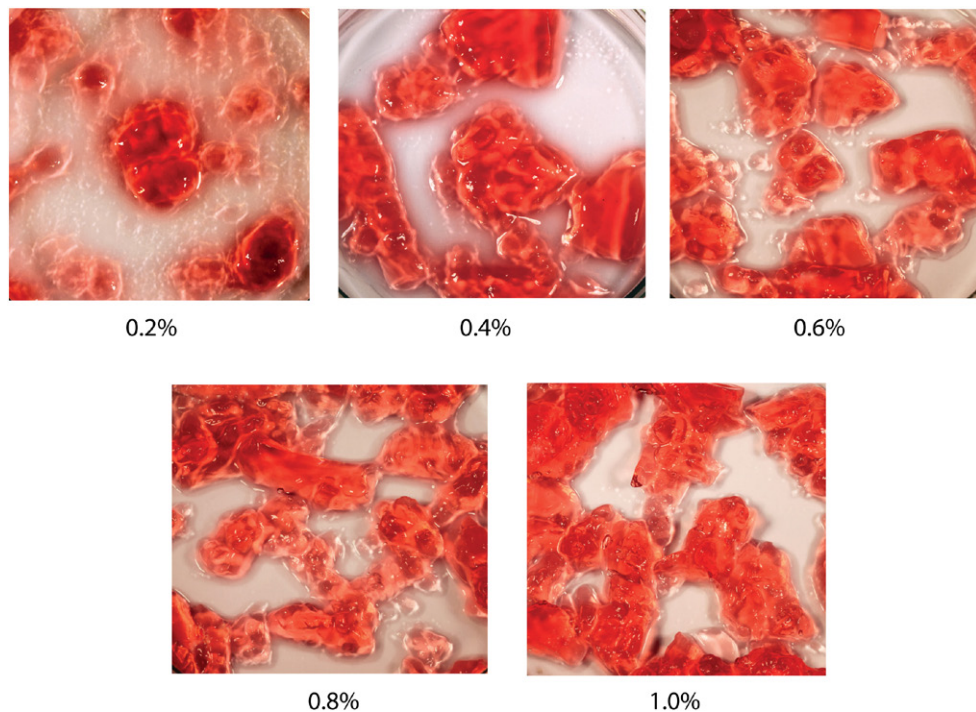


Figure 80. Bite pieces of agarose gels (unsweetened rosehip infusion) at different agarose concentrations. The free water at the surfaces of the pieces and their elasticity determine taste release and texture properties.

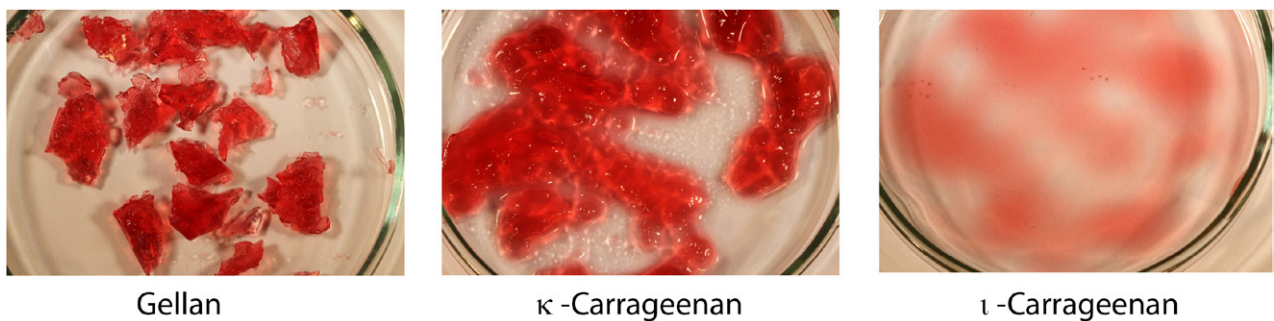


Figure 81. Bite pieces of gellan, κ - and ι -carrageenan gels. Each gel is free from sugar and salt and prepared with 1% of the gelling agent.

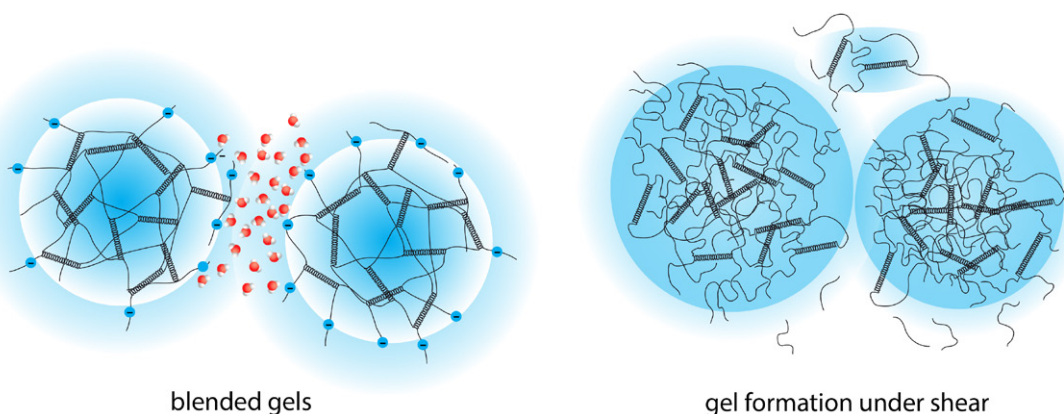


Figure 82. Formed gels (e.g. gellan or agarose) can be blended (left) to form a creamy structure with a pleasant mouth-feel. The water between the particles acts as a lubricant. Gelation under shear provides particle sizes defined by the shear rate (right).

Table 3. Typical food emulsifiers, their HLB values and their typical applications.

Emulsifier	Name	HLB	Typical applications
Phospholipids	PL	6–10	fat spreads, chocolate, bread
Mono-diglycerides	MG	2–5	margarine, whipped toppings, ice cream
Acetic acid esters of MG	ACETEM	7–8	fruits, nuts, pizza
Lactic acid ester of MG	LACTEM	7–8	baked products, whips
Citric acid ester of MG	CITREM	11	bakery, meat spreads, sauces
Diacetyl tartaric acid ester of MG	DATEM	7–8	bread, vegan product analogues
Polyglycerol ester of MG	PGE	5–7	icings, fillings, confectionery
Sodium stearoyl lactylate	SSL	10–15	bread, coffee whiteners, fat emulsions
Calcium stearoyl lactylate	CSL	5	bread, fat emulsions, cereals
Sucrose ester of fatty acids	—	6–15	sauces, sausages
Sorbitan monostearate	SMS	4–5	baking yeast, confectionery, ice cream
Polysorbate 60	PS60	15	forced fat crystallization, sauces

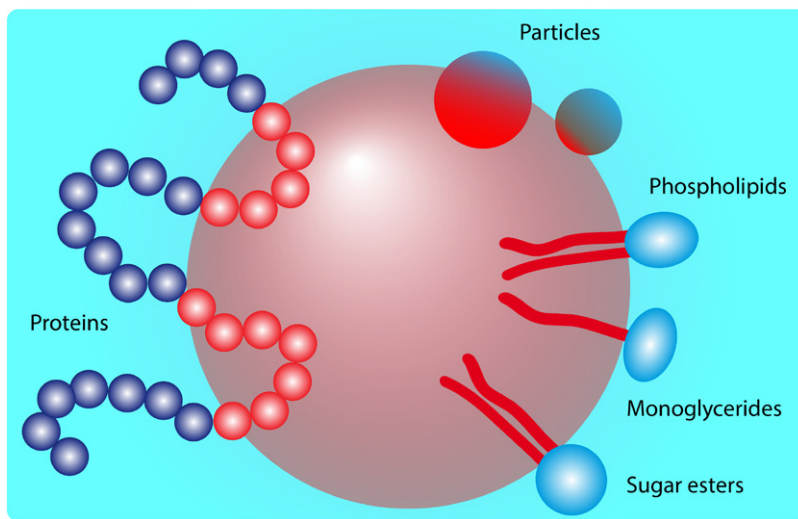


Figure 83. Schematic picture of the different types of emulsifiers arranged around an oil droplet. The hydrophilic head groups can be strongly polar (phospholipids), less polar (sugar esters) or weakly polar (monoglycerides). The particles can vary in size: some proteins are very useful emulsifiers due to their primary structure and sequence of hydrophilic/hydrophobic amino acids.

$$R \approx \left(\frac{k_B T}{6\pi\eta_s \gamma} \right)^{1/3} \quad (40)$$

where η_s is the viscosity of the sol phase.

Such considerations may appear oversimplified, but rheological and frictional properties in foods are essential during eating (Le Révérend *et al* 2010). Gels may serve as simple physical model systems to understand better the behavior of water-rich and structured foods in the mouth.

13. Emulsions and natural emulsions

13.1. General remarks

Foods are interface-dominated materials (Fischer and Windhab 2011, Israelachvili 2011). As already mentioned in the introduction most foods consist of carbohydrates, proteins, fat/oil and water as basic structural components. Oil and water do not mix; they are separated by interfaces, as for example in emulsions (Dickinson 1987, Dickinson *et al* 1988, McClements 1999, Friberg *et al* 2003, Norn 2014), foams (Prins *et al* 1988, Dickinson 2010), dairy foams (Anderson *et al* 1988, Allen *et al* 2006), dry foams like bread (della Valle

et al 2014) or complicated mixed systems like ice cream (Goff 1997b), which contains fat in liquid and solid phases, aqueous phases, solid, liquid and glassy water, sugars and proteins (Goff and Hartel 2013). Fat or meat spreads, margarine and iced foods (Heertje 2014) are other examples of interface-dominated food systems. Special attention is drawn to particle-stabilized emulsions (Dickinson 1987, Dickinson *et al* 1988, Frijters *et al* 2014), known also by the name Pickering emulsions (Sacanna *et al* 2007), which have a number of new applications in food systems (Dickinson 2010, Pawar *et al* 2011, Timgren *et al* 2011, Kargar *et al* 2012). Other aspects are multiple emulsions (Dickinson 2011, Muschiolik 2007), some with functional properties (Dagleish 2006, Weiss *et al* 2006). The detailed role of water in biological systems needs to be considered (Israelachvili and Wennerström 1996), as already pointed out in the previous section.

Emulsions can be classified into oil-in-water (O/W) emulsions and the ‘inverse’, water-in-oil (W/O) emulsions. In O/W emulsions, water is the continuous phase, oil the dispersed phase; in W/O emulsions it is vice versa. Most food emulsions belong to the O/W class, which means that the emulsifiers are first dissolved in the water phase before the oil is added while stirring. From that it follows that W/O emulsions require fat-soluble emulsifiers. Such requirements are of special interest for

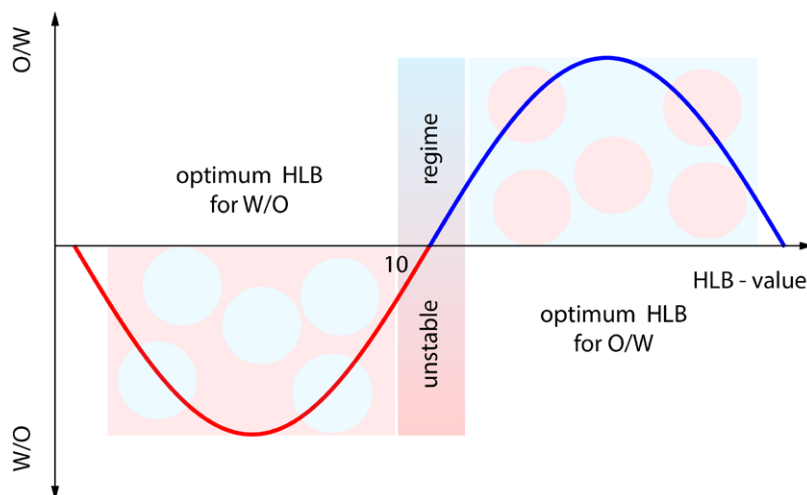


Figure 84. The HLB values discriminate between different types of emulsion. Emulsifiers with low HLB values can be used for W/O emulsions whereas emulsifiers with larger (than 10) HLB values are suitable for O/W emulsions.

multiple emulsions, i.e. O/W/O or W/O/W emulsions (or even of higher orders), where the oil droplets are themselves so-called ‘inverse emulsions’ (Matsumoto 1986, Garti 1997, Muschiolik 2007, Dickinson 2011, Sapei *et al* 2012, Jiménez-Colmenero 2013) for taste, aroma or textural improvements, or alternatively for functionally controlled drug release in pharmaceuticals.

13.2. Emulsifiers, classical emulsions in foods

In food systems a number of different emulsifiers are available (see figure 83). Best known are phospholipids (lecithin) from membranes, which carry two fatty acids and a polar or charged head group (Whitehurst 2008). Other emulsifiers are mono- and diglycerides, originating from triacylglycerols, where one or two fatty acids have been removed by enzymatic digestion (Krog 1977). Sugar esters carry fatty acids with sugars or polyols (Lauridsen 1976). These emulsifiers have a common structure: they contain small water-soluble groups and long-chain fatty acids. The different water solubilities of the head groups depend on the strength of polarity, charge and chemical structure (see section 12.8) so that the balance between the hydrophilicity of the head group and the lipophilicity of the fatty acids determines the action and strength of the emulsifier. The differences in the emulsifiers are measured with the so-called HLB value, which defines empirically the hydrophilic–lipophilic balance. The HLB concept appears empirical but turns out to be very useful for practical applications. The physical motivation is simple: the balance between the hydrophilic and lipophilic (hydrophobic) interactions of a surfactant is given by the polarity of the hydrophilic group, the length/molecular weight (and degree of saturation, see section 4) of the fatty acids and their solubility in the corresponding fatty/oily environment. The latter is determined by the mismatch of the molecular properties of the fatty acids of the emulsifier and the oil. Therefore, two basic equations for the HLB value have been proposed. Firstly, Griffith suggested for non-polar/ionic emulsifiers the equation

$$\text{HLB} = 20 \left(1 - \frac{M_h}{M} \right) \equiv 20 \frac{M_h}{M}, \quad (41)$$

where M_l and M_h are the molecular weights of the lipophilic and the hydrophilic groups, respectively, and $M = M_l + M_h$ the total molecular weight. This heuristic definition of the HLB value appears incomplete, because it only takes the size of the different groups into account. Alternatively, Davis proposed to consider the corresponding enthalpies of the different groups,

$$\text{HLB} = 7 + mN_h - nN_l, \quad (42)$$

where N_h and N_l describe the relative solubilities of the hydrophilic and lipophilic groups. The values m and n denote the number of times they appear in the emulsifier molecule. Both equations are empirical and need refinement by more elaborate physical and quantum chemical computations (Little 1978, Nakai 1983, Vaughan and Rice 1990, Hu *et al* 2010).

The HLB concept (for more discussions, see e.g. (Boyd *et al* 1972, O’Lenick and Parkinson 1996)) allows at least a general (rough) idea about the classification of emulsions. Low HLB values describe oil-soluble emulsifiers, which can be used to produce W/O emulsions. HLB values above 10 indicate stable O/W emulsions, as is indicated in figure 84. Often HLB values of around 10 do not produce long-term stable emulsions. This, however, depends on the precise nature of the water phase, e.g. ionic strength and pH value, and the oil phase, e.g. length and degree of saturation of the fatty acids used, and molecular mobility at the temperature of use. Indeed, the structure of the triacylglycerols of the oil phase and their molecular mobility become important, for example, when they crystallize partially, as is the case in margarine or butter.

Another stabilizing factor for O/W emulsions is the viscosity of the continuous water phase. Highly viscous emulsions are more stable; therefore, the long-term stability of food and cosmetic emulsions is ensured by the addition of thickening agents such as xanthan gum, guar gum or carrageenans, which contribute also to the ‘thickness’ and ‘creaminess’ of O/W emulsions (Akhtar *et al* 2005).

Typical food emulsifiers, their HLB values and their typical applications in various aspects of food technology are listed in table 4. The HLB values have been taken from Bennion *et al*

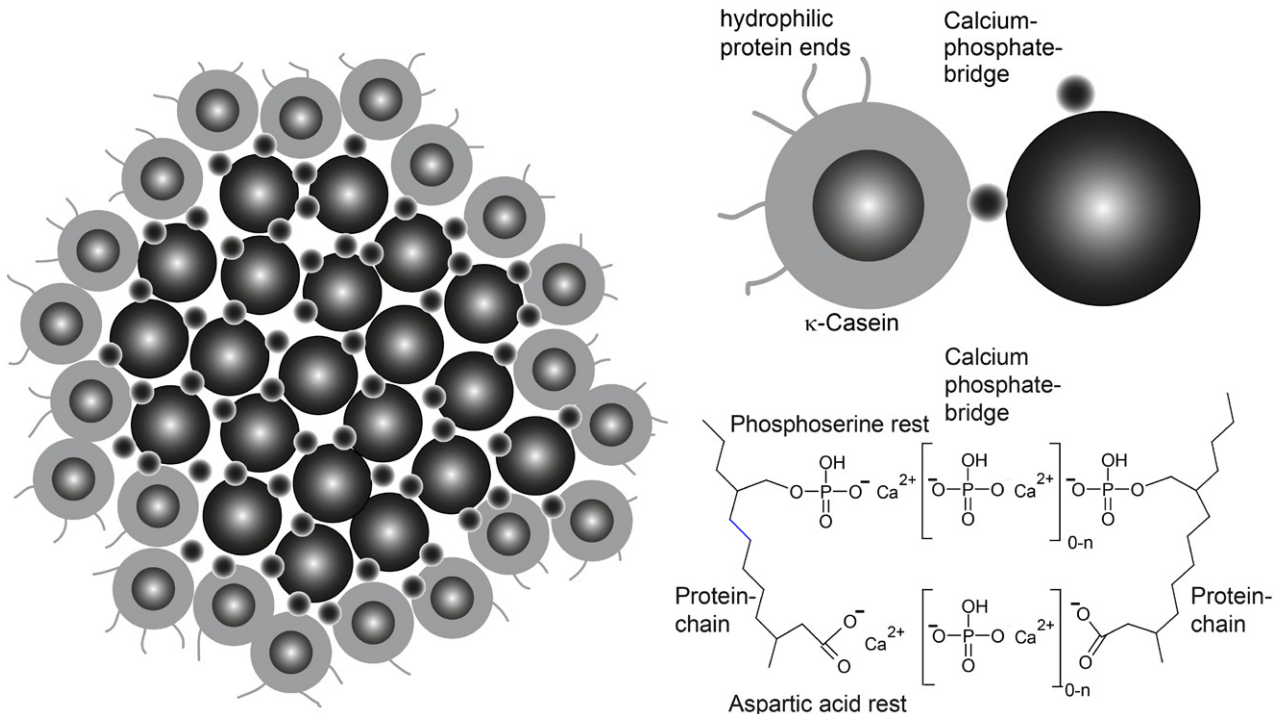


Figure 85. Schematic cartoon of the the classical model for casein micelles in raw (cow's) milk. The casein is bound by calcium phosphate bridges to micelles of about 120 nm size.

(1997), Leser *et al* (2006), Smith (1991) and Norn (2014). Indeed these emulsifiers can be used for home cooking to produce emulsions with special properties, ‘creaminess’, structures, textures and thus mouth-feel. The self-assembly of polar food lipids has been studied in detail by Leser *et al* (2006), Sagalowicz *et al* (2006), where the corresponding phase diagrams are discussed in detail.

The distribution of the droplet sizes itself is important for rheological properties (Mason *et al* 1996, Pal 1996, Malkin *et al* 2004) and thus for the mouth-feel and the textural perception (Truong *et al* 2014). For highly concentrated emulsions jamming takes place and dominates their shear properties (Clusel *et al* 2009) and the oral processing of cream-like or ‘semi-solid’ texture (Prinz *et al* 2007).

13.3. Natural animal emulsions: milk and egg yolks

Nature itself uses emulsions, which are so far unbeatable in structure, stability and application in food physics, and consequently in culinary use. Well-known examples are milk (Walstra *et al* 1984, Dalgleish and Corredig 2012), oil seeds and nuts (Huang 1992, Waschatko 2013) or egg yolks (Anton 2013). Natural raw milk is an emulsion, which contains water (whey), globular proteins dissolved in water, casein micelles and fat particles (Walstra *et al* 1984, 1999, Kanekanian 2005, Dalgleish and Corredig 2012). The casein micelles contain different proteins, which organize themselves into connected globules as shown schematically in figure 85. The casein micelles consist of large hydrophobic submicelles of α - and β -casein (dark circles in figure 85), which are connected via ionic interactions by colloidal calcium phosphate clusters. The outer shell consists of hydrophilic κ -caseins, which ensure

stability by negative net charges at pH values >4 . Their size has been determined by scattering methods to be 121 nm by De Kruif *et al* (2012), where it was also shown that the matrix inside the casein micelles is more or less homogeneous, and that the casein phosphate nanoclusters show a mean separation of 18 nm and a mean radius of 1–2 nm. The fat particles in raw milk are much larger: their average size is about 3 μm , but with a very broad distribution, which ranges from 1 μm to 20 μm and depends strongly on the diet, feed and race of the animal (Wiking *et al* 2004). From the physics point of view the structure of the fat globules is interesting. Milk fat contains a very broad distribution of triacylglycerols (TAG), which are composed of fatty acids ranging from C 4:0 up to C 18:0, and also contains unsaturated fatty acids C 18:1, C 18:3 and C 20:4 (Jensen *et al* 1991, Michalski 2009); the precise composition and distribution depend again on the feed. This broad distribution of fatty acids induces solid and liquid phases in the fat globules, which are partially crystalline. The solid phase forms a crystal layer at the perimeter of the fat globules whereas the liquid blend remains in the core at typical consumption temperatures of 4 °C (Lopez *et al* 2002, Michalski *et al* 2004, Lopez 2005). The triple layer of phospholipids also ensures stability of the fat globules even at high temperatures during processing or cooking, when the TAGs melt in the globule. Obviously nature selects a larger number of phospholipids with low HLB value, which show a higher fat solubility.

The broad size distribution of the fat globules in native milk implies creaming (Mulder and Walstra 1974, Walstra *et al* 1999). After some time natural milk shows a substantial cream layer at the top. The creaming velocity v of the fat globules can be simply estimated by classical Stokes theory:

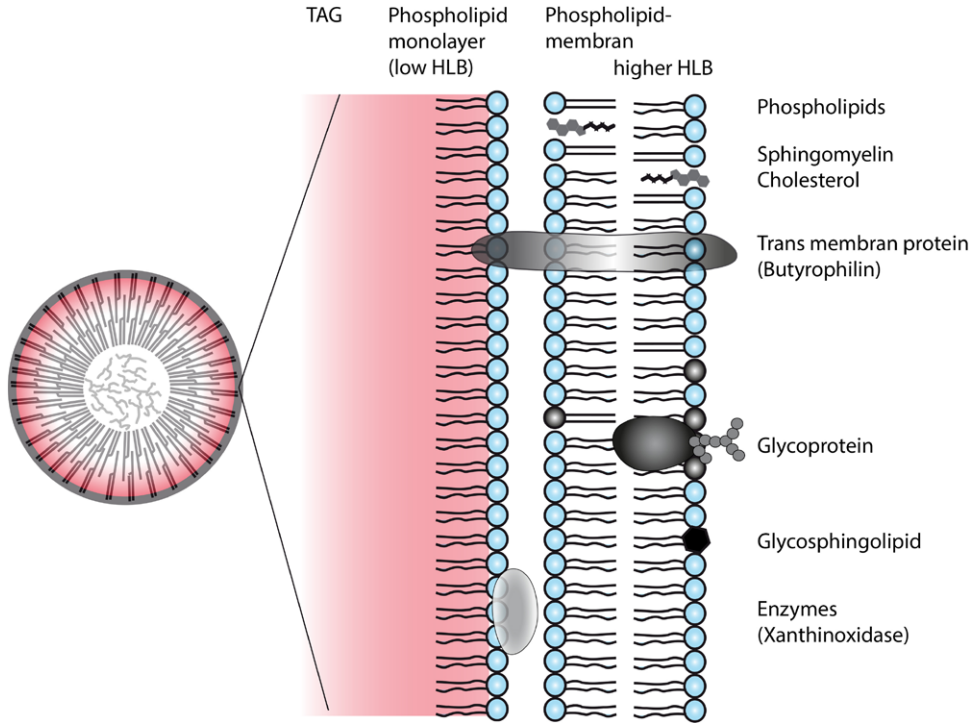


Figure 86. Semicrystalline milk fat globules (left); the liquid kernel also contains cholesterol esters. Their surface is covered with a monolayer of phospholipids of low HLB value and a membrane (double layer) which contains membrane proteins, glycoproteins and cholesterol, which defines the local flexibility and stability of the membrane.

$$\nu = \frac{2g}{9\eta}(\rho_{\text{fat}} - \rho_{\text{whey}})R^2 \quad (43)$$

where g is the gravitational acceleration, η the temperature-dependent viscosity of the whey, $\rho_{\text{fat}} = 0.9 \text{ g l}^{-1}$ the density of the fat globules, $\rho_{\text{whey}} \approx 1.02 \text{ g l}^{-1}$ the density of the whey (milk serum) and R the size of the fat globules; consequently larger particles show a higher creaming viscosity. However, during creaming fat globules may stick together by cold agglutination (Walstra 1995, Huppertz and Kelly 2006) and become larger in size, which makes the size R time-dependent. The agglutination process is more pronounced at low temperatures (e.g. in refrigerators) than at higher temperatures. The real creaming rate of the fat globules appears considerably higher as described by Stokes' law. The clustering of milk fat globules during cold storage resembles the agglutination of bacteria or red blood cells, due to the action of the immunoglobulin IgM, in terms of dependence on pH, concentration and valency of cations. Hence, the clustering of milk fat globules in the cold is referred to as cold agglutination, as was remarked by Huppertz and Kelly (2006). The physics of the creaming process depends on the temperature and can be used technologically for fractionation of raw milk (Ma and Barbano 2000).

To prevent creaming (e.g. for shelf stability), milk is homogenized. By pressing native milk through thin pores the maximum size of the fat globules is forced to be $R < 1 \mu\text{m}$. The high shear rate has strong effects on the interface of the fat particles. The membrane (see figure 86) gets ruptured and parts of the casein micelles become localized at the interface. The smaller size slows the creaming rate down, and the hydrophilic parts of the casein micelles ensure electrostatic

contributions to the stability of the homogenized milk as indicated in figure 87.

Another example of natural emulsions are hen's egg yolks (Strixner *et al* 2014). The state of the art of the egg yolk has recently been reviewed by Anton (2013). Fat globules, known as low density lipoproteins (LDL) and high density lipoproteins (HDL), are embedded in different hydrophilic matrices and structural levels. Yolk consists of soluble proteins and insoluble protein aggregates (granules) which are suspended in the plasma containing LDL. Plasma and granules can be easily separated by centrifugation. The granules contain 50% of the egg yolk proteins, phosvitin (Samaraweera *et al* 2011), the egg yolk lipids, which form the HDL droplets, see figure 88. They are ionically connected also by calcium phosphate bridges. The plasma consists of the LDL droplets and hydrophilic proteins, i.e. livetins (Anton and Gandemer 1997, Dauphas *et al* 2006, Anton 2013). Granules are composed of spherical complexes ranging in diameter from 0.3 to 2 μm , whereas the LDLs are spherical nanoparticles with sizes between 17 nm and 60 nm. For the context of this review, the structure of LDL is important. The fat globules of milk, triacylglycerides (and cholesterol esters), are bound to droplets and stabilized by phospholipids and apolipoproteins as surfactants. In contrast, the LDL droplets are surrounded by a monolayer of phospholipids, additionally stabilized by apolipoproteins, which are localized close to the interface, defined by the hydrophilic phospholipid heads, as shown schematically in figure 89. In different regions of the surface the apolipoproteins have different secondary conformations and structural elements, such as α -helices and β -sheets (Hevonoja *et al* 2000), to adjust to the hydrophilic and lipophilic nature of the interface boundary.

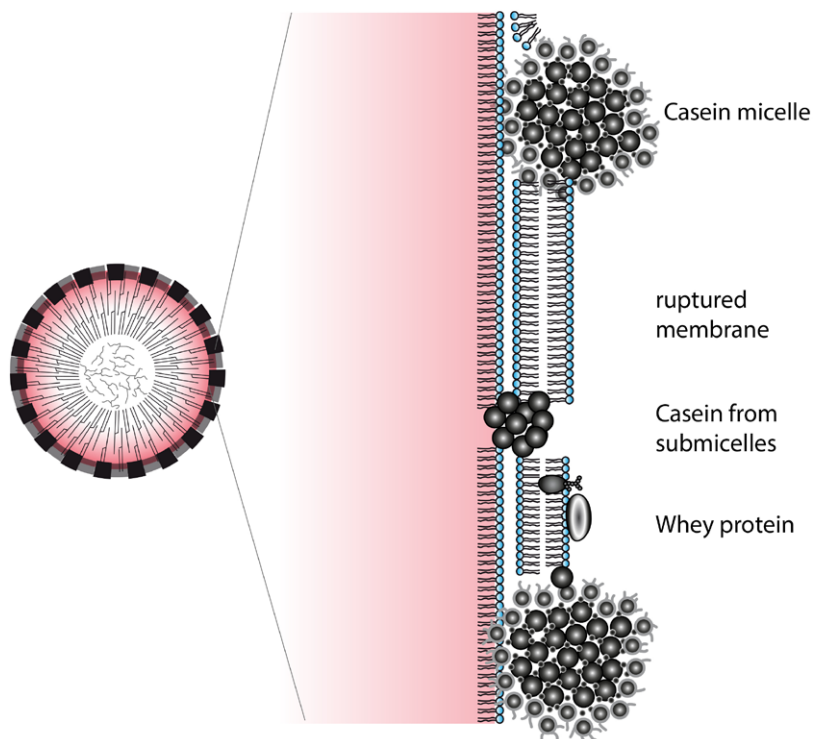


Figure 87. Schematic illustration of the interface of fat globules in homogenized milk. The stability of the emulsion is ensured by additional electrostatic repulsion of the casein micelles localized in the ruptured membrane.

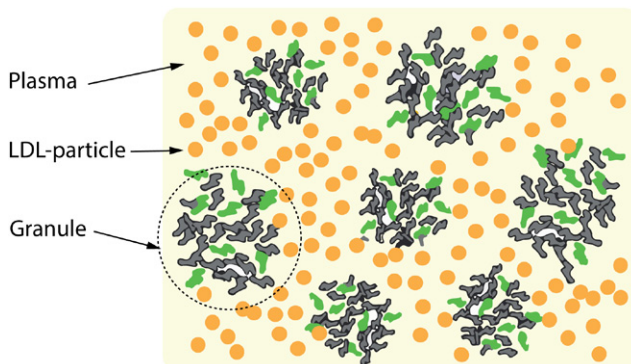


Figure 88. Illustration of the different scales in hen's egg yolks, which consist of granules (HDL and phosvitin) and the plasma that contains the LDL particles. Reproduced from Anton 2013 with permission.

Of special interest is the behavior of LDL particles at air–water interfaces, i.e. the study of their stability and phase behavior and their adsorption mechanisms (Anton 2013). These investigations can be carried out by Langmuir film balance experiments in combination with scattering and (Brewster angle) microscopic techniques, which show the concentration of LDL at the air–water interface, a technique that has been widely developed in the context of lipids, phospholipids and other surfactants (Lösche *et al* 1983, Miller *et al* 1986, Helm *et al* 1987, Kjaer *et al* 1987, Hönig and Möbius 1992, Brezesinski *et al* 1995). When emulsions (or lipid solutions) are immersed in the water sub-phase in the Langmuir tray, the lipids spread over the air–water interface into monolayers and form different phases, depending on the concentration and the pressure. For small concentrations (small pressures) the lipids form 2D gas-like phases, where

the mean distance between the lipids is large and quasi-free motion is ensured. Under compression liquid-like phases appear. The distance between the molecules becomes smaller, but the tails of the fatty acids are still disordered (molten). At high concentrations, the fatty acids of the lipids tilt and form gel and crystalline phases.

In contrast to simple (e.g. phospholipid-stabilized) emulsions, the surface of LDL droplets contains proteins; the droplets open at the interface and liberate their contents. Hydrophobic and amphiphilic molecules such as triacylglycerides, phospholipids, cholesterol and proteins are distributed on the surface. Depending on the pH value and ionic strength, proteins adsorb in different conformations at the interface, and the phase behavior is expected to be much richer. The basic process is shown schematically in figure 90. The complete phase diagram as a function of the ionic strength (using sodium chloride as monovalent salt) and the pH values been reported by Anton (2013). It is shown that at low pH values and low salt concentration only insoluble micelles ($1\text{--}8 \mu\text{m}$) appear. At higher salt concentration and pH values (larger than 7 above 0.75 mg l^{-1}) soluble micelles at about 200 nm are formed. At intermediate pH values and salt concentrations, small insoluble micelles coexist with the large micelles. It was also shown that extracted phosvitins undergo a phase transition from a loop structure, where the hydrophobic parts of the protein are localized at the interface, to a brush-like structure at higher pressures (Castellani *et al* 2006).

The different proteins forming the plasma content and granules show a very sensitive temperature dependence and enable a broad variety of textures (Vilgis 2010, Vega and Mercadé-Prieto 2011), which is of special interest in culinary science, confectioneries and sauces.

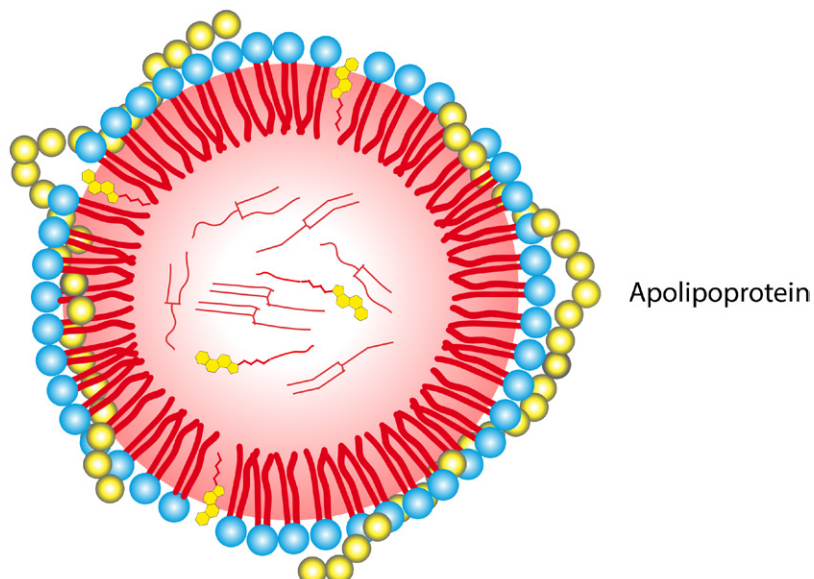


Figure 89. LDL particles are stabilized by a monolayer of phospholipids (with cholesterol) and surrounding apolipoproteins (drawn in yellow), which are localised close to the interface of the nanodroplets.

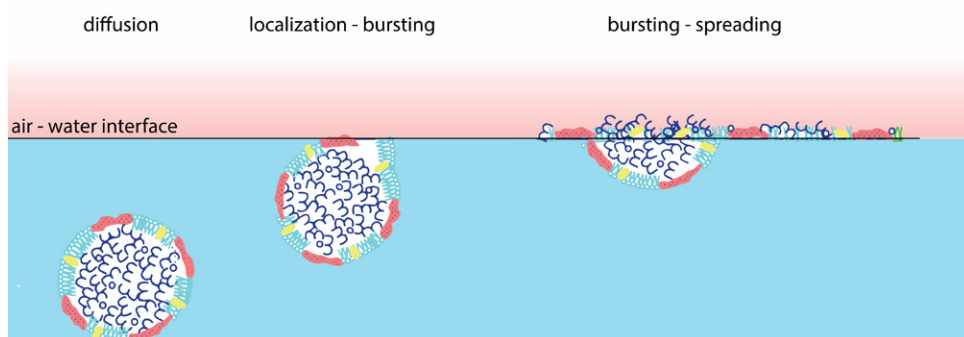


Figure 90. LDL particles at an air–water interface. The particles diffuse to the surface, where the hydrophobic parts anchor and localize. The droplet breaks up and the contents spread over the surface. (Redrawn from Anton (2013) with permission.)

13.4. Oleosomes

Important and so far less investigated natural emulsions are found in leguminous plants and oil seeds. Following Maurer (2014) for the next paragraphs, oleaginous plants (e.g. olives, lupines, soy beans), pseudo-cereals (amaranth) and oil seeds (peanuts, linseeds, sesame seeds, walnuts, ...) require a high energy input for germination, establishment of seedlings and biosynthesis. For their energy supply, neutral lipids are accumulated in plant tissue cells in the form of sub-cellular, micellae-like organelles, also referred to as oleosomes or oil bodies.

Integral or peripheral proteins and phospholipids, which form an intermediate monolayer between protein and lipid matrix, encapsulate the oleosomes. Proteins and phospholipids serve as surfactants, thus emulsifying the abundant hydrophobic lipids, mainly triacylglyceroles (TAG) and sterol esters, into relatively small hydrophilic oil droplets (Huang 1992, Frandsen *et al* 2001). In addition to phospholipids, oleosins play a major role in the oleosome stabilization, as well as in mobilization and degradation of oleosomes during active plant metabolism. Their amphiphilic N- and C-terminal

domains anchored by a hydrophobic domain in the oil matrix completely cover the oleosome surface. Oleosins partition into spherical individual entities with a high surface-to-volume ratio, and thus prevent droplets from coalescing and acting as lipase receptors during TAG hydrolysis. Partitioning of TAG into highly stable oil droplets helps plants to withstand periods of drought, coolness, rehydration and heating for months or years before the stored oleosomes are mobilized and degraded for the plant growth (Huang 1996, Frandsen *et al* 2001, Purkrtova *et al* 2008).

The size of oleosomes varies from 0.2 to 2 μm , depending on the nature of the oil seed. The size is also governed by the primary structure of the oleosin and thus by the oleosin-to-oil ratio that is mainly influenced by synthesis of oleosin in the respective plant species, as well as by environmental and nutritional conditions (Ting *et al* 1996, Siloto *et al* 2006). Tzen *et al* (1993) correlated the oleosome constituents with the size of oleosomes, which leads to structural insight into the oil particles. It has been shown that the amount of oleosin decreases with increasing oleosome size. Oleosomes of sesame seeds possess 0.57% protein and 97.37% oil at an average size of

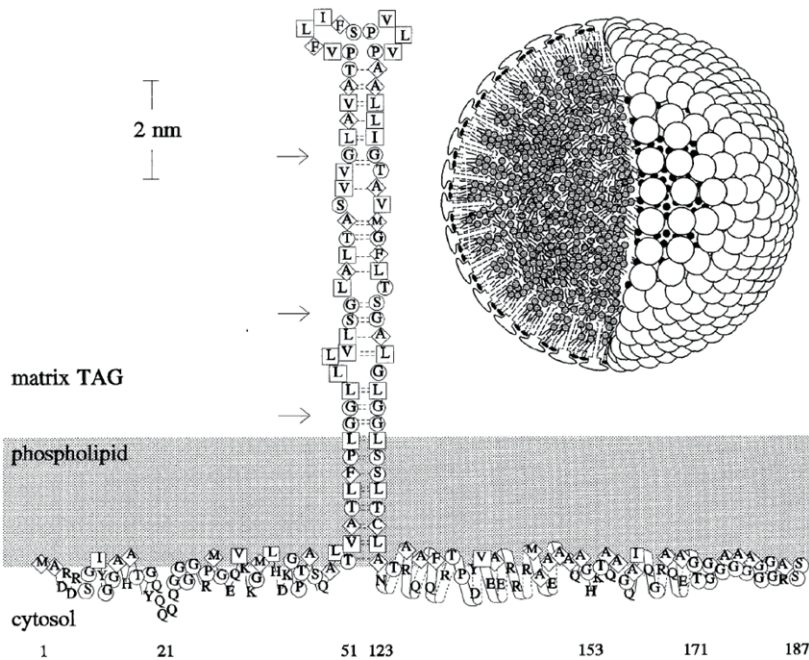


Figure 91. Current model of oleosomes (Huang 1996). The spherical particles are stabilized by phospholipids and specially folded proteins (oleosins) which stick into the oil phase with a long hairpin-shaped part.

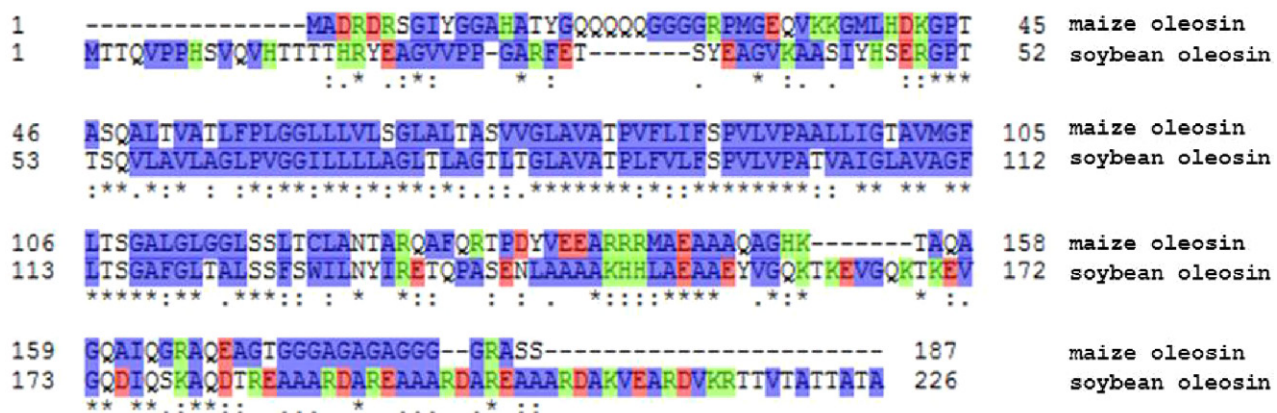


Figure 92. Primary structure of the oleosomes (TheUniProtConsortium 2014). The hydrophobic amino acids are shown in blue. The amino acids are abbreviated using the one-letter code (see figure 20).

2 µm, whereas rape seed oleosomes are composed of 3.46% protein and 94.21% oil at a size of 0.65 µm. The modulation of oleosome size by the oleosin level and thus the variation in the surface-to-volume ratio of the oleosomes is supposed to correlate with the physiological state of oleosomes during seed maturation and germination and plays an important role in the resistance of seeds to environmental stress factors (Siloto *et al* 2006, Purkrtova *et al* 2008, Shimada and Hara-Nishimura 2010, Jolivet *et al* 2011).

The structure of the oleosins and oleosomes is remarkable. Huang (1992) did pioneering work by modeling a whole maize germ oleosome with an unusual structure of oleosins in comparison to other proteins found in nature (figure 91). Its primary structure with the long hydrophobic sequences is shown in figure 92. The oleosin structure model is also based on theoretical assumptions supported by microscopic observations and preliminary sequence analysis by cDNA cloning tests. However, the model is confirmed by more profound

proteomic analysis of, e.g., rice oleosomes (Chuang *et al* 1996) and peanut oleosins (Cabanos *et al* 2011). Apart from the hydrophilic groups of oleosin, phospholipids and free fatty acids also contribute to the hydrophilic oleosome surface (Huang 1992).

The model for the structure of oleosomes is presented schematically in figure 93 and shows another way how nature stabilizes nano- and microemulsions (Waschatko *et al* 2012, Maurer *et al* 2013). Fat globules in milk are stabilized without direct interactions with proteins. A triple phospholipid layer is sufficient to provide thermal stability of the milk up to cooking temperatures, but is unstable under high shear stress (for example during homogenization processes). LDL particles in egg yolks involve a monolayer of phospholipids and different proteins that provide stable emulsions below a temperature of 63 °C, when the yolk begins to show an increase in viscosity by the denaturation of proteins (Vega and Mercadé-Prieto 2011). Oleosins contribute significantly

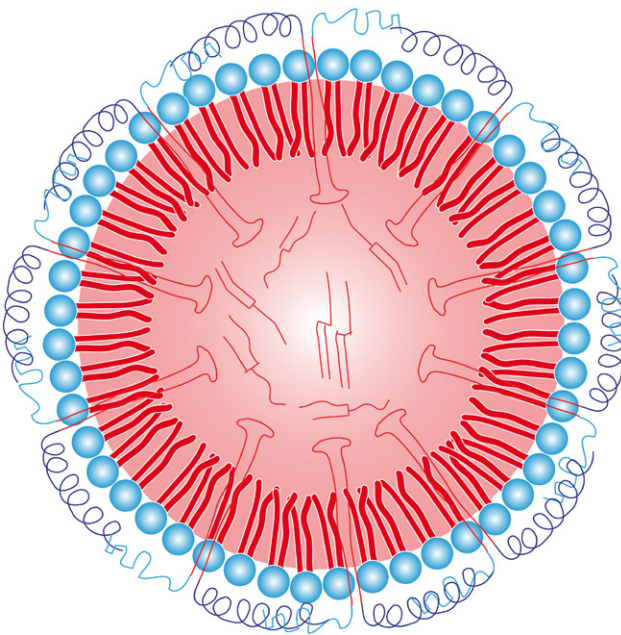


Figure 93. Schematic picture of the oleosome, stabilized with a phospholipid monolayer and oleosins.

to the extraordinary stability under changes of temperature and shear rates.

However, cleavage of the N- and C-terminal domains by protease digestion, yielding unstable oleosomes prone to coalescence, suggests that emulsifying and stabilizing properties are rather due to the peripheral amphiphatic than to the hydrophobic domains (Lacey *et al* 1998). Accordingly, stabilization of oleosomes by oleosins occurs via steric hindrance and electrostatic repulsion (Capuano *et al* 2007, Shimada and Haranishimura 2010).

The precise secondary structure of the hydrophobic part pointing in the oil phase of the oleosome is still under debate. According to the (theoretical) model shown in figure 91, an antiparallel β -sheet structure penetrating into the TAG matrix and stabilized by interstrand hydrogen bonding between adjacent pairing amino acid residues is suggested from information derived from circular dichroism (CD) and conventional secondary structure predictions based on the primary sequence. The formation into antiparallel β -sheets is attributed to the ‘proline-knot’ motif that acts as a loop folding back the β -strand. A relatively short sequence of 30–60 amino acids residues on the site of the C-terminus and close to the central domain is assigned to be α -helical. The secondary structure of the N-terminal domain could not be specified due to insufficient information about its sequence (Huang 1992, Tzen and Huang 1992). Results from CD and Fourier-transformed infrared spectroscopy (FTIR) measurements of oleosins from rape seeds (Li *et al* 1993) and peanuts (Jacks *et al* 1990) were consistent with this secondary structure prediction.

To facilitate a more refined secondary structure analysis, other researchers analysed only the hydrophobic domain from rape seed oleosin isolated by SDS-PAGE (sodium dodecyl sulfate polyacrylamide gel electrophoresis) and enzymatic digestion. Predominantly parallel intermolecular β -sheets (51%) were obtained with minor amounts of antiparallel structure

(12%) as revealed by CD and FTIR (Li *et al* 2002). A contribution of the ‘proline-knot’ to the topology of the oleosin structure is not assumed but rather its function in targeting oleosins into oleosomes during synthesis. A similar thing was done with the N-terminal domain expressed in *Escherichia coli* as a recombinant fusion protein (Li *et al* 1993). Reconstituted in liposomes, here regarded as the closest approximation to the oleosin situation *in vivo*, the N-terminal domain contains only a few α -helices, some random coil and mostly β -sheet structural elements. Comparative analysis of purified and reconstituted N-terminal domains demonstrated that structural changes occur by embedding them in the respective environment. Secondary structure analysis is recommended to be best performed in the natural environment of oleosins, respectively its domains. Here, N- and C-terminal domains of different origin are expected to adopt similar structures, which is probably not the case under other conditions due to variations in amino acid sequences among species (Li *et al* 1993). Secondary structure analysis by Lacey *et al* (1998) also considered a higher content of β -sheet structures in the N-terminal domain as likely but disagreed that the hydrophobic domain predominantly consists of β -sheets, either parallel or antiparallel. Instead, protease treatment of oleosins, both of sunflower and safflower, revealed distinct contents of α -helical structures, which is in accordance with early studies by Millichip *et al* (1996).

13.5. Interfacial behavior

Lipid droplets, such as oleosomes, fat milk globules and animal lipoprotein particles, are found to be ubiquitous in biological organisms, from prokaryotes to mammals and plants. All these droplets have something in common: the very hydrophobic lipid core is surrounded by a layer or layers of emulsifiers that keep lipid droplets suspended and stable against aggregation and coalescence. The emulsifiers are phospholipids and proteins or peptides with a hydrophobic–hydrophilic ‘block structure’ (Small *et al* 2009). A major difference between oleosomes and other lipid droplets is the unique structure of oleosins, which are structurally reminiscent of a chain surfactant (Vargo *et al* 2012).

Experimental approaches reported in the literature are diverse and controversially debated. Research on the interfacial behavior of oleosins is critical as the oleosin is strongly associated with the oleosome and isolation of them can result in structural conformation changes and in the formation of insoluble aggregates (Sessions *et al* 2002, Roux *et al* 2004). Although the isolation of oleosin not simple, it is of great interest to understand the interfacial behavior of pure oleosins in order to clarify their role in the stabilization and biological function of oleosomes. Furthermore, solutions of pure oleosins allow the emulsifying properties of oleosins to be assessed in comparison with other, commonly used proteins. Deleu *et al* (2010) focused on the emulsifying and oleosome-stabilizing properties of oleosins and phospholipids, both isolated from rape seeds, in relation to the competing effects of both with regard to their adsorption kinetics and interfacial rheological properties at the oil–water interface. Nikiforidis *et al* (2011)

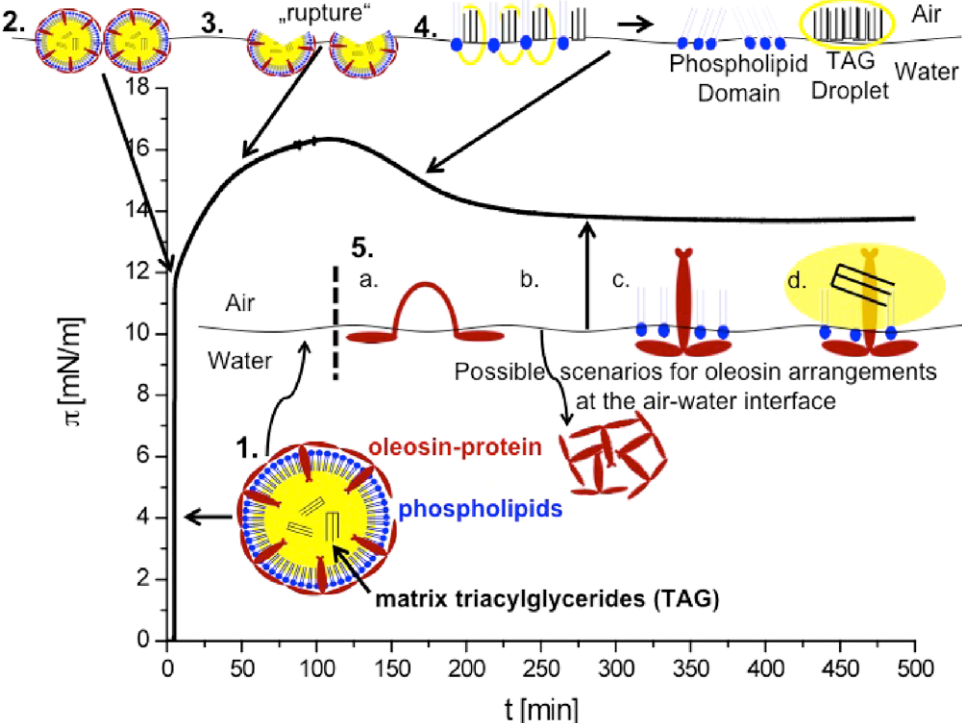


Figure 94. Schematic representation of the behavior of the oleosomes at the air–water-interface.

investigated the foaming properties of isolated maize germ oleosins by analyzing their surface activity and viscoelasticity at the air–water interface. In both studies, organic solvents are used for oleosin, respectively phospholipid isolation. Since organic solvents are considered to be detrimental for the oleosin structure, Roux *et al* (2004) analysed the interfacial properties of bacterially expressed oleosins from *Arabidopsis thaliana* at the oil–water interface of recombined oleosomes. The challenging task that all researchers have to deal with is the poor solubility of oleosins in aqueous solutions due to their long hydrophobic domain. However, to best mimic the natural environment of oleosin, the oleosome, the analysis of emulsifying and stabilizing properties of oleosins in aqueous solutions is indispensable. Despite the constraints with regard to solubilization of oleosins, the studies reached the conclusions that (i) adsorption of oleosins is very important for the stability of oleosomes and (ii) excesses of phospholipids at surfaces lead to droplet coalescence due to reduced steric repulsion forces provided by oleosins (Deleu *et al* 2010). The reduction in surface tension and the formation of relatively highly viscoelastic surface films are mainly based on synergistic effects between oleosins and phospholipids (Roux *et al* 2004, Deleu *et al* 2010). In general, oleosins are considered to have very good emulsifying properties, if not better ones than other proteins such as milk proteins. Adsorption of oleosins to the drop surface of a rape seed oil model occurred faster than is observed for lactoglobulin and casein, presumably to due the less globular and smaller, and thus more flexible, structure of oleosins (Deleu *et al* 2010). However, 0.8 g m^{-2} of oleosin are required to effectively stabilize the surface, which is significantly higher than the value reported for casein (1 mg m^{-2}) (Fang and Dalgleish 1993).

A first schematic model for the behavior of soybean oleosomes at an air–water interface is suggested by Waschatko *et al* (2012) (figure 94). It is shown how changes in surface pressure over time (example shown in figure 94) and compressing the surface area using a film balance were correlated with Brewster angle micrographs that visualized oleosome constituents at the first micrometer of the surface layer. The adsorption mechanism of oleosomes to the air–water interface is comparable with that of animal apolipoproteins. In particular, the LDL particles, found for example in egg yolk, have been extensively investigated and their interfacial behavior is well characterized (Anton 2006, Dauphas *et al* 2006). However, it is expected that oleosomes are much more stable than LDL particles due to the different arrangement of both proteins at the oil–water interface. The apolipoprotein is located peripherally on the lipid droplet and the oleosome is additionally integrated into oil core via its long hydrophobic domain (Hevona *et al* 2000, Jolivet *et al* 2006). Oleosomes immersed in the aqueous subphase diffuse to the air–water interface because of their amphiphilic nature and buoyancy forces, figure 94. Since it is energetically unfavourable for the hydrophilic protein groups to be in contact with hydrophobic air molecules (marked as 2), oleosomes rupture (3) and a 2D-surface film of spread TAG, phospholipids, free fatty acids and oleosins is formed at the interface (4, 5). Conformation, orientation and arrangement of oleosins within the 2D film depend on subphase conditions, the interfacial behavior of thermodynamically competing constituents and the oleosome concentration inserted (5). Four different scenarios (a)–(d) are assumed: (a) the oleosin structure unfolds with the hydrophilic domains remaining in the aqueous phase whilst the hydrophobic domains reach out into the air. (b) Oleosins

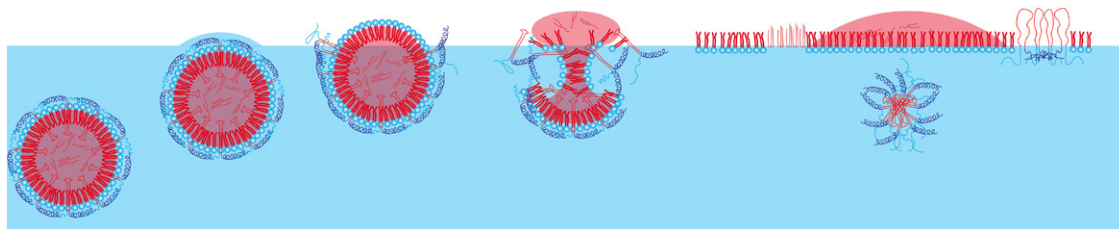


Figure 95. Schematic representation of the behavior of the oleosomes at the air–water-interface.

desorb from the interface with their hydrophobic domains joined to micellar, dense structures enclosed by hydrophilic domains. (c), (d) The hydrophobic domains of oleosins interact either with phospholipids or phospholipid and triacylglycerole film patches and the hydrophilic domains are exposed to the subphase. Changes in subphase conditions like the pH value and the ionic strength revealed that the charge distribution along the oleosin structure is the driving force in the interfacial behavior of oleosomes at air–water interfaces. At $\text{pH} = 5$, which is close to the oleosins' isoelectric point $\text{pI} = 5.3$, electrostatic repulsive interactions between adjacent oleosomes diminish as charged oleosin groups exposed to aqueous medium become neutral. Thus, short-ranged van der Waals and hydrophobic forces dominate, allowing oleosomes to pack more densely at the air–water interface. This results in a higher surface pressure than that in more alkaline/acidic subphase conditions. A similar effect is observed at high ionic strength ($I = 100\text{ mM}$) where the charge of oleosin groups is screened and thus the oleosome net surface charge becomes neutral (Waschatko *et al* 2012, Waschatko *et al* 2012).

The process of the rupture of native oleosomes at the water–air interface involves the denaturation of the hydrophilic parts of the oleosins. When the oil particles are located close to the interface, the effective charges of the amino acids reorient the water molecules at the surface (Smits *et al* 2007). The hydration shell stabilizes the oleosomes in the close range of the interface (see figure 95) before the proteins denature and liberate oil by reorienting the phospholipids at the interface.

The stability of the oleosomes can be influenced strongly by enzymatic treatment of the oleosins by proteases, such as trypsin (Maurer *et al* 2013), when the hydrophilic parts of the oleosin are cleaved. The structure changes significantly and the electrostatic contribution to the stability becomes reduced. Emulsions from partially digested oleosomes are less stable, and the droplets coagulate quickly (Waschatko *et al* 2012, Maurer *et al* 2013). As a consequence of the digestion the ζ -potential, which is related to the effective surface charge at the corresponding pH value, and the aggregation behavior of oleosomes change. The steric stabilization through the oleosin termini disappears and coalescence of the oil droplet is likely to occur. The behavior at air liquid surfaces becomes changed completely as indicated in figure 96.

13.6. Physicochemical stability of isolated oleosomes and their application

The stability of emulsions composed of oleosomes is comparable to technically prepared emulsions (Chen *et al* 2012).

Therefore, using oleosomes in industrial manufacturing, such as food, cosmetics or pharmaceutical products, can offer many benefits over using commonly produced emulsions. Highly energy-consuming processes such as homogenization involved in the production of a sufficiently stable oil-in-water emulsion become negligible as oleosomes already provide a well-stabilized pre-emulsified oil. Commonly emulsions are prepared from compounds that were previously thoroughly extracted, often under environmentally unfriendly and unhealthy conditions. Moreover, oleosomes are recovered from renewable and environmentally more friendly sources, i.e. exclusively plants (Bhatla *et al* 2010). Plant oil is believed to be healthier than animal fats due to its high content of unsaturated fatty acids (although there is no hard scientific evidence). Additionally, oleosomes can act as a carrier system for bioactive ingredients such as vitamins (Fisk and Gray 2011), flavors, aromas (Fisk *et al* 2013) and drug agents (Tzen 2012) to protect them against degradation during processing and storage and to deliver them to the desired host.

Oleosomes are predominantly used in pharmaceutical and cosmetic products, for example in drug delivery (Chiang *et al* 2011) and skin care products (Deckers *et al* 2001). Their usage in food products is still fairly uncommon. However, particularly with regard to the steadily increasing demand for vegetarian or vegan products, oleosomes and their constituents are suitable replacements for ingredients of animal origin, like egg yolk or milk-based additives. Applications are conceivable in ice creams, mayonnaise, salad dressings, juices, vinaigrettes, pet food etc (Bhatla *et al* 2010). Concerning food-relevant quality criteria, a detailed knowledge of the physicochemical stability of oleosomes against the various environmental stresses that they encounter during processing and storage is crucial. Lipid oxidation imparts undesirable odors and flavors (Fisk and Gray 2011, Chen *et al* 2012). High temperatures and dehydration during preservation and freeze–thaw cycles can result in phase separation following oil droplet aggregation, which in turn alters texture and other rheological properties (Wu *et al* 2012).

Furthermore, interactions between oleosomes and other food ingredients can influence the stability and function of oleosomes (Chen *et al* 2012). An ensemble of isolated oleosomes forms a natural, predominantly protein-stabilized emulsion. Its stability depends on colloidal interactions of the surfactant-stabilized droplets, which in turn are determined by the interfacial composition. Changes in the electrolyte concentration and pH value can have a tremendous impact on the stability of an emulsion (Guzey and McClements 2006). When the pH value of the continuous phase is far enough

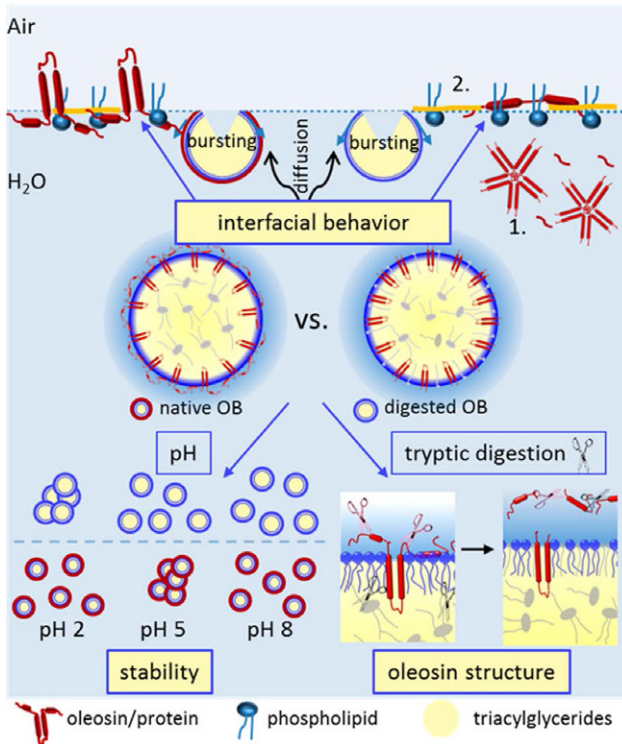


Figure 96. Comparison of native oleosomes and oleosomes with digested oleosins at the air–water interface (from Maurer *et al* (2013)).

from the isoelectric point of the proteins, in either the alkaline or acidic regime, electrostatic repulsive interactions dominate, which prevent coalescence or flocculation. Close to or directly at the pI, short-ranged interactions, such as van der Waals or hydrophobic interactions, presumably result in droplet aggregation and subsequent phase separation. Regarding ionic influences, four different scenarios might occur: droplet repulsion is reduced due to electrostatic screening; ions bind to droplets of emulsion, thereby weakening electrostatic repulsion; the structural organization of water molecules is altered, resulting in increased hydration repulsion between droplets; hydrophobic interactions between non-polar groups are changed (McClements 1999, Israelachvili 2011). In addition to the interfacial composition, also the volume fraction of the dispersed phase, as well as the droplet size and distribution, can have an influence on the emulsion's stability (White *et al* 2008).

It was shown that the interfacial composition of oleosomes is crucial for their physicochemical stability and depends significantly on the extraction procedure of oleosomes (Iwanaga *et al* 2008, Chen *et al* 2012, 2014, Karkani *et al* 2013, Nikiforidis *et al* 2013). Extraction conditions, particularly the pH and usage of organic solvent, determine the type of protein that remains associated with oleosomes after washing and centrifugation (Chen and Ono 2010, Nikiforidis *et al* 2013). Comparative studies of maize germ and sunflower oleosomes revealed that the same procedure applied yields different results: whereas maize germ oleosomes are free of any non-oleosome associated proteins after extensive washing with sucrose at a mildly alkaline pH value, residual seed proteins

are detected on sunflower oleosomes. However, long-term stability, i.e. no changes in average particle size, charge distribution on droplet surface and intermolecular droplet interactions over 15 days, only applies to oleosomes with an additional surface layer of extraneous proteins (Nikiforidis *et al* 2013). Soybean oleosomes remain stable after temperature treatment at 90 °C or lower for 30 min and after additions of NaCl no higher than 50 mM. However, the presence of extraneous proteins is not excluded (Iwanaga *et al* 2007). At pH values close to the pI values of proteins, between 4.5 and 5.5 depending on the protein type, flocculation or coalescence occurs between oleosomes. To improve the stability in slightly acidic environments, often encountered in foods such as juices and salad dressings, hydrocolloids like xanthan gum (Nikiforidis and Kiosseoglou 2010), citrus peel pectin (Iwanaga *et al* 2008) and carrageenan (Wu *et al* 2011) are added. Coatings of pectin or carrageenan and the presence of sucrose yield oleosome solutions that are stable to freeze–thaw cycles (Iwanaga *et al* 2008, Wu *et al* 2012).

14. Some culinary aspects based on soft matter physics

Interface-dominated foods have widespread culinary aspects. The collective behavior during oral processing yields strong effects in the mouth and indicates textural pleasures. A few examples will be discussed in the following.

14.1. Particle-based emulsions

A simple culinary model system for a particle-based Pickering emulsion can be produced with starch oil and a tasty water-based fluid (e.g. chicken broth, lemon juice/vinegar-based and spiced water). Starch is available in different grain sizes. The emulsion is easy to produce: starch grains are immersed in the water-based fluid to form a suspension. Then the oil is added under continuous mixing until a stable, highly viscous O/W emulsion forms. For spherical particles the interfacial energy depends strongly on the contact angle,

$$U = \pi r^2 \gamma (1 - |\cos \theta|)^2, \quad (44)$$

where r is the particle radius, γ the interface tension and θ the contact angle defined by the penetration depth of the particle (see inset in figure 97). However, such an emulsion only achieves any culinary value when it is heated up to 70–75 °C, slightly above the gelatinization temperature of the starch. The starch granules form a gelatinized layer around the oil droplets and encapsulate the oil permanently. The oil is trapped in the fragile starch matrix. From the point of view of perception the gelatinized starch granules form a solid network with pore size defined by the encapsulated oil droplets.

Timgren *et al* (2011) discussed possible pharmaceutical applications of these ideas; Yusoff and Murray (2011) investigated the effect of various starch modifications on the stability of starch-based Pickering emulsions. Typical sizes for the oil droplets are about 20–100 μm, whereas the starch granule size ranges from 1 μm to 5 μm depending on the species. The

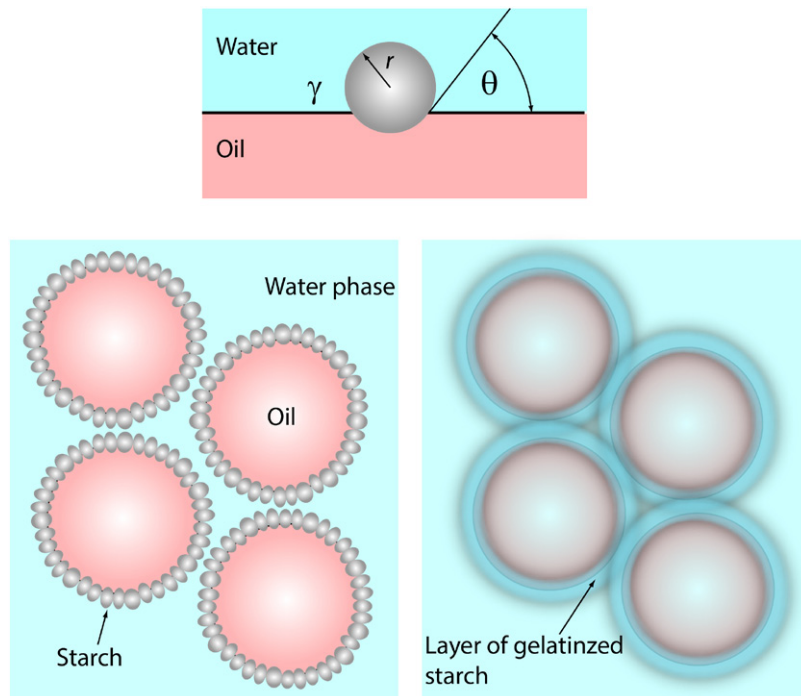


Figure 97. Model of a starch-stabilized emulsion before (left) and after (right) heating. The energy of an individual particle at given contact angle is shown in the upper part of the figure. (From Vilgis (2013a) with permission.)

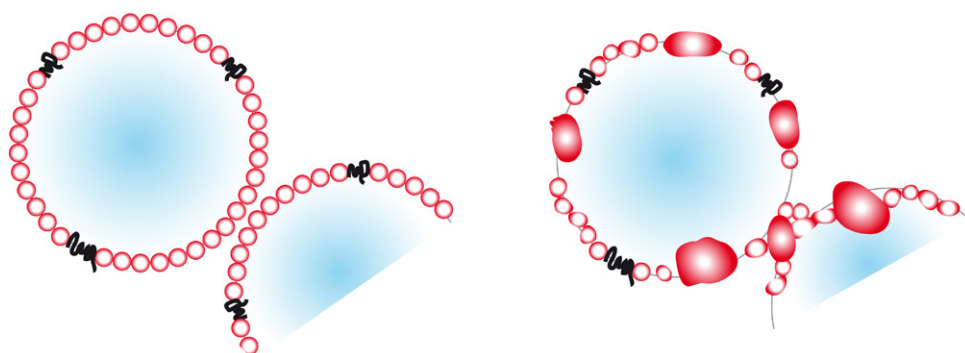


Figure 98. Schematic model of whipped cream. The partially solid fat globules act as emulsifiers (left). When the whipped cream is heated, the fat globules melt and may coagulate and the structure breaks down. Casein micelles and sub-micelles have been omitted. The fat globules are only drawn schematically, omitting their detailed surface structure. Surface-active whey proteins support the stability. (Redrawn from Vilgis (2012a) with permission.)

solid emulsion is very stable after ‘baking’ and can be cut into pieces—discs or other shapes. In these forms it can be added to complex food plates as a ‘textural’ and taste element. The mouth-feel can be described as somewhere between solid, brittle and similarly melting, because the oil becomes released during oral processing, when physical structures, i.e. the network with micrometer pore sizes, transform into textures and thus their perception (Çakır *et al* 2012, Koç *et al* 2013).

14.2. Dairy foams

Foams from whipped milk (Stanley *et al* 1996) used in cappuccino or other coffee drinks are one of the most well-known foams. Milk foams are easy to produce, but they are not always very stable. Their culinary value appears attractive, because the densely packed air bubbles collect the volatile milk aroma

compounds, which get released during processing, and burst in the mouth. In addition, the soft texture of the foamy structure appears as very pleasant.

In contrast, whipping cream produces stable foams, if the cream is sufficiently cold. Cold cream forms particle-stabilized foams (Rousseau 2000, Sajedi *et al* 2014), where the fat globules mainly play the role of the emulsifier, as in particle-stabilized emulsions. The ratio of the water content, whey proteins, casein micelles and fat globules is very well balanced in whipping cream, which allows the formation of relatively stable foams where air bubbles are stabilized by fat globules and form Pickering-type emulsions, as presented schematically in figure 98. At low temperatures (between 0 °C and 4 °C) triacylglycerols containing longer saturated fatty acids crystallize and the particles are solid and act as a Pickering emulsifier (Goff 1997a). When whipped cream is heated above

the melting temperature of the triacylglycerols the particles become liquid and may coagulate. In addition, the fat globules are released from the interface when the thermal energy $k_B T$ becomes larger than the surface energy in equation (44), and the structure breaks down.

The stability of the foamy fat/water/air based structure is essential when it is frozen and turned into ice cream (Goff and Hartel 2013). In most cases sugar and hydrocolloids are added and the local chemical properties of the low-molecular-weight carbohydrates matter (see section 12.8). The frozen food melting in the mouth determines the entire perception of the temperature, up to the release of taste and aroma until the swallowing process. Water crystals need to be small and the distribution of the different phases needs to be controlled during the production process. Such multicomponent and multiphase materials require systematic investigation in order to control all the physical and process parameters. In a remarkable study (Pinzer *et al* 2012) investigated ‘model ice cream’ preparations to obtain information on the distribution and sizes of the different structural elements, such as bubble size and crystal growth. Using x-ray microtomography, it was possible to carry out time lapse studies of the development of microstructure in model ice cream, and the three-dimensional distribution and coarsening of the three main phases—air, unfrozen sugar solution and ice crystals—could be systematically investigated, for example as a function of the heat cycles.

As a short aside, the crema of coffee (Piazza *et al* 2008) has, apart from its textural and bitter taste, another physically useful function: the foamy structure conducts heat very purely. Cremas keep Italian-style espressi and coffee hotter for quite a long time. This has also some importance for the taste. In addition, the bitter taste, not liked very much by some people, appears more pronounced at lower temperatures.

14.3. Mayonnaise

Mayonnaises are perhaps the best known food emulsions. Classical recipes use egg yolk mayonnaise, where unheated yolks are slightly salted and beaten with oil (and some acids, such as lemon juice, spiced vinegars, mustard etc). Classical examples use egg yolk as a natural emulsifier (Kiosseoglou 2003), where different lipoproteins contribute to stability and rheology (Kiosseoglou and Sherman 1983). Depree and Savage (2001) discussed the synergistic interplay of different emulsifiers, e.g. proteins, phospholipids, mono- and diglycerides, at the interface of yolk emulsion, and Guilmeneau and Kulozik (2007) investigated the influence of different forms of heat treatment of yolk on the resulting emulsions.

Pure egg white contains proteins that denature when mechanical energy is applied (see section 8.1) and it forms stable foams (Campbell *et al* 2003). The proteins act as emulsifiers as indicated in figure 83. This implies that unheated egg whites can be used as the basis for stable emulsions, which can be demonstrated in a simple kitchen table experiment. Egg white is beaten slightly, salted and spiced before the oil is added while mixing. The result is a creamy emulsion with a much clearer oil taste than the classical yolk version. In addition, the emulsion can be heated to 71 °C, when

ovalbumin forms sulfur cross-links. The emulsion solidifies and the oil droplets will be immobilized in the protein matrix. Another possibility is the use of spray-dried egg white where the water can be replaced by tasty fluids, such as juices or broths (stocks), and the oil, for example, by liquid, but not hot butter ($T < 40$ °C), to prevent protein denaturation before the emulsification. Afterwards the emulsion is either cooled, to crystallize the milk fat, or heated, to cross-link the proteins. This ‘buttery gel’ can be served below 36 °C (with crystallized butter) or hot, above 40 °C, with liquid butter droplets: one system, two different physical phases, two different culinary functions. This example shows again the utility of physical ideas in the kitchen.

In addition, other proteins, e.g. soybean (soymilk), pea etc, show well defined emulsifying properties too (see Lam and Nickerson (2013) for a recent review and Nishinari *et al* (2014), especially for soybean protein applications). The use of hydrocolloids in the water component in emulsions allows more stable mayonnaise, due to higher viscosity and slowed diffusion processes. Moreover, they extend the oral processing time. The mouth-feel and sensory aspects are ‘enhanced’ due to significant changes in the texture.

The exceptional range of culinary applications of the natural emulsion yolk (Vega and Mercadé-Prieto 2011) has already been addressed. However, another aspect needs to be added here. Frozen (below 10 °C) egg yolks show an impressive creamy texture and retain their natural raw flavor, as was remarked decades ago (Powrie *et al* 1963) and investigated further more recently (Telis and Kieckbusch 1997, 1998). Chang *et al* (1977) investigated the changes of entire yolk and plasma by freeze–thaw gelation. The increase in the moduli and mechanical properties cannot be attributed exclusively to the plasma. Together with electrophoresis measurements a strong immobilization of the LDL particles has been found. In addition the increase of the moduli is found to be more pronounced with increasing storage time.

This method offers quite a number of culinary possibilities. When whole eggs are frozen and then thawed, the egg white can be removed easily (and reused as emulsifier, for foams, baking). The yolk is gelled and remains in its spherical form, but retains its original flavour. It can be served ‘raw’; alternatively it can be heated up to 65 °C to add a ‘boiled’ flavor, without changing the creaminess and the texture.

14.4. Oil thickening, inverse emulsions and foams

According to table 3, mono- and diglycerides are possible candidates for inverse emulsions in the kitchen laboratory. These emulsifiers dissolve in slightly warmed oil (60–65 °C). The viscosity of the oil increases after cooling, which already allows unusual effects on plating, because the highly viscous oil can be served in the form of stable drops. When the prepared oil is filled into syphons and loaded, whipped cream-like textures can be sprayed out. The oil forms very stable foams, which appear light and airy, in contrast to the liquid oil and solid/waxy fats. Especially with colorful and tasty oils such as green pumpkin oils from Austria or golden-green oils like

olive oils, this method provides nice extensions of the special ‘plating’ in avant-garde cuisine. When water-based liquids are added to such inverse emulsions, tasty spreads of all kinds can be produced very easily. A simple example is the combination of olive oil and honey. The emulsifiers are added to the slightly heated oil before the honey is added. The resulting inverse emulsion can be spread on plates or in spots, droplets or form-stable tappets on plate arrangements for additional flavors and textures.

Oils with low crystallization temperatures (such as sunflower and nut oils) that are treated with mono- and diglycerides appear more viscous after cooling. The emulsifiers induce a forced crystallization especially by mono- and diglycerides (Munk *et al* 2013) and change the texture and appearances of the low-viscosity oils significantly, allowing new gastronomic applications.

15. Next challenges for (food) physics

The main topic in this review has been the physical aspects of food, its molecular structure and its structural changes during preparation. This context showed a number of interactions between the food structure and taste, which are not obvious at first sight, but an important point in food systems. The basic taste qualities, sweet, salty, sour, bitter and umami, are induced by polar molecules and ions, which have a strong interplay with structure-determining macromolecules in foods via electrostatic and pH-changing effects. The scents induced by volatile aroma compounds have so far been completely ignored, although most of these issues can be attributed to aroma and food chemistry with its immense literature (Reineccius 2004) and the large number of aroma compounds of very different chemical structure and very different olfactory descriptions. The need for some basic scent–structure relationships has been an unrealised dream for a long time. Only in recent years, when molecular sensory science made significant progress, have relevant connections and a basis for the connections between molecular structures and perception been found (Dunkel *et al* 2014), and they offer very new and different perspectives in finding the real key aroma compounds and their interaction. Apart from such fundamental observations and findings, the scent of foods is closely related to the physical properties of the matrix that couples the release of aroma with the food’s structure, temperature, state and other physical properties.

There are, for example, clear and important interactions of aroma compounds and salts (and pH values) involved in perception. Simple systems, such as vegetable soups, appear to have more flavor and be richer in aroma when they are salted (Mitchell *et al* 2011). The effect can be measured by headspace analysis, and it is shown that the concentration of volatile aroma compounds (liberated from the soup), apart from some terpenes and sulfur compounds, is higher when the salt concentration is higher. This corresponds to the salting-out effects and the interplay of the different solubilities of hydrophobic aroma compounds and ions in water. Here details of hydrophobic hydration (Lazaridis and Paulaitis 1992, Lee and

Graziano 1996) and the competition for water play an important role.

Apart from taste and scent, trigeminal effects on chemos- and thermal receptors, such as temperature sensitivity, are of physical (via the thermal energy $k_B T$) and molecular origin (the ‘hot’ effects of individual molecules—capsaicin in chilli, piperins in pepper) and cannot be ignored (Jelen 2011).

The other important aspects concern the processing of the food in the mouth. As mentioned earlier, most oral processes concern the physics of foods. During mastication food is crushed and reformed into a bolus with certain properties required by the swallowing process (Chen and Engelen 2012). However, the changing size of the particles, their additional wetting with saliva and the cohesive properties of the bolus follow complicated physical laws, which connect their (non-linear) viscosity, the frictional properties, shear thinning and the nonlinear structural breakdown during the high shear rates involved in swallowing (Lucas *et al* 2002, Lillford 2011, Vilgis *et al* 2015). Apart from such considerations, the human response to taste is strongly coupled to the physical properties of the food and the resulting bolus, as has been demonstrated and modeled recently with specific examples (Le Révérend *et al* 2013). Already these few examples show that sensory science needs a larger input from molecular physics and physical chemistry.

Other issues concern interstitial digestion, which can nowadays be investigated *in vitro* (Hur *et al* 2011, Scheuble *et al* 2014). In digestion food pieces swallowed in the bolus must undergo structural changes induced by changes in pH value (from stomach to small intestine), enzymatic digestion (pancreas) and a wide variety of shear rates (peristalsis). The way in which the structural changes progress defines the basic nutritional values of foods and allows special designs of food structures for special nutritional or medical needs (Zimmermann and Windhab 2010). How the emulsion structure influences the stability of droplets and the digestive process can be clearly seen by direct comparison of the digestion of fat droplets from native (raw) milk with homogenized milk (see figures 86 and 87) that is structurally modified (Ye *et al* 2010, Berton *et al* 2012, Gallier *et al* 2012). Soft matter physics even helps us to understand such structural and dynamical processes much better, and rule out many speculations. In foods all length and time scales remain important, and food without a large portion of physics appears incomplete—and feels too much like a reducing diet.

Last but not least, molecules in food are hardly in equilibrium and (nearly) every phase change in food depends on the path of the process. This will require the development of new methods to understand the non equilibrium process dependent structure changes, taste developments, and aroma release, on all length and time scales: challenges enough for physics, chemistry, biology and engineering.

Acknowledgment

The author is indebted to the members (past and present) of the Mainz food group, chefs and others: S Beccard, F Bröcker,

N Chatti, J Dahl, H Enzmann, J Franz, M Ghebremedhin, A Junghans, J Mann, S Maurer, S Muthuramalingam, D Nordqvist, B Mert, N Russ, B Viezenz, G Waschatko, J Zidek, B Zielbauer. Warm thanks also go to T Bühner, B Conde-Petit, P Fischer, K Kremer, H Limbach, U Neumann, S Parekh, H Tzscherer, T Weidner, F Wiebe and J Wissler for valuable discussions and support.

References

- Adrià F, Adrià A and Soler J 2010 *A Day at El Bulli* (New York: Phaidon)
- Adrià F, Blumenthal H, Keller T and McGee H 2006 Statement on the new cookery *The Observer* **10**
- Adrià F, Soler J and Adrià A 2002 *El Bulli, 1998–2002* (New York: Phaidon)
- Aduriz A L 2012 *Mugaritz: a Natural Science of Cooking* (New York: Phaidon)
- Aguilera J M, Cadoche L, López C and Gutierrez G 2001 Microstructural changes of potato cells and starch granules heated in oil *Food Res. Int.* **34** 939–47
- Aguilera J M and Lillford P J 2008 *Food Materials Science* (Berlin: Springer) pp 229–53
- Aharony A and Stauffer D 2003 *Introduction to Percolation Theory* (London: Taylor and Francis)
- Ahmadi L, Wright A J and Marangoni A G 2009 Structural and mechanical behavior of tristearin/triolein-rich mixtures and the modification achieved by interesterification *Food Biophys.* **4** 64–76
- Ahmed J and Rahman M S 2014 Glass transition in foods *Engineering Properties of Foods* (Hoboken: Taylor and Francis) p 93
- Akhtar M, Stenzel J, Murray B S and Dickinson E 2005 Factors affecting the perception of creaminess of oil-in-water emulsions *Food Hydrocolloids* **19** 521–6
- Akita C, Kawaguchi T and Kaneko F 2006 Structural study on polymorphism of cis-unsaturated triacylglycerol: triolein *J. Phys. Chem. B* **110** 4346–53
- Alexander S and Orbach R 1982 Density of states on fractals: fractons *J. Physique Lett.* **43** 625–31
- Allen K E, Dickinson E and Murray B 2006 Acidified sodium caseinate emulsion foams containing liquid fat: a comparison with whipped cream *LWT—Food Sci. Technol.* **39** 225–34
- Anderson M *et al* 1988 Dairy foams *Advances in Food Emulsions and Foams* (New York: Elsevier) pp 221–55
- Ang S, Kogulanathan J, Morris G A, Kök M S, Shewry P R, Tatham A S, Adams G G, Rowe A J and Harding S E 2010 Structure and heterogeneity of gliadin: a hydrodynamic evaluation *Eur. Biophys. J.* **39** 255–61
- Angell C and Tucker J 1980 Heat capacity changes in glass-forming aqueous solutions and the glass transition in vitreous water *J. Phys. Chem.* **84** 268–72
- Angyal S J 1969 The composition and conformation of sugars in solution *Angew. Chem. Int. Ed. Engl.* **8** 157–66
- Anton M 2006 Recent advances concerning the functional properties of egg yolk low-density lipoproteins *12th European Poultry Conf. (Verona, Italy, 10–14 September 2006)* paper 352
- Anton M 2013 Egg yolk: structures, functionalities and processes *J. Sci. Food Agric.* **93** 2871–80
- Anton M and Gandemer G 1997 Composition, solubility and emulsifying properties of granules and plasma of egg yolk *J. Food Sci.* **62** 484–7
- Armisen R 1997 *Thickening and Gelling Agents For Food* (Berlin: Springer) pp 1–21
- Arnott S, Fulmer A, Scott W, Dea I, Moorhouse R and Rees D 1974 The agarose double helix and its function in agarose gel structure *J. Mol. Biol.* **90** 269–84
- Aussenac T, Carceller J L and Kleiber D 2001 Changes in SDS solubility of glutenin polymers during dough mixing and resting 1 *Cereal Chem.* **78** 39–45
- Awad T S, Rogers M A and Marangoni A G 2004 Scaling behavior of the elastic modulus in colloidal networks of fat crystals *J. Phys. Chem. B* **108** 171–9
- Aye M 2014 *Noodle: 100 Amazing Authentic Recipes* (London: Bloomsbury)
- Aymard P, Martin D R, Plucknett K, Foster T J, Clark A H and Norton I T 2001 Influence of thermal history on the structural and mechanical properties of agarose gels *Biopolymers* **59** 131–44
- Bailey A J 1972 The basis of meat texture *J. Sci. Food Agric.* **23** 995–1007
- Baldwin D E 2012 Sous vide cooking: a review *Int. J. Gastron. Food Sci.* **1** 15–30
- Ball R 1989 Fractal colloidal aggregates: consolidation and elasticity *Phys. D: Nonlinear Phenom.* **38** 13–5
- Ball R and Edwards S F 1980 Elasticity and stability of a dense gel *Macromolecules* **13** 748–61
- Barbosa-Cánovas G V, Fontana A J Jr, Schmidt S J and Labuza T P 2008 *Water Activity in Foods: Fundamentals and Applications* vol 13 (13: New York)
- Barham B 2013 Physics in the kitchen *Flavour* **2** 5
- Barham P, Skibsted L H, Bredie W L, Bom Frøst M, Møller P, Risbo J, Snitkjær P and Mortensen L M 2010 Molecular gastronomy: a new emerging scientific discipline *Chem. Rev.* **110** 2313–65
- Barrat J L and Joanny J F 1993 Persistence length of polyelectrolyte chains *Europhys. Lett.* **24** 333
- Barrat J L and Joanny J F 1997 Theory of polyelectrolyte solutions *Adv. Chem. Phys.* **94** 1
- Bashford D and Karplus M 1990 pKa's of ionizable groups in proteins: atomic detail from a continuum electrostatic model *Biochemistry* **29** 10219–25
- Bashford D and Karplus M 1991 Multiple-site titration curves of proteins: an analysis of exact and approximate methods for their calculation *J. Phys. Chem.* **95** 9556–61
- Baynes J W *et al* 2005 *The Maillard Reaction: Chemistry at the Interface of Nutrition, Aging, and Disease* (New York: New York Academy of Sciences)
- Bechtel P J 2012 *Muscle as Food* (Amsterdam: Elsevier)
- Beckett S T 2000 *The Science of Chocolate* (Cambridge, UK: Royal Society of Chemistry)
- Belitz H D, Grosch W and Schieberle P 2009 *Food Chemistry* (Berlin: Springer)
- Belton P 1999 Mini review: on the elasticity of wheat gluten *J. Cereal Sci.* **29** 103–7
- Belton P 2005 New approaches to study the molecular basis of the mechanical properties of gluten *J. Cereal Sci.* **41** 203–11
- Bennion E B, Bent A and Bamford G 1997 *The Technology of Cake Making* (Berlin: Springer)
- Bertazzon A, Tian G, Lamblin A and Tsong T Y 1990 Enthalpic and entropic contributions to actin stability: calorimetry, circular dichroism, and fluorescence study and effects of calcium *Biochemistry* **29** 291–8
- Berton A, Rouvellac S, Robert B, Rousseau F, Lopez C and Crenon I 2012 Effect of the size and interface composition of milk fat globules on their in vitro digestion by the human pancreatic lipase: native versus homogenized milk fat globules *Food Hydrocolloids* **29** 123–34
- Bhatla S C, Kaushik V and Yadav M K 2010 Use of oil bodies and oleosins in recombinant protein production and other biotechnological applications *Biotechnology* **28** 293–300
- Biliaderis C G and Galloway G 1989 Crystallization behavior of amylose-v complexes: structure-property relationships *Carbohydr. Res.* **189** 31–48
- Biroli G 2011 *Glasses and Grains* (Berlin: Springer) pp 41–76
- Bloksma A 1990 Dough structure, dough rheology, and baking quality *Cereal Foods World* **35** 237–44

- Blumenthal H 2008 *The Fat Duck Cookbook* (New York: Bloomsbury)
- Blumenthal H 2009 *In Search of Total Perfection* (London: Bloomsbury)
- Boskou D, Blekas G and Tsimidou M 1996 Olive oil composition *Olive Oil: Chem. Technol.* **1996** 52–83
- Bourne M 2002 *Food Texture and Viscosity: Concept and Measurement* (New York: Academic)
- Bouzidi L and Narine S S 2012 Relationships between molecular structure and kinetic and thermodynamic controls in lipid systems. Part II: phase behavior and transformation paths of sss, pss and pps saturated triacylglycerols effect of chain length mismatch *Chem. Phys. Lipids* **165** 77–88
- Boyd J V, Parkinson C and Sherman P 1972 Factors affecting emulsion stability, and the hlb concept *J. Colloid Interface Sci.* **41** 359–70
- Brady J F 1983 The einstein viscosity correction in n dimensions *Int. J. Multiph. Flow* **10** 113–4
- Branca C, Magazù S, Maisano G, Migliardo F, Migliardo P and Romeo G 2001 α , α -trehalose/water solutions. 5 hydration and viscosity in dilute and semidilute disaccharide solutions *J. Phys. Chem. B* **105** 10140–5
- Brezesinski G, Scalas E, Struth B, Möhwald H, Bringezu F, Gehlert U, Weidemann G and Vollhardt D 1995 Relating lattice and domain structures of monoglyceride monolayers *J. Phys. Chem.* **99** 8758–62
- Brézin E and Zinn-Justin J 1990 *Fields, Strings and Critical Phenomena* (Amsterdam: North-Holland)
- Broadhurst M G 1966 The melting temperatures of the n-paraffins and the convergence temperature for polyethylene *J. Res. Natl Bur. Stand.* **70** 481–6
- Brown W and Ball R 1985 Computer simulation of chemically limited aggregation *J. Phys. A: Math. Gen.* **18** L517
- Bruce Litchfield J and Okos M R 1992 Moisture diffusivity in pasta during drying *J. Food Eng.* **17** 117–42
- Brüggemann D A, Bremer J, Risbo J and Bagatolli L 2010 Second harmonic generation microscopy: a tool for spatially and temporally resolved studies of heat induced structural changes in meat *Food Biophys.* **5** 1–18
- Bryngelson J and Wolynes P 1987 Spin-glasses and the statisticalmechanics of protein folding *Proc. Natl Acad. Sci.* **84** 7524–8
- Buléon A, Colonna P, Planchot V and Ball S 1998 Starch granules: structure and biosynthesis *Int. J. Biol. Macromol.* **23** 85–112
- Burchard W and Ross-Murphy S B 1990 *Physical Networks-Polymers and Gels* (London: Elsevier)
- Cabanos C, Katayama H, Tanaka A, Utsumi S and Maruyama N 2011 Expression and purification of peanut oleosins in insect cells *Protein J.* **30** 457–63
- Cai T and Chang K C 1999 Processing effect on soybean storage proteins and their relationship with tofu quality *J. Agric. Food Chem.* **47** 720–7
- Caine W, Aalhus J, Best D, Dugan M and Jeremiah L 2003 Relationship of texture profile analysis and Warner-Bratzler shear force with sensory characteristics of beef rib steaks *Meat Sci.* **64** 333–9
- Cakir E, Vinyard C J, Essick G, Daubert C R, Drake M and Foegeding E A 2012 Interrelations among physical characteristics, sensory perception and oral processing of protein-based soft-solid structures *Food Hydrocolloids* **29** 234–45
- Cameron R and Donald A 1992 A small-angle x-ray scattering study of the annealing and gelatinization of starch *Polymer* **33** 2628–35
- Campbell L, Raikos V and Euston S R 2003 Modification of functional properties of egg-white proteins *Food/Nahrung* **47** 369–76
- Campo V L, Kawano D F, Silva D B D Jr and Carvalho I 2009 Carrageenan: biological properties, chemical modifications and structural analysis—a review *Carbohydr. Polym.* **77** 167–80
- Campos R and Marangoni A G 2014 Crystallization dynamics of shear worked cocoa butter *Cryst. Growth Des.* **14** 1199–210
- Capron I, Robert P, Colonna P, Broglly M and Planchot V 2007 Starch in rubbery and glassy states by ftir spectroscopy *Carbohydr. Polym.* **68** 249–59
- Capuano F, Beaudoin F, Napier J A and Shewry P R 2007 Properties and exploitation of oleosins *Biotechnol. Adv.* **25** 203–6
- Carrapiso A I 2007 Effect of fat content on flavour release from sausages *Food Chem.* **103** 396–403
- Carrillo-Navas H, Avila-de la Rosa G, Gómez-Luría D, Meraz M, Alvarez- Ramirez J and Vernon-Carter E 2014 Impact of ghosts on the viscoelastic response of gelatinized corn starch dispersions subjected to small strain deformations *Carbohydr. Polym.* **110** 156–62
- Castellani O, Belhomme C, David-Briand E, Guérin-Dubiard C and Anton M 2006 Oil-in-water emulsion properties and interfacial characteristics of hen egg yolk phosvitin *Food Hydrocolloids* **20** 35–43
- Cates M 1985 Brownian dynamics of self-similar macromolecules *J. Phys.* **46** 1059–77
- Cates M and Edwards S 1984 Linear theory of disordered fibre-reinforced composites *Proc. R. Soc.* **395** 89–109
- Cebula D J, McClements D J, Povey M J and Smith P R 1992 Neutron diffraction studies of liquid and crystalline trilaurin *J. Am. Oil Chem. Soc.* **69** 130–6
- Chaiquin P M and Lubensky T 2000 *Principles of Condensed Matter Physics* (Cambridge: Cambridge University Press)
- Chaiseri S and Dimick P S 1989 Lipid and hardness characteristics of cocoa butters from different geographic regions *J. Am. Oil Chem. Soc.* **66** 1771–6
- Chang C, Powrie W and Fennema O 1977 Studies on the gelation of egg yolk and plasma upon freezing and thawing *J. Food Sci.* **42** 1658–65
- Chapin F S, Schulze E D and Mooney H A 1990 The ecology and economics of storage in plants *Annual Review of Ecology and Systematics* (Palo Alto, CA: Annual Reviews) pp 423–47
- Charalambides M N, Wanigasooriya L, Williams J G, Goh S M and Chakrabarti S 2006 Large deformation extensional rheology of bread dough *Rheol. Acta* **46** 239–48
- Cheah P and Ledward D 1996 High pressure effects on lipid oxidation in minced pork *Meat Sci.* **43** 123–134
- Chen B, McClements D J, Gray D A and Decker E A 2012 Physical and oxidative stability of pre-emulsified oil bodies extracted from soybeans *Food Chem.* **132** 1514–20
- Chen J and Engelen L 2012 *Food Oral Processing: Fundamentals of Eating and Sensory Perception* (New York: Wiley)
- Chen Y and Ono T 2010 Simple extraction method of non-allergenic intact soybean oil bodies that are thermally stable in an aqueous medium *J. Agric. Food Chem.* **58** 7402–7
- Chen Y, Zhao L, Cao Y, Kong X and Hua Y 2014 Oleosins (24 and 18 kda) are hydrolyzed not only in extracted soybean oil bodies but also in soybean germination *J. Agric. Food Chem.* **62** 956–65
- Chiang C J, Lin C C, Lu T L and Wang H F 2011 Functionalized nanoscale oil bodies for targeted delivery of a hydrophobic drug *Nanotechnology* **22** 1–9
- Choe E and Min D 2007 Chemistry of deep-fat frying oils *J. Food Sci.* **72** R77–86
- Christensen L, Ertbjerger P, Aaslyngb M D and Christensen M 2011 Effect of prolonged heat treatment from 48° C to 63° C on toughness, cooking loss and color of port *Meat Sci.* **88** 280–5
- Chuang R L C, Chen J C, Chu J and Tzen J T 1996 Characterization of seed oil bodies and their surface oleosin isoforms from rice embryos *J. Biochem.* **120** 74–81
- Clementi C 2008 Coarse-grained models of protein folding: toy models or predictive tools? *Curr. Opin. Struct. Biol.* **18** 10–5
- Clusel M, Corwin E I, Siemens A O and Brujić J 2009 A granocentricmodel for random packing of jammed emulsions *Nature* **460** 611–5

- Costa M C, Rolemberg M P, Meirelles A J, Coutinho J A and Krähenbühl M 2009a The solid–liquid phase diagrams of binary mixtures of even saturated fatty acids differing by six carbon atoms *Thermochim. Acta* **496** 30–7
- Costa M C, Sardo M, Rolemberg M P, Coutinho J A, Meirelles A J, Ribeiro-Claro P and Krähenbühl M 2009b The solid–liquid phase diagrams of binary mixtures of consecutive, even saturated fatty acids *Chem. Phys. Lipids* **160** 85–97
- Costa M C, Sardo M, Rolemberg M P, Ribeiro-Claro P, Meirelles A J, Coutinho J A and Krähenbühl M 2009c The solid–liquid phase diagrams of binary mixtures of consecutive, even saturated fatty acids: differing by four carbon atoms *Chem. Phys. Lipids* **157** 40–50
- Cunningham S, McMinn W, Magee T and Richardson P 2007 Modelling water absorption of pasta during soaking *J. Food Eng.* **82** 600–7
- Cuq B, Gonçalves F, François Mas J, Vareille L and Abecassis J 2003 Effects of moisture content and temperature of spaghetti on their mechanical properties *J. Food Eng.* **59** 51–60
- Dalgleish D G 2006 Food emulsions: their structures and structure-forming properties *Food Hydrocolloids* **20** 415–22
- Dalgleish D G and Corredig M 2012 The structure of the casein micelle of milk and its changes during processing *Annu. Rev. Food Sci. Technol.* **3** 449–67
- Daniels P H and Cabrera A 2014 Plasticizer compatibility testing: dynamic mechanical analysis and glass transition temperatures *J. Vinyl Additive Technol.*
- Danno G and Hoseney R 1982 Changes in flour proteins during dough mixing *Cereal Chemistry (USA)*
- Daoud M and Joanny J 1981 Conformation of branched polymers *J. Phys.* **42** 1359–71
- Daoud M and Leibler L 1988 Randomly branched polymers: semidilute solutions *Macromolecules* **21** 1497–501
- Dauphas S, Beaumal V, Riaublanc A and Anton M 2006 Hen egg yolk low-density lipoproteins film spreading at the air-water and oil-water interfaces *J. Agric. Food Chem.* **54** 3733–7
- Davis J and Foegeding E 2007 Comparisons of the foaming and interfacial properties of whey protein isolate and egg white proteins *Colloids Surf.* **54** 200–10
- de Bruijne D W and Bot A 1999 Fabricated fat-based foods *Food Texture: Measurement and Perception* (Gaithersburg, MD.: Aspen Publishers) pp 185–227
- de Carvalho W and Djabourov M 1997 Physical gelation under shear for gelatin gels *Rheol. Acta* **36** 591–609
- de Gennes P G 1979 *Scaling Concepts in Polymer Physics* (Ithaca, NY: Cornell University Press)
- De Gennes P G and Prost J 1993 *The Physics of Liquid Crystals* vol 23 (23: Oxford)
- De Kruif C G, Huppertz T, Urban V S and Petukhov A V 2012 Casein micelles and their internal structure *Adv. Colloid Interface Sci.* **171** 36–52
- de Solier I 2010 Liquid nitrogen pistachios: molecular gastronomy, elbulli and foodies *Eur. J. Cultural Stud.* **13** 155–70
- Debet M R and Gidley M J 2007 Why do gelatinized starch granules not dissolve completely? Roles for amylose, protein, and lipid in granule ghost integrity *J. Agric. Food Chem.* **55** 4752–60
- Deckers H M, van Rooijen G, Boothe J, Goll J and Moloney M M 2001 Oil body based personal care products
- Delcour J and Hoseney R C 2010 *Principles of Cereal Science and Technology* (St. Paul, MN: AACC International)
- Deleu M, Vaca-Medina G, Fabre J F, Roiza J, Valentin R and Moulongui Z 2010 Interfacial properties of oleosins and phospholipids from rapeseed for the stability of oil bodies in aqueous medium *Colloids Surf.* **80** 125–32
- della Valle G, Chiron H, Cicerelli L, Kansou K, Katina K, Ndiaye A, Whitworth M and Poutanen K 2014 Basic knowledge models for the processing of bread as a solid foam *Key Eng. Mater.* **611** 901–8
- Depree J and Savage G 2001 Physical and flavour stability of mayonnaise *Trends Food Sci. Technol.* **12** 157–63
- des Cloizeaux J and Jannink G 1990 *Polymers in Solution; Their Modelling and Structure* (Oxford: Clarendon)
- Deszczyński M, Kasapis S, MacNaughton W and Mitchell J R 2003a Effect of sugars on the mechanical and thermal properties of agarose gels *Food Hydrocolloids* **17** 793–9
- Deszczyński M, Kasapis S and Mitchell J R 2003b Rheological investigation of the structural properties and aging effects in the agarose/co-solute mixture *Carbohydr. Polym.* **53** 85–93
- Di Luca A, Mullen A M, Elia G, Davey G and Hamill R M 2011 Centrifugal drip is an accessible source for protein indicators of pork ageing and water-holding capacity *Meat sci.* **88** 261–70
- Dickinson E 1987 *Food Emulsions and Foams* (Amsterdam: Elsevier)
- Dickinson E 2010 Food emulsions and foams: stabilization by particles *Curr. Opin. Colloid Interface Sci.* **15** 40–9
- Dickinson E 2011 Double emulsions stabilized by food biopolymers *Food Biophys.* **6** 1–11
- Dickinson E *et al* 1988 *Advances in Food Emulsions and Foams* (Amsterdam: Elsevier)
- Dikeman M E, Obuz E, Gök V, Akkaya L and Stroda S 2013 Effects of dry, vacuum, and special bag aging; usda quality grade; and end-point temperature on yields and eating quality of beef longissimus lumborum steaks *Meat sci.* **94** 228–33
- Dill K 1999 Polymer principles and protein folding *Prot. Sci.* **8** 1166–80
- Dimick P S 1999 Compositional effect on crystallization of cocoa butter *Physical Properties of Fats, Oils and Emulsifiers* (Champaign, IL: AOCS Press) pp 140–62
- Dobrynin A V and Rubinstein M 2005 Theory of polyelectrolytes in solutions and at surfaces *Prog. Polym. Sci.* **30** 1049–118
- Doi M and Edwards S F 1986 *The Theory of Polymer Dynamics* (Oxford: Clarendon)
- Donald A M 1994 Physics of foodstuffs *Rep. Prog. Phys.* **57** 1081–135
- Donati I, Holtan S, Mørch Y A, Borgogna M, Dentini M and Skjåk-Bræk G 2005 New hypothesis on the role of alternating sequences in calcium–alginate gels *Biomacromolecules* **6** 1031–40
- Donovan J W and Mapes C J 1976 A differential scanning calorimetric study of conversion of ovalbumin to s-ovalbumin in eggs *J. Sci. Food Agric.* **27** 197–204
- Draget K, Skjåk Bræk G and Smidsrød O 1994 Alginic acid gels: the effect of alginate chemical composition and molecular weight *Carbohydr. Polym.* **25** 31–8
- Duckworth R 1974 *Water Relations of Foods Proc. of an Int. Symp. (Glasgow, September 1974)* (New York: Academic)
- Dufour E, Mazerolles G, Devaux M, Duboz G, Dupoyer M and Mouhous Riou N 2000 Phase transition of triglycerides during semi-hard cheese ripening *Int. Dairy J.* **10** 81–93
- Dufresne A 2014 Crystalline starch based nanoparticles *Curr. Opin. Colloid Interface Sci.* **19** 397–408
- Dunkel A, Steinhaus M, Kotthoff M, Nowak B, Krautwurst D, Schieberle P and Hofmann T 2014 Genuine geruchssignaturen der natur–perspektiven aus der lebensmittelchemie für die biotechnologie *Angew. Chem.* **126** 7250–71
- Eastwood E and Dadmun M 2002 Multiblock copolymers in the compatibilization of polystyrene and poly (methyl methacrylate) blends: role of polymer architecture *Macromolecules* **35** 5069–77
- Ebashi S and Endo M 1968 Calcium and muscle contraction *Prog. Biophys. Mol. Biol.* **18** 123–83
- Ebbinghaus S, Kim S J, Heyden M, Yu X, Heugen U, Gruebele M, Leitner D M and Havenith M 2007 An extended dynamical hydration shell around proteins *Proc. Natl Acad. Sci.* **104** 20749–52
- Edwards S and Vilgis T A 1988 The tube model theory of rubber elasticity *Rep. Prog. Phys.* **51** 243

- Edwards S and Vilgis T 1986 The dynamics of the glass transition *Phys. Scr.* **1986** 7
- Einstein A 1906 Effect of suspended rigid spheres on viscosity *Ann. Phys.* **19** 289–306
- Engelsen S B and Pérez S 1996 The hydration of sucrose *Carbohydr. Res.* **292** 21–38
- Evans I and Haisman D 1980 Rheology of gelatinised starch suspensions *J. Texture Stud.* **10** 347–70
- Fang Y and Dalgeish D G 1993 Dimensions adsorption on the surfaces of oil-in-water emulsions modified by lecithin *Colloids Surf.* **1** 357–64
- Farhat I and Blanshard J 1997 On the extrapolation of the melting temperature of dry starch from starch-water data using the Flory-Huggins equation *Carbohydr. Polym.* **34** 263–5
- Feder J 1988 *Fractals* (New York: Plenum)
- Fellows P J 2009 *Food Processing Technology - Principles and Practice* (Woodhead Publishing) (Cambridge: CRC Press)
- Ferreira M, Hofer C and Raemy A 1997 A calorimetric study of egg white proteins *J. Therm. Anal. Calorim.* **48** 683–90
- Ferry J D 1980 *Viscoelastic Properties of Polymers* (New York: Wiley)
- Finkelstein A V and Ptitsyn O 2002 *Protein Physics: a Course of Lectures* (New York: Academic)
- Fioretto D, Comez L, Corezzi S, Paolantoni M, Sassi P and Morresi A 2013 Solvent sharing models for non-interacting solute molecules: the case of glucose and trehalose water solutions *Food Biophys.* **8** 177–82
- Fischer P and Windhab E J 2011 Rheology of food materials *Curr. Opin. Colloid Interface Sci.* **16** 36–40
- Fisk I D and Gray D A 2011 Soybean (Glycine max.) oil bodies and their associated phytochemicals *J. Food Sci. C: Food Chem.* **76** 1349–54
- Fisk I D, Linforth R, Trophard G and Gray D 2013 Entrapment of a volatile lipophilic aroma compound (d-limonene) in spray dried water-washed oil bodies naturally derived from sunflower seeds (*Helianthus annus*) *Food Res. Int.* **54** 861–6
- Flory P and Vrij A 1963 Melting points of linear-chain homologs. The normal paraffin hydrocarbons *J. Am. Chem. Soc.* **85** 3548–53
- Flory P 1989 *Statistical Mechanics of Chain Molecules*. 1969 (New York: Interscience) p 308
- Flory P J and Rehner J Jr 1943 Statistical mechanics of cross-linked polymer networks II. Swelling *J. Chem. Phys.* **11** 521–6
- Foegeding E A and Davis J P 2011 Food protein functionality: a comprehensive approach *Food Hydrocolloids* **25** 1853–64
- Forrest J C et al 1975 *Principles of Meat Science* (San Francisco: Freeman)
- Förster S and Schmidt M 1995 *Physical Properties of Polymers* (Berlin: Springer) pp 51–133
- Frandsen G I, Mundy J and Tzen J T C 2001 Oil bodies and their associated proteins, oleosin and caleosin *Physiol. Plant.* **112** 301–7
- Friberg S, Larsson K and Sjöblom J 2003 *Food Emulsions* (Boca Raton, FL: CRC Press)
- Frijters S, Günther F and Harting J 2014 Domain and droplet sizes in emulsions stabilized by colloidal particles *Phys. Rev. E* **90** 042307
- Frings C, Tvaroska I, Mazeau K, Rinaudo M and Desbrieres J 1995 Hydration of maltose and amylose: molecular modelling and thermodynamics study *Carbohydr. Res.* **278** 27–41
- Frisullo P, Laverse J, Marino R and Del Nobile M 2009 X-ray computed tomography to study processed meat microstructure *J. Food Eng.* **94** 283–9
- Fryer P and Pinschöwer K 2000 The materials science of chocolate *MRS Bull.* **25** 25–9
- Funami T 2011 Next target for food hydrocolloid studies: texture design of foods using hydrocolloid technology *Food Hydrocolloids* **25** 1904–14
- Gallier S, Ye A and Singh H 2012 Structural changes of bovine milk fat globules during in vitro digestion *J. Dairy Sci.* **95** 3579–92
- Garel T and Orland H 1988 Mean-field model for protein folding *Europhys. Lett.* **6** 307
- Garrec D A and Norton I T 2012 Boundary lubrication by sodium salts: a Hofmeister series effect *J. Colloid Interface Sci.* **379** 33–40
- Garti N 1997 Progress in stabilization and transport phenomena of double emulsions in food applications *LWT-Food Sci. Technol.* **30** 222–35
- Garti N and Sato K 1988 *Crystallization and Polymorphism of Fats and Fatty Acids (Surfactant Science series)* (New York: Dekker)
- Giovambattista N, Angell C A, Sciotino F and Stanley H E 2004 Glass-transition temperature of water: a simulation study *Phys. Rev. Lett.* **93** 047801
- Godet M, Bizot H and Buléon A 1995 Crystallization of amylose-fatty acid complexes prepared with different amylose chain lengths *Carbohydr. Polym.* **27** 47–52
- Goff H 1997a Instability and partial coalescence in whippable dairy emulsions *J. Dairy Sci.* **80** 2620–30
- Goff H D 1997b Colloidal aspects of ice cream—a review *Int. Dairy J.* **7** 363–73
- Goff H D and Hartel R W 2013 Ice cream structure *Ice Cream* (Berlin: Springer) pp 313–52
- Goll D E, Thompson V F, Li H, Wei W and CONG J 2003 The calpain system *Physiol. Rev.* **83** 731–801
- Gombotz W R and Wee S F 2012 Protein release from alginate matrices *Adv. Drug Delivery Rev.* **64** 194–205
- Gomez A, Ferrero C, Calvelo A, Anon M and Puppo M 2011 Effect of mixing time on structural and rheological properties of wheat flour dough for breadmaking *Int. J. Food Prop.* **14** 583–98
- Gosline J M 1978 The temperature-dependent swelling of elastin *Biopolymers* **17** 697–707
- Granvogl M, Beksan E and Schieberle P 2012 New insights into the formation of aroma-active strecker aldehydes from 3-oxazolines as transient intermediates *J. Agric. Food Chem.* **60** 6312–22
- Gras P, Carpenter H and Anderssen R 2000 Modelling the developmental rheology of wheat-flour dough using extension tests *J. Cereal Sci.* **31** 1–13
- Gregory J, Clary D, Liu K, Brown M and Saykally R 1997 The water dipole moment in water clusters *Science* **275** 814–7
- Greiner M, Reilly A M and Briesen H 2012 Temperature-and pressure-dependent densities, self-diffusion coefficients, and phase behavior of monoacid saturated triacylglycerides: toward molecular-level insights into processing *J. Agric. Food Chem.* **60** 5243–9
- Grønbech-Jensen N, Mashl R J, Bruinsma R F and Gelbart W M 1997 Counterion-induced attraction between rigid polyelectrolytes *Phys. Rev. Lett.* **78** 2477
- Guérin-Dubiard C, Pasco M, Mollé D, Désert C, Croguennec T and Nau F 2006 Proteomic analysis of hen egg white *J. Agric. Food Chem.* **54** 3901–10
- Guilmineau F and Kulozik U 2007 Influence of a thermal treatment on the functionality of hens egg yolk in mayonnaise *J. Food Eng.* **78** 648–54
- Güler S, Köksel H and Ng P 2002 Effects of industrial pasta drying temperatures on starch properties and pasta quality *Food Res. Int.* **35** 421–7
- Guzey D and McClements D J 2006 Formation, stability and properties of multilayer emulsions for application in the food industry *Adv. Colloid Interface Sci.* **128–30** 227–48
- Ha B Y and Liu A J 1997 Counterion-mediated attraction between two like-charged rods *Phys. Rev. Lett.* **79** 1289
- Hachiya I, Koyano T and Sato K 1989a Seeding effects on solidification behavior of cocoa butter and dark chocolate. I. Kinetics of solidification *J. Am. Oil Chem. Soc.* **66** 1757–62

- Hachiya I, Koyano T and Sato K 1989b Seeding effects on solidification behavior of cocoa butter and dark chocolate. II. Physical properties of dark chocolate *J. Am. Oil Chem. Soc.* **66** 1763–70
- Hailing P J and Walstra P 1981 Protein-stabilized foams and emulsions *Crit. Rev. Food Sci. Nutrition* **15** 155–203
- Hamley I W 2005 *Block Copolymers in Solution: Fundamentals and Applications* (New York: Wiley)
- Hamoen J, Vollebregt H and Van der Sman R 2013 Prediction of the time evolution of pH in meat *Food Chem.* **141** 2363–72
- Hanft F and Koehler P 2006 Studies on the effect of glucose oxidase in bread making *J. Sci. Food Agric.* **86** 1699–704
- Hayakawa T, Yoshida Y, Yasui M, Ito T, Iwasaki T, Wakamatsu J, Hattori A and Nishimura T 2012 Heat-induced gelation of myosin in a low ionic strength solution containing l-histidine *Meat sci.* **90** 77–80
- Hedrick H B 1994 *Principles of Meat Science* (Dubuque, Iowa: Kendall/Hunt)
- Heertje I 2014 Structure and function of food products: a review *Food Struct.* **1** 3–23
- Helm C, Möhwald H, Kjaer K and Als-Nielsen J 1987 Phospholipid monolayers between fluid and solid states *Biophys. J.* **52** 381–90
- Herald T J and Smith D M 1992 Heat-induced changes in the secondary structure of hen egg s-ovalbumin *J. Agric. Food Chem.* **40** 1737–40
- Hess B, Holm C and van der Vegt N 2006a Modeling multibody effects in ionic solutions with a concentration dependent dielectric permittivity *Phys. Rev. Lett.* **96** 147801
- Hess B, Holm C and van der Vegt N 2006b Osmotic coefficients of atomistic nacl (aq) force fields *J. Chem. Phys.* **124** 164509
- Hevonenja T, Pentikainen M O, Hyvonen M T, Kovanen P T and Ala-Korpela M 2000 Structure of low density lipoprotein (LDL) particles: basis for understanding molecular changes in modified LDL *Biochem. Biophys. Ata* **1488** 189–210
- Höhne G, Hemminger W and Flammersheim H J 2003 *Differential Scanning Calorimetry* (Berlin: Springer)
- Holm C, Joanny J, Kremer K, Netz R, Reineker P, Seidel C, Vilgis T and Winkler R 2004 Polyelectrolyte theory *Polyelectrolytes with Defined Molecular Architecture II* (Berlin: Springer) pp 67–111
- Hong L and Lei J 2009 Scaling law for the radius of gyration of proteins and its dependence on hydrophobicity *J. Polym. Sci.* **47** 207–14
- Hönig D and Möbius D 1992 Reflectometry at the brewster angle and brewster angle microscopy at the air-water interface *Thin Solid Films* **210** 64–8
- Hopkins D, Toohey E, Kerr M and van de Ven R 2011 Comparison of two instruments (g2 tenderometer and a lloyd texture analyser) for measuring the shear force of cooked meat *Animal Prod. Sci.* **51** 71–6
- Hu J, Zhang X and Wang Z 2010 A review on progress in qspr studies for surfactants *Int. J. Mol. Sci.* **11** 1020–47
- Huang A H C 1992 Oil bodies and oleosin in seeds *Ann. Rev. Plant Physiol. Plant Mol. Biol.* **43** 177–200
- Huang A H C 1996 Oleosins and oil bodies in seeds and other organs *Plant Physiol.* **110** 1055–61
- Huang Q, Qiu N, Ma M, Jin Y, Yang H, Geng F and Sun S 2012 Estimation of egg freshness using s-ovalbumin as an indicator *Poultry Sci.* **91** 739–43
- Huber G and Vilgis T A 2002 On the mechanism of hydrodynamic reinforcement in elastic composites *Macromolecules* **35** 9204–10
- Huber G, Vilgis T A and Heinrich G 1996 Universal properties in the dynamical deformation of filled rubbers *J. Phys.: Condens. Matter* **8** L409
- Huff-Lonergan E, Zhang W and Lonergan S M 2010 Biochemistry of postmortem muscle-lessons on mechanisms of meat tenderization *Meat Sci.* **86** 184–195
- Hui Y H, Nip W K and Rogers R 2001 *Meat Science and Applications* (Boca Raton, FL: CRC Press)
- Hummer G, Pratt L R and García A E 1996 Free energy of ionic hydration *J. Phys. Chem.* **100** 1206–15
- Huppertz T and Kelly A 2006 *Advanced Dairy Chemistry Volume 2 Lipids* (Berlin: Springer) pp 173–212
- Hur S J, Lim B O, Decker E A and McClements D J 2011 In vitro human digestion models for food applications *Food Chem.* **125** 1–12
- Ikeda A, Berthier L and Sollich P 2012 Unified study of glass and jamming rheology in soft particle systems *Phys. Rev. Lett.* **109** 018301
- Imeson A 2011 *Food Stabilisers, Thickeners and Gelling Agents* (New York: Wiley)
- Israelachvili J N 2011 *Intermolecular and Surface Forces: Revised Third Edition* (New York: Academic)
- Israelachvili J and Wennerström H 1996 Role of hydration and water structure in biological and colloidal interactions
- Iwanaga D, Gray D A, Decker E A, Weiss J and McClements D J 2008 Stabilization of soybean oil bodies using protective pectin coatings formed by electrostatic deposition *J. Agric. Food Chem.* **56** 2240–5
- Iwanaga D, Gray D A, Fisk I D, Decker E A, Weiss J and McClements D J 2007 Extraction and characterization of oil bodies from soy beans: a natural source of pre-emulsified soybean oil *J. Agric. Food Chem.* **55** 8711–6
- Jacks T J, Hensarling T P, Neucere J N, Yatsu L Y and Barker R H 1990 Isolation and physicochemical characterization of the half-unit membranes of oilseed lipid bodies *JOACS* **67** 353–61
- Jacobson A L, Devin G and Braun H 1981 Thermal denaturation of beef cardiac troponin and its subunits with and without calcium ion *Biochemistry* **20** 1694–701
- Jain A, Yang G and Yalkowsky S H 2004 Estimation of melting points of organic compounds *Ind. Eng. Chem. Res.* **43** 7618–21
- Jekle M and Becker T 2011 Dough microstructure: novel analysis by quantification using confocal laser scanning microscopy *Food Res. Int.* **44** 984–91
- Jelen H 2011 *Food Flavors: Chemical, Sensory and Technological Properties* (Boca Raton, FL: CRC Press)
- Jenkins P J and Donald A M 1998 Gelatinisation of starch: a combined saks/waxs/dsc and sans study *Carbohydr. Res.* **308** 133–47
- Jensen R G, Ferris A M and Lammi-Keefe C J 1991 The composition of milk fat *J. Dairy Sci.* **74** 3228–43
- Jiménez-Colmenero F 2013 Potential applications of multiple emulsions in the development of healthy and functional foods *Food Res. Int.* **52** 64–74
- Johns P and Courts A 1977 Relationship between collagen and gelatin *The Science and Technology of Gelatin* (New York: Academic) pp 137–77
- Jolivet P, Boulard C, Beaumal V, Chardot T and Anton M 2006 Protein components of low-density lipoproteins purified from hen egg yolk *J. Agric. Food Chem.* **54** 4424–9
- Jolivet P, Boulard C, Bellamy A, Valot B, d'Andrea S, Zivy M, Nesi N and Chardot T 2011 Oil body proteins sequentially accumulated throughout seed development in Brassica napus *J. Plant Physiol.* **168** 2015–20
- Jovanovich G, Zamponi R A, Lupano C E and Anon M C 1992 Effect of water content on the formation and dissociation of the amylose-lipid complex in wheat flour *J. Agric. Food Chem.* **40** 1789–93
- Joye I J, Lagrain B and Delcour J A 2009 Endogenous redox agents and enzymes that affect protein network formation during breadmaking—a review *J. Cereal Sci.* **50** 1–10
- Kanekanian A 2005 Dairy technology-principles of milk properties and processes *Int. J. Dairy Technol.* **58** 237–7
- Kaneko F, Yano J and Sato K 1998 Diversity in the fatty-acid conformation and chain packing of cis-unsaturated lipids *Curr. Opin. Struct. Biol.* **8** 417–25

- Kara S, Arda E, Dolastir F and Pekcan Ö 2011 Thermal phase transitions of agarose in various compositions: a fluorescence study *J. Fluoresc.* **21** 1871–7
- Kargar M, Fayazmanesh K, Alavi M, Spyropoulos F and Norton I T 2012 Investigation into the potential ability of pickering emulsions (food-grade particles) to enhance the oxidative stability of oil-in-water emulsions *J. Colloid Interface Sci.* **366** 209–15
- Karkani O A, Nenadis N, Nikiforidis C V and Kiosseoglou V 2013 Effect of recovery methods on the oxidative and physical stability of oil body emulsions *Food Chem.* **139** 640–8
- Karmas R, Pilar Buera M and Karel M 1992 Effect of glass transition on rates of nonenzymic browning in food systems *J. Agric. Food Chem.* **40** 873–9
- Kasapis S, Al-Marhoobi I M, Deszcynski M, Mitchell J R and Abeysekera R 2003 Gelatin versus polysaccharide in mixture with sugar *Biomacromolecules* **4** 1142–9
- Katkov I I and Levine F 2004 Prediction of the glass transition temperature of water solutions: comparison of different models *Cryobiology* **49** 62–82
- Kawai H, Sakurai M, Inoue Y, Chujo R and Kobayashi S 1992 Hydration of oligosaccharides: anomalous hydration ability of trehalose *Cryobiology* **29** 599–606
- Kawakami K and Norisuye T 1991 Second virial coefficient for charged rods: sodium xanthan in aqueous sodium chloride *Macromolecules* **24** 4898–903
- Khokhlov A R and Khalatur P G 1998 Protein-like copolymers: computer simulation *Physica* **249** 253–61
- Khokhlov A R, Starodubtzev S G and Vasilevskaya V V 1993 Conformational transitions in polymer gels: theory and experiment *Responsive Gels: Volume Transitions I* (Berlin: Springer) pp 123–71
- Kijowski J and Mast M 1988 Thermal properties of proteins in chicken broiler tissues *J. Food Sci.* **53** 363–6
- Kim Y H B, Warner R D and Rosenvold K 2014 Influence of high pre-rigor temperature and fast pH fall on muscle proteins and meat quality: a review *Animal Prod. Sci.* **54** 375–95
- Kim Y R, Cornillon P, Campanella O, Stroshine R, Lee S and Shim J Y 2008 Small and large deformation rheology for hard wheat flour dough as influenced by mixing and resting *J. Food Sci.* **73** E1–8
- Kiosseoglou V 2003 Egg yolk protein gels and emulsions *Curr. Opin. Colloid Interface Sci.* **8** 365–70
- Kiosseoglou V and Sherman P 1983 The influence of egg yolk lipoproteins on the rheology and stability of o/w emulsions and mayonnaise *Colloid Polym. Sci.* **261** 502–7
- Kjaer K, Als-Nielsen J, Helm C, Laxhuber L and Möhwald H 1987 Ordering in lipid monolayers studied by synchrotron x-ray diffraction and fluorescence microscopy *Phys. Rev. Lett.* **58** 2224
- Knoester M, De Bruijne P and Van Den Tempel M 1972 The solid-liquid equilibrium of binary mixtures of triglycerides with palmitic and stearic chains *Chem. Phys. Lipids* **9** 309–19
- Knothe G and Dunn R O 2009 A comprehensive evaluation of the melting points of fatty acids and esters determined by differential scanning calorimetry *J. Am. Oil Chem. Soc.* **86** 843–56
- Koç H, Vinyard C, Essick G and Foegeding E 2013 Food oral processing: conversion of food structure to textural perception *Ann. Rev. Food Sci. Technol.* **4** 237–66
- Kodali D R, Atkinson D, Redgrave T G and Small D M 1987 Structure and polymorphism of 18-carbon fatty acyl triacylglycerols: effect of unsaturation and substitution in the 2-position *J. Lipid Res.* **28** 403–13
- Kokawa M, Fujita K, Sugiyama J, Tsuta M, Shibata M, Araki T and Nabetani H 2012 Quantification of the distributions of gluten, starch and air bubbles in dough at different mixing stages by fluorescence fingerprint imaging *J. Cereal Sci.* **55** 15–21
- Kokawa M, Sugiyama J, Tsuta M, Yoshimura M, Fujita K, Shibata M, Araki T and Nabetani H 2013 Development of a quantitative visualization technique for gluten in dough using fluorescence fingerprint imaging *Food Bioprocess Technol.* **6** 3113–23
- Kokelaar J, Van Vliet T and Prins A 1996 Strain hardening properties and extensibility of flour and gluten doughs in relation to breadmaking performance *J. Cereal Sci.* **24** 199–214
- Krog N 1977 Functions of emulsifiers in food systems *J. Am. Oil Chem. Soc.* **54** 124–31
- Krystyjan M, Sikora M, Adamczyk G and Tomasik P 2012 Caramel sauces thickened with combinations of potato starch and xanthan gum *J. Food Eng.* **112** 22–8
- Kuktaite R, Larsson H, Marttila S and Johansson E 2005 Effect of mixing time on gluten recovered by ultracentrifugation studied by microscopy and rheological measurements *Cereal Chem.* **82** 375–84
- Kunz W, Henle J and Ninham B W 2004 zur lehre von der wirkung der salze(about the science of the effect of salts): Franz hofmeister's historical papers *Curr. Opin. Colloid Interface Sci.* **9** 19–37
- Kurti N 1980 The physicist in the kitchen *New Sci.* **88** 786–9
- Kurti N and This-Benckhard H 1994 Chemistry and physics in the kitchen *Sci. Am.* **270** 44–51
- Kyte J and Doolittle R F 1982 A simple method for displaying the hydrophobic character of a protein *J. Mol. Biol.* **157** 105–32
- Laakkonen E, Sherbon J and Wellington G 1970 Low-temperature, long-time heating of bovine muscle 3 collagenolytic activity *J. Food Sci.* **35** 181–4
- Labropoulos K, Niesz D, Danforth S and Kevrekidis P 2002 Dynamic rheology of agar gels: theory and experiments. part II: gelation behavior of agar sols and fitting of a theoretical rheological model *Carbohydr. Polym.* **50** 407–15
- Lacey D J, Wellner N, Beaudoin F, Napier J A and Shewry P R 1998 Secondary structure of oleosins in oil bodies isolated from seeds of safflower (*Carthamus tinctorius* L.) and sunflower (*Helianthus annuus* L.) *Biochem. J.* **334** 469–77
- Lam R S and Nickerson M T 2013 Food proteins: a review on their emulsifying properties using a structure–function approach *Food Chem.* **141** 975–84
- Langer J 2014 Theories of glass formation and the glass transition *Rep. Prog. Phys.* **77** 042501
- Lanier T C, Yongsawatdigul J and Carvajal-Rondanelli P 2013 Surimi gelation chemistry 4 *Surimi and Surimi Seafood* (Boca Raton, FL: CRC Press) p 101
- Lauridsen J B 1976 Food emulsifiers: surface activity, edibility, manufacture, composition, and application *J. Am. Oil Chem. Soc.* **53** 400–7
- Lawless H T and Heymann H 2010 *Sensory Evaluation of Food: Principles and Practices* vol 5999 (Berlin: Springer)
- Lazaridis T and Paulaitis M E 1992 Entropy of hydrophobic hydration: a new statistical mechanical formulation *J. Phys. Chem.* **96** 3847–55
- Le Révérend B J, Norton I T and Bakalis S 2013 Modelling the human response to saltiness *Food & function* **4** 880–888
- Le Révérend B J, Norton I T, Cox P W and Spyropoulos F 2010 Colloidal aspects of eating *Curr. Opin. Colloid Interface Sci.* **15** 84–9
- Leander R, Hedrick H, Brown M and White J 1980 Comparison of structural changes in bovine long and semitendinosus muscles during cooking *J. Food Sci.* **45** 1–6
- Lechevalier V, Jeantet R, Arhaliass A, Legrand J and Nau F 2007 Egg white drying: influence of industrial processing steps on protein structure and functionalities *J. Food Eng.* **83** 404–13
- Leclerc E and Daoud M 1997 Multiblock copolymers at interfaces: concentration and selectivity effects *Macromolecules* **30** 293–300
- Ledward D *et al* 2000 Gelatin *Handbook of Hydrocolloids* (Boca Raton, FL: CRC Press) pp 67–86

- Lee B and Graziano G 1996 A two-state model of hydrophobic hydration that produces compensating enthalpy and entropy changes *J. Am. Chem. Soc.* **118** 5163–8
- Lee H, Jang E H, Lee J S, Hong W S, Kim Y S and Han J A 2012 Textural and sensory properties of rice noodle blended with hydrocolloids *Korean J. Food Cookery Sci.* **28** 703–9
- Lee K Y and Mooney D J 2012 Alginate: properties and biomedical applications *Prog. Polym. Sci.* **37** 106–26
- Lee Y, Ristic R, DeMatos L and Martin C 2010 Crystallisation pathways of polymorphic triacylglycerols induced by mechanical energy *J. Phys.: Conf. Ser.* **247** 012049
- Leser M E, Sagalowicz L, Michel M and Watzke H J 2006 Self-assembly of polar food lipids *Adv. Colloid Interface Sci.* **123** 125–36
- Levitsky D I, Pivovarova A V, Mikhailova V V and Nikolaeva O P 2008 Thermal unfolding and aggregation of actin *Febs J.* **275** 4280–95
- Levy Y and Onuchic J N 2004 Water and proteins: a love–hate relationship *Proc. Natl Acad. Sci.* **101** 3325–26
- Lewicki P P 2004 Water as the determinant of food engineering properties. A review *J. Food Eng.* **61** 483–95
- Li M, Keddie J S, Smith L J, Clark D C and Murphy D J 1993 Expression and characterization of the n-terminal domain of an oleosin protein from sunflower *J. Biol. Chem.* **268** 17504–12
- Li M, Murphy D J, Lee K H K, Wilson R, Smith L J, Clark D C and Sung J Y 2002 Purification and structural characterisation of the central hydrophobic domain of oleosin *J. Biol. Chem.* **277** 37888–95
- Lberman V 2014 Molecular gastronomy
- Lii C Y, Tsai M L and Tseng K H 1996 Effect of amylose content on the rheological property of rice starch *Cereal Chem.* **73** 415–20
- Lillford P 2001 Mechanisms of fracture in foods *J. Texture Stud.* **32** 397–417
- Lillford P J 2011 The importance of food microstructure in fracture physics and texture perception *J. Texture Stud.* **42** 130–6
- Little R C 1978 Correlation of surfactant hydrophile-lipophile balance (hlb) with solubility parameter *J. Colloid Interface Sci.* **65** 587–8
- Liu A J and Nagel S R 2001 *Jamming and Rheology: Constrained Dynamics on Microscopic and Macroscopic Scales* (Boca Raton, FL: CRC Press)
- Liu J, Ruusunen M, Puolanne E and Ertbjerg P 2014 Effect of pre-rigor temperature incubation on sarcoplasmic protein solubility, calpain activity and meat properties in porcine muscle *LWT-Food Sci. Technol.* **55** 483–9
- Liu S, Joshi S C and Lam Y 2008 Effects of salts in the Hofmeister series and solvent isotopes on the gelation mechanisms for hydroxypropylmethylcellulose hydrogels *J. Appl. Polym. Sci.* **109** 363–72
- Lomiwes D, Farouk M, Wiklund E and Young O 2014 Small heat shock proteins and their role in meat tenderness: a review *Meat sci.* **96** 26–40
- Lopez C 2005 Focus on the supramolecular structure of milk fat *Reprod. Nutrition Dev.* **45** 497–511
- Lopez C, Bourgaux C, Lesieur P and Ollivon M 2002 Crystalline structures formed in cream and anhydrous milk fat at 4 °C *Le Lait* **82** 317–35
- Lösche M, Sackmann E and Möhwald H 1983 A fluorescence microscopic study concerning the phase diagram of phospholipids *Ber. Bunsenges. Phys. Chem.* **87** 848–52
- Lucas P, Prinz J, Agrawal K and Bruce I 2002 Food physics and oral physiology *Food Qual. Preference* **13** 203–13
- Luther P K 2009 The vertebrate muscle z-disc: sarcomere anchor for structure and signalling *J. Muscle Res. Cell Motility* **30** 171–85
- Ma Y and Barbano D 2000 Gravity separation of raw bovine milk: fat globule size distribution and fat content of milk fractions *J. Dairy Sci.* **83** 1719–27
- MacRitchie F 2014 Theories of glutenin/dough systems *J. Cereal Sci.* **60** 4–6
- Malik R, Hall C K and Genzer J 2013 Effect of protein-like copolymers composition on the phase separation dynamics of a polymer blend: a monte carlo simulation *Macromolecules* **46** 4207–14
- Malkin A Y, Masalova I, Slatter P and Wilson K 2004 Effect of droplet size on the rheological properties of highly-concentrated w/o emulsions *Rheol. Acta* **43** 584–91
- Mandelkern L 1964 *Crystallization of Polymers* vol 38 (38: New York)
- Mann J, Schiedt B, Baumann A, Conde-Petit B and Vilgis T A 2013 Effect of heat treatment on wheat dough rheology and wheat protein solubility *Food Sci. Technol. Int.* **20** 341–51
- Manning G 2011 Counterion condensation theory of attraction between like charges in the absence of multivalent counterions *Eur. Phys. J.* **34** 1–18
- Marangoni A G 2002 The nature of fractality in fat crystal networks *Trends Food Sci. Technol.* **13** 37–47
- Marangoni A G and McGauley S E 2003 Relationship between crystallization behavior and structure in cocoa butter *Cryst. Growth Des.* **3** 95–108
- Marangoni A G and Rogers M A 2003 Structural basis for the yield stress in plastic disperse systems *Appl. Phys. Lett.* **82** 3239–41
- Marangoni A G and Rousseau D 1996 Is plastic fat rheology governed by the fractal nature of the fat crystal network? *J. Am. Oil Chem. Soc.* **73** 991–4
- Marina A, Man Y C, Nazimah S and Amin I 2009 Chemical properties of virgin coconut oil *J. Am. Oil Chem. Soc.* **86** 301–7
- Mark J E, Erman B and Roland M 2013 *The Science and Technology of Rubber* (New York: Academic)
- Marshall M E and Deutsch H 1951 Distribution of egg white proteins in chicken blood serum and egg yolk *J. Biol. Chem.* **189** 1–9
- Martens H, Stabursvik E and Martens M 1982 Texture and colour changes in meat during cooking related to thermal denaturation of muscle proteins *J. Texture Stud.* **13** 291–309
- Mason T, Bibette J and Weitz D 1996 Yielding and flow of monodisperse emulsions *J. Colloid Interface Sci.* **179** 439–48
- Matsumoto S 1986 W/o/w-type multiple emulsions with a few to possible food applications *J. Texture Stud.* **17** 141–59
- Matsuoka H, Hachisuka M, Uda K, Onishi T and Ozoe S 2012 Why ionic amphiphilic block copolymer can be non-surface active? comparison of homopolymer, block and random copolymers of poly (styrenesulfonate) *Chem. Lett.* **41** 1063–5
- Maurer S 2014 Spray drying of soybean oleosomes *PhD Thesis*, TU Berlin
- Maurer S, Junghans A and Vilgis T A 2012 Impact of xanthan gum, sucrose and fructose on the viscoelastic properties of agarose hydrogels *Food Hydrocolloids* **29** 298–307
- Maurer S, Waschatho G, Schach D, Zielbauer B I, Dahl J, Weidner T, Bonn M and Vilgis T A 2013 The role of intact oleosin for stabilization and function of oleosomes *J. Phys. Chem.* **117** 13872–83
- Maurstad G and Stokke B T 2004 Metastable and stable states of xanthan polyelectrolyte complexes studied by atomic force microscopy *Biopolymers* **74** 199–213
- Maximo G J, Costa M C, Coutinho J A and Meirelles A 2014 Trends and demands in solid-liquid equilibrium of lipidic mixtures *RSC Adv.* **4** 31840–50
- Mayama H 2009 Blooming theory of tristearin *Soft Matter* **5** 856–9
- McClements D J 1999 *Food Emulsion: Principles, Practice and Techniques* (Boca Raton, FL: CRC Press)

- Menjivar J A 1990 Fundamental aspects of dough rheology *Dough Rheology and Baked Product Texture* (Berlin: Springer) pp 1–28
- Meste M L, Champion D, Roudaut G, Blond G and Simatos D 2002 Glass transition and food technology: a critical appraisal *J. Food Sci.* **67** 2444–58
- Meyer L C and Wright N T 2013 Structure of giant muscle proteins *Frontiers Physiol.* **4** 368
- Miao B, Vilgis T A, Poggendorf S and Sadowski G 2010 Effect of finite extensibility on the equilibrium chain size *Macromol. Theory Simul.* **19** 414–20
- Michalski M C 2009 Specific molecular and colloidal structures of milk fat affecting lipolysis, absorption and postprandial lipemia *Eur. J. Lipid Sci. Technol.* **111** 413–31
- Michalski M C, Ollivon M, Briard V, Leconte N and Lopez C 2004 Native fat globules of different sizes selected from raw milk: thermal and structural behavior *Chem. Phys. Lipids* **132** 247–61
- Micka U and Kremer K 1996 Persistence length of the debye-hückel model of weakly charged flexible polyelectrolyte chains *Phys. Rev.* **54** 2653
- Mietsch F, Halász A and Farkas J 1994 Untersuchung über änderungen von fleischproteinen während der gefrierlagerung *Food/Nahrung* **38** 47–52
- Miller A, Knoll W and Möhwald H 1986 Fractal growth of crystalline phospholipid domains in monomolecular layers *Phys. Rev. Lett.* **56** 2633
- Millichip M, Tatham A S, Jackson F, Griffiths G, Shewry P R and Stobart A K 1996 Purification and characterization of oil-bodies (oleosomes) and oil-body boundary proteins (oleosins) from the developing cotyledons of sunflower (*Helianthus Annuus L.*) *Biochemistry* **31** 433–7
- Mills T, Spyropoulos F, Norton I T and Bakalis S 2011 Development of an in vitro mouth model to quantify salt release from gels *Food Hydrocolloids* **25** 107–13
- Mine Y 1995 Recent advances in the understanding of egg white protein functionality *Trends Food Sci. Technol.* **6** 225–32
- Mine Y, Noutomi T and Haga N 1990 Thermally induced changes in egg white proteins *J. Agric. Food Chem.* **38** 2122–5
- Mitchell M, Brunton N P and Wilkinson M G 2011 Impact of salt reduction on the instrumental and sensory flavor profile of vegetable soup *Food Res. Int.* **44** 1036–43
- Mohammed Z H, Hember M, Richardson R and Morris E 1998 Kinetic and equilibrium processes in the formation and melting of agarose gels *Carbohydr. Polym.* **36** 15–26
- Møller A 1981 Analysis of warner-bratzler shear pattern with regard to myofibrillar and connective tissue components of tenderness *Meat Sci.* **5** 247–60
- Monsón F, Sañudo C and Sierra I 2004 Influence of cattle breed and ageing time on textural meat quality *Meat Sci.* **68** 595–602
- Morell P, Fiszman S, Varela P and Hernando I 2014 Hydrocolloids for enhancing satiety: relating oral digestion to rheology, structure and sensory perception *Food Hydrocolloids* **41** 343–53
- Morris E R, Nishinari K and Rinaudo M 2012 Gelation of gellan—a review *Food Hydrocolloids* **28** 373–411
- Mulder H and Walstra P 1974 *The Milk Fat Globule* (Slough: Commonwealth Agricultural Bureaux)
- Munk M B, Marangoni A G, Ludvigsen H K, Norn V, Knudsen J C, Risbo J, Ipsen R and Andersen M L 2013 Stability of whippable oil-in-water emulsions: effect of monoglycerides on crystallization of palm kernel oil *Food Res. Int.* **54** 1738–45
- Murphy R, Marks B and Marcy J 1998 Apparent specific heat of chicken breast patties and their constituent proteins by differential scanning calorimetry *J. Food Sci.* **63** 88–91
- Muschiolik G 2007 Multiple emulsions for food use *Curr. Opin. Colloid Interface Sci.* **12** 213–20
- Myhrvold N and Smith R M 2011 *Modernist Cuisine* (Cologne: Taschen)
- Nakai S 1983 Structure-function relationships of food proteins: with an emphasis on the importance of protein hydrophobicity *J. Agric. Food Chem.* **31** 676–83
- Narine S S and Marangoni A G 1999a Fractal nature of fat crystal networks *Phys. Rev. E* **59** 1908
- Narine S S and Marangoni A G 1999b Relating structure of fat crystal networks to mechanical properties: a review *Food Res. Int.* **32** 227–48
- N'da Kouamé V, Handschin S, Derungs M, Amani G and Conde-Petit B 2011 Thermal properties of new varieties of yam starches *Starch—Stärke* **63** 747–53
- Neri L, Pittia P, Di Mattia C D, Bertolo G, Mastrolola D and Sacchetti G 2014 Multiple effects of viscosity, water activity and glass transition temperature on peroxidase activity in binary and ternary carbohydrate solutions *Food Biophys.* **9** 260–6
- Ngapo T, Babare I, Reynolds J and Mawson R 1999 Freezing and thawing rate effects on drip loss from samples of pork *Meat Sci.* **53** 149–58
- Nikiforidis C V, Karkani O A and Kiosseoglou V 2011 Exploitation of maize germ for the preparation of a stable oil-body nanoemulsion using a combined aqueous extraction—ultrafiltration method *Food Hydrocolloids* **25** 1122–7
- Nikiforidis C V and Kiosseoglou V 2010 Physicochemical Stability of Maize Germ Oil Body Emulsions As Influenced by Oil Body Surface-Xanthan Gum Interactions *J. Agric. Food Chem.* **58** 527–32
- Nikiforidis C V, Kiosseoglou V and Scholten E 2013 Oil bodies: an insight on their microstructure—maize germ versus sunflower seed *Food Res. Int.* **52** 136–41
- Nilsson M 2014 Fine tuiles aux grains de lin *Yam Mag. Chefs* **19** 76–77
- Nishinari K, Fang Y, Guo S and Phillips G 2014 Soy proteins: a review on composition, aggregation and emulsification *Food Hydrocolloids* **39** 301–18
- Nishinari K and Watase M 1992 Effects of sugars and polyols on the gel-sol transition of kappa-carrageenan gels *Thermochim. Acta* **206** 149–62
- Nishinari K, Watase M, Kohyama K, Nishinari N, Oakenfull D, Koide S, Ogino K, Williams P A and Phillips G O 1992 The effect of sucrose on the thermo-reversible gel-sol transition in agarose and gelatin *Polym. J.* **24** 871–7
- Nordqvist D and Vilgis T A 2011 Rheological study of the gelation process of agarose-based solutions *Food Biophys.* **6** 450–60
- Normand V, Lootens D L, Amici E, Plucknett K P and Aymard P 2000 New insight into agarose gel mechanical properties *Biomacromolecules* **1** 730–8
- Norn V 2014 *Emulsifiers in Food Technology* (New York: Wiley)
- Norton I, Frith W and Ablett S 2006 Fluid gels, mixed fluid gels and satiety *Food Hydrocolloids* **20** 229–39
- Ogawa T 2014 Drying and rehydration kinetics of pasta
- Ohtaki H and Radnai T 1993 Structure and dynamics of hydrated ions *Chem. Rev.* **93** 1157–204
- O'Lenick A J Jr and Parkinson J K 1996 Three-dimensional hlb *Cosmetics Toiletries* **111** 37–46
- Ollivier D, Artaud J, Pinatel C, Durbec J P and Guérere M 2006 Differentiation of french virgin olive oil rdos by sensory characteristics, fatty acid and triacylglycerol compositions and chemometrics *Food Chem.* **97** 382–93
- Olsson P and Teitel S 2007 Critical scaling of shear viscosity at the jamming transition *Phys. Rev. Lett.* **99** 178001
- Onuchic J N and Wolynes P G 2004 Theory of protein folding *Curr. Opin. Struct. Biol.* **14** 70–5
- Osada Y and Khokhlov A 2001 *Polymer Gels and Networks* (Boca Raton, FL: CRC Press)
- Pal R 1996 Effect of droplet size on the rheology of emulsions *AIChE J.* **42** 3181–90
- Parsons D F, Boström M, Nostro P L and Ninham B W 2011 Hofmeister effects: interplay of hydration, nonelectrostatic

- potentials, and ion size *Phys. Chem. Chem. Phys.* **13** 12352–67
- Pawar A B, Caggioni M, Ergun R, Hartel R W and Spicer P T 2011 Arrested coalescence in pickering emulsions *Soft Matter* **7** 7710–6
- Pearson A M 2012 *Muscle and Meat Biochemistry* (Amsterdam: Elsevier)
- Phillips G O and Williams P A 2009 *Handbook of Hydrocolloids* (Amsterdam: Elsevier)
- Piazza L, Gigli J and Bulbarello A 2008 Interfacial rheology study of espresso coffee foam structure and properties *J. Food Eng.* **84** 420–9
- Pinzer B, Medebach A, Limbach H, Dubois C, Stampanoni M and Schneebeli M 2012 3d-characterization of three-phase systems using x-ray tomography: tracking the microstructural evolution in ice cream *Soft Matter* **8** 4584–94
- Plotkin S S and Onuchic J N 2002 Understanding protein folding with energy landscape theory. Part I basic concepts *Quart. Rev. Biophys.* **35** 111–67
- Pospiech E, Greaser M L, Mikolajczak B, Chiang W and Krzywdzińska M 2002 Thermal properties of titin from porcine and bovine muscles *Meat sci.* **62** 187–92
- Powrie W, Little H and Lopez A 1963 Gelation of egg yolk *J. Food Sci.* **28** 38–46
- Precht D 1988 Fat crystal structure in cream and butter *Crystallization and Polymorphism of Fats and Fatty Acids* vol 31 (New York: M Dekker)
- Prins A *et al* 1988 Principles of foam stability *Advances in Food Emulsions and Foams* (New York: Elsevier) pp 91–122
- Prinz J, Janssen A and De Wijk R 2007 In vitro simulation of the oral processing of semi-solid foods *Food Hydrocolloids* **21** 397–401
- Purkrbova Z, Jolivet P, Miquel M and Chardot T 2008 Structure and function of seed lipid body-associated proteins *C. R. Biol.* **331** 746–54
- Purslow P P 1985 The physical basis of meat texture: Observations on the fracture behaviour of cooked bovine m. semitendinosus *Meat Sci.* **12** 39–60
- Purslow P P 2005 Intramuscular connective tissue and its role in meat quality *Meat Sci.* **70** 435–47
- Purslow P P 2014 New developments on the role of intramuscular connective tissue in meat toughness *Ann. Rev. Food Sci. Technol.* **5** 133–53
- Qiu S, Yadav M P, Liu Y, Chen H, Tatsumi E and Yin L 2015 Effects of corn fiber gum with different molecular weights on the gelatinization behaviors of corn and wheat starch *Food Hydrocolloids*
- Raikos V, Campbell L and Euston S R 2007 Rheology and texture of hen's egg protein heat-set gels as affected by pH and the addition of sugar and/or salt *Food Hydrocolloids* **21** 237–44
- Rajah K K 2014 *Fats in Food Technology* (New York: Wiley)
- Rao M A 2014 Rheology of food gum and starch dispersions *Rheology of Fluid, Semisolid, and Solid Foods* (Berlin: Springer) pp 161–229
- Raven P H, Evert R F and Eichhorn S E 2005 *Biology of Plants* (London: Macmillan)
- Rayment I, Holden H M, Whittaker M, Yohn C B, Lorenz M, Holmes K C and Milligan R A 1993 Structure of the actin-myosin complex and its implications for muscle contraction *Science* **261** 58–65
- Rees D A 1977 *Polysaccharide Shapes* (London: Chapman and Hall)
- Rees D A and Welsh E J 1977 Secondary and tertiary structure of polysaccharides in solutions and gels *Angew. Chem. Int. Ed. Engl.* **16** 214–24
- Reineccius G 2004 *Flavor Chemistry and Technology* (Boca Raton, FL: CRC press)
- Rognså G H, Rathe M, Paulsen M T, Petersen M A, Brüggemann D A, Sivertsvik M and Risbo J 2014 Preparation methods influence gastronomical outcome of hollandaise sauce *Int. J. Gastronomy Food Sci.* **2** 32–45
- Ross-Murphy S B 1987 Physical gelation of biopolymers *Food Hydrocolloids* **1** 485–95
- Ross-Murphy S B 1992 Structure and rheology of gelatin gels: recent progress *Polymer* **33** 2622–7
- Ross-Murphy S B 1995 Structure—property relationships in food biopolymer gels and solutions *J. Rheol.* **39** 1451–63
- Roura P, Fort J and Saurina J 2000 How long does it take to boil an egg? A simple approach to the energy transfer equation *Eur. J. Phys.* **21** 95
- Rousseau D 2000 Fat crystals and emulsion stability: a review *Food Res. Int.* **33** 3–14
- Roux E, Baumberger S, Axelos M A V and Chardot T 2004 Oleosins of *Arabidopsis thaliana*: expression in *Escherichia coli*, purification, and functional properties *J. Agric. Food Chem.* **52** 5245–9
- Russ N, Zielbauer B I, Koynov K and Vilgis T A 2013 Influence of nongelling hydrocolloids on the gelation of agarose *Biomacromolecules* **14** 4116–24
- Russ N, Zielbauer B I and Vilgis T A 2014 Impact of sucrose and trehalose on different agarose-hydrocolloid systems *Food Hydrocolloids* **41** 44–52
- Sacanna S, Kegel W and Philipse A 2007 Thermodynamically stable pickering emulsions *Phys. Rev. Lett.* **98** 158301
- Saenger 1987 Structure and dynamics of watersurrounding biomolecules *Ann. Rev. Biophys. Chem.* **16** 93–114
- Sagalowicz L, Leser M, Watzke H and Michel M 2006 Monoglyceride self-assembly structures as delivery vehicles *Trends Food Sci. Technol.* **17** 204–14
- Saha D and Bhattacharya S 2010 Hydrocolloids as thickening and gelling agents in food: a critical review *J. Food Sci. Technol.* **47** 587–97
- Sajedi M, Nasirpour A, Keramat J and Desobry S 2014 Effect of modified whey protein concentrate on physical properties and stability of whipped cream *Food Hydrocolloids* **36** 93–101
- Samaraweera H, Zhang W g, Lee E J and Ahn D U 2011 Egg yolk phosphitin and functional phosphopeptides—review *J. Food Sci.* **76** R143–50
- Sapei L, Naqvi M A and Rousseau D 2012 Stability and release properties of double emulsions for food applications *Food hydrocolloids* **27** 316–23
- Sato K 2001 Crystallization behaviour of fats and lipids—a review *Chem. Eng. Sci.* **56** 2255–65
- Sato K and Ueno S 2014 *Physical Properties of Fats in Food I* (New York: Wiley)
- Schenk H and Peschar R 2004 Understanding the structure of chocolate *Radiat. Phys. Chem.* **71** 829–35
- Scheuble N, Geue T, Windhab E J and Fischer P 2014 Tailored interfacial rheology for gastric stable adsorption layers *Biomacromolecules* **15** 3139–45
- Schiedt B, Baumann A, Conde-Petit B and Vilgis T A 2013 Short-and long-range interactions governing the viscoelastic properties during wheat dough and model dough development *J. Texture Stud.* **44** 317–32
- Seiffert S and Sprakel J 2012 Physical chemistry of supramolecular polymer networks *Chem. Soc. Rev.* **41** 909–30
- Sessions L A R B, Clarke A R, Tatham A S, Shewry P R and Napier J A 2002 Characterization and modelling of the hydrophobic domain of a sunflower oleosin *Planta* **214** 546–51
- Sfatos C, Gutin A and Shakhnovich E 1993 Phase diagram of random copolymers *Phys. Rev. E* **48** 465
- Shakhnovich E I 1997 Theoretical studies of protein-folding thermodynamics and kinetics *Curr. Opin. Struct. Biol.* **7** 29–40
- Sheikh F, Bang M L, Lange S and Chen J 2007 “z”eroing in on the role of cypher in striated muscle function, signaling, and human disease *Trends Cardiovasc. Med.* **17** 258–62

- Shewry H M and Stokes J R 2015 Analytically predicting the viscosity of hard sphere suspensions from the particle size distribution *J. Non-Newtonian Fluid Mech.* **222** 72–81
- Shewry P R, Halford N G, Belton P S and Tatham A S 2002 The structure and properties of gluten: an elastic protein from wheat grain *Phil. Trans. R. Soc. Lond.* **357** 133–42
- Shewry P and Tatham A 1997 Disulphide bonds in wheat gluten proteins *J. Cereal Sci.* **25** 207–27
- Shih W H, Shih W Y, Kim S I, Liu J and Aksay I A 1990 Scaling behavior of the elastic properties of colloidal gels *Phys. Rev. A* **42** 4772
- Shimada T L and Hara-Nishimura I 2010 Oil-body-membrane proteins and Their physiological functions in plants *Biol. Pharm. Bull.* **33** 360–3
- Shimizu S and Matubayasi N 2014 Gelation: the role of sugars and polyols on gelatin and agarose *J. Phys. Chem. B* **118** 13210–6
- Shimoni E, Dirks E and Labuza T 2002 The relation between final popped volume of popcorn and thermal—physical parameters *LWT-Food Sci. Technol.* **35** 93–8
- Shogren R 1992 Effect of moisture content on the melting and subsequent physical aging of cornstarch *Carbohydr. Polym.* **19** 83–90
- Siloto R M P, Findlay K, Lopez-Villalobos A, Yeung E C and Nykiforuk C L 2006 The accumulation of oleosins determines the size of seed oilbodies in arabidopsis *Plant Cell* **18** 1961–74
- Silva R C, Soares F A S D M, Maruyama J M, Dagostinho N R, Silva Y A, Calligaris G A, Ribeiro A P B, Cardoso L P and Gioielli L A 2014 Effect of diacylglycerol addition on crystallization properties of pure triacylglycerols *Food Res. Int.* **55** 436–44
- Singh H and MacRitchie F 2001 Application of polymer science to properties of gluten *J. Cereal Sci.* **33** 231–43
- Skerritt J H, Hac L and Bekes F 1999 Depolymerization of the glutenin macropolymer during dough mixing: I. Changes in levels, molecular weight distribution, and overall composition *Cereal Chem.* **76** 395–401
- Slade L and Levine H 1991 A food polymer science approach to structure-property relationships in aqueous food systems: non-equilibrium behavior of carbohydrate-water systems *Water Relationships in Foods* (Berlin: Springer) pp 29–101
- Slade L, Levine H and Reid D S 1991 Beyond water activity: recent advances based on an alternative approach to the assessment of food quality and safety *Crit. Rev. Food Sci. Nutrition* **30** 115–360
- Small D, Wang L and Mitsche M A 2009 The adsorption of biological peptides and proteins at the oil/water interface. A potentially important but largely unexplored field *J. Lipid Res.* **50** 329–34
- Smith J 1991 *Food Additive User's Handbook* (Berlin: Springer)
- Smits M, Ghosh A, Sterrer M, Müller M and Bonn M 2007 Ultrafast vibrational energy transfer between surface and bulk water at the air–water interface *Phys. Rev. Lett.* **98** 098302
- Smulders F, Hofbauer P and Geesink G H 2014 The conversion of muscle to meat *Meat Inspection and Control in the Slaughterhouse* (Chichester: Wiley) pp 399–421
- Squire J M 1997 Architecture and function in the muscle sarcomere *Curr. Opin. Struct. Biol.* **7** 247–57
- Stanley D, Goff H and Smith A 1996 Texture-structure relationships in foamed dairy emulsions *Food Res. Int.* **29** 1–13
- Stanley H E 1971 *Introduction to Phase Transitions and Critical Phenomena* (Oxford: Oxford University Press)
- Steiger G, Müller-Fischer N, Cori H and Conde-Petit B 2014 Fortification of rice: technologies and nutrients *Ann. N.Y. Acad. Sci.* **1324** 29–39
- Strixner T, Sterr J, Kulozik U and Gebhardt R 2014 Structural study on hen-egg yolk high density lipoprotein (hdl) granules *Food Biophys.* **9** 314–21
- Sun X D and Holley R A 2011 Factors influencing gel formation by myofibrillar proteins in muscle foods *Compr. Rev. Food Sci. Food Saf.* **10** 33–51
- Szopinski D, Kulicke W M and Luinstra G A 2015 Structure—property relationships of carboxymethyl hydroxypropyl guar gum in water and a hyperentanglement parameter *Carbohydr. Polym.* **119** 159–66
- Talbot G 2014 Fats for chocolate and sugar confectionery 1 *Fats in Food Technology* (Chichester: Wiley) p 169
- Tan C and Che Man Y 2002 Differential scanning calorimetric analysis of palm oil, palm oil based products and coconut oil: effects of scanning rate variation *Food Chem.* **76** 89–102
- Tanford C and Roxby R 1972 Interpretation of protein titration curves. application to lysozyme *Biochemistry* **11** 2192–8
- Tang D and Marangoni A G 2006 Quantitative study on the microstructure of colloidal fat crystal networks and fractal dimensions *Adv. Colloid Interface Sci.* **128** 257–65
- Tatham A S and Shewry P R 2000 Elastomeric proteins: biological roles, structures and mechanisms *Trends Biochem. Sci.* **25** 567–71
- Tatham A and Shewry P 2008 Rubber elasticity and wheat gluten proteins *Food Materials Science* (Berlin: Springer) pp 83–94
- Taylor W R and Lin K 2003 Protein knots: a tangled problem *Nature* **421** 25
- Telis V and Kieckbusch T 1998 Viscoelasticity of frozen/thawed egg yolk as affected by salts, sucrose and glycerol *J. Food Sci.* **63** 20–4
- Telis V R N and Kieckbusch T 1997 Viscoelasticity of frozen/thawed egg yolk *J. Food Sci.* **62** 548–50
- TheUniProtConsortium 2014 Activities at the universal protein resource (uniprot) *Nucl. Acids Res.* **42** D191–8
- Thirumalai D 1995 From minimal models to real proteins: time scales for protein folding kinetics *J. Phys.* **5** 1457–67
- This H 2005 Modelling dishes and exploring culinary precisions: the two issues of molecular gastronomy *Br. J. Nutrition* **93** S139–46
- Tielrooij K, Garcia-Araez N, Bonn M and Bakker H 2010 Cooperativity in ion hydration *Science* **328** 1006–9
- Tielrooij K J, Hunger J, Buchner R, Bonn M and Bakker H J 2010 Influence of concentration and temperature on the dynamics of water in the hydrophobic hydration shell of tetramethylurea *J. Am. Chem. Soc.* **132** 15671–8
- Timgren A, Rayner M, Sjöö M and Dejmek P 2011 Starch particles for food based pickering emulsions *Proc. Food Sci.* **1** 95–103
- Timms R 1984 Phase behaviour of fats and their mixtures *Prog. Lipid Res.* **23** 1–38
- Ting J T L, Lee K Y, Ratnayake C and Platt K A 1996 Oleosin genes in maize kernels having diverse oil contents constitutively expressed independent of oil contents—size and shape of intracellular oil bodies are determined by the oleosins oils ratio *Planta* **199** 158–65
- Tolstoguzov V 2003 Some thermodynamic considerations in food formulation *Food Hydrocolloids* **17** 1–23
- Tomozawa M 1996 Fracture of glasses *Ann. Rev. Mater. Sci.* **26** 43–74
- Tornberg E 2005 Effects of heat on meat proteins—implications on structure and quality of meat products *Meat Science* **70** 493–508
- Treloar L R G 1975 *The Physics of Rubber Elasticity* (Oxford: Oxford University Press)
- Troller J and Christian J 2012 *Water Activity and Food* (New York: Elsevier)
- Truong T, Bansal N and Bhandari B 2014 Effect of emulsion droplet size on foaming properties of milk fat emulsions *Food Bioprocess Technol.* **7** 3416–28
- Tuhumury H, Small D and Day L 2014 The effect of sodium chloride on gluten network formation and rheology *J. Cereal Sci.* **60** 229–37
- Tzen J T C 2012 Integral proteins in plant oil bodies *Int. Scholarly Res. Netw. Bot.* **2012** 1–16
- Tzen J T C, Cao Y Z, Laurent P, Ratnayake C and Huang A H C 1993 Lipids, proteins, and structure of seed oil bodies from diverse species *Plant Physiol.* **101** 267–276

- Tzen J T C and Huang A H C 1992 Surface structure and properties of plant seed oil bodies *J. Cell Biol.* **117** 327–35
- Tzschirner H and Vilgis T 2013 *Sous Vide* (Cologne: Fackelträger)
- Uedaira H, Ikura M and Uedaira H 1989 Natural-abundance oxygen-17 magnetic relaxation in aqueous solutions of carbohydrates *Bull. Chem. Soc. Japan* **62** 1–4
- Unsworth J and Duarte F 1979 Heat diffusion in a solid sphere and fourier theory: an elementary practical example *Am. J. Phys.* **47** 981–3
- Vaclavik V A, Christian E W and Christian E W 2008 *Essentials of Food Science* vol 42 (42: Berlin)
- Valanis K and Landel R 1967 The strain-energy function of a hyperelastic material in terms of the extension ratios *J. Appl. Phys.* **38** 2997–3002
- van de Velde F, van Riel J and Tromp R H 2002 Visualisation of starch granule morphologies using confocal scanning laser microscopy (cslm) *J. Sci. Food Agric.* **82** 1528–36
- van der Linden E, McClements D J and Ubbink J 2008 Molecular gastronomy: a food fad or an interface for science-based cooking? *Food Biophys.* **3** 246–54
- Van der Maarel J R 2008 *Introduction to Biopolymer Physics* (Singapore: World Scientific)
- Van der Sman R 2007 Moisture transport during cooking of meat: an analysis based on Flory–Rehner theory *Meat sci.* **76** 730–8
- Van der Sman R 2012 Thermodynamics of meat proteins *Food Hydrocolloids* **27** 529–35
- Van der Sman R and Meinders M 2011 Prediction of the state diagram of starch water mixtures using the Flory–Huggins free volume theory *Soft Matter* **7** 429–42
- Van der Sman R and Meinders M 2013 Moisture diffusivity in food materials *Food Chem.* **138** 1265–74
- Van Kleef F, Boskamp J and Van den Tempel M 1978 Determination of the number of cross-links in a protein gel from its mechanical and swelling properties *Biopolymers* **17** 225–35
- van Mechelen J B, Peschar R and Schenk H 2006a Structures of mono-unsaturated triacylglycerols. I. The 1 polymorph *Acta Crystallogr.* **62** 1121–30
- van Mechelen J B, Peschar R and Schenk H 2006b Structures of mono-unsaturated triacylglycerols. II. The 2 polymorph *Acta Crystallogr.* **62** 1131–8
- van Vlijmen H W, Schaefer M and Karplus M 1998 Improving the accuracy of protein pka calculations: conformational averaging versus the average structure *Proteins: Struct. Funct. Bioinform.* **33** 145–58
- Varela P, Pintor A and Fiszman S 2014 How hydrocolloids affect the temporal oral perception of ice cream *Food Hydrocolloids* **36** 220–8
- Vargo K B, Parthasarathy R and Hammera D A 2012 Self-assembly of tunable protein suprastructures from recombinant oleosin *Proc. Natl Acad. Sci. USA* **109** 11657–62
- Vaughan C D and Rice D A 1990 Predicting o/w emulsion stability by the required hlb equation *J. Dispers. Sci. Technol.* **11** 83–91
- Vega C and Mercadé-Prieto R 2011 Culinary biophysics: on the nature of the 6X°C egg *Food Biophys.* **6** 152–9
- Vega C and Ubbink J 2008 Molecular gastronomy: a food fad or science supporting innovative cuisine? *Trends Food Sci. Technol.* **19** 372–82
- Vermeylen R, Derycke V, Delcour J A, Goderis B, Reynaers H and Koch M H 2006 Gelatinization of starch in excess water: beyond the melting of lamellar crystallites. A combined wide- and small-angle x-ray scattering study *Biomacromolecules* **7** 2624–30
- Vetharaniam I, Thomson R A, Devine C and Daly C 2010 Modelling muscle energy-metabolism in anaerobic muscle *Meat sci.* **85** 134–48
- Viebke C 2005 Order-disorder conformational transition of xanthan gum *Polysaccharides: Structural Diversity and Functional Versatility* vol 2 (New York: Marcel Dekker)
- Vilgis T 1987 Swollen and condensed states of polymeric fractals *Phys. Rev. A* **36** 1506
- Vilgis T 1992 Scaling theory for the size of crumpled membranes in presence of linear polymers and other objects *J. Phys.* **II 2** 1961–72
- Vilgis T 2000 Polymer theory: path integrals and scaling *Phys. Rep.* **336** 167–254
- Vilgis T 2007 *Die Molekularküche—das Kochbuch* (Wiesbaden: Tre Torri)
- Vilgis T 2009 *Molekularküche: Geschmack, Aromen, Flavour* (Wiesbaden: Tre Torri)
- Vilgis T 2010 *Das Moleküll-Menü: Molekulare Grundlagen für Kreative Köche* (Stuttgart: Hirzel)
- Vilgis T 2012a Aber bitte mit sahne *Phys. unserer Zeit* **43** 102
- Vilgis T 2013a Die stärke der stärke *Phys. unserer Zeit* **44** 102
- Vilgis T A 2012b Hydrocolloids between soft matter and taste: culinary polymer physics *Int. J. Gastronomy Food Sci.* **1** 46–53
- Vilgis T A 2013b Texture, taste and aroma: multi-scale materials and the gastrophysics of food *Flavour* **2** 12
- Vilgis T A, Heinrich G and Klüppel M 2009 *Reinforcement of Polymer Nano-Composites: Theory, Experiments and Applications* (Cambridge: Cambridge University Press)
- Vilgis T A, Lendner I and Caviezel R 2015 *Ernährung bei Pflegebedürftigkeit und Demenz* (Berlin: Springer)
- Vilgis T and Caviezel R 2012 *Das Moderne Küchenhandwerk* (Wiesbaden: Tre Torri)
- Virot E and Ponomarenko A 2015 Popcorn: critical temperature, jump and sound *J. R. Soc. Interface* **12** 20141247
- Vujadinović D, Gruijić R, Tomović V and Torbica A 2013 Effects of temperature and method of heat treatment on myofibrillar proteins of pork *Chem. Ind. Chem. Eng. Q.* **20** 407–15
- Waananen K M and Okos M R 1996 Effect of porosity on moisture diffusion during drying of pasta *J. Food Eng.* **28** 121–37
- Walstra P 1995 Physical chemistry of milk fat globules *Adv. Dairy Chem.* **2** 131–78
- Walstra P 2007 *Physical Chemistry of Foods* (Boca Raton, FL: CRC Press)
- Walstra P, Geurts T and Noomen A 1999 *Dairy Technology: Principles of Milk Properties and Processes (Food Science and Technology)* (New York: Marcel Dekker)
- Walstra P *et al* 1984 *Dairy Chemistry and Physics* (New York: Wiley)
- Wang R, Tang P, Qiu F and Yang Y 2005 Aggregate morphologies of amphiphilic abc triblock copolymer in dilute solution using self-consistent field theory *J. Phys. Chem. B* **109** 17120–7
- Warner M, Gelling K and Vilgis T 1988 Theory of nematic networks *J. Chem. Phys.* **88** 4008–13
- Warriss P D 2010 *Meat Science: an Introductory Text* (Cambridge: Cambridge University Press)
- Waschatsko G, Junghans A and Vilgis T A 2012 Soy milk oleosome behaviour at the air–water interface *Faraday Discuss.* **158** 157–69
- Waschatsko G M 2013 Oleosome *PhD Thesis* Univesity of Mainz
- Waschatsko G, Schiedt B, Vilgis T A and Junghans A 2012 Soybean oleosomes behavior at the air–water interface *J. Phys. Chem. B* **116** 10832–41
- Watase M, Kohyama K and Nishinari K 1992 Effects of sugars and polyols on the gel-sol transition of agarose by differential scanning calorimetry *Thermochim. Acta* **206** 163–73
- Weegels P, Hamer R and Schofield J 1997 Functional properties of low m r wheat proteins. III. Effects on composition of the glutenin macropolymer during dough mixing and resting *J. Cereal Sci.* **25** 165–73
- Weiss J, Takhistov P and McClements D J 2006 Functional materials in food nanotechnology *J. Food Sci.* **71** R107–16
- Weiss R G and Terech P 2006 *Molecular Gels* (Berlin: Springer)
- West A, Melrose J and Ball R 1994 Computer simulations of the breakup of colloid aggregates *Phys. Rev. E* **49** 4237
- White D, Fisk I, Mitchell J, Wolf B, Hill S and Gray D 2008 Sunflower-seed oil body emulsions: rheology and stability assessment of a natural emulsion *Food Hydrocolloids* **22** 1224–32

- Whitehurst R J 2008 *Emulsifiers in Food Technology* (New York: Wiley)
- Wieser H 2007 Chemistry of gluten proteins *Food Microbiol.* **24** 115–9
- Wiklund L, Stagsted J, Björck L and Nielsen J H 2004 Milk fat globule size is affected by fat production in dairy cows *Int. Dairy J.* **14** 909–13
- Wille R and Lutton E 1966 Polymorphism of cocoa butter *J. Am. Oil Chem. Soc.* **43** 491–6
- Williams C D 1998 The science of boiling an egg
- Witten T and Pincus P 1986 Colloid stabilization by long grafted polymers *Macromolecules* **19** 2509–13
- Witten T, Rubinstein M and Colby R 1993 Reinforcement of rubber by fractal aggregates *J. Phys.* **3** 367–83
- Wollny M and Peleg M 1994 A model of moisture-induced plasticization of crunchy snacks based on fermi's distribution function *J. Sci. Food Agric.* **64** 467–73
- Wright A, Scanlon M, Hartel R and Marangoni A 2001 Rheological properties of milkfat and butter *J. Food Sci.* **66** 1056–71
- Wright D J, Leach I B and Wilding P 1977 Differential scanning calorimetric studies of muscle and its constituent proteins *J. Sci. Food Agric.* **28** 557–64
- Wu H and Morbidelli M 2001 A model relating structure of colloidal gels to their elastic properties *Langmuir* **17** 1030–6
- Wu N, Huang X, Yang X Q, Guo J, Zheng E L, Yin S W, Zhu J H, Qi J R, He X T and Zhang J B 2012 Stabilization of soybean oil body emulsions using ι -carrageenan: effects of salt, thermal treatment and freeze-thaw cycling *Food Hydrocolloids* **28** 110–20
- Wu N, Yang X, Teng Z, Yin S, Zhu J and Qi J 2011 Stabilization of soybean oil body emulsions using kappa, gamma, lambda-carrageenan at different pH values *Food Res. Int.* **44** 1059–68
- Wuestenberg T 2014 *Cellulose and Cellulose Derivatives in the Food Industry: Fundamentals and Applications* (New York: Wiley)
- Wyatt N B, Gunther C M and Liberatore M W 2011 Increasing viscosity in entangled polyelectrolyte solutions by the addition of salt *Polymer* **52** 2437–44
- Wyatt N B and Liberatore M W 2009 Rheology and viscosity scaling of the polyelectrolyte xanthan gum *J. Appl. Polym. Sci.* **114** 4076–84
- Wyrwisz J, Półtorak A, Zalewska M, Zaremba R and Wierzbicka A 2012 Analysis of relationship between basic composition, pH, and physical properties of selected bovine muscles *Bull. Veterinary Inst. Pulawy* **56** 403–9
- Xu C, Li Y and Yu H 2014 Effect of far-infrared drying on the water state and glass transition temperature in carrots *J. Food Eng.* **136** 42–7
- Yamamoto K 1990 Electron microscopy of thermal aggregation of myosin *J. Biochem.* **108** 896–8
- Yamashita H, Ishibashi J, Hong Y H and Hirose M 1998 Involvement of ovotransferrin in the thermally induced gelation of egg white at around 65 °C *Biosci. Biotechnol. Biochem.* **62** 593–5
- Yang A S, Gunner M, Sampogna R, Sharp K and Honig B 1993 On the calculation of pkas in proteins *Proteins: Struct. Funct. Bioinform.* **15** 252–65
- Yang A S and Honig B 1993 On the pH dependence of protein stability *J. Mol. Biol.* **231** 459–74
- Ye A, Cui J and Singh H 2010 Effect of the fat globule membrane on in vitro digestion of milk fat globules with pancreatic lipase *Int. Dairy J.* **20** 822–9
- Yin W, Zhang H, Huang L and Nishinari K 2008 Effects of the lyotropic series salts on the gelation of konjac glucomannan in aqueous solutions *Carbohydr. Polym.* **74** 68–78
- Yuan Y, Zhang N, Tao W, Cao X and He Y 2014 Fatty acids as phase change materials: a review *Renew. Sustainable Energy Rev.* **29** 482–98
- Yusoff A and Murray B S 2011 Modified starch granules as particle-stabilizers of oil-in-water emulsions *Food Hydrocolloids* **25** 42–55
- Zhang B, Dhital S, Flanagan B M and Gidley M J 2014 Mechanism for starch granule ghost formation deduced from structural and enzyme digestion properties *J. Agric. Food Chem.* **62** 760–71
- Zhou W, Therdthai N and Hui Y 2014 *Introduction to Baking and Bakery Products* (Hoboken: Wiley)
- Zielbauer B, Franz J, Viezenz B and Vilgis T A 2015 Physical aspects of meat cooking: time and temperature dependence or protein denaturation and water loss *Food Biophys.* accepted
- Zimmermann M B and Windhab E J 2010 Encapsulation of iron and other micronutrients for food fortification *Encapsulation Technologies for Active Food Ingredients and Food Processing* (Berlin: Springer) pp 187–209
- Zobel H 1988 Molecules to granules: a comprehensive starch review *Starch—Stärke* **40** 44–50